การปรับคุณภาพพลอยคอรันดัมบางชนิดจากประเทศมาดากัสการ์ ด้วยความร้อน

นางสาวกฤตยา ปัทมาลัย

สถาบันวิทยบริการ
จุฬาลงกรณ์มหาวิทยาลัย

วิทยานิพนธ์นี้เป็นส่วนหนึ่งของการศึกษาตามหลักสูตรปริญญาวิทยาศาสตร์มหาบัณฑิต
สาขาวิชาธรณีวิทยา ภาควิชาธรณีวิทยา
คณะวิทยาศาสตร์ จุฬาลงกรณ์มหาวิทยาลัย
ปีการศึกษา 2545

ISBN 974-17-2833-6

ลิขสิทธิ์ของจุฬาลงกรณ์มหาวิทยาลัย

HEAT TREATMENT OF SOME CORUNDUM FROM MADAGASCAR

Miss Krittaya Pattamalai

สถาบันวิทยบริการ
จุฬาลงกรณ์มหาวิทยาลัย

A Thesis Submitted in Partial Fulfillment of the Requirements
for the Degree of Master of Science in Geology

Department of Geology
Faculty of Science
Chulalongkorn University

Academic Year 2002

ISBN 974-17-2833-6

Thesis Title	Heat Treatment of some corundum from Madagascar
By	Miss Krittaya Pattamalai
Field of study	Geology
Thesis Advisor	Associate Professor Visut Pisutha-Arnond, Ph.D.
Thesis Co-advisor	Mr. Rak Hansawek

Accepted by the Faculty of Science, Chulalongkorn University in Partial Fulfillment of the Requirements for the Master 's Degree

…….. Dean of Faculty of Science
(Associate Professor Wanchai Phothiphichitr, Ph.D.)

THESIS COMMITTEE

…….. Chairman
(Mr. Chakkaphan Sutthirat, Ph.D.)

……. Thesis Advisor
(Associate Professor Visut Pisutha-Arnond, Ph.D.)

…….. Thesis Co-advisor
(Mr. Rak Hansawek, M.Sc.)

…….. Member
(Assistant Professor Sompop Vedchakanchana, M.Sc.)

สถาบันวิทยบริการ
จุฬาลงกรณ์มหาวิทยาลัย

กฤตยา ปัทมาลัย : การปรับคุณภาพพลอยคอรันดัมบางชนิดจากประเทศมาดากัสการ์ด้วยความร้อน อ. ที่ปรึกษา : รองศาสตราจารย์ ดร.วิสุทธิ์ พิสุทธอานนท์, อ. ที่ปรึกษาร่วม : นายรัก หรรษาเวก จำนวนหน้า 178 หน้า. ISBN 974-17-2833-6

การปรับคุณภาพพลอยคอรันดัมด้วยความร้อนหรือการเผาพลอยนับเป็นกรรมวิธีเพิ่มคุณภาพที่สำคัญอันเป็นที่รู้จักและยอมรับในตลาดการค้าระหว่างประเทศ ปัจจุบันประเทศไทยนำเข้าพลอยคอรันดัมเป็นจำนวนมากจากประเทศมาดากัสการ์ โดยที่พลอยส่วนใหญ่จะต้องผ่านกรรมวิธีการปรับคุณภาพด้วยความร้อน เพื่อทำให้พลอยมีสีสวยและเนื้อใสสะอาดดีขึ้นก่อนที่จะนำไปใช้ในอุตสาหกรรมอัญมณีและเครื่องประดับ

ตัวอย่างพลอยแซปไฟร์จำนวนมากกว่า 270 ตัวอย่าง ที่ได้จากแหล่งพลอยทุติยภูมิของแหล่งอิลากากา-ซาการาฮา ซึ่งอยู่ทางตะวันตกเฉียงใต้ของประเทศมาดากัสการ์ สามารถจัดแบ่งเป็นกลุ่มสีต่าง ๆ ตามความแตกต่างของสีได้ 7 กลุ่ม คือ กลุ่มสีชมพู น้ำเงิน ม่วง ม่วงแดง ขาว เหลือง และเขียว ตัวอย่างพลอยกลุ่มสีที่ใช้ในการปรับคุณภาพด้วยความร้อนในการศึกษานี้ คือ กลุ่มสีชมพู ม่วงแดง และม่วง โดยนำมาทดลองเผาที่อุณหภูมิสูงสุดตั้งแต่ 800^{O}C, 1000^{O}C, 1200^{O}C, 1400^{O}C และ 1600^{O}C และคงอุณหภูมิสูงสุดเป็นเวลานาน 1 ชั่วโมง ในบรรยากาศการเผาแบบออกซิไดซิง ผลการศึกษาพบว่าช่วงอุณหภูมิที่เหมาะสมในการลดหรือกำจัดสีอมม่วงหรือแกมน้ำเงินในกลุ่มพลอยสีชมพู คือ 1000^{O}C ถึง 1200^{O}C นอกจากนี้ยังพบว่า แร่เซอร์คอน ซึ่งเป็นมลทินภายในพลอยแสดงความขุ่นขาว สามารถใช้เป็นตัวบ่งชี้การเผาได้ จากการเปรียบเทียบสเปกตรัมการดูดกลืนแสงในช่วงอัลตราไวโอเลตถึงอินฟราเรดระยะใกล้ของพลอยก่อนและหลังเผา รวมทั้งนำผลการวิเคราะห์ปริมาณธาตุร่องรอยของกลุ่มพลอยที่ศึกษาเทียบกับแบบจำลองธาตุมลทินระหว่าง Mg, Ti และ Fe ของ Haeger (2001) ทำให้ทราบถึงสาเหตุของการเกิดสีและการเปลี่ยนแปลงสีภายหลังการเผาว่าเกี่ยวข้องกับ Mg, Ti และ Fe ซึ่งเป็นธาตุร่องรอยภายในพลอย โดยอัตราส่วน Mg : Ti ของพลอยส่วนใหญ่มีค่าใกล้เคียง 1 เมื่อเผาพลอยในบรรยากาศแบบออกซิไดซิง จะทำให้ Mg และ Ti เกิดเป็นกลุ่มของ $MgTiO_3$ ซึ่งไม่มีสีในโครงสร้างของพลอย และยังทำให้ Fe^{2+} ถูกออกซิไดซ์ เป็น Fe^{3+} ดังนั้น สีแกมน้ำเงินที่เกิดจากการแลกเปลี่ยนประจุระหว่าง Fe^{2+} กับ Ti^{4+} จะถูกกำจัดทำให้พลอยมีสีชมพู

ภาควิชา.....ธรณีวิทยา..... ลายมือชื่อนิสิต.....
สาขาวิชา.....ธรณีวิทยา..... ลายมือชื่ออาจารย์ที่ปรึกษา.....
ปีการศึกษา.....2545..... ลายมือชื่ออาจารย์ที่ปรึกษาร่วม.....

4272208423 : MAJOR Geology

KEY WORD: heat treatment / corundum / sapphire / oxidizing atmosphere

Krittaya Pattamalai : Heat Treatment of some corundum from Madagascar THESIS ADVISOR : Associate Professor Visut Pisutha-Arnond, Ph.D., THESIS CO-ADVISOR : Mr.Rak Hansawek, M.Sc., 178 pp., ISBN 974-17-2833-6.

Heat treatment is an important technique for improving the color and clarity of corundum. It is the most popular method accepted and adopted by the international trade. At present, Thailand imports a large volume of corundum from Madagascar, most of which is heat-treated before it is supplied to the gems and jewelry industry.

More than 270 sapphires from secondary gem deposits in Ilakaka-Sakaraha area, southwestern Madagascar, were categorized into 7 color groups including pink, blue, violet, purple, colorless, yellow and green sapphires. Most pink and purple and medium violet sapphires were selected for heat-treatment study. These sapphires were examined in great details on gem characteristics using basic equipment and advanced instruments. Step-heating experiments were performed under oxidizing atmosphere at different maximum temperatures (i.e., 800^{O}C, 1000^{O}C, 1200^{O}C, 1400^{O}C and 1600^{O}C) for one hour soaking time at each temperature. Characteristics of all samples were examined after each heating step for comparison. Results of this study show that most sapphire samples can be treated ultimately to reduce their blue color in oxidizing atmosphere at 1000^{O}C-1200^{O}C. The criterion for detecting the heat treatment is the turbidity of zircon inclusion. Causes of color and its changing are obviously explained using UV-VIS-NIR absorption spectra and trace elements. Based on the interaction model of Mg, Ti and Fe by Haeger (2001), the causes of color can be explained in all studied sample groups. Most samples have Mg/Ti ratios close to 1. This data suggest that when heat-treated those sapphires in oxidizing atmosphere, most of Mg and Ti would be tied up with the formation of colorless $MgTiO_3$ clusters and at the same time the Fe^{2+} might have been oxidized into Fe^{3+}. Hence the blue overcast originated from Fe^{2+}/Ti^{4+} IVCT process would have been eliminated and the stones should turn in pure pink color.

Department……Geology…… Student's signature……..

Field of study……..Geology…… Advisor's signature…….

Academic year……2002……. Co-advisor's signature…….

ACKNOWLEDGEMENTS

The author would like to thank Associate Professor Dr. Visut Pisutha-Arnond and Mr. Rak Hansawek for their suggestion and supervision throughout the completion of this thesis.

The author sincerely appreciates the Department of Geology, Faculty of Science, Chulalongkorn University for providing sample preparation. Many thanks are also due to The Gem and Jewelry Institute of Thailand (GIT) for the permission to use laboratory instruments, i.e., Laser Raman Spectroscope, Fourier Transform Infrared Spectrophotometer (FTIR) and photographic equipment. Thanks are due to the Physical Analysis Section, Mineral Resources Analysis Division, Department of Mineral Resources (DMR) for providing Energy Dispersive X-ray Fluorescence Spectrometer (EDXRF), especially Mr. Boonthavee Sriprasert who assisted in the EDXRF analysis. Many thanks are also given to the Gemstone Section, Economic Geology Division, DMR for permission to use basic and advanced instruments, i.e., gemological microscope, UV-VIS-NIR Spectrophotometer, electric furnace and computer. Thanks are also given to Center of Gemstone Research, Institute of Geosciences, University of Mainz, Germany for providing Electron Probe Micro-Analyzer (EPMA).

The author is very grateful to GIT for some financial support through the Heat Treatment of Ruby and Sapphire Research Project. Sincere gratitude is expressed to Dr. Chakkaphan Sutthirat who assisted in the EPMA analysis. Special thanks are also delivered to laboratory staff members of the GIT and many people, who are not named here for various kinds of help to finish this thesis.

ศูนย์วิทยทรัพยากร
จุฬาลงกรณ์มหาวิทยาลัย

CONTENTS

PAGE

ABSTRACT IN THAI iv
ABSTRACT IN ENGLISH v
ACKNOWLEDGEMENTS vi
LIST OF TABLES ix
LIST OF FIGURES x
CHAPTER I INTRODUCTION 1
The purpose of study 1
Method of study 2
CHAPTER II GEOLOGY 5
Locality and access 5
Regional geology 6
Mining and production 9
CHAPTER III PHYSICAL AND OPTICAL PROPERTIES 13
Visual appearance and Crystal habits 13
Classification and Preparation 13
Physical and Optical properties 15
Internal Characteristics 26
CHAPTER IV ABSORPTION SPECTRA 38
FTIR Spectrophotometer 38
FTIR spectra 39
UV-VIS-NIR Spectrophotometer 39
UV-VIS-NIR spectra 44
CHAPTER V STUDY AFTER HEAT TREAMENT 53
Introduction 53
The effect of heat treatment on the color appearance 55
The effect of heat treatment on the internal characteristics 62
FTIR spectra 86
UV-VIS-NIR spectra 91
CHAPTER VI CHEMICAL ANALYSIS 97
Energy Dispersive X-ray Fluorescence Spectrometer 97

CONTENTS (CONTINUED)

PAGE

Trace Element Analysis by EDXRF 98
Trace Element Analysis by EPMA 105
Comparison of trace element content by EDXRF and EPMA 111
CHAPTER VII DISCUSSION AND CONCLUSIONS 118
Cause of color change in sapphire after heat treatment 118
Conclusions 122
REFERENCES 125
APPENDICES 127
APPENDIX I 128
Table I.1 Showing the gemological properties of some Ilakaka-Sakaraha sapphires 129
Table II.2 Color codes of pink, purple and medium violet sapphires before heating based on GIA GemSet color specimens (Retail Set) 136
APPENDIX II FTIR spectra of sapphire before and after heating 140
APPENDIX III UV-VIS-NIR spectra of sapphire before and after heating 149
APPENDIX IV 166
Table IV.1 Showing the trace elements analyzes of some Ilakaka-Sakaraha sapphires by Energy Dispersive X-ray Fluorescence (in weight %). The analyzes were performed before heating 167
Table IV.2 Showing the major and trace elements content of some selected pink, purple and violet sapphires (16 samples) by Electron Probe Micro-Analyzer. The analyzes were performed after the step-heating up to 1600^{O}C 173
BIOGRAPHY 178

LIST OF TABLES

TABLE PAGE

3.1 Summary of the gemological properties of some Ilakaka–Sakaraha sapphires..... 21

3.2 Color comparison of sapphires before heating by GIA GemSet..... 25

3.3 Major Raman Shift peaks of the common inclusions in this study 27

5.1 Color codes of sapphires before and after heating at 800^{O}C, 1000^{O}C, 1200^{O}C, 1400^{O}C and 1600^{O}C by GIA GemSet..... 56

6.1 EDXRF analyzes of some Ilakaka-Sakaraha sapphires (in weight %)..... 99

6.2 Some trace elements content of selected pink, purple and violet sapphires (16 samples) by Electron Probe Micro-Analyzer. The analyzes were performed after the step-heating up to 1600^{O}C..... 107

สถาบันวิทยบริการ
จุฬาลงกรณ์มหาวิทยาลัย

LIST OF FIGURES (CONTINUED)

FIGURE PAGE

1.1 Diagram of method of study 3
2.1 Location map of Ilakaka-Sakaraha area, southwestern Madagascar 5
2.2 Generalized geologic map of southwestern Madagascar 8
2.3 Alluvial gemstone deposit at Ilakaka 10
2.4 Hand-miner digging at Ilakaka. During the digging for sapphire, sometimes a hole collapses. Since 1998 approximately 900 diggers died during their dangerous work 10
2.5 Washing the gravels in a nearby stream 11
2.6 Overview of the whole of the GMRC test mine. The Isalo mountain range is in the background 11
2.7 Showing the mining operation by heavy machine at the GMRC test mine: Scrapers remove overburden. The sapphire-bearing paydirt is loaded onto the trucks and sent to the machanised processing plant 12
3.1 Crystal habits observed in Ilakaka-Sakaraha sapphires 14
3.2 Showing 4 types of polished pink sapphires
(A-B) purplish pink; (C) light purplish pink; (D) light orangey pink;
(E) orangey pink 16
3.3 Showing 3 types of polished blue sapphires
(A) very dark blue; (B) dark blue; (C), (E) and (G) medium blue
(B) observed under the day light lamp; (D) and (F) medium blue observed under the tungsten lamp 17
3.4 Showing 4 types of blue sapphires
(A), (C) and (D) light blue observed under the day light lamp;
(B) light blue observed under the tungsten lamp; (E)-(G) very light blue; (H)-(I) extremely light blue; (J) light greenish blue 18
3.5 Showing 3 types of polished violet sapphires
(A) dark violet observed under the day light lamp; (B) dark violet observed under the tungsten lamp; (C) and (E) medium violet

LIST OF FIGURES (CONTINUED)

FIGURE PAGE

observed under the day light lamp; (D) medium violet observed under the tungsten lamp; (F) light violet..... 19

3.6 Showing 3 types of polished purple sapphires (A) purple; (B)-(C) pinkish purple; (D) brownish purple..... 19

3.7 Showing 4 types of colorless sapphires (A) colorless; (B) very light bluish white; (C) very light yellowish white; (D) colorless with blue patch..... 20

3.8 Showing 2 types of yellow sapphires; orangey yellow (left) and light yellow (right)..... 20

3.9 Showing 2 types of green sapphires; light yellowish green (left) and medium green with blue patch (right)..... 20

3.10 GIA GemSet color specimens..... 24

3.11 Characteristics of zircon inclusions occurring in pink sapphires;
(A) as single inclusion (sample no. LP3, 70X)
(B) as cluster of inclusions (sample no. PP6, 140X)
(C) as single inclusion with tension disc (sample no. PP15, 70X)
(D) as cluster of inclusions with tension disc (sample no. LP3, 140X)..... 28

3.12 Raman spectrum of a zircon inclusion in light purplish pink sapphire (sample no. LP3, zircon peaks at 442, 977, 1017, 1055, 1089 and 1144 cm^{-1}, corundum peaks at 225, 363, 400, 417, 576 and 750 cm^{-1})..... 28

3.13 Cluster of zircon inclusions with tension disc and a monazite inclusion in purplish pink sapphire (sample no. PP4, 140X)..... 29

3.14 Raman spectrum of a zircon inclusion in purplish pink sapphire (sample no. PP4, zircon peaks at 356, 1006, 1054, 1089 and 1144 cm^{-1}, corundum peaks at 400 and 749 cm^{-1})..... 29

3.15 Raman spectrum of a monazite inclusion in purplish pink sapphire (sample no. PP4, monazite peaks at 463, 624, 975 and 1063 cm^{-1}, corundum peaks at 403, 416, and 575 cm^{-1})..... 29

LIST OF FIGURES (CONTINUED)

FIGURE PAGE

3.16 Rutile inclusions occurring in purplish pink sapphire as black to dark brown, rounded and short prismatic crystal (sample no. PP3, 30X)..... 30
3.17 Raman spectrum of a rutile inclusion in purplish pink sapphire (sample no. PP3, rutite peaks at 240, 444 and 611 cm^{-1})..... 30
3.18 Abundant colorless zircon inclusions and a hexagonal platy mica inclusion in light purplish pink sapphire (sample no. LP3, 70X)..... 31
3.19 Raman spectrum of a mica inclusion in light purplish pink sapphire (sample no. LP3, mica peaks at 262, 698 and 908 cm^{-1}, corundum peaks at 378, 417, 575, 642 and 750 cm^{-1})..... 31
3.20 Fingerprints (healed fractures) in purplish pink sapphire (sample no. PP3, 15X)..... 32
3.21 Showing the white dust or minute particles (sample no. PP3, 70X)..... 32
3.22 Rutile needles in purplish pink sapphire (sample no. PP3, 70X)..... 32
3.23 Zircon inclusions occurring in purple sapphires as
(A) single crystal (sample no. P16, 140X)
(B) single crystal with tension disc (sample no. P5, 70X)
(C) crystal cluster with tension disc (sample no. P5, 140X)..... 34
3.24 Raman spectrum of a zircon inclusion in purple sapphire (sample no. P16, zircon peaks at 359, 439. 979, 1014, 1090 and 1147 cm^{-1}, corundum peaks at 400, 416, and 749 cm^{-1})..... 34
3.25 Zircon and mica inclusions in pinkish purple sapphire (sample no. P6, 70X). Abundance of zircon inclusions such as this photo is a locality characteristic of the Ilakaka-Sakaraha pink and purple sapphires..... 35
3.26 Raman spectrum of a mica inclusion in pinkish purple sapphire (sample no. P6, mica peaks at 262, 700 and 905 cm^{-1}, corundum peaks at 416, 576, 641 and 749 cm^{-1})..... 35
3.27 Raman spectrum of a fuchsite inclusion in purple sapphire (sample no. P16, fuchsite peaks at 263, 490 and 698 cm^{-1}, corundum peaks at 378, 414, 576, 641 and 750 cm^{-1})..... 35

LIST OF FIGURES (CONTINUED)

FIGURE PAGE

3.28 Monazite inclusion occurring in purple sapphire as white rounded crystal (sample no. P16, 70X) 36
3.29 Raman spectrum of a monazite inclusion in purple sapphire (sample no. P16, monazite peaks at 465, 622, 974 and 1059 cm^{-1}, corundum peaks at 377, 416, 573 and 643 cm^{-1}) 36
3.30 Fingerprint and rutile needles in medium violet sapphire (sample no. MV5, 40X) 37
3.31 Rutile needles oriented 3 directions and intersecting at $60^{o}/120^{o}$ angles in medium violet sapphire (sample no. MV2, 50X) 37
3.32 White dust which appear milky and fingerprint in medium violet sapphire (sample no. MV5, 20X) 37
4.1 Nicolet FTIR Spectrophotometer (model NEXUS 670) 38
4.2 FTIR spectra of unheated purplish pink sapphire (total 10 samples) 40
4.3 FTIR spectra of unheated light purplish pink sapphire (total 8 samples) 40
4.4 FTIR spectra of unheated light orangey and orangey pink sapphires (total 6 samples) 41
4.5 FTIR spectra of unheated purple sapphire (total 3 samples) 41
4.6 FTIR spectra of unheated pinkish purple sapphire (total 10 samples) 42
4.7 FTIR spectra of unheated brownish purple sapphire (total 3 samples) 42
4.8 FTIR spectra of unheated medium violet sapphire (total 4 samples) 43
4.9 Hitachi UV-VIS-NIR Spectrophotometer (model U4001) 44
4.10 UV-VIS-NIR spectra of unheated (A) purplish pink (PP11) and (B) light orangey pink (PP15) sapphires 45
4.11 UV-VIS-NIR spectra of unheated light purplish pink sapphire (A) low Fe content (LP7) (B) high Fe content (LP9) 46
4.12 UV-VIS-NIR spectra of unheated orangey pink sapphire (A) low Fe content (PP17) (B) high Fe content (PP16) 47

LIST OF FIGURES (CONTINUED)

FIGURE PAGE

4.13 UV-VIS-NIR spectra of unheated (A) purple (P16) and (B) brownish purple (P11) sapphires 48
4.14 UV-VIS-NIR spectra of unheated pinkish purple sapphire (A) low Fe content (P10) (B) high Fe content (P6) 49
4.15 UV-VIS-NIR spectra of unheated violet sapphire (A) with color-change effect (MV2) (B) without color-change effect (MV5) 50
4.16 UV-VIS-NIR spectra comparison of unheated ruby and pink sapphire (A) Thai ruby that related to basaltic-type origin (B) Mogok ruby that related to metamorphic-type origin (C) low iron Ilakaka-Sakaraha pink sapphire 52
5.1 Lindberg electric furnace (Model 59256-E6) and accessory 54
5.2 Color appearance in purplish pink sapphire samples 57
5.3 Color appearance in light purplish pink sapphire samples 57
5.4 Color appearance in light orangey pink sapphire (sample no. PP15) 58
5.5 Color appearance in orangey pink sapphire (sample no. PP17) 58
5.6 Color appearance in purple sapphire (sample no. P16) 60
5.7 Color appearance in pinkish purple sapphire samples 60
5.8 Color appearance in brownish purple sapphire (sample no. P11) 61
5.9 Color appearance in medium violet sapphire samples 61
5.10 Most zircon inclusions in these two sapphire samples were still unchanged after the step-heating from 800^{O}C to 1600^{O}C, each step was hold for 1 hour soaking time 63
5.11 A zircon inclusion with slight tension crack was still unchanged after the step-heating from 800^{O}C to 1600^{O}C (sample no. PP15, 70X) 64
5.12 A cluster of zircon inclusions was still unchanged after the step-heating from 800^{O}C to 1600^{O}C (sample no. PP6, 140X) 64

LIST OF FIGURES (CONTINUED)

FIGURE PAGE

5.13 Another cluster of zircon inclusion with slight tension disc (in circle) was still unchanged after the step-heating from 800^{O}C to 1600^{O}C (sample no. P16, 70X) 65

5.14 Many clusters of zircon inclusions with tension cracks (in circle) were still unchanged after the step-heating from 800^{O}C to 1600^{O}C..... 66

5.15 Most of individual zircon inclusions were still unchanged after the step-heating from 800^{O}C-1600^{O}C whereas the zircon cluster (in circle) showed slight development of tension crack after heating up to 1000^{O}C. When re-heating up to 1400^{O}C and 1600^{O}C, this tension crack became more obvious (sample no. P6, 70X)..... 67

5.16 A zircon inclusion with slight tension crack was still unchanged after heating to 800^{O}C. When re-heating up to 1000^{O}C-1600^{O}C, this tension crack was obviously expanded (sample no. P5, 140X) 67

5.17 A relatively large and clear zircon inclusion (in circle) was still unchanged after heating at 800^{O}C. However, when re-heating up to 1000^{O}C, the crystal began to alter into whitish, cloudy appearance (turbid) with slight development of tension crack. The tension crack became more obvious after re-heating up to 1400^{O}C. The crystal showed stronger decomposition after re-heating up to 1600^{O}C (sample no. P6, 70X)..... 68

5.18 Zircon inclusions (in circle) showed the development of tension crack after heating up to 1200^{O}C. When re-heating up to 1600^{O}C, they began to decompose into whitish, cloudy appearance (turbid) with obvious tension crack (sample no. P6, 70X) 69

5.19 Most zircon inclusions were still unchanged after the step-heating from 800^{O}C to 1600^{O}C except the crystal in circle began to alter with slight development of tension crack after heating up to 1400^{O}C. When re-heating up to 1600^{O}C, it was obviously altered into whitish, cloudy

LIST OF FIGURES (CONTINUED)

FIGURE PAGE

appearance (turbid) with well developed tension crack surrounding it (sample no. LP9, 140X) 69

5.20 Most of the zircon inclusions were still unchanged after the step-heating from 800^{O}C to 1600^{O}C except some crystals in circle appear turbid after heating at 1600^{O}C (sample no. PP6, 140X) 70

5.21 Most of the zircon inclusions were still unchanged after the step-heating from 800^{O}C to 1600^{O}C except some crystals in circle appear turbid after heating at 1600^{O}C (sample no. LP3, 140X) 70

5.22 Most of the zircon inclusions were still unchanged after the step-heating from 800^{O}C to 1600^{O}C except some crystals in circle appear turbid after heating at 1600^{O}C 71

5.23 Most of the zircon inclusions were still unchanged after the step-heating from 800^{O}C to 1600^{O}C except some crystals in circle appear turbid after heating at 1600^{O}C 72

5.24 Showing zircon clusters with minor tension discs before heating. The tension discs were noticeably expanded after heating at 800^{O}C and became more obvious after reheating at higher temperatures. It should also be noted that some crystals in zircon clusters appear turbid after heating at 1200^{O}C. The decomposition of those zircon crystals became more pronounced after re-heating to higher temperatures. (sample no. PP11, 70X) 73

5.25 A zircon clusters was still unchanged after heating at 800^{O}C. The tension discs began to develop after re-heating to 1000^{O}C. After re-heating from 1400^{O}C to 1600^{O}C, these tension discs became more obvious (sample no. PP4, 140X) 74

5.26 A zircon cluster was still unchanged after heating at 800^{O}C but showed a strong development of tension discs after re-heating from 1000^{O}C to 1600^{O}C. Furthermore, most crystals in the cluster appear

LIST OF FIGURES (CONTINUED)

FIGURE PAGE

turbid after heating up to 1400^{O}C while a monazite inclusion began to alter at 1600^{O}C (sample no. PP4, 140X) 74

5.27 Showing zircon clusters with slight tension crack before heating. After heating at 800^{O}C to 1200^{O}C, they were still unchanged (sample no. PP6, 140X)

(A) When re-heating up to 1400^{O}C, some zircon crystals in the clusters began to decompose into whitish cloudy appearance and became obviously decomposed after re-heating up to 1600^{O}C

(B) After re-heating up to 1400^{O}C, tension crack was extended and some zircon crystals in the clusters began to decompose. These crystals were obviously decomposed when heated up to 1600^{O}C 75

5.28 Showing zircon clusters with slight tension crack before heating. After heating at 800^{O}C to 1200^{O}C, they were still unchanged. When re-heating up to 1400^{O}C, some zircon crystals in the clusters began to decompose into whitish cloudy appearance and the tension crack was expanded. After re-heating up to 1600^{O}C, the crack appeared more expansive and the crystals clearly turn turbid (sample no. LP3, 70X) 76

5.29 A monazite inclusion was still unchanged after the step-heating from 800^{O}C to 1600^{O}C (sample no. P16, 70X) 78

5.30 A mica inclusion was still remain the same after heating at 800^{O}C. When re-heating up to 1000^{O}C, the crystal began to alter and were obviously altered at higher temperatures. The tension crack start to form around the inclusion at 1200^{O}C, it became more and more obvious when re-heating up to 1400^{O}C and 1600^{O}C (sample no. P6, 70X) 79

5.31 Another mica inclusion was still unchanged after heating at 800^{O}C. When re-heating up to 1000^{O}C, it was partially altered or appeared slightly turbid with small development of tension crack. The alteration

LIST OF FIGURES (CONTINUED)

FIGURE PAGE

and tension crack became more and more obvious when re-heating at 1200^{O}C, 1400^{O}C and 1600^{O}C (sample no. LP3, 70X) 80

5.32 Some rutile inclusions changed color from dark brown-black to red with slight development of tension crack after heating at 800^{O}C. When re-heating up to higher temperature (1400^{O}C to 1600^{O}C) the red color were more intense and tension cracks became obvious (sample no. PP3) 81

5.33 Black rutile inclusion slightly changed to red after heating at 800 ^{O}C. They became obviously red color and formed melted boundary at higher temperatures (sample no. PP3, 70X) 82

5.34 Rutile needles intersecting each other at 60^{O}/120^{O} angles was still unchanged after heating at 800^{O}C-1400^{O}C but was partially dissolved in the host sapphire creating dot-like pattern after heating at 1600^{O}C (sample no. MV2) 82

5.35 Rutile silk or needles completely dissolved in the host sapphire after heating at 1600 ^{O}C but was still unchanged after heating at lower temperatures 83

5.36 Milky or dust zone became clearer when heated at 1600^{O}C 84

5.37 Sapphire showed slight development of the fingerprint after heating at 800^{O}C and obviously developed at 1000^{O}C. When re-heating up to 1600^{O}C the fluid inclusion in the fingerprint would be developed into fine pattern (sample no. P6, 70X) 85

5.38 Fingerprints in a unheated sapphire were expanded after heating at 1200^{O}C and 1600^{O}C (sample no. PP6, 50X) 85

5.39 FTIR spectra of purplish pink sapphire before and after heating (sample no. PP4) 87

5.40 FTIR spectra of purplish pink sapphire before and after heating (sample no. LP9) 87

LIST OF FIGURES (CONTINUED)

FIGURE PAGE

5.41 FTIR spectra of light orangey pink sapphire before and after heating (sample no. PP15) 88

5.42 FTIR spectra of light orangey pink sapphire before and after heating (sample no. PP17) 88

5.43 FTIR spectra of purple sapphire before and after heating (sample no. P16) 89

5.44 FTIR spectra of pinkish purple sapphire before and after heating (sample no. P10) 89

5.45 FTIR spectra of brownish purple sapphire before and after heating (sample no. P11) 90

5.46 FTIR spectra of medium bluish violet sapphire before and after heating (sample no. MV5) 90

5.47 The UV-VIS-NIR absorption spectra of the purple sapphire sample (P16) on the vibration plane perpendicular to the c-axis (o-ray)

(A) The spectra of before (purple, unheat) and after (pink) heat treatment at 1200^{O}C

(B) The remaining (residue) spectrum after subtraction of before and after heat-treatment at 1200^{O}C 93

5.48 The UV-VIS-NIR absorption spectra of the medium violet sapphire sample (MV2) on the vibration plane perpendicular to the c-axis (o-ray)

(A) The spectra of before (medium violet, unheat) and after heat treatment at 1200^{O}C (pale bluish purple) and at 1600^{O}C (bluish purple)

(B) The remaining spectra after subtraction of before and after heat-treatment at 1200^{O}C and 1600^{O}C 94

5.49 The UV-VIS-NIR absorption spectra of the orangey pink sapphire sample (PP17) on the vibration plane perpendicular to the c-axis (o-ray)

(A) The spectra of before (orangey pink, unheat) and after heat treatment at 800^{O}C (pale pink) and at 1600^{O}C (pale pink)

LIST OF FIGURES (CONTINUED)

FIGURE PAGE

(B) The remaining spectra after subtraction of before and after heat-treatment at 800^{O}C and 1600^{O}C 95

6.1 Variation diagram of V_2O_3 versus Cr_2O_3 shows the average and one standard deviation of vanadium and chromium contents of 7 sapphire groups by EDXRF 102

6.2 Variation diagram of Fe_2O_3 versus TiO_2 shows the average and one standard deviation of iron and titanium contents of 7 sapphire groups by EDXRF 103

6.3 Variation diagram of Ga_2O_3 versus Cr_2O_3 shows the average and one standard deviation of gallium and chromium contents of 7 sapphire groups by EDXRF 104

6.4 Variation diagram of V_2O_3 versus Cr_2O_3 shows the average and one standard deviation of vanadium and chromium contents of 8 sapphire types by EPMA 108

6.5 Variation diagram of Fe_2O_3 versus TiO_2 shows the average and one standard deviation of iron and titanium contents of 8 sapphire types by EPMA 109

6.6 Variation diagram of Ga_2O_3 versus Cr_2O_3 shows the average and one standard deviation of gallium and chromium contents of 8 sapphire types by EPMA 110

6.7 Titanium content of some selected pink, purple and violet sapphires (4 samples) by EPMA versus EDXRF; titanium content in PP15/1 is lower than detection limit (<0.01 weight % TiO_2). 113

6.8 Chromium content of some selected pink, purple and violet sapphires (4 samples) by EPMA versus EDXRF 114

6.9 Vanadium content of some selected pink, purple and violet sapphires (4 samples) by EPMA versus EDXRF; vanadium contents in P10/3,

LIST OF FIGURES (CONTINUED)

FIGURE PAGE

P10/5, PP11/2, PP11/4, P16/3 and MV5/3 are lower than detection limit (<0.01 weight % V_2O_3) 115

6.10 Gallium content of some selected pink, purple and violet sapphires (4 samples) by EPMA versus EDXRF; gallium contents in PP17/1 and LP3/5 are lower than detection limit (<0.01 weight % Ga_2O_3) 116

6.11 Iron content of some selected pink, purple and violet sapphires (4 samples) by EPMA versus EDXRF 117

7.1 Model of sapphires heated at 1850°C in oxidizing atmospheres (Haeger, 2001) 119

7.2 Model of corundum heated at 1750°C in oxidizing atmospheres (Haeger, 2001) 119

7.3 Mg, Fe and Ti contents of 16 sapphire samples by EPMA. The analysis was performed after the step-heating up to 1600°C in oxidizing atmosphere. These contents were normalized to 100% and plot in Mg-Fe-Ti triangle in comparison to Al-$Fe_{(total)}$-Ti-Mg model of corundum heated at 1750°C in oxidizing atmospheres 121

สถาบันวิทยบริการ
จุฬาลงกรณ์มหาวิทยาลัย

CHAPTER I

INTRODUCTION

Thailand is known as one of the important precious stones cutting and jewelry manufacturing and exporting center. Approximately 80% of ruby and sapphire trading in the world has been supplied from Thailand. Rough gemstones have been imported from foreign countries especially from African countries such as Tanzania and Madagascar. The stones, ruby and sapphire in particular, were normally heat-treated, then cut and subsequently exported or setting in jewelry before being exported. Recently, Madagascar produces more than 50 varieties of gemstone, for example, ruby and sapphire, aquamarine, morganite, tourmaline, emerald and garnet. Most ruby and sapphire deposits are located in the central and southern parts of the country, such as Antanifotsy, Andranondambo, Vatomandry, Betroka-Ihosy, Gogogogo, Ejeda, and Ilakaka-Sakaraha (Schwarz and Schmetzer, 2001). In late 1998, pink, blue and fancy-colored sapphires were discovered in Ilakaka-Sakaraha area. Most of them have been thermally enhanced to improve their color and clarity. After heat treatment, blue sapphires look similar to materials from Sri Lanka and pinkish-orange varieties also correspond to Sri Lankan padparadschas (Milisenda and others, 2001). So gem dealers from overseas including Thai traders have been actively mining or purchasing the stones from the Ilakaka-Sakaraha area.

Gemstone heat treatment has been one of several techniques commonly practiced by Thai gem traders. Thermal enhancement of ruby and sapphire is a well-known and acceptable method in gem industry. The detailed heating processes and techniques of the heat treatment have never been disclosed. The heat treatment was mainly done by trial and error. It is therefore the author's motive to study heat treatment of some sapphires from Ilakaka-Sakaraha by applying scientific approach.

The purpose of study

The purpose of this research is to study the gemmological properties and to observe internal characteristics of some Ilakaka-Sakaraha sapphires that could

be developed during heat treatment. The method is to compare the features of both before and after thermal treatment, such as color, absorption spectra and internal characteristics. This study aims at illustrating the changes of these characteristics at different temperatures which will not only help finding identification criteria for the heat treated sapphire but also gain some knowledge for the effective heat treatment method for the Ilakaka-Sakaraha sapphires.

Method of study

The method of study can be summarized as follows (Figure 1.1) :

1. Literature survey of the previous works related to this study,

2. Classifying the samples based on the color appearance,

3. Selecting suitable sets of samples for thermal treatment,

4. Locating the c-axis of samples using a polariscope,

5. Cutting and polishing the samples both perpendicular and parallel to c-axis,

6. Determining the physical and optical properties such as refractive index (RI), birefringence, specific gravity (SG), and luminescence under short wave (SW, 254 nm) and long wave (LW, 365 nm),

7. Observation of the internal characteristics and taking photos for comparison with those of after heat treatment,

8. Measurement of the absorption spectra of the samples before heat treatment by UV-VIS-NIR Spectrophotometer at Department of Mineral Resources (DMR) and FTIR Spectrophotometer at The Gem and Jewelry Institute of Thailand (GIT),

9. Semi-quantitative analyzes of trace element contents (total Fe_2O_3, TiO_2, Cr_2O_3, V_2O_3 and Ga_2O_3) by Energy Dispersive X-ray Fluorescence (EDXRF) at the DMR,

10. Performing step-heat treatment in an electric furnace at $800^{O}C$, $1000^{O}C$, $1200^{O}C$, $1400^{O}C$ and $1600^{O}C$ for one hour soaking time at the DMR,

11. Observation of the internal characteristics and the absorption spectra after each heating condition,

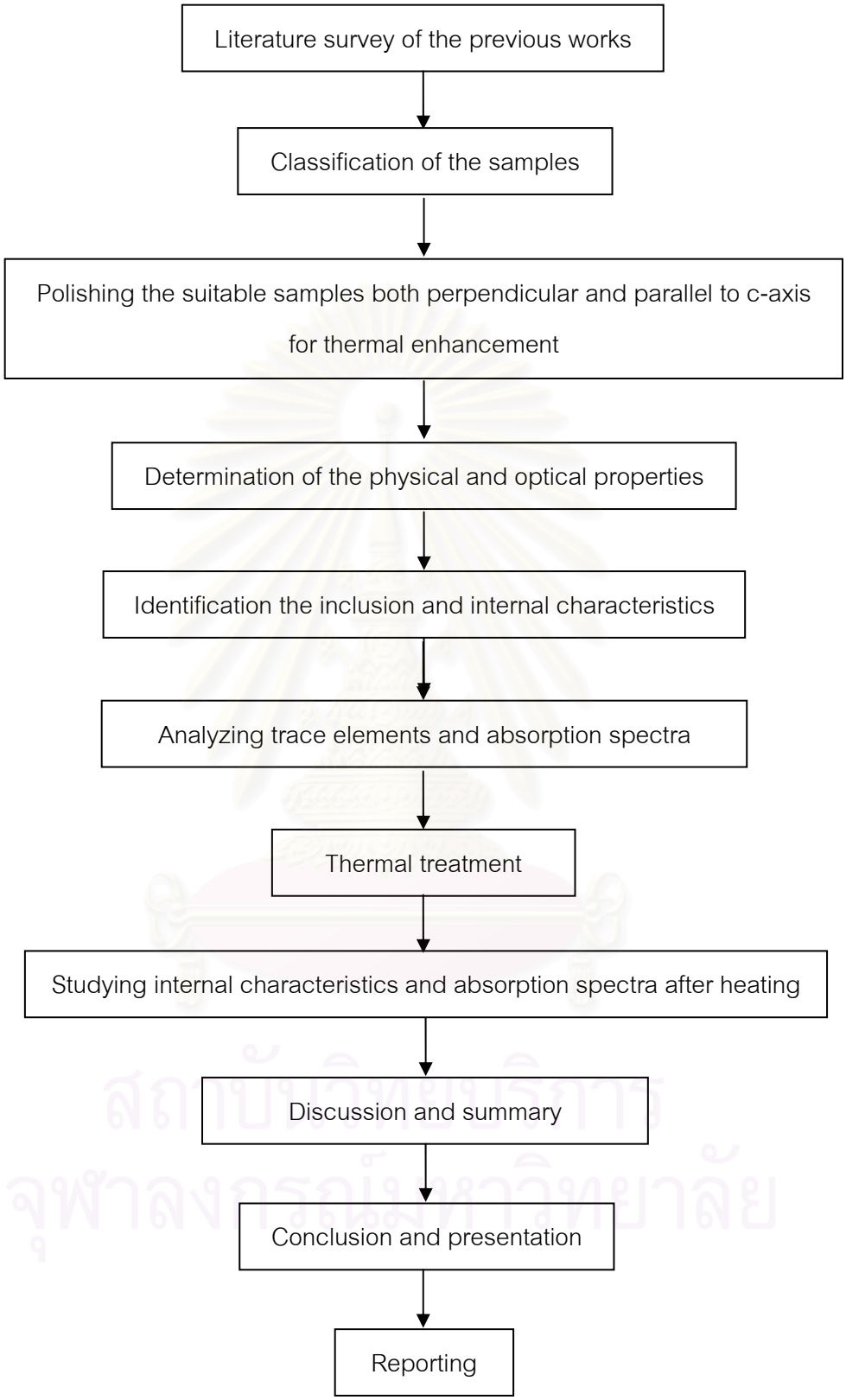

Figure 1.1 Diagram of method of study

12. Quantitative analyzes of trace element contents (total Fe_2O_3, TiO_2, Cr_2O_3, V_2O_3, Ga_2O_3, MgO, MnO and SiO_2) by Electron Probe Micro-Analyzer (EPMA) at Center of Gemstone Research, University of Meinz, Germany,

13. Discussion and summary,

14. Thesis reporting

สถาบันวิทยบริการ
จุฬาลงกรณ์มหาวิทยาลัย

CHAPTER II

GEOLOGY

Locality and access

Ilakaka-Sakaraha deposit is located about 210 kilometers northeast of Tulear in the southwestern Madagascar. It extends from the south of the Isalo National Park near the town of Sakahara (Sakaraha) up to Ilakaka (Figure 2.1) (Milisenda and others, 2001). Accessing to this area can be done on a pave road from Tulear to Ilakaka for 3 hours. The climate is 11 hot and dry months of the year with torrential rains a few days in each summer (between November and March). The average temperature is 26^{O}C (Gem Mining Resources, 2002).

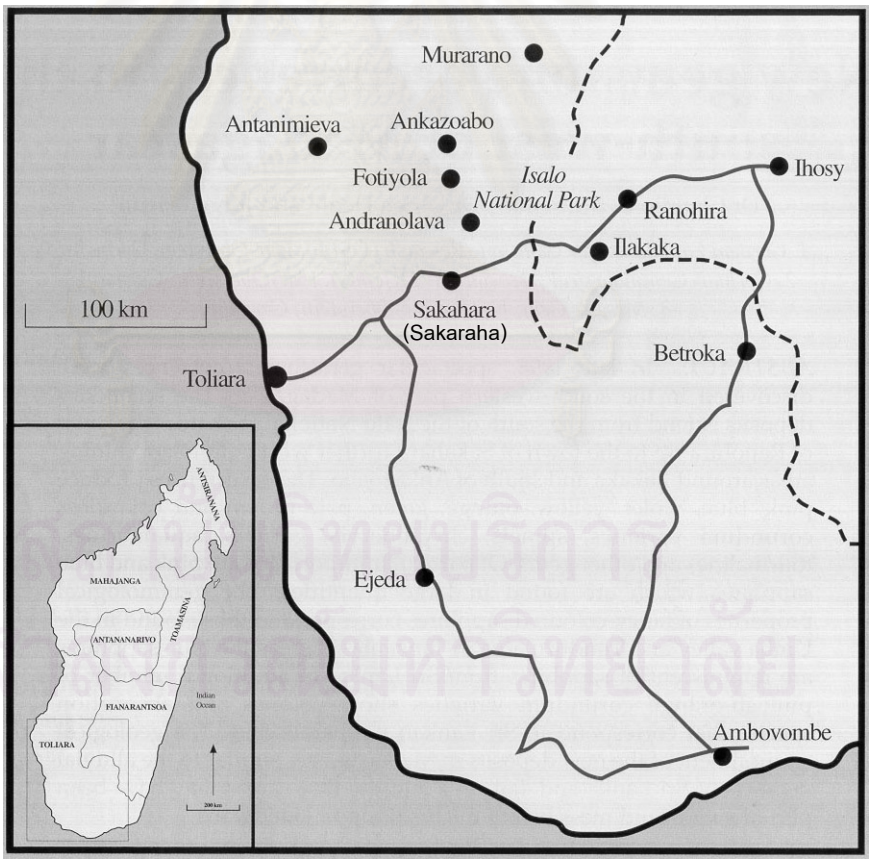

Figure 2.1 Location map of Ilakaka-Sakaraha area, southwestern Madagascar (Milisenda and others, 2001)

Regional Geology

Madagascar is the world's fourth largest island. It extends over 600,000 square kilometers. It separated from the mainland of Africa and drifted about 400 kilometers east into the Indian Ocean. The geology of Madagascar is closely related to the geological evolution of East Africa. Southern Madagascar is characterized by Precambrian basement rocks, which mainly consist of medium to high grade metamorphosed gneisses and metasediments. These rocks represent terrains of continental sediments, which were accumulated and primarily metamorphosed in Archean age about 2,600 million years (Ma) ago (Kiefert and others, 1996). In a reconstruction of the Gondwana supercontinent, the high grade rocks of Madagascar formed the eastern part of the Mozambique belt, which was regarded as a collision structure resulting from collision of East Gondwana (India-Antarctica-Australia) and West Gondwana (Africa-South America) some 600 Ma ago (Milisenda and others, 2001).

The Ilakaka-Sakaraha deposit is located within the Morandava basin. The sedimentary Morandava basin of western and southwestern Madagascar form part of a larger basin which finds its continuation on the East African continent. The sediments in this basin were deposited from Carboniferous (about 345 Ma ago) to the Tertiary (less than 60 Ma ago). The separation of the basin was due to the break of Gondwana and continental drifting some 165 Ma ago. In Africa, the thick continental succession of rocks ranging in age from Upper Carboniferous to Lower Jurassic is commonly defined as Karroo. This Karroo Supergroup can be subdivided into three groups as follows: (Milisenda and others, 2001)

1. The Sakoa Group is the base unit and Carboniferous to Middle Triassic in age with predominantly sandstone and argillitic layers as well as coal beds.

2. The Sakamena Group is Upper Permian to Middle Triassic age with alternating argillitic and sandstone layers.

3. The Isalo Group is Upper Triassic to Upper Jurassic and consisting of alternating sandstone and red argillitic layers. Ilakaka gems are recovered from Isalo Group sediments which were deposited about 200 Ma ago.

According to Radelli (1975), Sakoa and Sakamena Groups are marine and continental sediments in respective Middle to Lower Permian and Upper Permian to Lower Triassic age. The Isalo Group is Middle Triassic to Liassic (Jurassic) in age and includes 2 formations as Isalo I and Isalo II. The Isalo I formation consists chiefly of piedmont deposits, including stream deposits. They are coarse, generally crossbedded, poorly consolidated feldspathic sandstone, but some salt-bearing terrain indicates local evaporitic conditions. The Isalo II formation differs from the Isalo I in that it contains not only sandstone but also several red claystone deposits. The sandstones are light and generally less coarse than Isalo I. There are also several small evaporitic deposits. Locally brown-coal deposits are present. The generalized geologic map of southwestern Madagascar is showed in Figure 2.2.

Gem Mining Resources (2002) reported that sapphires and associated minerals in the deposits from the Ranohira, Ilakaka, Bezaha and Sakaraha regions are alluvium type. They consist mainly of secondary deposits. The sapphires (blue, violet, pink and translucent) and accompanying minerals (zircon, spinel, garnet, topaz and chrysoberyl) were found in the upper and lower terraces. The layer, commonly known as “lalambato” in the region, is a layer of stones of many different sizes mixed with various rock types and medium grain sand. All this is imbedded in clayey mixture made up primarily of calcareous limestone deposits of a yellowish, whitish and locally light gray color. The minerals are mostly concentrated below the layers consisting of blocks of rock. These layers containing the minerals are distributed, and various thickness and density. There are 2 containing mineral layers, which are separated by clayey sand. The upper layer, which can be seen on the surface, contains lesser quality and quantity minerals than lower layer. Sometimes there is only one layer enriched with minerals. These single layers are much less interesting for mechanized mining when they were thin (20-50 centimeters) and shallow layers.

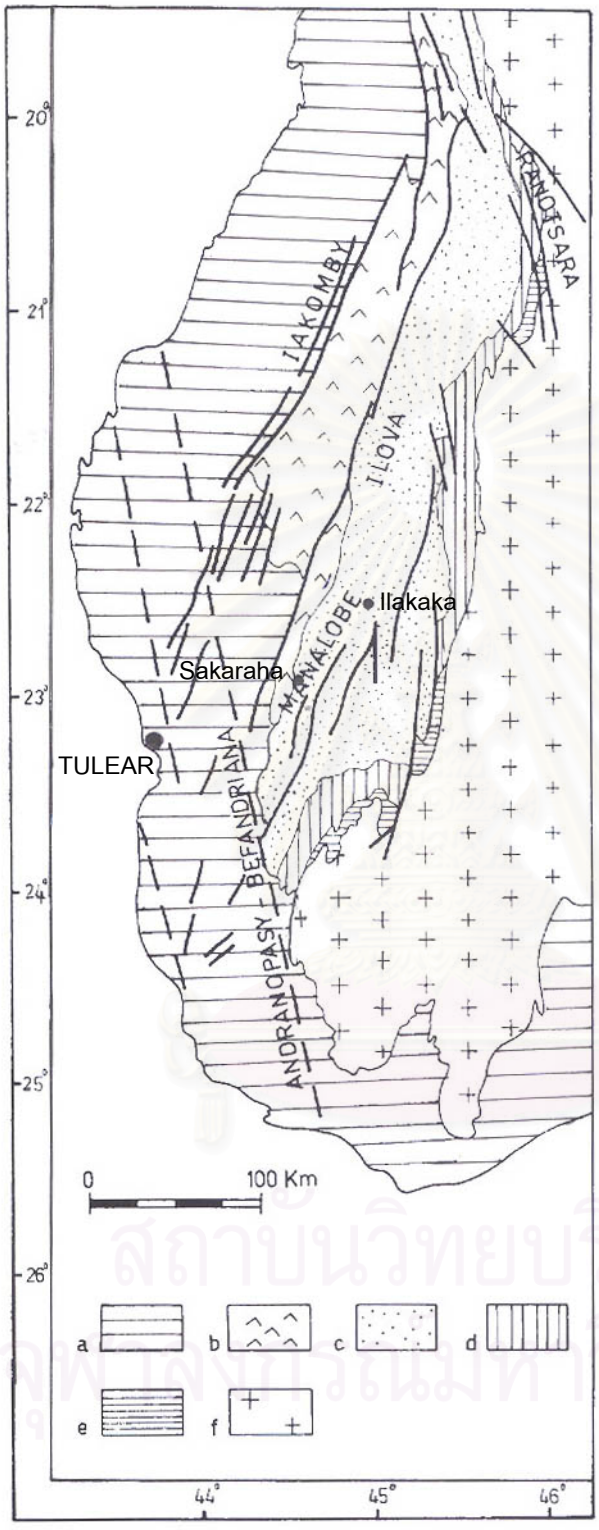

EXPLANATION

a : marine Liassic (Jurassic) to Tertiary

b : marine Liassic and mixed facies Dogger (Sakaraha Group)

c : continental Middle Triassic and Liassic (Isalo Group)

d : Upper Permian to Lower Triassic (Sakamena Group)

e : Lower to Middle Permian (Sakoa Group)

f : Precambrian crystalline basement

Figure 2.2 Generalized geologic map of southwestern Madagascar (Radelli, 1975)

According to Hansawak (2001), Ilakaka-Sakaraha sapphires are found as secondary deposits in alluvial plain and river terrace (Figure 2.3). The paydirt thickness averages from 0.5 to 1.5 meters or 3-5 meters in some places, and is overlain by sediments (0.5-5.0 meters thick and in some places up to 21 meters thick). The bedrock underlying the paydirt is Triassic sandstone.

Mining and production

Milisenda and others (2001) reported that three main areas have been mined in the Ilakaka-Sakaraha deposit since summer 1999. The first region included a 90x20 kms wide belt between Ranohira and Sakaraha (Sakahara). Intensive mining takes place around the village of Ilakaka which is now well-known for the blue sapphire production. A second important mining area covers a 30x20 kms wide zone around Fotiyola and Andranolava, north of Sakaraha with interesting occurrences of pink sapphires. Third area sites around Murarano which has rich deposits of blue and pink sapphires. Mining is controlled by the Ministry of Mines and hundreds of claims have been conferred, each measuring approximately 2.4x4 kms. As reported by Gem Mining Resources (2002), there were an estimated 300,000 hand-miners in the Ilakaka area working in the field during that time. The gem gravels were excavated by using simple hand tools from numerous pits. Some hand-miners dig up to 15 meters below the surface (Figure 2.4). Gems were separated from gravels by washing in nearby streams (Figure 2.5). In September 1999 a mining test in real field condition was began by EGT, the construction company of the Tatienne group of companies, provided some earth moving equipment and a washing plant was acquired on the spot. Mining on this parcel was located at $N^{O}17$, permit $N^{O}H56\text{-}98\text{-}47/E$ III (about 10 kilometers north of Ilakaka, see Figure 2.6) and chosen by a GMRC (Gem Mining Resources Corporation) geologist. The mine operated from early November 1999 to late December 1999 (Figure 2.7). The production was reported between November 5th, 1999 and December 23rd, 1999. During the 38 days of production, approximately 43,000 grams of gemstones were accumulated. The total production consisted of 96% sapphire which were 58% pink

Figure 2.3 Alluvial gemstone deposit at Ilakaka (Milisenda and others, 2001).

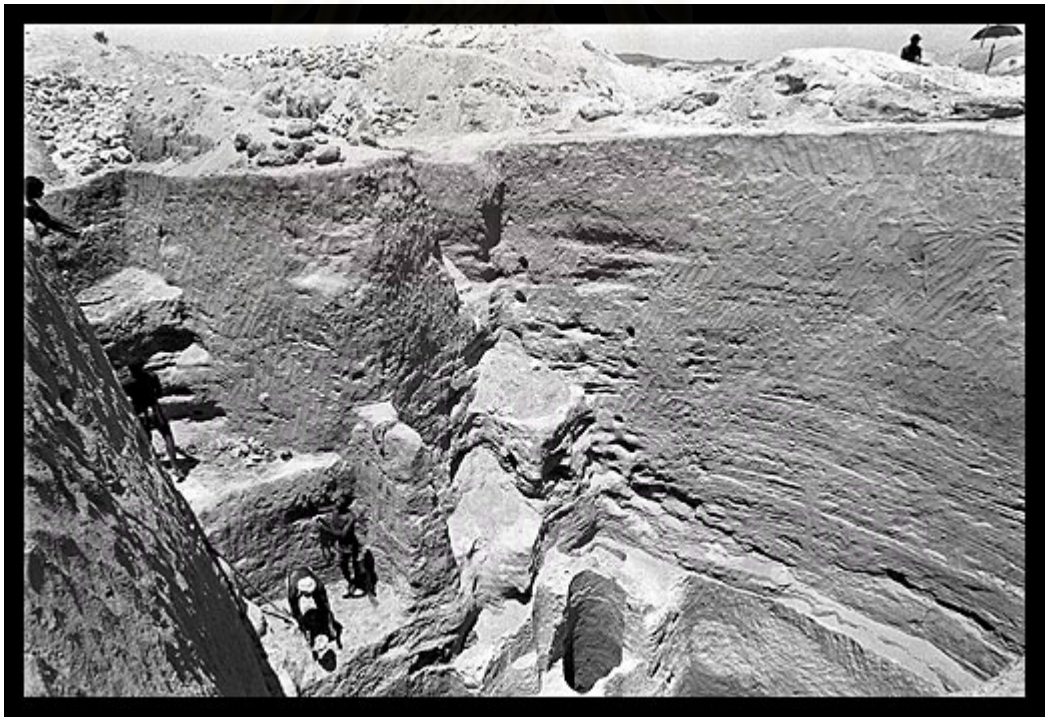

Figure 2.4 Hand-miner digging at Ilakaka. During the digging for sapphire, sometimes a hole collapses. Since 1998 approximately 900 diggers died during their dangerous work (Doomernik, 2001).

sapphire (composition of light to dark pink, light to dark purple and red), 30% light to dark blue sapphire, 8% other colors of sapphire (yellow, padparadscha and color change). The others were semi-precious stones, volcanic glass and ruby.

Figure 2.5 Washing the gravels in a nearby stream (Left: Doomernik, 2001 and Right: Milisenda and others, 2001)

Figures 2.6 Overview of the whole of the GMRC test mine. The Isalo mountain range is in the background (Gem Mining Resources, 2002).

Figure 2.7 Showing the mining operation by heavy machine at the GMRC test mine: Scrapers remove overburden. The sapphire-bearing paydirt is loaded onto the trucks and sent to the mechanised processing plant (Gem Mining Resources, 2002).

จุฬาลงกรณ์มหาวิทยาลัย

CHAPTER III

PHYSICAL AND OPTICAL PROPERTIES

Visual appearance and Crystal habits

Altogether 275 rough samples of corundum from Ilakaka-Sakaraha area were initially acquired for this study. They were a mixture of many hue and tone, such as very dark to very light blue, colorless, orangey yellow, yellowish green, violet, purple, pinkish purple, purplish pink and orangey pink. Some colorless and green sapphires contain blue patches. Almost all the stones are transparent and vitreous luster. Their sizes vary from 3 to 8 millimeters and weights are from 0.5 to 3.0 carats. The samples are mostly water-worn crystals and irregular in shape (anhedral crystal) but some samples show recognizable crystal form. Their habits are barrel-shaped crystal, hexagonal prism, pyramid, tabular and bipyramid crystals (Figure 3.1). Rhombohedral crystals are very rare.

Classification and Preparation

The rough sapphires were classified into 7 groups based on the color shade observed under the day light lamp as follows:

1. Pink group: Pink sapphires were devided into 4 types as follows:
   - 1.1 Purplish pink sapphires
   - 1.2 Light purplish pink sapphires
   - 1.3 Light orangey pink sapphires
   - 1.4 Orangey pink sapphires

2. Blue group: Blue sapphires were devided into 7 types as follows:
   - 2.1 Very dark blue sapphires
   - 2.2 Dark blue sapphires (with and without color-change effects)
   - 2.3 Medium blue sapphires (with and without color-change effects)
   - 2.4 Light blue sapphires (with and without color-change effects)
   - 2.5 Very light blue sapphires
   - 2.6 Extremely light blue sapphires
   - 2.7 Light greenish blue sapphires

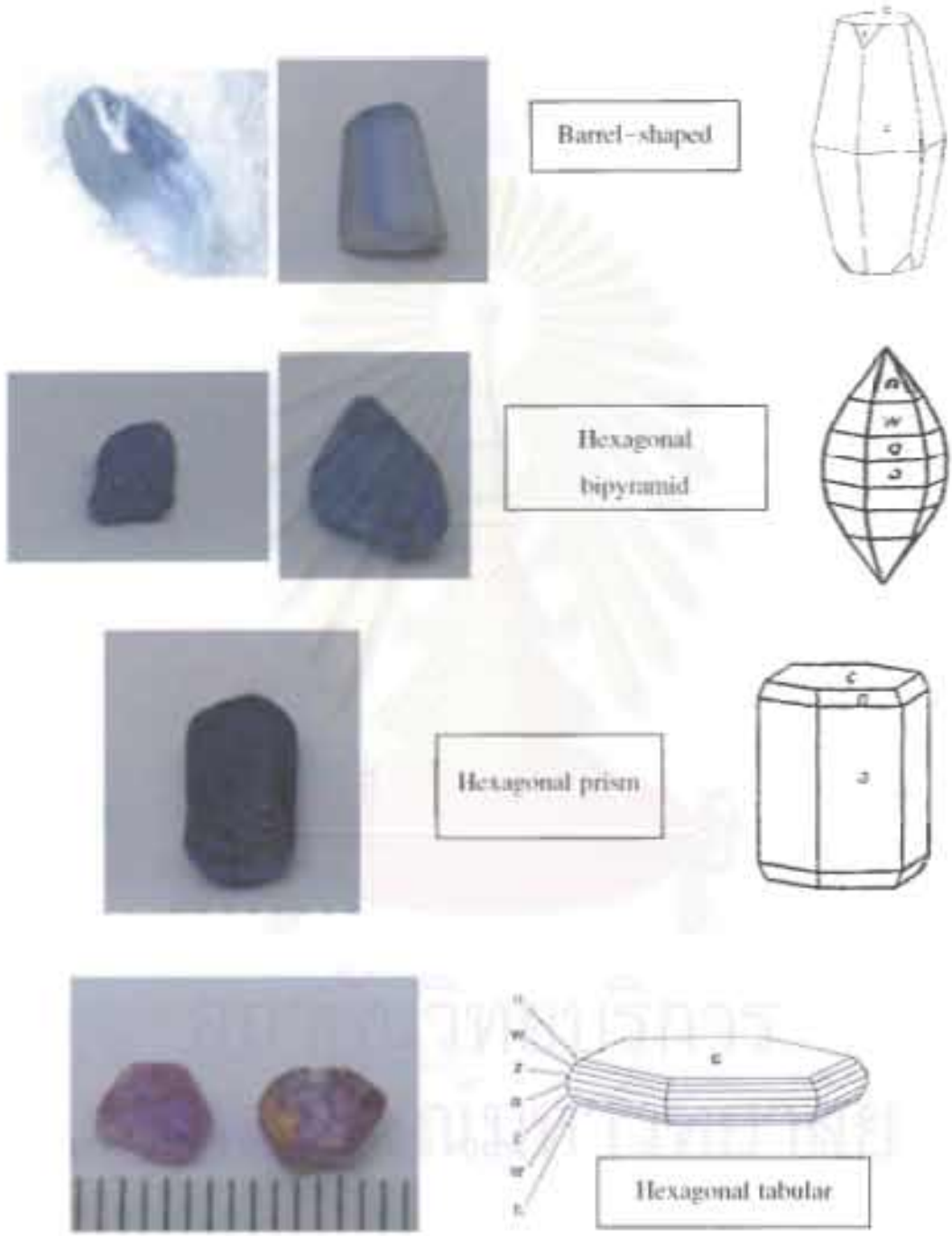

Figure 3.1 Crystal habits observed in Ilakaka-Sakaraha sapphires.

3. **Violet group**: Violet sapphires were devided into 3 types as follows:

   3.1 Dark violet sapphires (with color-change effects).

   3.2 Medium violet sapphires (with and without color-change effects).

   3.3 Light violet sapphires

4. **Purple group**: Purple sapphires were devided into 3 types as follows:

   4.1 Purple sapphires

   4.2 Pinkish purple sapphires

   4.3 Brownish purple sapphires

5. **Colorless group**: Colorless sapphires were devided into 4 types as follows:

   5.1 Colorless sapphires

   5.2 Very light bluish sapphires

   5.3 Very light yellowish sapphires

   5.4 Colorless sapphires with blue patch

6. **Yellow group**: Orangey yellow and light yellow sapphires

7. **Green group**: Light yellowish green and medium green sapphires with blue patched

Out of 275 rough stones, 123 samples were selected for cutting and polishing into flat surface perpendicular and parallel to the c-axis (Figures 3.2 to 3.9). They were used for measurement of gemological properties. Only 44 pink, purple and medium violet sapphires were selected for detailed study.

Physical and Optical properties

Almost all groups of sapphires, except light greenish blue, very light yellowish and colorless sapphires with blue patch, were examined for their gemological properties, such as specific gravity (SG), refractive index (RI), birefringence, and fluorescence (see Table I.1 in Appendix I for all the details). The result of this study (see Table 3.1 for the summary) shows that the basic gemological properties of

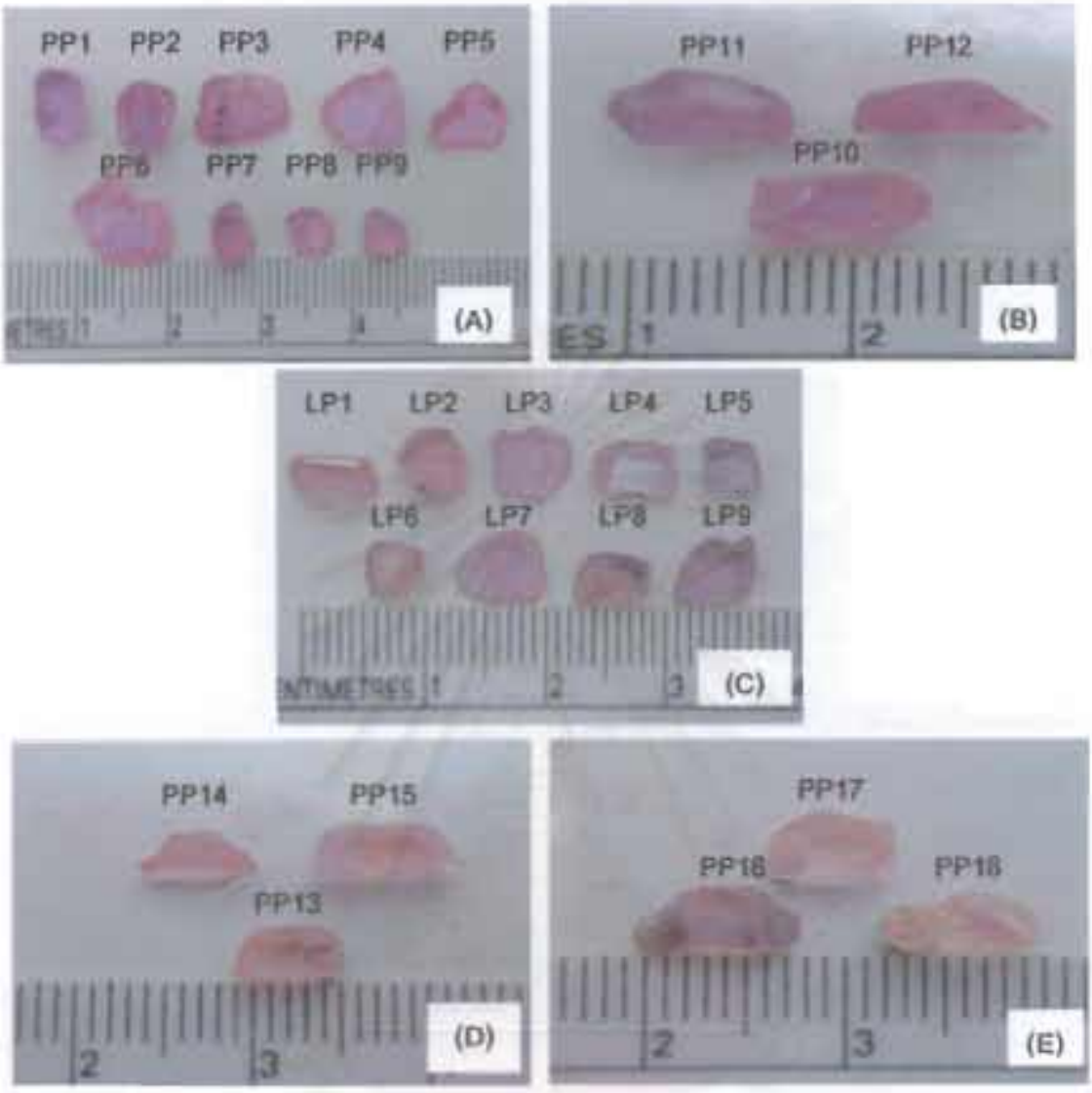

Figure 3.2 Showing 4 types of polished pink sapphires

(A-B) purplish pink; (C) light purplish pink; (D) light orangey pink;

(E) orangey pink

all sapphire groups fall into a normal range of corundum. It should be noted that most pink, violet and purple sapphires show moderate to strong fluorescence in pink to orange color under LWUV which suggest that they may belong to a low iron suit of probably metamorphic-type origin rather than the high iron suit of basaltic-type origin (see other supporting evidence in later section).

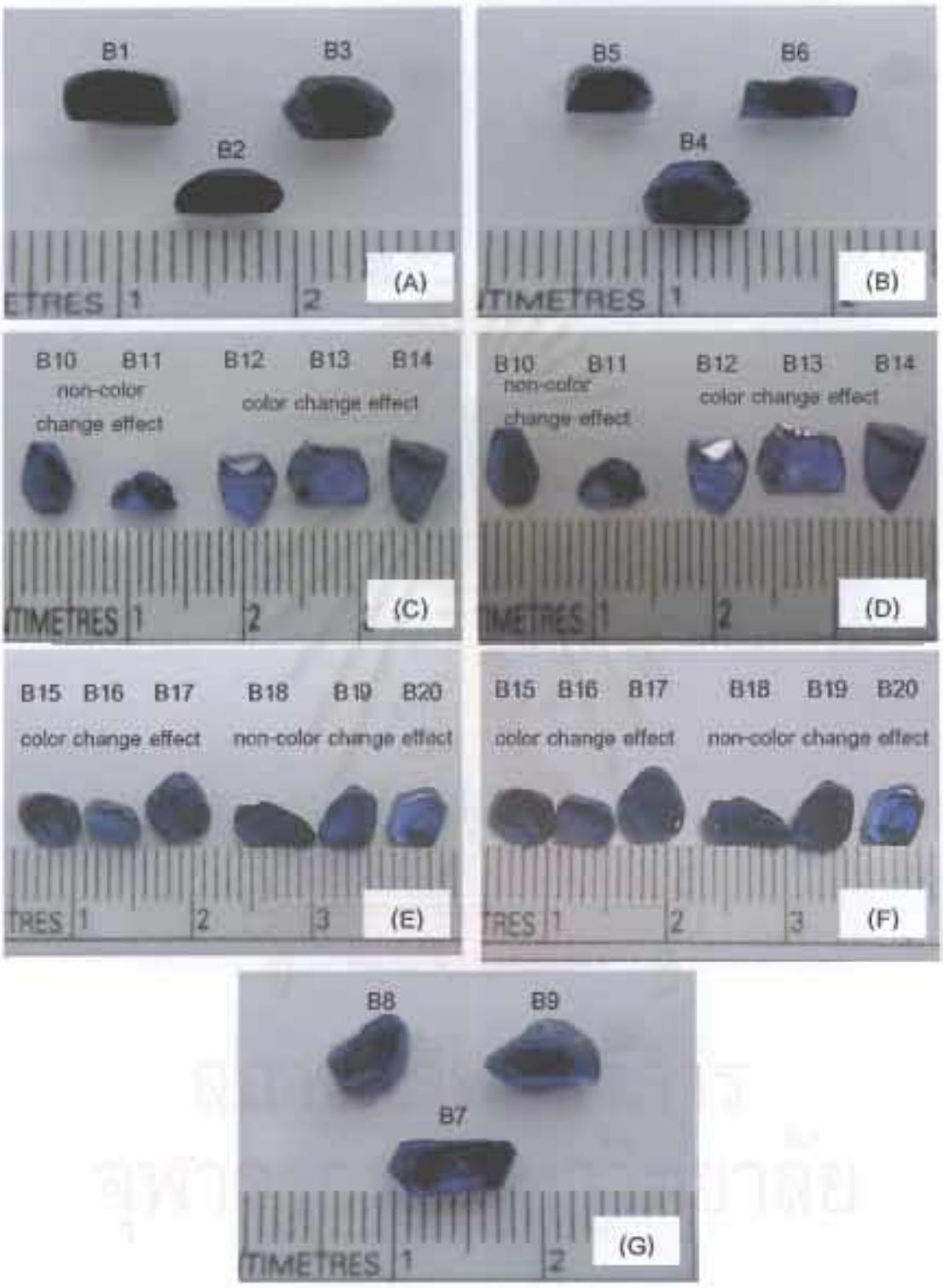

Figure 3.3 Showing 3 types of polished blue sapphires

(A) very dark blue; (B) dark blue; (C), (E) and (G) medium blue observed under the day light lamp; (D) and (F) medium blue observed under the tungsten lamp

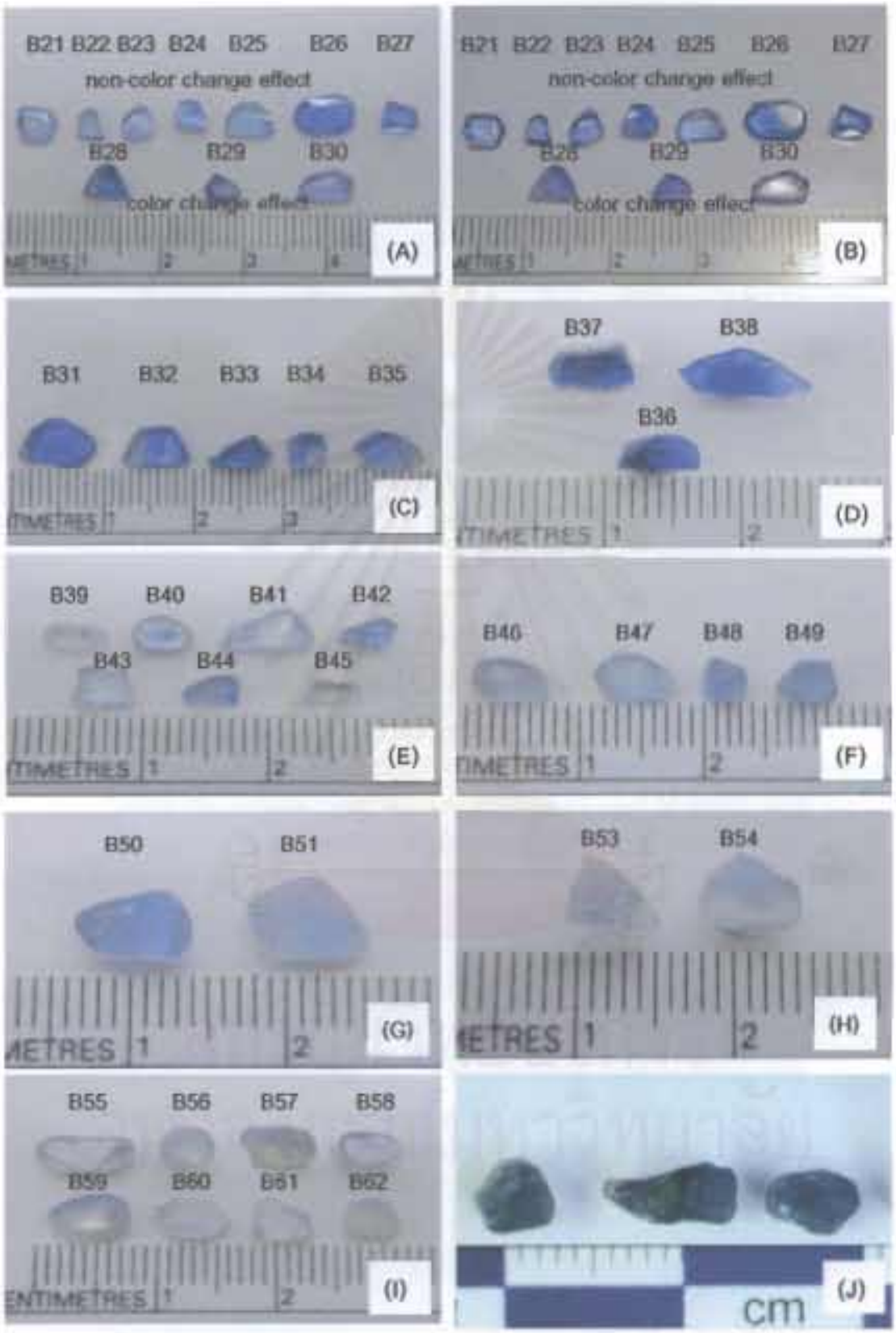

Figure 3.4 **Showing 4 types of blue sapphires**

(A), (C) and (D) light blue observed under the day light lamp; (B) light blue observed under the tungsten lamp; (E)-(G) very light blue; (H)-(I) extremely light blue; (J) light greenish blue

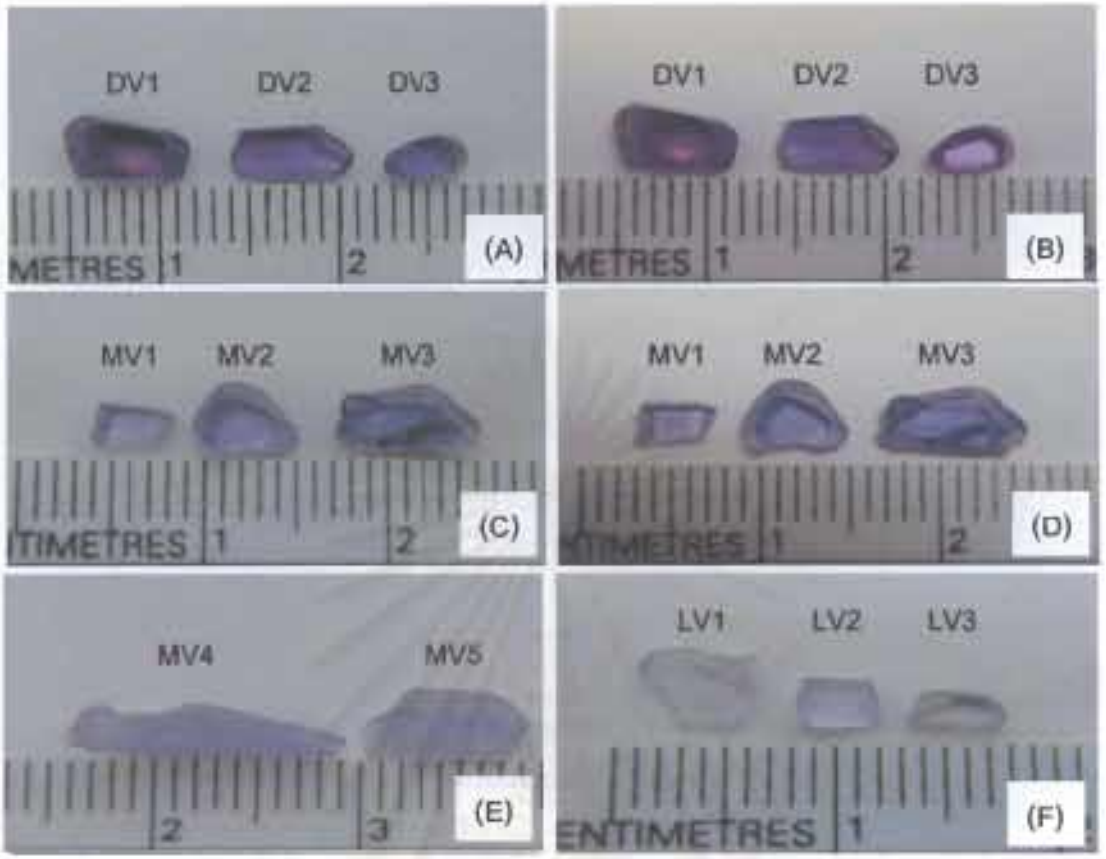

Figure 3.5 Showing 3 types of polished violet sapphires

(A) dark violet observed under the day light lamp; (B) dark violet observed under the tungsten lamp; (C) and (E) medium violet observed under the day light lamp; (D) medium violet observed under the tungsten lamp; (F) light violet

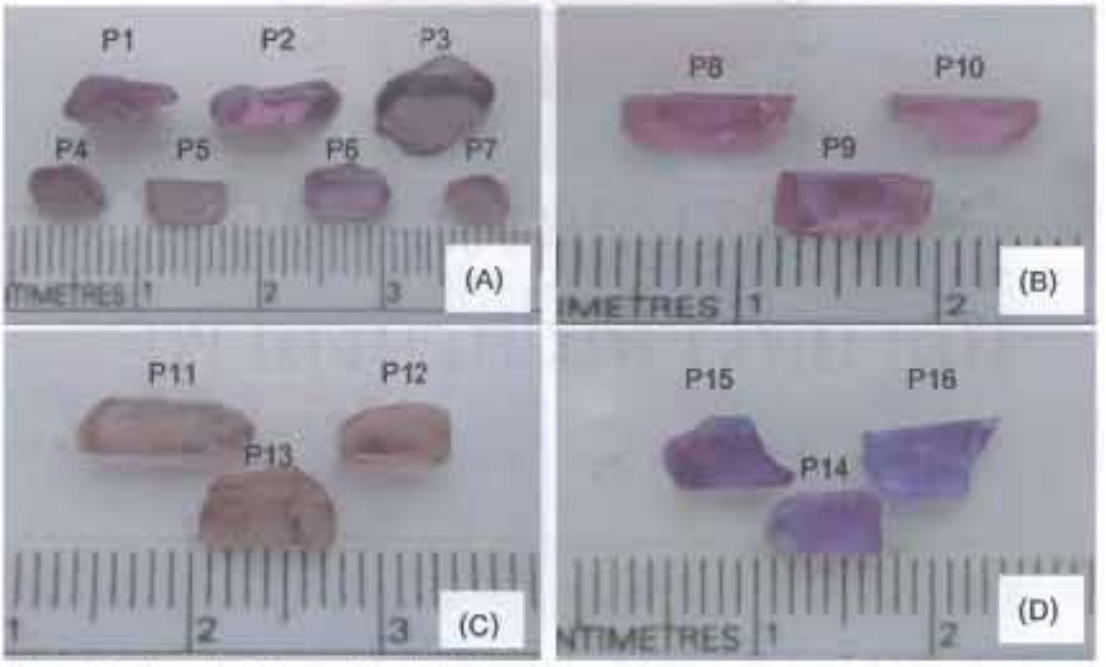

Figure 3.6 Showing 3 types of polished purple sapphires

(A)-(B) pinkish purple; (C) brownish purple; (D) purple

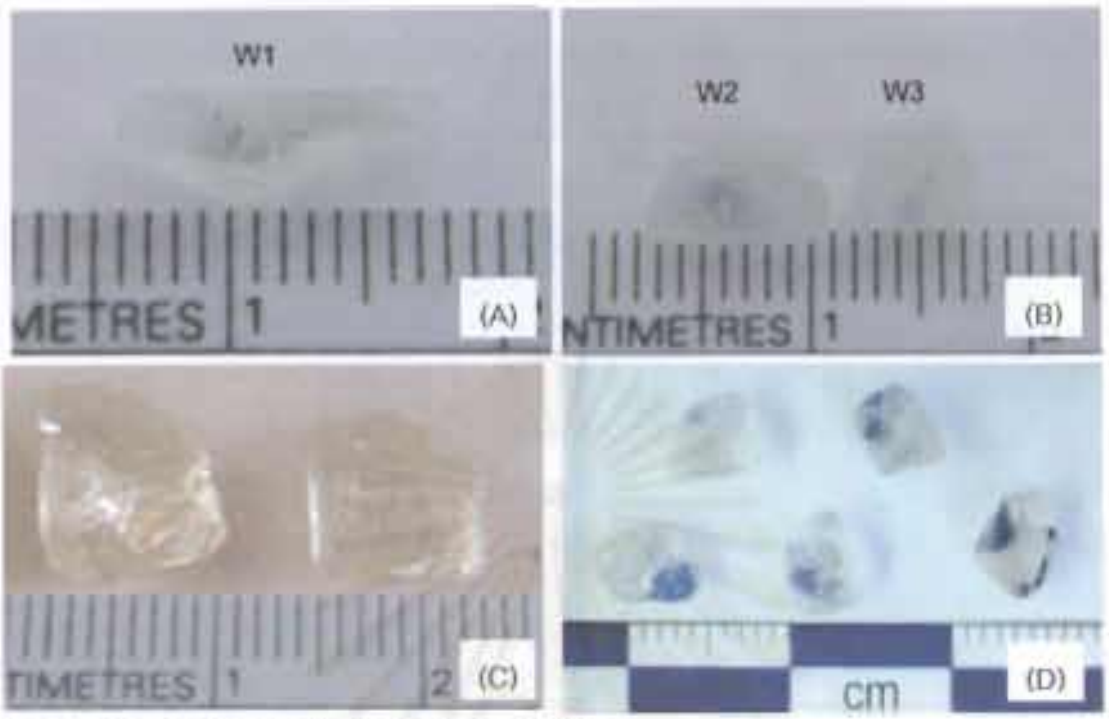

Figure 3.7 Showing 4 types of colorless sapphires
(A) colorless; (B) very light bluish; (C) very light yellowish;
(D) colorless with blue patch

Figure 3.8 Showing 2 types of yellow sapphires; orangey yellow (left) and light yellow (right)

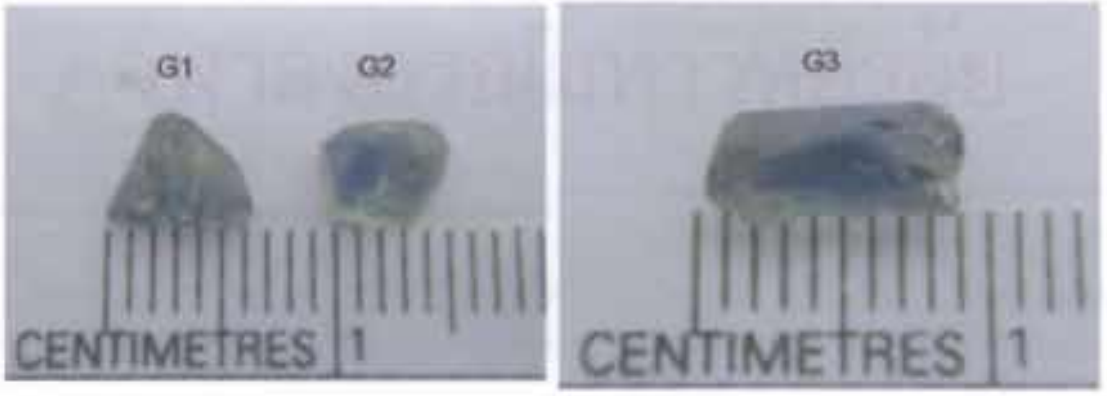

Figure 3.9 Showing 2 types of green sapphires; light yellowish green (left) and medium green with blue patch (right)

Table 3.1 Summary of the gemological properties of some Ilakaka-Sakaraha sapphires.

Type	SG	RI		birefringence	fluorescence	
		n_o	n_e		SWUV	LWUV
Pink group						
Purplish pink (PP1-PP12)	3.94-3.99	1.768-1.769	1.760	0.008-0.009	inert-very weak pink	moderate–strong pink
Light purplish pink (LP1-LP9)	3.92-3.99	1.768-1.770	1.760-1.762	0.008	inert	weak–moderate pink
Light orangey pink (PP13-PP15)	3.98-4.01	1.768	1.760	0.008	very weak-weak pink	strong orange-pinkish orange
Orangey pink (PP16-PP18)	4.00-4.01	1.768-1.772	1.760-1.764	0.008	inert-weak pink	very weak pink-strong orange
Blue group						
Very dark blue (B1-B3)	3.97-3.99	1.768	1.760	0.008	inert	inert
Dark blue without color-change (B4-B5)	3.93-3.99	1.768	1.760	0.008	inert	inert
Dark blue with color-change (B6)	3.97	1.770	1.762	0.008	inert	very weak reddish orange
Medium blue without color-change (B7, B9, B10, B12, B18-B20)	3.94-4.04	1.768-1.770	1.760-1.761	0.008-0.009	inert	inert
Medium blue with color-change (B8, B11, B13-B17)	3.92-4.04	1.768-1.770	1.760-1.761	0.008-0.009	inert	weak-moderate reddish orange

Table 3.1 Summary of the gemological properties of some Ilakaka-Sakaraha sapphires (continued).

Type	SG	RI		birefringence	fluorescence	
		n_o	n_e		SWUV	LWUV
Light blue without color-change (B21-B27, B31-B35, B37-B38)	3.92-4.04	1.768-1.770	1.760-1.761	0.008-0.009	inert	inert-very weak reddish orange
Light blue with color-change (B28-B30, B36)	3.96-4.01	1.768-1.770	1.760	0.008-0.010	inert	weak-moderate reddish orange
Very light blue (B39-B52)	3.91-4.02	1.768-1.769	1.760	0.008-0.009	inert	inert–moderate reddish orange
Extremely light blue (B53-B62)	3.94-4.00	1.768-1.769	1.760	0.008-0.009	inert	inert–moderate orange
Violet group						
Dark violet with color-change (DV1-DV3)	3.95-3.99	1.769-1.770	1.760-1.761	0.008-0.010	inert	moderate orange
Medium violet without color-change (MV4-MV6)	3.94-3.99	1.768	1.760	0.008	very very weak-very weak orange	weak reddish orange-moderate pinkish orange
Medium violet with color-change (MV1-MV3)	3.94-4.02	1.769-1.770	1.760-1.762	0.008-0.010	inert	inert-moderate pinkish orange
Light violet (LV1-LV3)	3.91-3.96	1.769-1.771	1.760-1.761	0.009-0.010	inert	weak-moderate pinkish orange
Purple group						
Pinkish purple (P1-P10)	3.96-4.02	1.768-1.770	1.760-1.762	0.008-0.009	inert-very weak pink	weak–strong pink

Table 3.1 Summary of the gemological properties of some Ilakaka-Sakaraha sapphires (continued).

Type	SG	RI		birefringence	fluorescence	
		n_o	n_e		SWUV	LWUV
Brownish purple (P11-P13)	3.96-3.99	1.770	1.762	0.008	inert	very weak pink
Purple (P14-P16)	4.00-4.02	1.768	1.760	0.008	very weak pink	strong pink
Colorless group						
Colorless (W1)	4.00	1.768	1.760	0.008	inert	inert
Very light bluish (W2-W3)	4.00	1.768	1.760	0.008	inert	inert
Yellow group						
Orangey yellow (Y1)	3.99	1.768	1.760	0.008	very weak reddish orange	moderate reddish orange
Light yellow (Y2-Y4)	3.96-3.97	1.768	1.760	0.008	very weak-weak orange	moderate-strong orange
Green group						
Medium green (G1)	4.00	1.771	1.763	0.008	inert	inert
Light yellowish green (G2-G3)	3.98-4.01	1.771	1.763	0.008	inert	inert-very very weak orange

RI were measured by Krüss refractometer.

Colors of 44 unheated pink, purple and medium violet sapphires were compared with the standard gem color of Gemological Institute of America (GIA GemSets, Figures 3.10) under the day light lamp. These color comparisons are listed in Table 3.2. The color code comprises tone, saturation and hue. Hue is the pure spectral sensation. Tone is the lightness to darkness of the hue; the higher number is the darker tone (scale 0-10). Saturation is the strength and purity of the hue; the higher number is the stronger the hue (scale 1-6). For example in Table 3.2, PR/RP 4/2; hue is PR/RP (red-purple or purple-red), tone is 4 (medium light) and saturation is 2 (slightly grayish or brownish). All unheated sapphire color codes are given in the Table I.2 in Appendix I.

Figure 3.10 GIA GemSet color specimens.

Table 3.2 Color comparison of sapphires before heating by GIA GemSet.

Sample Type	GIA GemSet color specimens	
	Code	Tone, Saturation Hue
Purplish pink (PP1-PP12)	PR/RP 4/2 to PR/RP 6/4	medium light – medium dark , slightly brownish – moderately strong Purple - Red
Light purplish pink (LP1-LP9)	PR/RP 4/3	medium light, very slightly brownish Purple – Red
Light orangey pink (PP13-PP15)	RO/OR 2/3 to PR/RP 2/3 + rO 2/3	very light, very slightly brownish Orange- Red to very light, very slightly brownish Purple – Red + very light, very slightly brownish reddish Orange
Orangey pink (PP16-PP18)	RO/OR 3/2, to slpR 2/3 + rO 2/3	light, slightly brownish Orange- Red to very light, very slightly brownish slightly purplish Red + very light, very slightly brownish reddish Orange
Pinkish purple (P1-P10)	PR/RP 6/3 to PR/RP 7/4	medium dark – dark, very slightly brownish - moderately strong Purple – Red
Brownish purple (P11-P13)	PR/RP 6/3 + oR 4/3 to rP 5/3 + PR/RP 5/3	medium dark, very slightly brownish Purple – Red + medium light, very slightly brownish orangey Red to medium, very slightly brownish reddish Purple + medium, very slightly brownish Purple – Red
Purple (P14-P16)	P 4/5 to P 6/3	medium light – medium dark, very slightly brownish – strong Purple

Table 3.2 Color comparison of sapphires before heating by GIA GemSet (continued).

Sample Type	GIA GemSet color specimens	
	Code	Tone, Saturation Hue
Medium violet without color-change effect (MV4-MV5)	V 4/4 + rP 5/3 to V 4/3	medium light, moderately strong Violet + medium, very slightly brownish reddish Purple to medium light, very slightly grayish Violet
Medium violet with color-change effect (MV1-MV3)	V 4/3	medium light, very slightly grayish Violet
	*bP 4/4 to bP 6/3	*medium light – medium dark, moderately strong – very slightly grayish bluish Purple

*under tungsten lamp

Internal Characteristics

Identification of inclusions in a gemstone is of considerable importance as the inclusions yield information about genesis of gemstone. Therefore it may be with some restrictions, essential for determining genuineness (i.e. natural versus synthetic) or even the origin of a gemstone.

Much of the pink, purple and violet sapphires are rather clean. Out of 44 stones, only 16 samples (PP3, PP4, PP6, PP11, PP15, PP17, LP3, LP4, LP9, P5, P6, P10, P11, P16, MV2 and MV5) contain mineral inclusions and internal features. Some mineral inclusions were identified by the Renishaw Laser Raman spectroscope (Model 1000) at the GIT. Not all the mineral inclusions, however, were able to identify due to the depth of the inclusions. If they were too deep, the signal would be too weak for identification. So the best condition were obtained when the inclusion was exposed or closed to the surface of the sample. Williams and others (1997) summarized major Raman Shift peaks of the gemological and mineralogical materials. The Raman peaks of common inclusions in these sapphires are shown in Table 3.3. All of the internal features were

Table 3.3 Major Raman Shift peaks of the common inclusions in this study (Williams and others, 1997).

Minerals	Major Raman Shift peaks at 200-2000 cm^{-1}
Corundum	225, 363, 377-379, 380-382, 400-403, 414-417, 432, 573-576, 641-643, 746 (or 748-751), 805, 848
Fuchsite	263-264, 407, 490, 698, 704-705
Monazite	300, 395, 463-465, 514, 622-624, 974-975, 1059, 1063-1067, 1072
Muscovite	258-262, 406-408, 658, 698-700, 905-908, 1107-1111
Rutile	240-242, 444 (or 448-449), 610-613, 800
Zircon	353 (or 356, 359), 439-442, 500, 882, 977-980, 1006-1008, 1014-1017, 1054-1055, 1089-1090, 1144-1147, 1201, 1223

observed under the gemological microscopes and their photos were taken by a digital camera.

Pink sapphires

This group of sapphires contains many different species of the mineral inclusions. The most common one is zircon which typically occurs as well-formed, somewhat rounded, stubby or elongate crystals up to 80 micrometers (μm) in size. They commonly occur as single inclusion or as cluster of inclusions with or without tension disc or crack (see Figures 3.11 and 3.13). Raman spectra of zircon inclusions are shown in Figures 3.12 and 3.14. Monazite inclusion (only one crystal was found) is small and rounded shape (Figure 3.13). Raman spectrum of monazite inclusion is shown in Figure 3.15. Rutile inclusions occur as rounded, black to dark brown, short prismatic crystals (Figure 3.16). Rutile needles were found in only one sample (Figure 3.22). Raman spectrum of rutite inclusion is shown in Figure 3.17. A mica inclusion was found in only one sample as colorless hexagonal platy crystal (Figure 3.18). Raman spectrum of mica inclusion is shown in Figure 3.19. The internal features in pink sapphires are fingerprints (healed fractures) and white dust or minute particles (Figures 3.20 and 3.21).

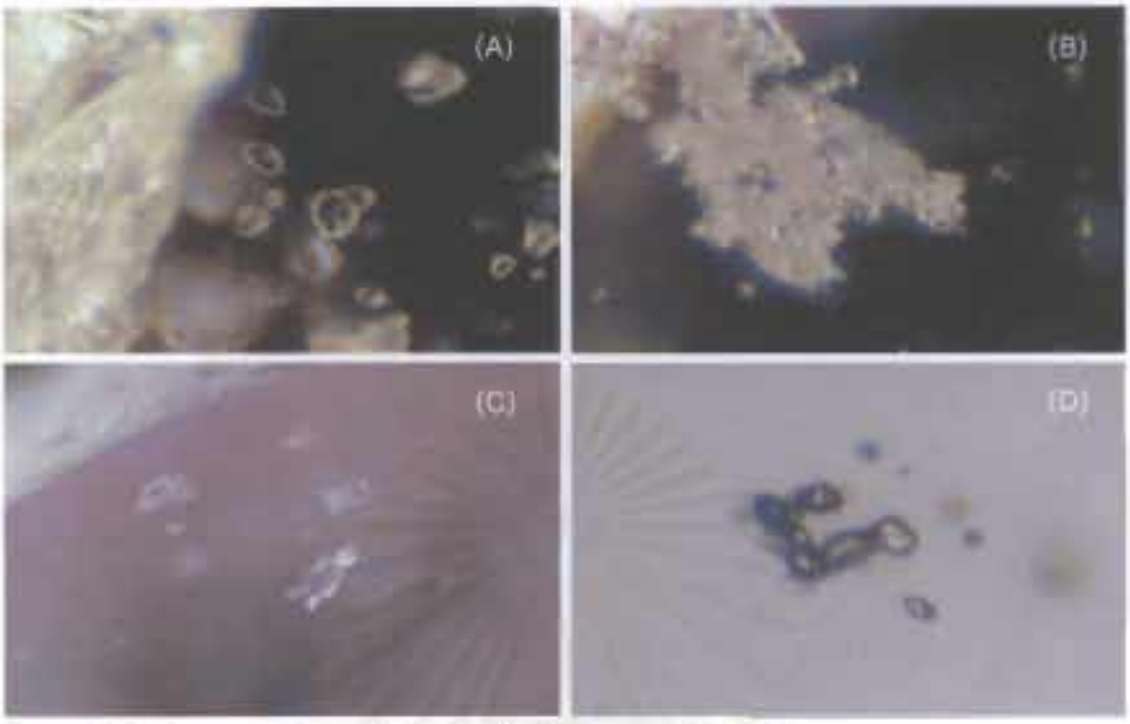

Figure 3.11 Characteristics of zircon inclusions occurring in pink sapphires:
(A) as single inclusion (sample no. LP3, 70X)
(B) as cluster of inclusions (sample no. PP8, 140X)
(C) as single inclusion with tension disc (sample no. PP15, 70X)
(D) as cluster of inclusions with tension disc (sample no. LP3, 140X)

Figure 3.12 Raman spectrum of a zircon inclusion in light purplish pink sapphire (sample no. LP3, zircon peaks at 442, 977, 1017, 1055, 1089 and 1144 cm^{-1}, corundum peaks at 225, 363, 400, 417, 576 and 750 cm^{-1})

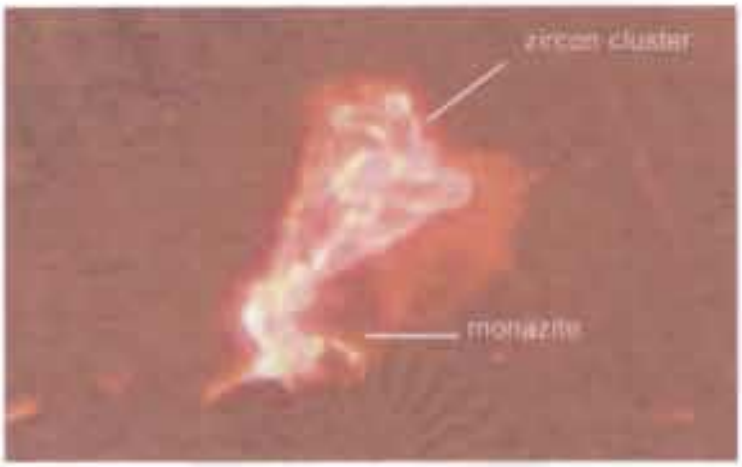

Figure 3.13 Cluster of zircon inclusions with tension disc and a monazite inclusion in purplish pink sapphire (sample no. PP4, 140X)

Figure 3.14 Raman spectrum of a zircon inclusion in purplish pink sapphire (sample no. PP4, zircon peaks at 356, 1006, 1054, 1089 and 1144 cm^{-1}, corundum peaks at 400 and 749 cm^{-1})

Figure 3.15 Raman spectrum of a monazite inclusion in purplish pink sapphire (sample no. PP4, monazite peaks at 463, 624, 975 and 1063 cm^{-1}, corundum peaks at 403, 416, and 575 cm^{-1})

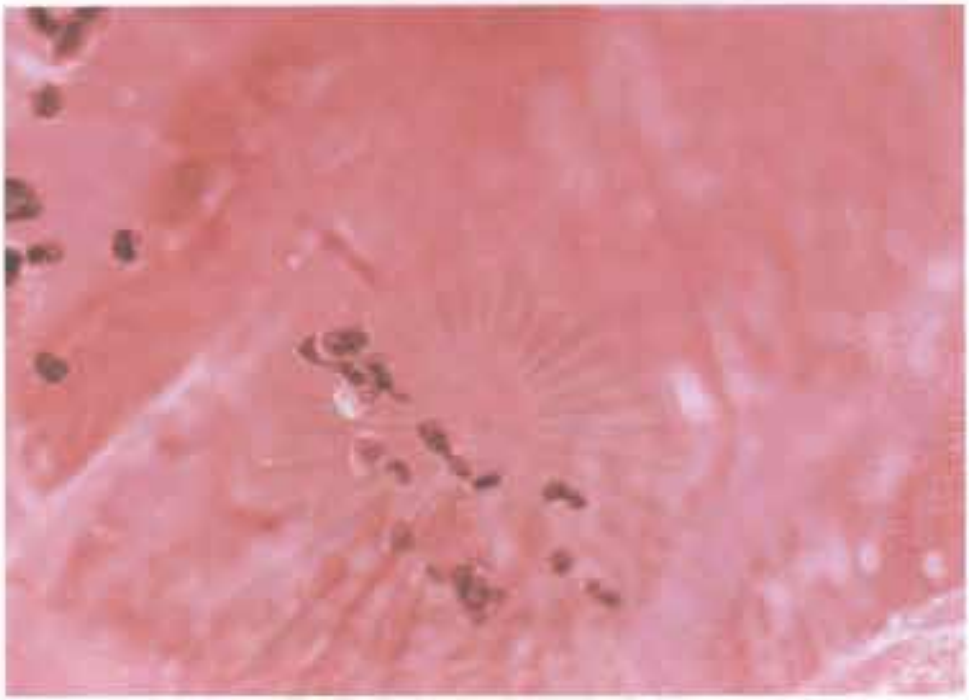

Figure 3.16 Rutile inclusions occurring in purplish pink sapphire as black to dark brown, rounded and short prismatic crystals (sample no. PP3, 30X)

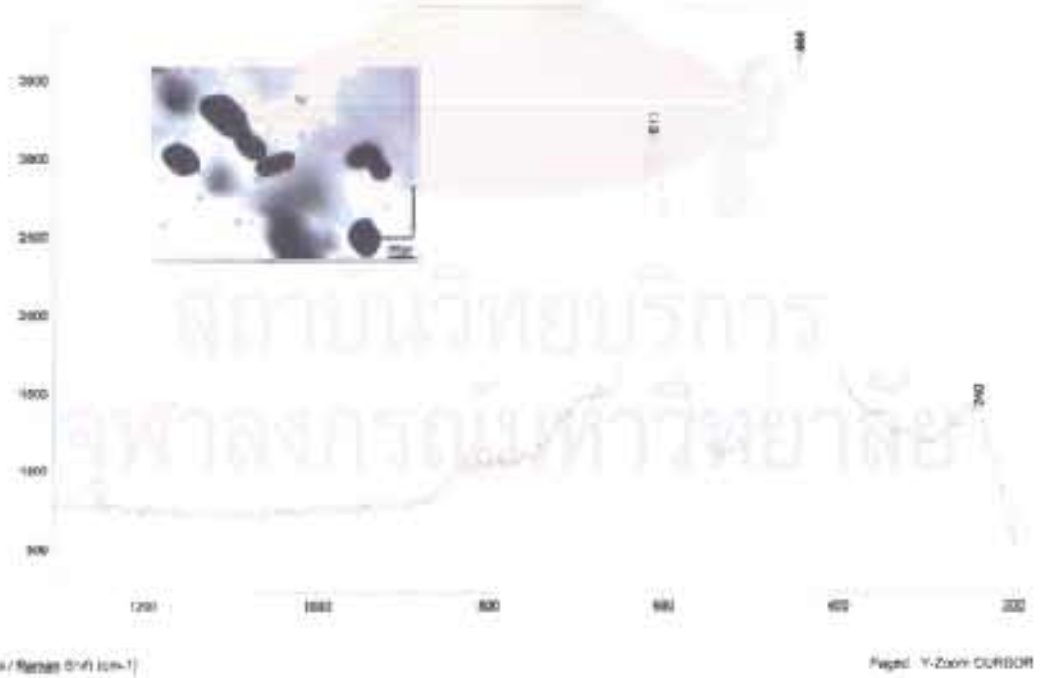

Figure 3.17 Raman spectrum of a rutile inclusion in purplish pink sapphire (sample no. PP3, rutite peaks at 240, 444 and 611 cm^{-1})

Figure 3.18 Abundant colorless zircon inclusions and a hexagonal platy mica inclusion in light purplish pink sapphire (sample no. LP3, 70X)

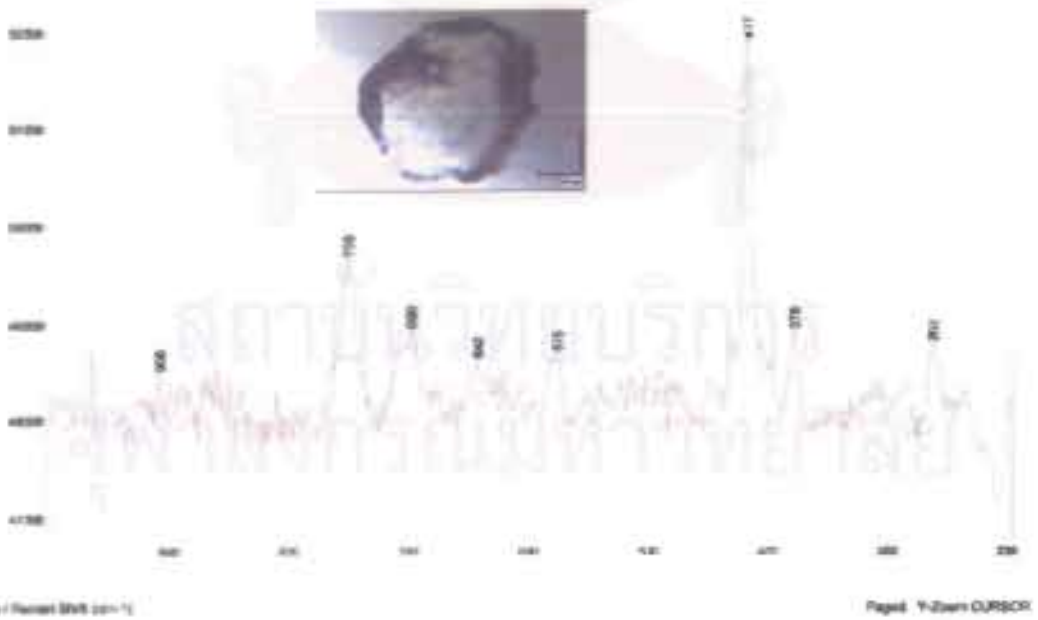

Figure 3.19 Raman spectrum of a mica inclusion in light purplish pink sapphire (sample no. LP3, mica peaks at 262, 698 and 908 cm^{-1}, corundum peaks at 378, 417, 575, 642 and 750 cm^{-1})

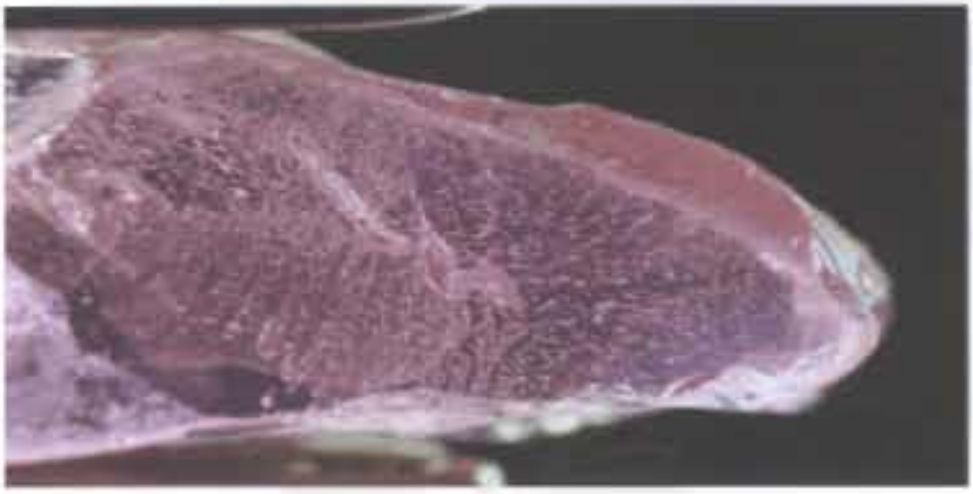

Figure 3.20 Fingerprints (healed fractures) in purplish pink sapphire (sample no. PP3,15X)

Figure 3.21 Showing the white dust or minute particles (sample no. PP3, 70X)

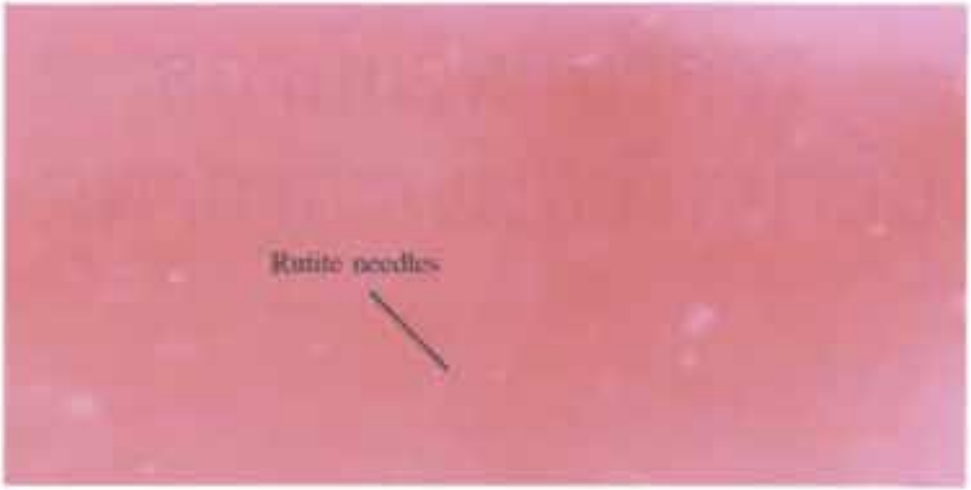

Figure 3.22 Rutile needles in purplish pink sapphire (sample no. PP3, 70X)

Purple sapphires

This group of sapphires contains similar mineral inclusions and internal characteristics as those in pink sapphires. Again, zircon inclusions are very common and typically show single inclusion and cluster of inclusions occasionally with tension disc (Figure 3.23). Raman spectrum of zircon inclusion is shown in Figure 3.24. Mica inclusions were found as colorless pseudohexagonal platy crystal (Figure 3.25) and green anhedral platy crystal of fuchsite (Figure 3.27). Raman spectra of colorless mica and fuchsite inclusions are shown in Figures 3.26 and 3.27. Monazite inclusions occur as white rounded crystals (Figure 3.28). Raman spectrum of a monazite inclusion is shown in Figure 3.29. It should be noticed that there is no color zone in pink and purple sapphires.

Medium violet sapphires

The internal features observed in medium violet sapphires are healed fractures or fingerprints, rutile needles oriented 3 directions and intersecting at $60^{\circ}/120^{\circ}$ angles, and white dust or minute particles that appear milky (Figures 3.30 to 3.32).

สถาบันวิทยบริการ
จุฬาลงกรณ์มหาวิทยาลัย

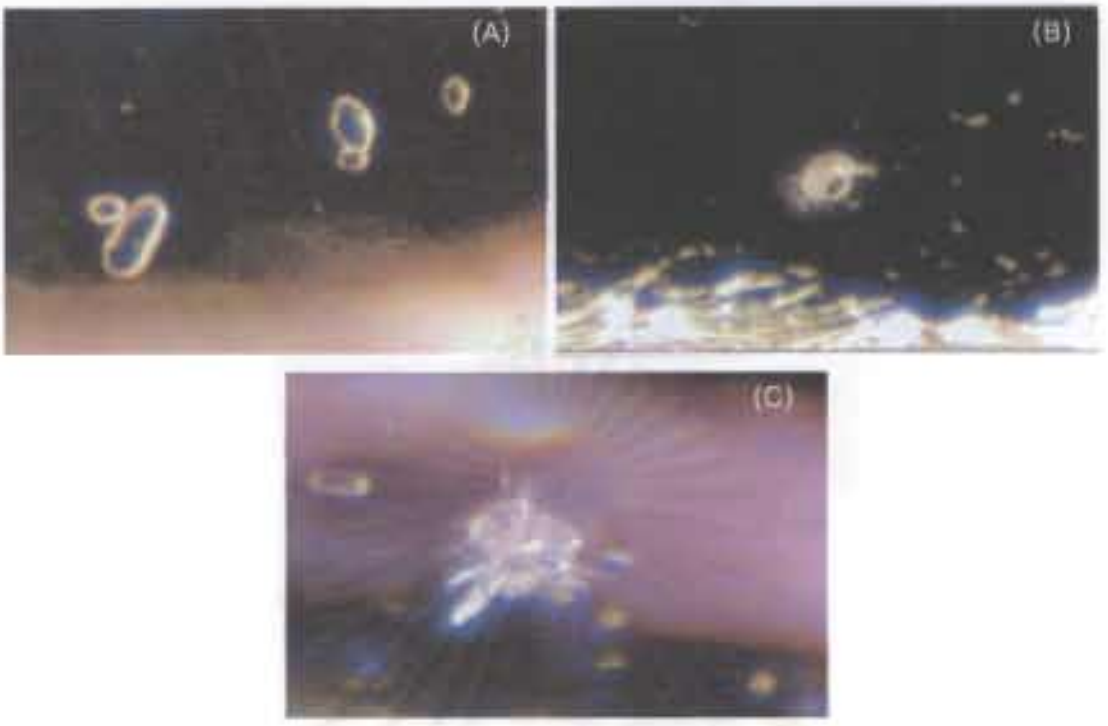

Figure 3.23 Zircon inclusions occurring in purple sapphires as

(A) single crystal (sample no. P16, 140X)

(B) single crystal with tension disc (sample no. P5, 70X)

(C) crystal cluster with tension disc (sample no. P5, 140X)

Figure 3.24 Raman spectrum of a zircon inclusion in purple sapphire (sample no. P16, zircon peaks at 359, 439, 979, 1014, 1090 and 1147 cm^{-1}, corundum peaks at 400, 416, and 749 cm^{-1})

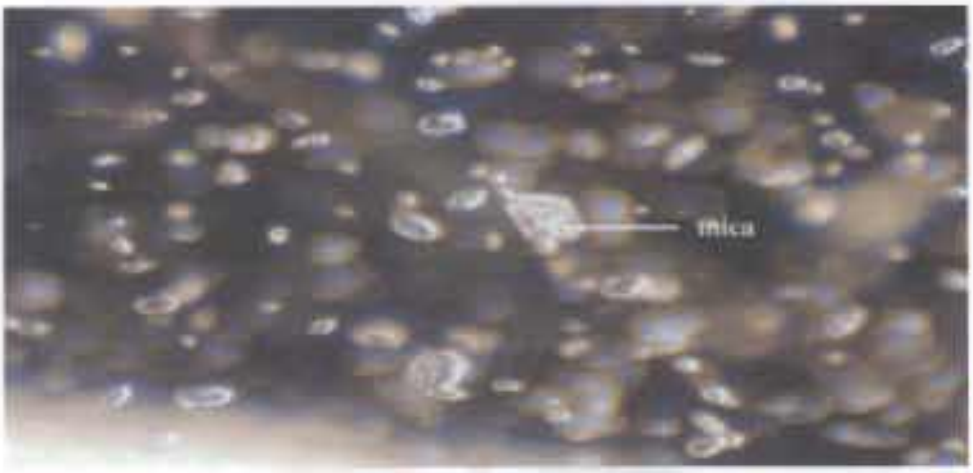

Figure 3.25 Zircon and mica inclusions in pinkish purple sapphire (sample no. P6, 70X). Abundance of zircon inclusions such as this photo is a locality characteristic of the Ilakaka-Sakaraha pink and purple sapphires

Figure 3.26 Raman spectrum of a mica inclusion in pinkish purple sapphire (sample no. P6, mica peaks at 262, 700 and 905 cm^{-1}, corundum peaks at 416, 576, 641 and 749 cm^{-1})

Figure 3.27 Raman spectrum of a fuchsite inclusion in purple sapphire (sample no. P16, fuchsite peaks at 263, 490 and 698 cm^{-1}, corundum peaks at 378, 414, 576, 641 and 750 cm^{-1})

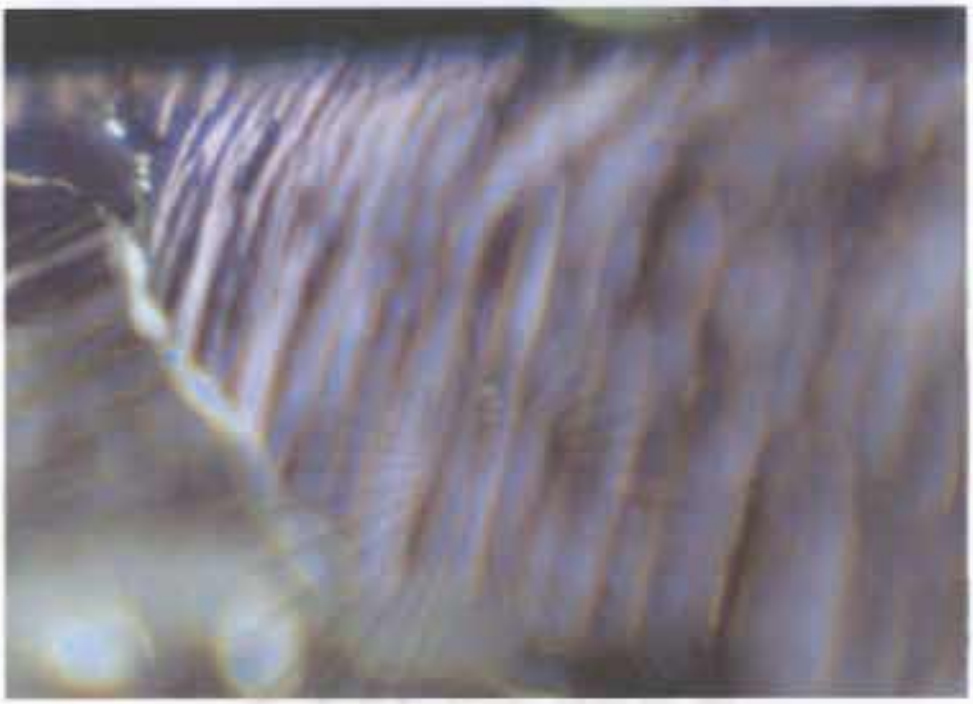

Figure 3.28 Monazite inclusion occurring in purple sapphire as white rounded crystal (sample no. P16, 70X)

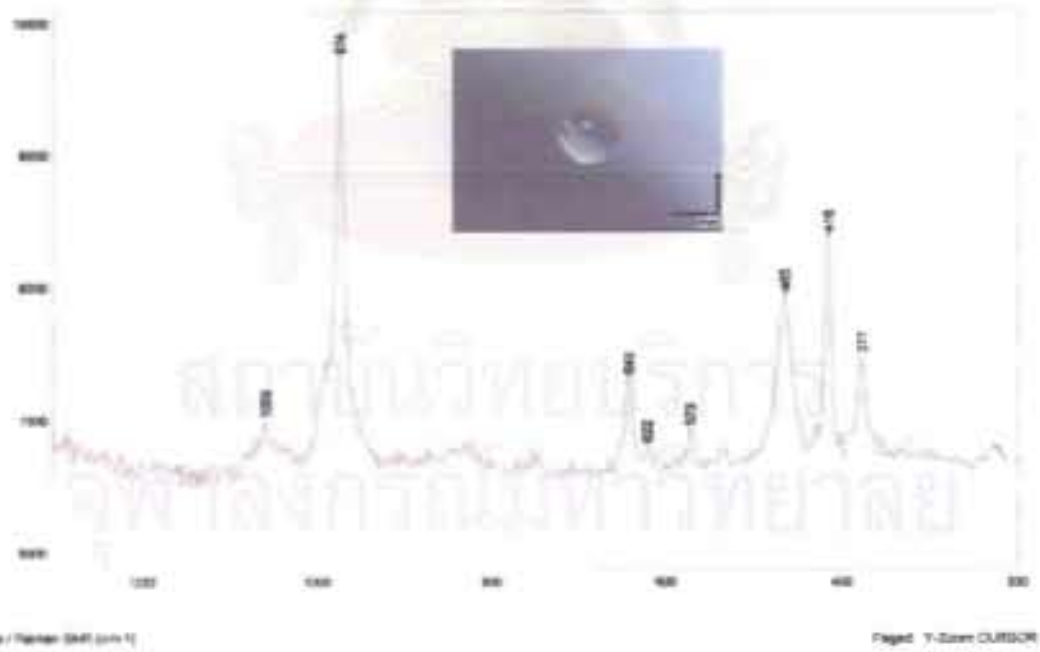

Figure 3.29 Raman spectrum of a monazite inclusion in purple sapphire (sample no. P16, monazite peaks at 465, 622, 974 and 1059 cm^{-1}, corundum peaks at 377, 416, 573 and 643 cm^{-1})

Figure 3.30 Fingerprint and rutile needles in medium violet sapphire (sample no. MV5, 40X)

Figure 3.31 Rutile needles oriented 3 directions and intersecting at 60°/120° angles in medium violet sapphire (sample no. MV2, 50X)

Figure 3.32 White dust which appear milky and fingerprint in medium violet sapphire (sample no. MV5, 20X)

CHAPTER IV

ABSORPTION SPECTRA

Each mineral or gemstone has its particular molecular structures and may contain different chromophoric elements which can absorbed light differently. So absorption or transmission spectra of a gemstone can be used to understand some of its molecular structure and color causing mechanism of that variety of gemstone. The IR-VIS-UV spectra of 8 types of pink, purple and violet sapphires before heating (total 44 samples) were therefore examined by FTIR Spectrophotometer and UV-VIS-NIR Spectrophotometer.

FTIR Spectrophotometer

Fourier Transform Infrared (FTIR) Spectrophotometer can be used for measuring the absorption or transmission spectra in the range of near to far infrared. In this study the FTIR spectra were measured with the transmission mode in the mid infrared range (400-4000 cm^{-1} wavenumber) by Nicolet FTIR Spectrophotometer (model NEXUS 670, see Figure 4.1) at the GIT. This range is particularly useful because the absorption features relating to structural OH group and water stretching frequencies (Smith, 1995).

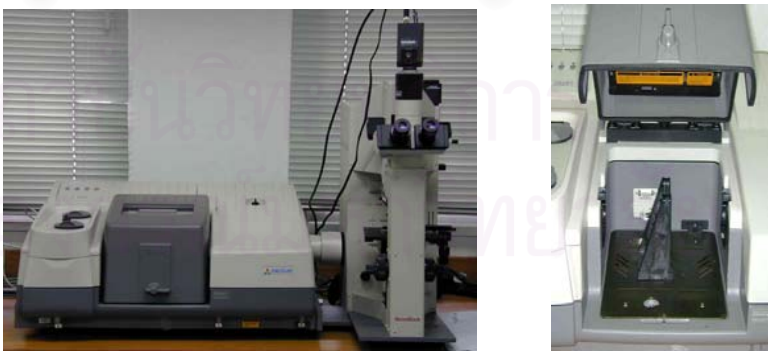

Figure 4.1 Nicolet FTIR Spectrophotometer (model NEXUS 670)

FTIR spectra

The FTIR spectra (in % transmittance) of sapphires before heating were displayed in Figures 4.2 to 4.8. The FTIR spectra of all types appear essentially the same pattern. They generally show almost complete absorption at wavenumber below 1500 cm^{-1}, which is typical for most corundum. The FTIR spectra of all the sapphires also show absorption peaks at 3900-3400 cm^{-1} due to moisture, 2925-2918 and 2852-2850 cm^{-1} due to C-H stretching, 2365-2360 and 2350-2340 cm^{-1} due to CO_2 (Smith, 1995). The moisture (H_2O) and CO_2 probably originate from the air in the chamber or on the surface or in open fracture of sample whereas the C-H stretching is likely to come from contamination of organic substance on sapphire surface.

In this study, about 50% of sapphires, except light purplish pink sapphires, show a very small absorption peak at 3309 cm^{-1} and/or broad absorption band in 3400-3300 cm^{-1} that could be due to O-H bonding (Volynets and others, 1972 cited in Smith, 1995). According to Smith (1995), the structural OH groups (which may or may not be related to the presence of diaspore or boehmite inclusion) are much more typically recorded in heat-treated blue sapphires from basaltic terrains such as Thailand, Cambodia, Southern Vietnam and Australia than those for rubies or sapphires from metamorphic provinces.

UV-VIS-NIR Spectrophotometer

The UV-VIS-NIR Spectrophotometer use a monochromatic light that can be tuned automatically and scanned over the visible, near infrared (NIR) and ultraviolet (UV) wavelengths. The resulting transmission or absorption spectrum is detected with a photocell, and either displayed on a monitor or plotted as a graph. This instrument is widely used in gemstone analysis because it relates to color and can be detected even weak absorption.

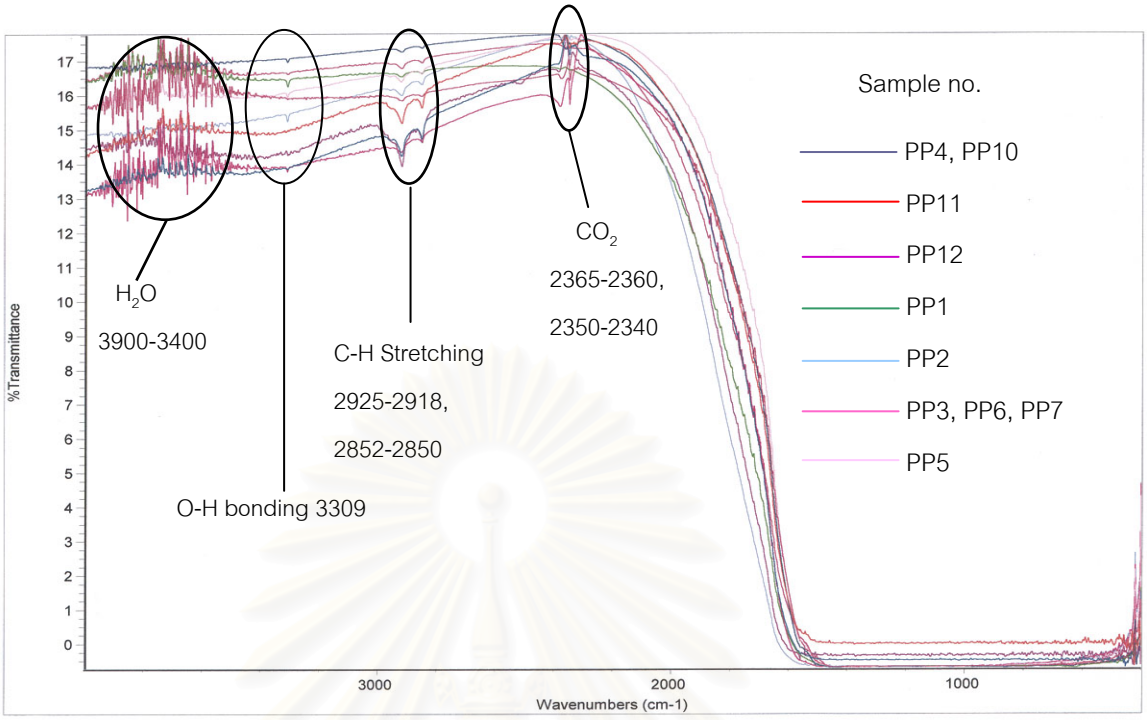

Figure 4.2 FTIR spectra of unheated purplish pink sapphire (total 10 samples)

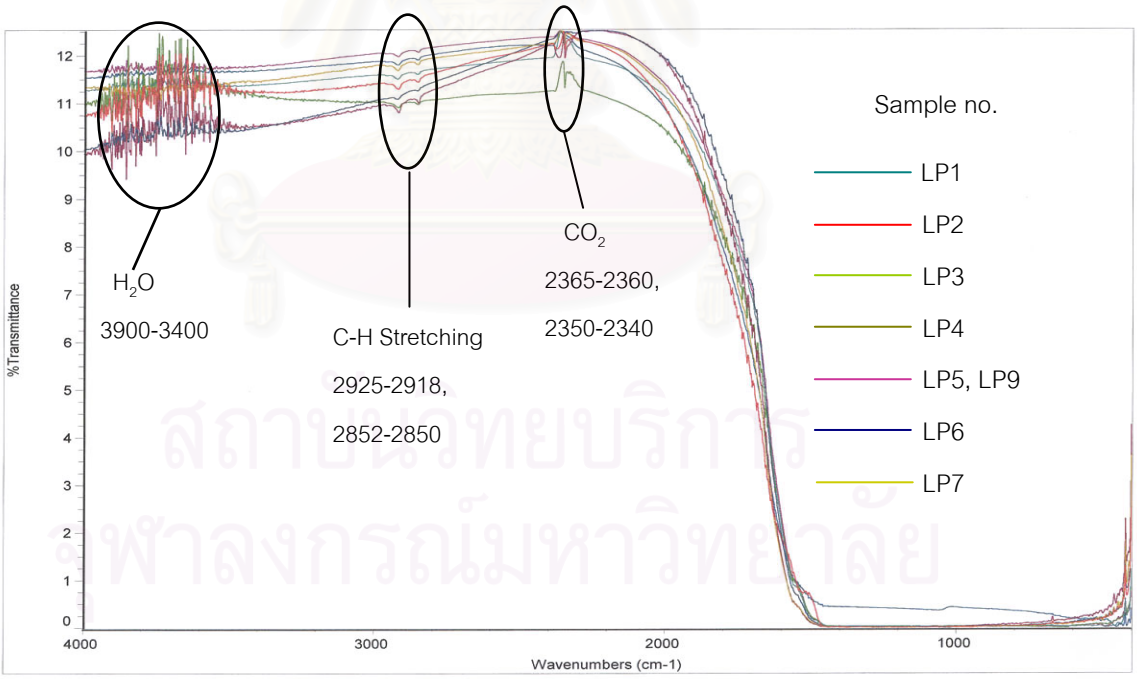

Figure 4.3 FTIR spectra of unheated light purplish pink sapphire (total 8 samples)

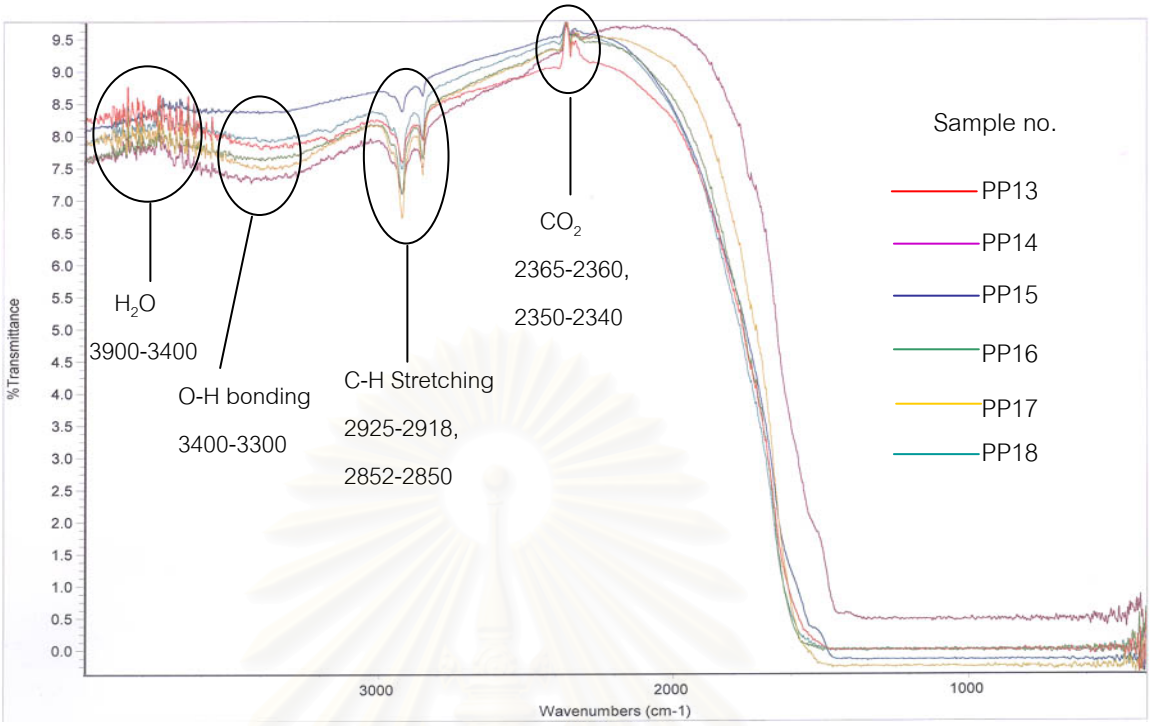

Figure 4.4 FTIR spectra of unheated light orangey and orangey pink sapphires (total 6 samples)

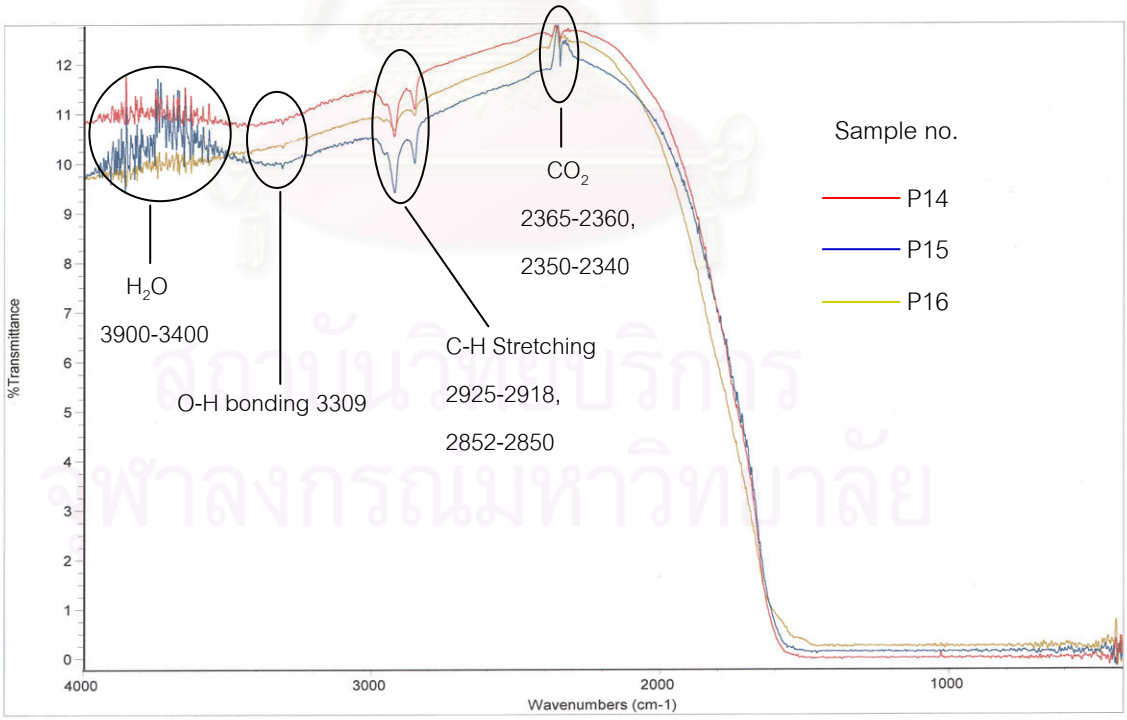

Figure 4.5 FTIR spectra of unheated purple sapphire (total 3 samples)

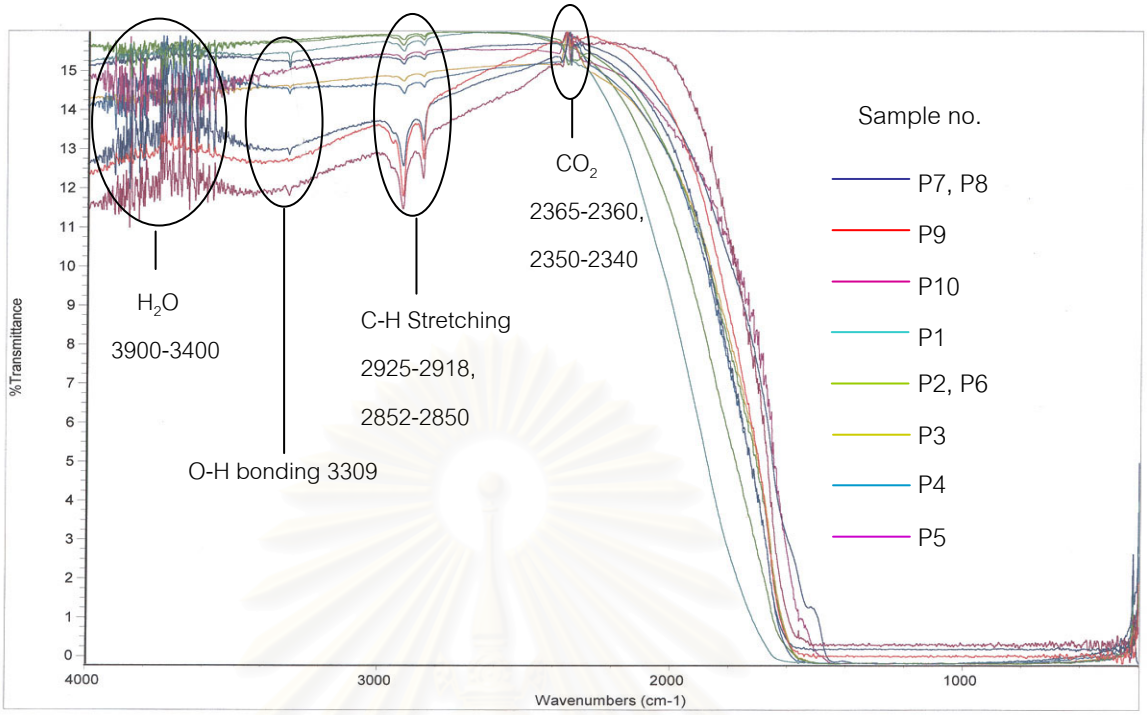

Figure 4.6 FTIR spectra of unheated pinkish purple sapphire (total 10 samples)

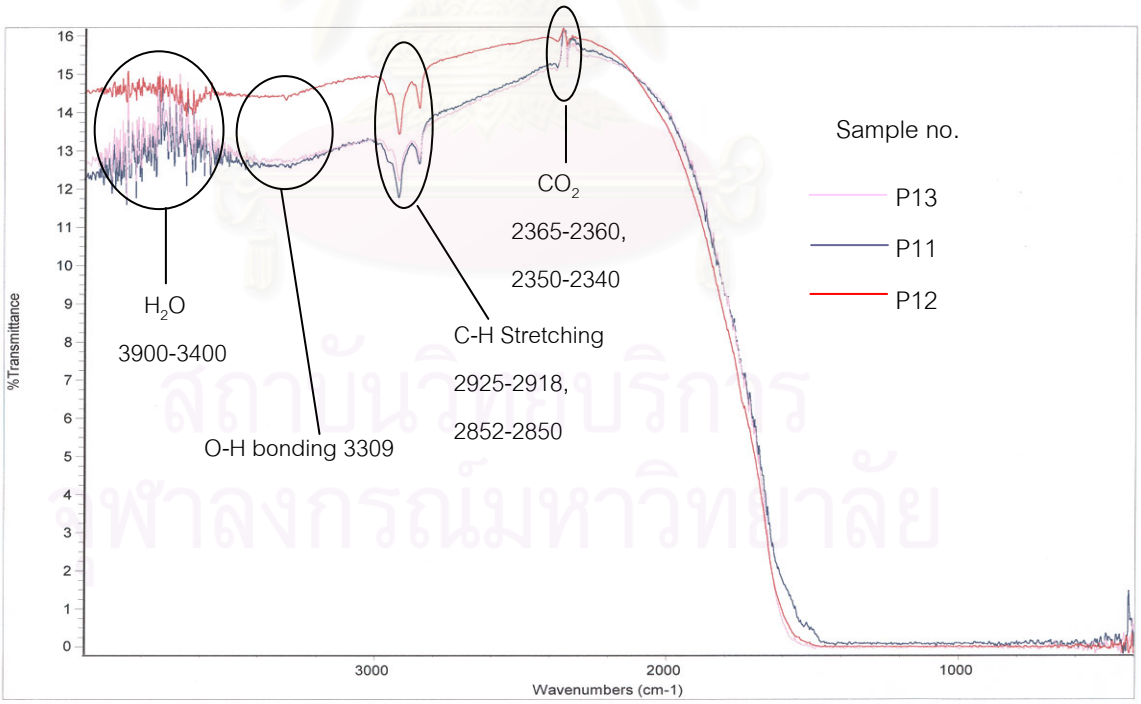

Figure 4.7 FIIR spectra of unheated brownish purple sapphire (total 3 samples)

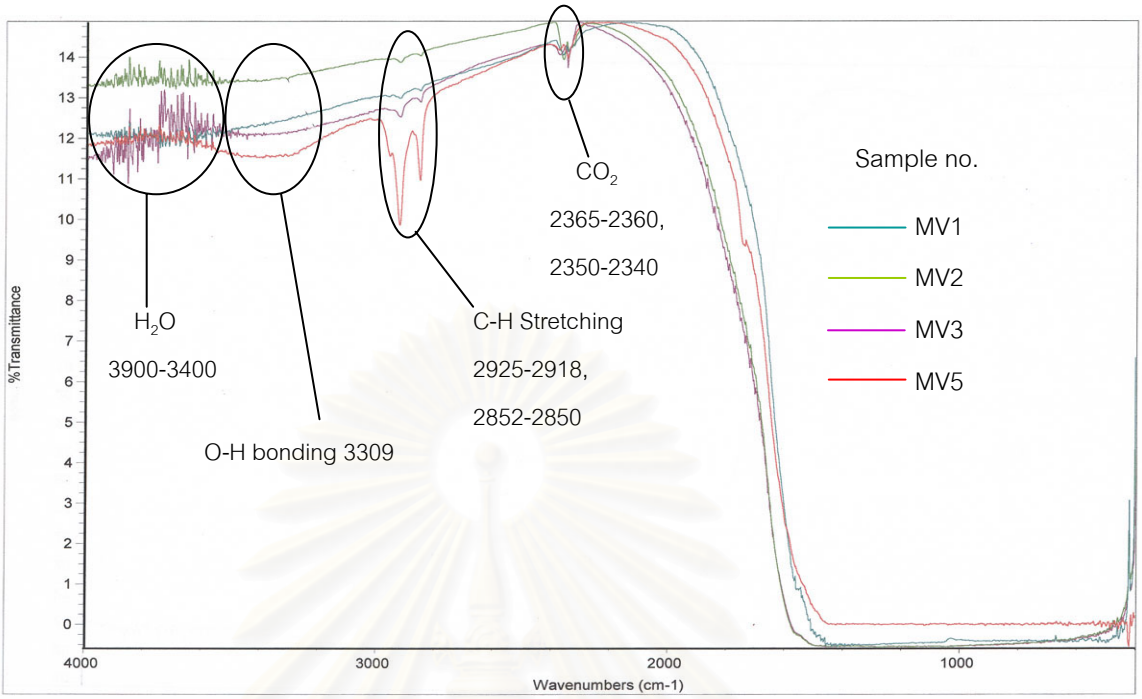

Figure 4.8 FTIR spectra of unheated medium violet sapphire (total 4 samples)

The sapphires may show the difference in wavelength absorption, which produces the appearance of color when perceives by the eyes. Some selected absorption of seven types of unheated sapphires were examined at 250-1500 nanometers (nm), with a spectral resolution of 2 nm by using Hitachi UV-VIS-NIR Spectrophotometer (model U4001, see Figure 4.9) at the DMR. This instrument has double beams. A beam of light is switched between a reference path and a sample path, which are recombined at the detector, which thus compares the two beams. The signal from the reference path is subtracted from that of the sample path to give a spectrum of the sample. Each sample was run twice, one for the parallel to c-axis spectrum (extraordinary (e) ray) and another for the perpendicular to c-axis spectrum (ordinary (o) ray).

Figure 4.9 Hitachi UV-VIS-NIR Spectrophotometer (model U4001)

UV-VIS-NIR spectra

The UV-VIS-NIR spectra of unheated pink (PP11, PP15, PP16, PP17, LP7 and LP9), purple (P6, P10, P11 and P16) and violet sapphires (MV2 and MV5) are displayed in Figures 4.10 to 4.15. Generally they dominantly exhibit 2 broad bands and a small peak of Cr^{3+} centered at 401-412 nm, 553-560 nm and 692-693 nm, respectively in o-ray. This 692 or 693 peak is prominent in o-ray. These spectra can be divided into 2 groups. The first group (LP9, PP16, P6, P11 and MV2) exhibits additional peaks at 385-388 and 449-450 nm in o-ray due to Fe^{3+} and Fe^{3+}/Fe^{3+} pairs (Ferguson and Fielding, 1971 and 1972; Krebs and Maisch, 1971 cited in Emmett and Douthit, 1993). The samples in this group have Fe content (Fe_2O_3) more than 0.2 weight % (anlyzed by EDXRF). The second group (PP11, PP15, PP17, LP7, P10, P16 and MV5) does not show peaks of Fe^{3+} and Fe^{3+}/Fe^{3+} pairs which has lower Fe content than the first group (less than 0.2 weight %). When these low Fe content spectra of unheated pink sapphires are compared with those of unheated rubies from Thailand and Mogok (Myanmar) derived respectively from basaltic and metamorphic source (Hughes, 1997). The absorption spectra are similar to those of Mogok ruby (Figure 4.16). Also Junprapasri (2000) interpreted the UV-VIS-NIR spectra of some sapphires from Ilakaka area as being derived from metamorphic origin. Hence sapphires from Ilakaka-Sakaraha area, the low iron group in particular, are likely to derive metamorphic origin.

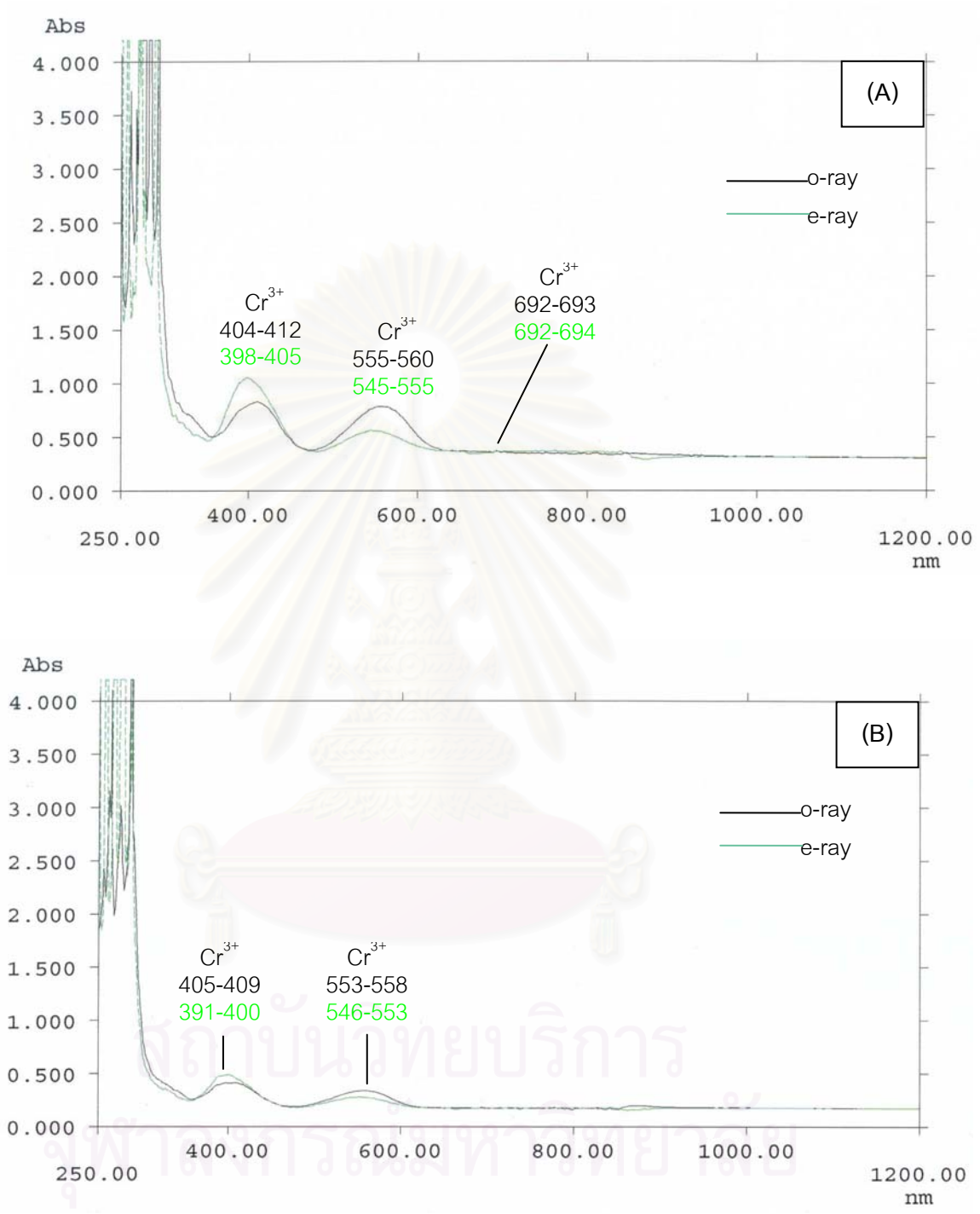

Figure 4.10 UV-VIS-NIR spectra of unheated (A) purplish pink (PP11) and (B) light orangey pink (PP15) sapphires

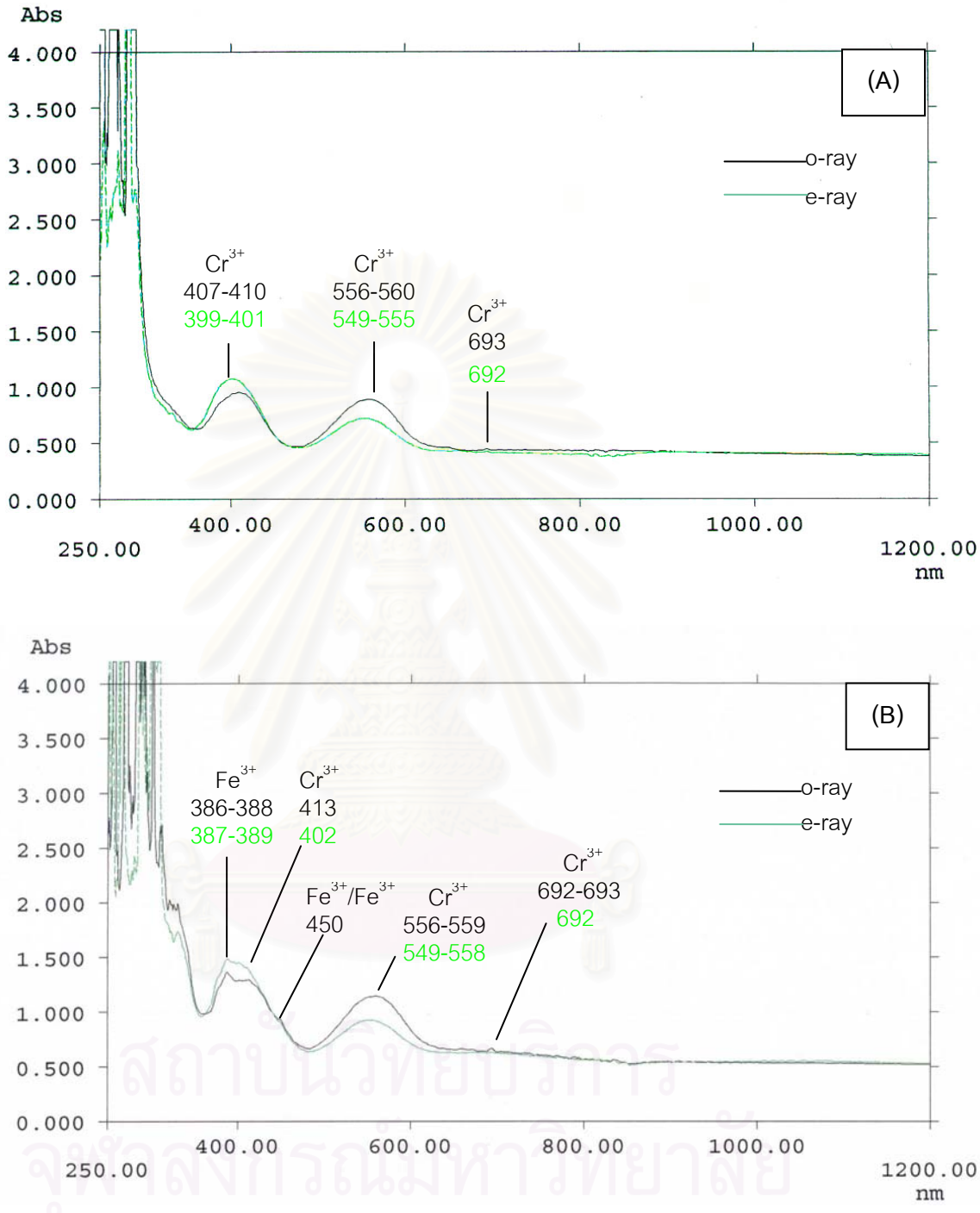

Figure 4.11 UV-VIS-NIR spectra of unheated light purplish pink sapphire
(A) low Fe content (LP7) (B) high Fe content (LP9)

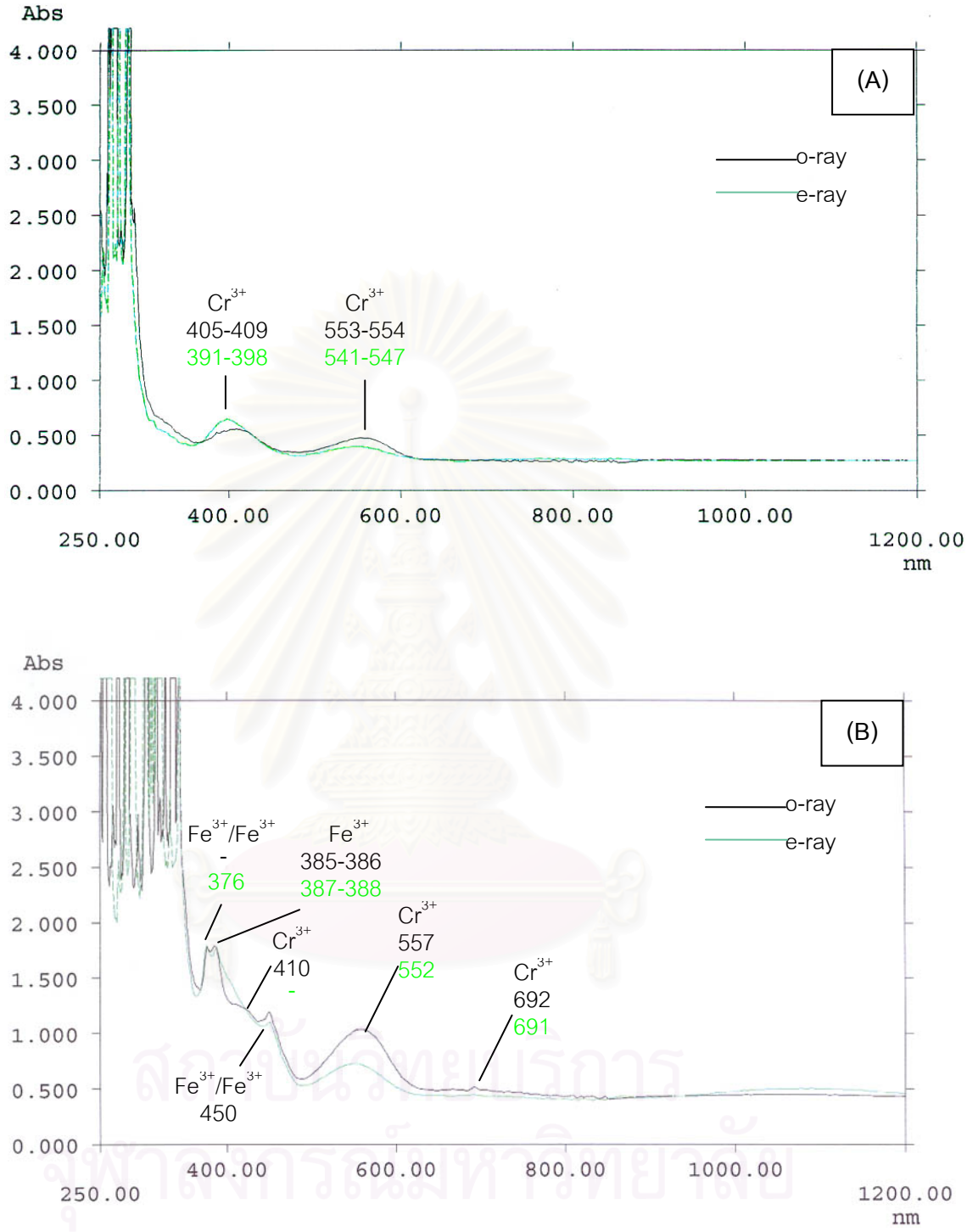

Figure 4.12 UV-VIS-NIR spectra of unheated orangey pink sapphire

(A) low Fe content (PP17) (B) high Fe content (PP16)

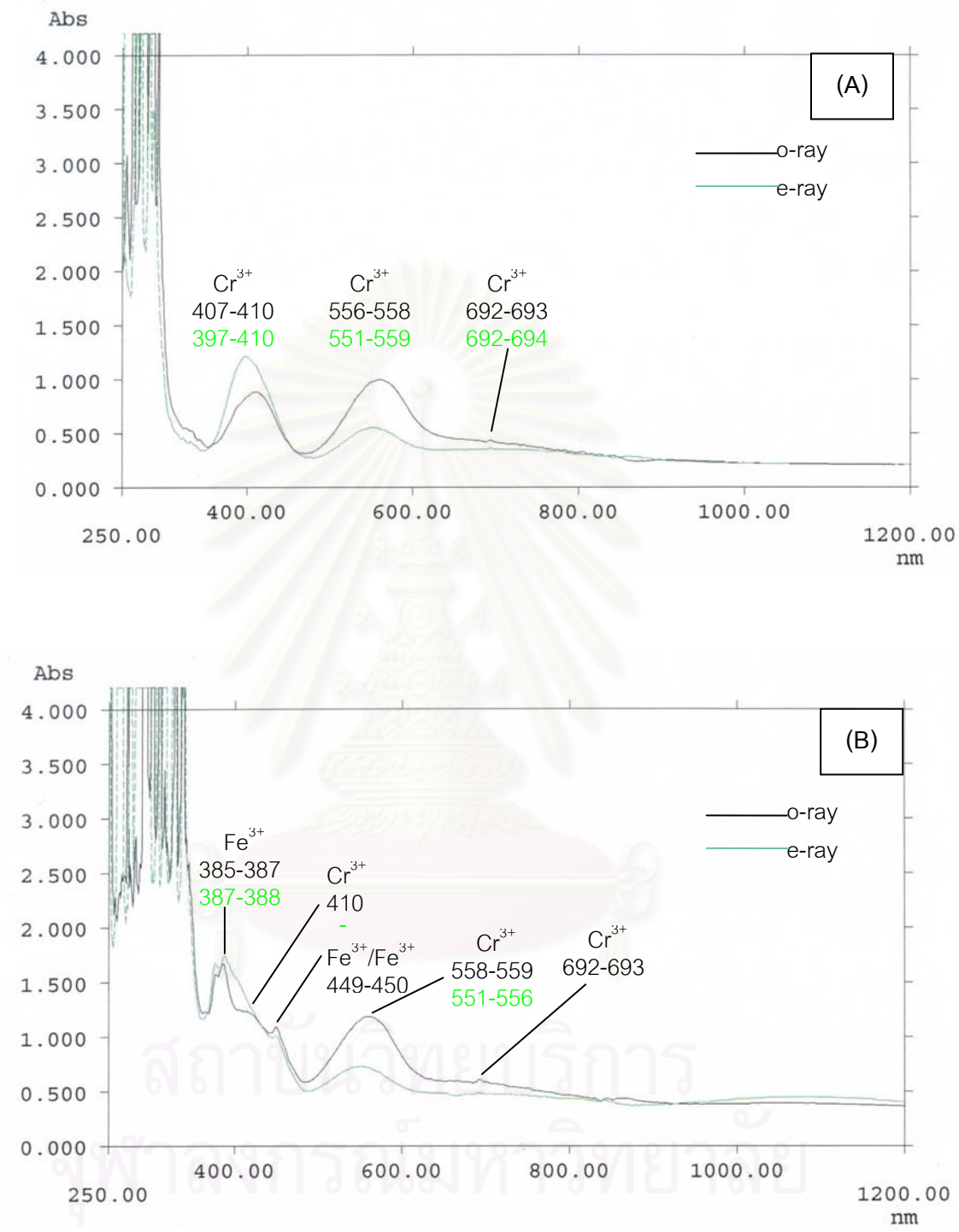

Figure 4.13 UV-VIS-NIR spectra of unheated (A) purple (P16) and (B) brownish purple (P11) sapphires

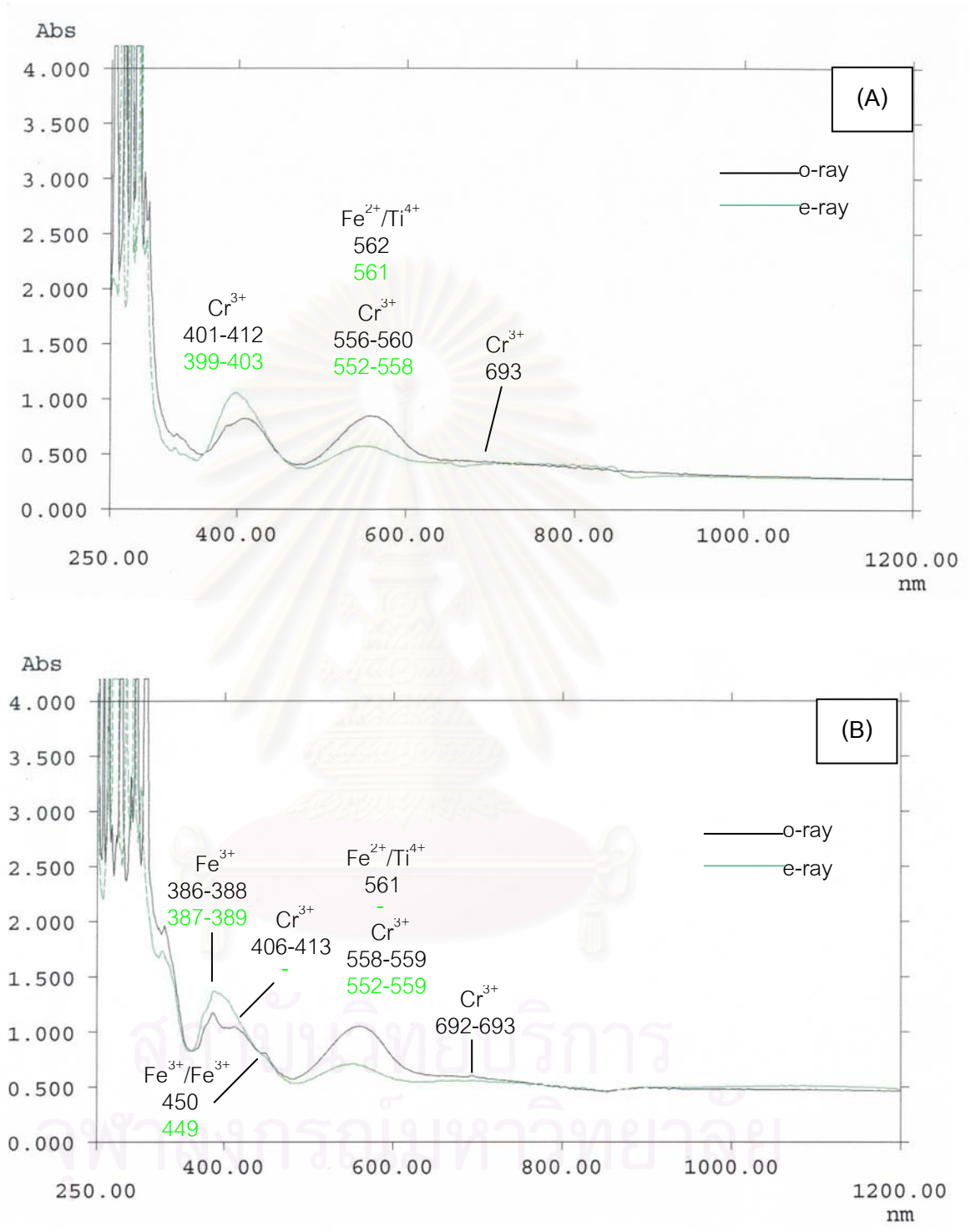

Figure 4.14 UV-VIS-NIR spectra of unheated pinkish purple sapphire

(A) low Fe content (P10) (B) high Fe content (P6)

The violet sapphires with color-change effect (bluish in fluorescent light and purplish in incandescent light) show Cr^{3+} absorption peaks at 410 nm (o-ray) and 405 nm (e-ray), Fe^{3+} absorption peaks at 386-388 (o-ray) and 388-389 nm (e-ray) and Fe^{3+}/Fe^{3+} pairs absorption peaks at 449-450 nm (o-ray and e-ray) and Fe^{2+}/Ti^{4+} intervalence charge transfer (IVCT) at 563-568 nm (o-ray) and 563-566 nm (e-ray) (Figure 4.15 A). The violet sapphires that do not show color-change effect show all absorption peaks similar to those of the violet sapphires with color-change effect except the Fe^{3+}/Fe^{3+} peak is missing (Figure 4.15 B). Schmetzer and others (1980) cited in Fritsch and Rossman (1988) reported the cause of color-change effect in corundum is due to Cr^{3+} and/or V^{3+} in which the positions of the V^{3+} absorption bands are very close those of Cr^{3+}. As also shown in Chapter VI, the sapphires with color-change effect contain higher Cr and V content than those without color-change effect.

All absorption peaks of sapphires relate to chromorphic impurities or transition ion. Themelis (1992) explained that the coloration of the ruby and pink sapphire are due to trivalent chromium (Cr^{3+}) present in the alumina substance in isomorphous replacement as chromium oxide (Cr_2O_3) impurities. About 0.1% of Cr_2O_3 in the corundum substance produces red color. As the concentration of the Cr_2O_3 is reduced, the red color is reduced accordingly; thus, about 0.04% of Cr_2O_3 will produce intense pink, whereas about 0.03% of Cr_2O_3 will produce light pink. The overall appearances of the ruby and pink sapphire are modified by various chromophoric impurities. For example, iron impurities may produce brownish overcasted coloration, while concentrated amounts of iron may form orange or brownish stains. When titanium and iron are present in ruby or pink sapphire, an overcasted bluish, violetish or purplish coloration may be produced. Traces of vanadium may modify the overall appearance, producing purplish or violetish overcasted coloration. As the content of these chromophic impurities increases, the overcasted coloration produced intense. In some orangey pink, orange and yellow sapphires, the yellow component is due to crystal lattice defects, such as color center. The color of purple and violet sapphire is cause by Cr^{3+} and Fe^{2+}/Ti^{4+} IVCT. The bluish color component in violet and purple sapphires is a result of Fe^{2+}/Ti^{4+} IVCT (Schmetzer and Bank, 1981 cited in Fritsch and Rossman, 1988).

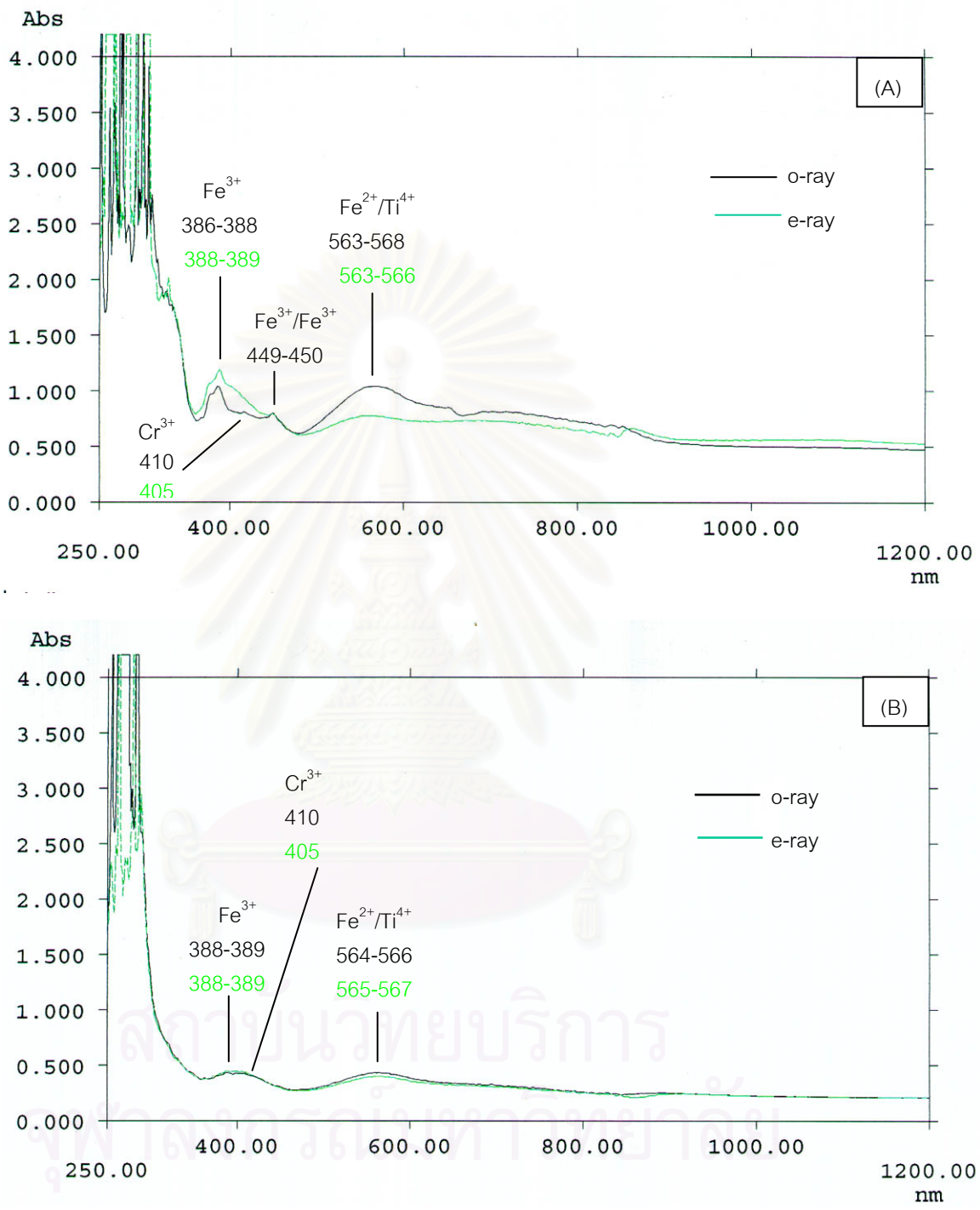

Figure 4.15 UV-VIS-NIR spectra of unheated violet sapphire

(A) with color-change effect (MV2) (B) without color-change effect (MV5)

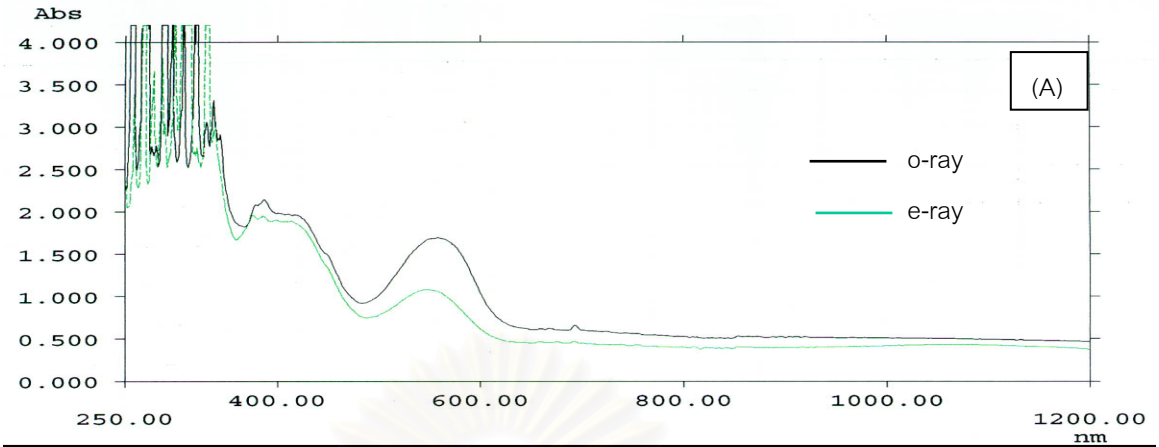

Figure 4.16 UV-VIS-NIR spectra comparison of unheated ruby and pink sapphire

(A) Thai ruby that related to basaltic-type origin

(B) Mogok ruby that related to metamorphic-type origin

(C) low iron Ilakaka-Sakaraha pink sapphire

CHAPTER V

STUDY AFTER HEAT TREATMENT

Introduction

Eight types of pink, purple and violet sapphires (16 samples) that have been studied for their gemological properties were used for heating experiment. The samples were heated each time at 5 different maximum temperatures for 1 hour (soaking time) under oxidizing atmosphere, so they were heated 5 times (at 800°C, 1000°C, 1200°C, 1400°C and 1600°C). These heating conditions were selected because according to Somboon (2000) 1000°C for 3 hours soaking time is a heating condition that can be observed some change in the internal characteristics and color, such as development of tension disc (discoid), slightly alter fingerprints and decreasing pink color. Hence in order to verity the lowest possible heating effect, 800°C heating condition was also selected for the minimum temperature used for this study. Previous works (Somboon, 2000; Bootsri and Bussal, 2001; Inraikhing and Rumpang, 2001) reveal that 3 hours soaking time was enough to observe the difference in color transparency and internal characteristics. So in order to examine the shortest possible heating time, 1 hour soaking time was chosen for this study. To avoid contamination, for example iron stains or secondary silicate minerals which may have coated the sample surface or stuck within the cracks, the samples were soaked in hydrofluoric acid (HF) for 1 day and then washed thoroughly with water. The cleaned samples are placed in an alumina crucible for heating in the determined conditions. The furnace and heating cycle used for heating experiment are outlined in the following paragraphs.

จุฬาลงกรณ์มหาวิทยาลัย

Furnace

The furnace used in this work is a Lindberg electric furnace Model 59256-E6 (Figure 5.1) at the DMR. This electric furnace can produce an oxidizing atmosphere at temperatures up to 1700°C. The furnace consists of a heating chamber and control section. The heating chamber is heated by U-shaped molybdenumdisilicide ($MoSi_2$) elements suspended from the roof to freely along the side

walls. The chamber is insulated with special high temperature refractory fiber broad. The sapphires were put in a small size (4 centimeters in diameter) alumina crucible which was placed in heating chamber.

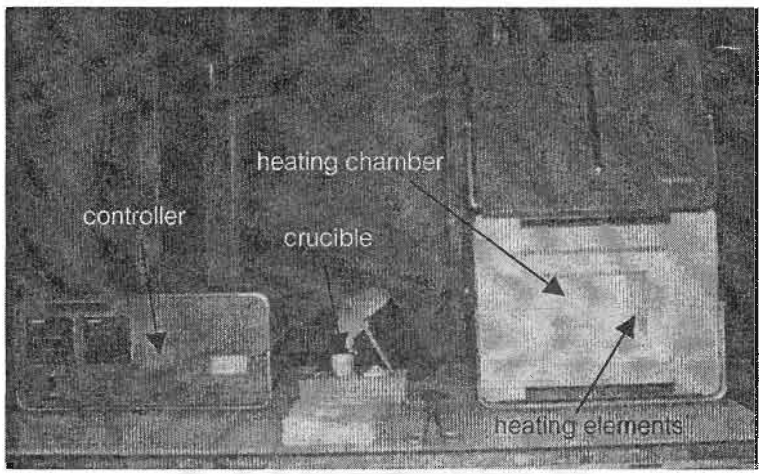

Figure 5.1 Lindberg electric furnace (Model 59256-E6) and accessory.

Heating Cycle

Every heating process is characterized by successive segments: heat-up, processing (soaking), and cool-down. The temperature in an electric furnace was controlled in all segments of the heating process, using the temperature controller.

The heat-up is a heating segment from 75°C (beginning controllable temperature) to the maximum temperature. The rate of temperature increase was controlled at about 4°C/minute for all heating conditions.

The processing or soaking segment means the period which the maximum temperature is sustained. In each condition, the soaking time was 1 hour.

The cool-down segment is initiated from the temperature starting to decrease from the processing segment until it eventually reaches a determined temperature, normally at about 600°C before taking sapphires out the furnace. The cool-down rate depends on the conductivity of the furnace. In this study, the cool-down rate was selected at 15°C/minute.

The effect of heat treatment on the color appearance

The GIA GemSet was used for documenting the color code of unheated and heated sapphires which are shown in Table 5.1.

Purplish and light purplish pink sapphires

The color appearance of four purplish pink sapphire samples (PP3, PP4 PP6 and PP11) and three light purplish pink sapphire samples (LP3, LP4 and LP9) before and after step-heating at 800°C, 1000°C, 1200°C, 1400°C and 1600°C are displayed in Figures 5.2 and 5.3.

Generally, when rubies or pink sapphires, overcasted by a purplish coloration are heated in an oxidizing atmosphere, their purplish coloration is reduced. As the overcasted color is reduced or removed, the red or pink color is light or pure, giving the impression that the ruby or pink sapphire has lost some red color, which in fact, it has not. This is because it is not possible to change the valence of the Cr^{3+} and remove the chromium content from ruby or pink sapphire by simple heating (Themelis, 1992). In this study, the purplish overcasted color in pink sapphires was reduced at 1000°C to 1200°C. The color was still unchanged when the sapphires were heated at 1400°C to 1600°C. While purplish overcasted color in light pink sapphires was reduced at 800°C to 1000°C. When they were heated at higher temperatures (1200°C to 1600°C), their color was still remain the same as they were heated at 800°C to 1000°C.

Light orangey and orangey pink sapphires

The color appearance of a light orangey (PP15) and an orangey (PP17) pink sapphire samples before and after heating are shown in Figures 5.4 and 5.5. The coloration of orange and orangey pink sapphires is a result of Cr^{3+}, Fe^{3+} and/or color center (Themelis, 1992). Most light orangey and orangey pink sapphires when heated in an oxidizing atmosphere tends to increase the yellow or orange coloration. In this study, however, the orangey overcasted color in light pink and pink sapphires was removed at 1200°C and 800°C, respectively. The cause of orange disappearance in two pink sapphire samples was explained in the later section.

Table 5.1 Color codes of sapphires before and after heating at 800°C, 1000°C, 1200°C, 1400°C and 1600°C by GIA GemSet (List of hue, tone, and saturation terms for describing gem color are shown in Appendix I).

Sample	Hue Tone Saturation					
no.	Unheat	Heat 800°C	Heat 1000°C	Heat 1200°C	Heat 1400°C	Heat 1600°C
Purplish pink						
PP 3	PR/RP 6/4	PR/RP 6/4	PR/RP 4/5	PR/RP 4/5	PR/RP 4/5	PR/RP 4/5
PP 4	PR/RP 5/3	PR/RP 5/3	PR/RP 5/3	PR/RP 4/3	PR/RP 4/3	PR/RP 4/3
PP 6	PR/RP 5/3	PR/RP 5/3	PR/RP 5/3	PR/RP 4/3	PR/RP 4/3	PR/RP 4/3
PP 11	PR/RP 5/3	PR/RP 5/3	PR/RP 4/3	PR/RP 4/3	PR/RP 4/3	PR/RP 4/3
Light purplish pink						
LP 3	PR/RP 4/3	PR/RP 4/3	rP 2/3	rP 2/3	rP 2/3	rP 2/3
LP 4	PR/RP 4/3	PR/RP 4/3	rP 2/3	rP 2/3	rP 2/3	rP 2/3
LP 5	PR/RP 4/3	PR/RP 3/3	PR/RP 3/3	PR/RP 3/3	PR/RP 3/3	PR/RP 3/3
Light orangey pink						
PP 15	PR/RP 2/3 + rO 2/3	PR/RP 2/3 + rO 2/3	PR/RP 2/3	PR/RP 2/3	PR/RP 2/3	PR/RP 2/3
Orangey pink						
PP 17	slpR2/3 + rO 2/3	PR/RP 3/3	PR/RP 2/3	PR/RP 2/3	PR/RP 2/3	PR/RP 2/3
Purple						
P 16	P 6/3	P 4/5	PR/RP 5/3	PR/RP 4/3	PR/RP 4/3	PR/RP 4/3
Pinkish purple						
P 5	PR/RP 6/3	PR/RP 6/3	PR/RP 4/2	PR/RP 4/2	PR/RP 4/2	PR/RP 4/2
P 6	PR/RP 7/4	PR/RP 7/4	PR/RP 5/3	PR/RP 5/3	PR/RP 5/3	PR/RP 5/3
P 10	rP 5/3	rP 4/4	rP 3/4	rP 3/4	rP 3/4	rP 3/4
Brownish purple						
P 11	PR/RP 6/3+ rO 4/3	slpR 6/3+ rO 4/3	stpR 5/4 + rO 4/3	stpR 5/4 + O 5/2	stpR 5/4 + O 5/2	stpR 5/4 + O 5/2
Medium violet						
MV 5	V 4/3	bP 2/3	P 3/1	P 3/1	P 2/1	P 2/1
MV 2	V 4/3	bP 4/4	bP 3/3	bP 2/3	bP 2/3	bP 2/3
	*bP 6/3	*P 6/3	*P 6/3	*bP 3/3	*bP 3/3	bP 3/3

*under tungsten light

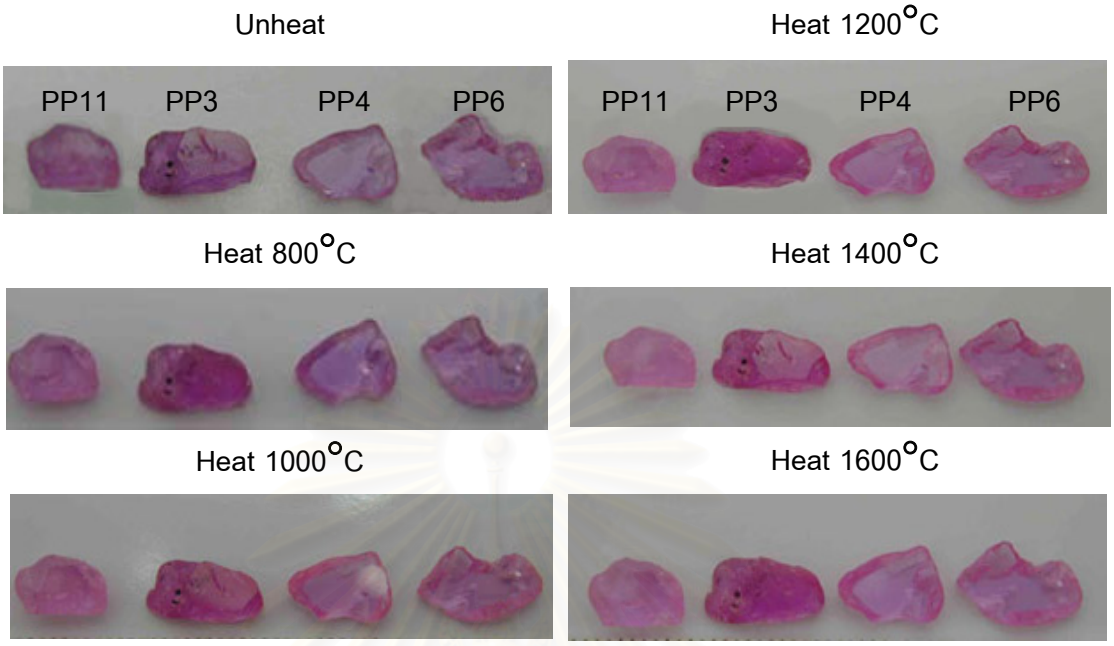

Figure 5.2 Color appearance in purplish pink sapphire samples.

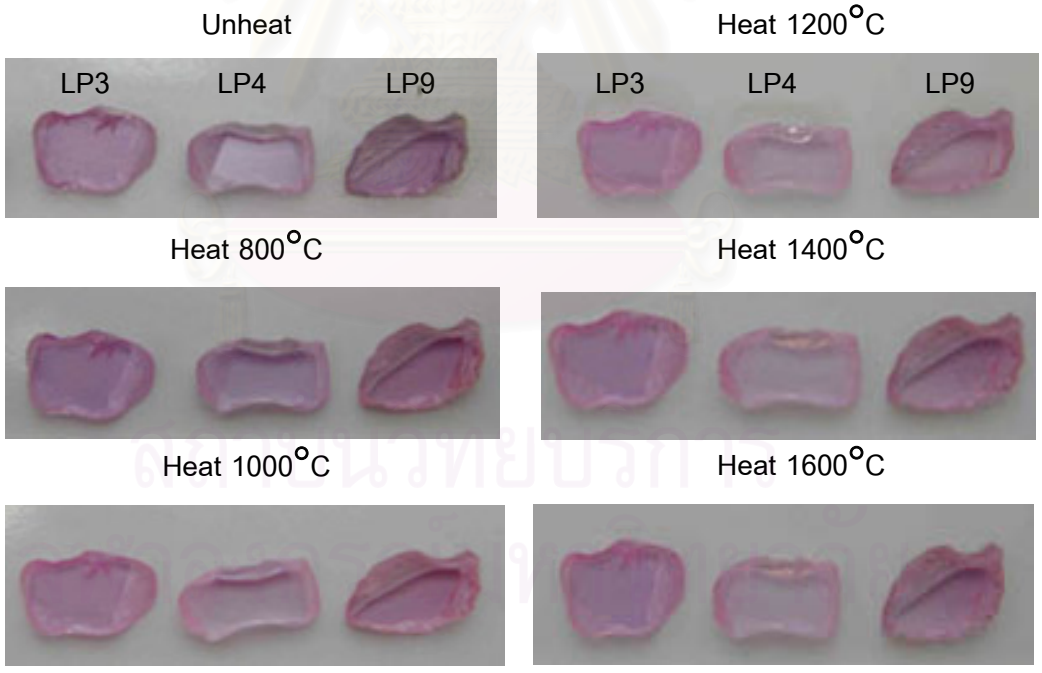

Figure 5.3 Color appearance in light purplish pink sapphire samples.

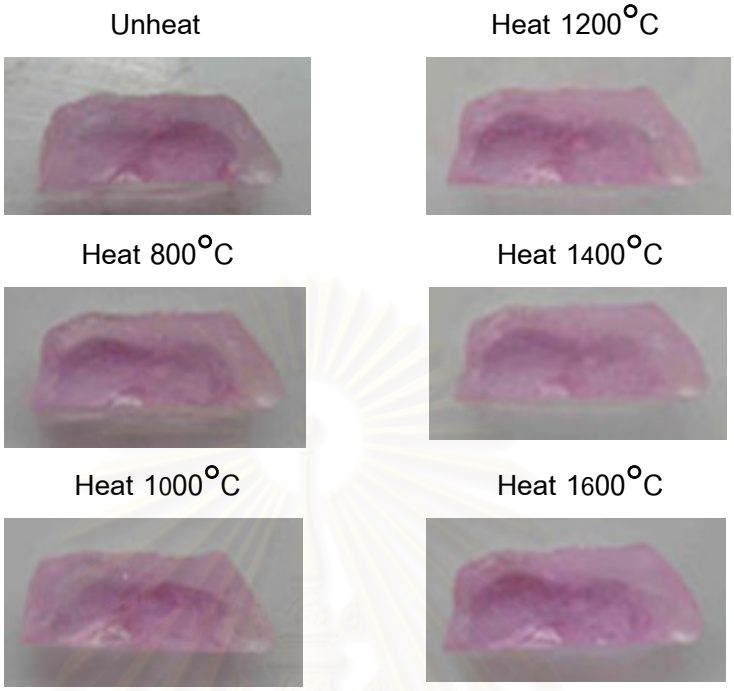

Figure 5.4 Color appearance in light orangey pink sapphire (sample no. PP15).

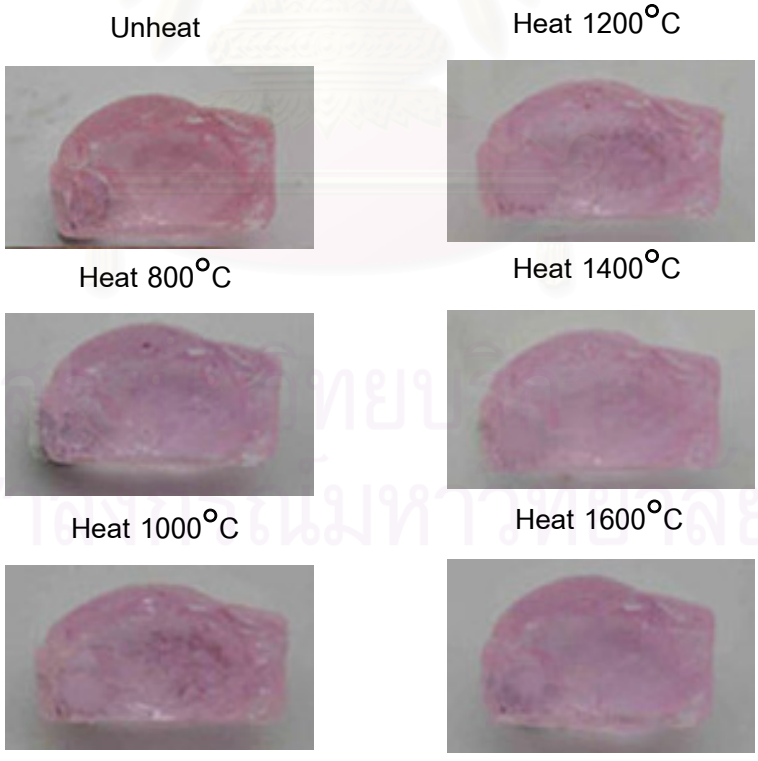

Figure 5.5 Color appearance in orangey pink sapphire (sample no. PP17).

Purple and pinkish purple sapphires

The color appearance of a purple (P16) and three pinkish purple sapphire samples (P5, P6 and P10) before and after step-heating at 800°C, 1000°C, 1200°C, 1400°C and 1600°C are displayed in Figures 5.6 and 5.7. When purple sapphire was heated at 1000°C, purple color was changed to pink and slightly changed to purer pink color at higher temperatures than 1000°C. To remove purple color in pinkish purple sapphires, they were heated at 800°C to 1000°C.

Brownish purple sapphire

The color appearance of a brownish purple sapphire (P11) before and after heating is revealed in Figure 5.8. According to Themelis (1992), the brownish overcasted color in pink sapphire is increased when it was heated in an oxidizing atmosphere. In this study, the brownish coloration in purple sapphire was slightly increased at 800°C to 1000°C. After heating at 1200°C, the brownish coloration was removed and the red color appears purer. The color was still unchanged when the sapphire was heated at 1400°C to 1600°C.

Medium violet sapphire

Two medium violet sapphires were selected for heat treatment. One sample (MV2) showed a color change from bluish violet under fluorescent light into purplish violet under tungsten light. Another sample (MV5) did not show this effect. The color appearance of two medium violet sapphire samples before and after heating are displayed in Figure 5.9. In this study, violet color was changed to bluish purple at 800°C and bluish overcasted color was slightly reduced at high temperature (1000°C to 1400°C). At 1600°C, bluish color was slightly re-produced in one sample (MV5). For medium violet with color-change effect, this effect was lost and the color turned to bluish purple.

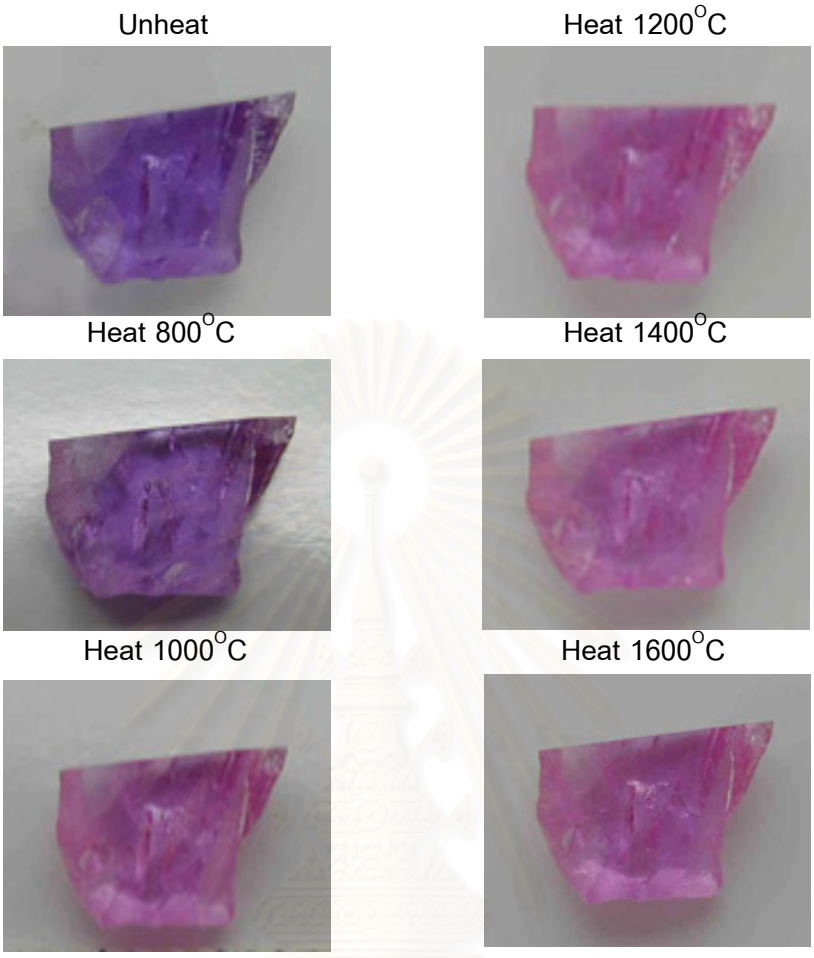

Figure 5.6 Color appearance in purple sapphire (sample no. P16).

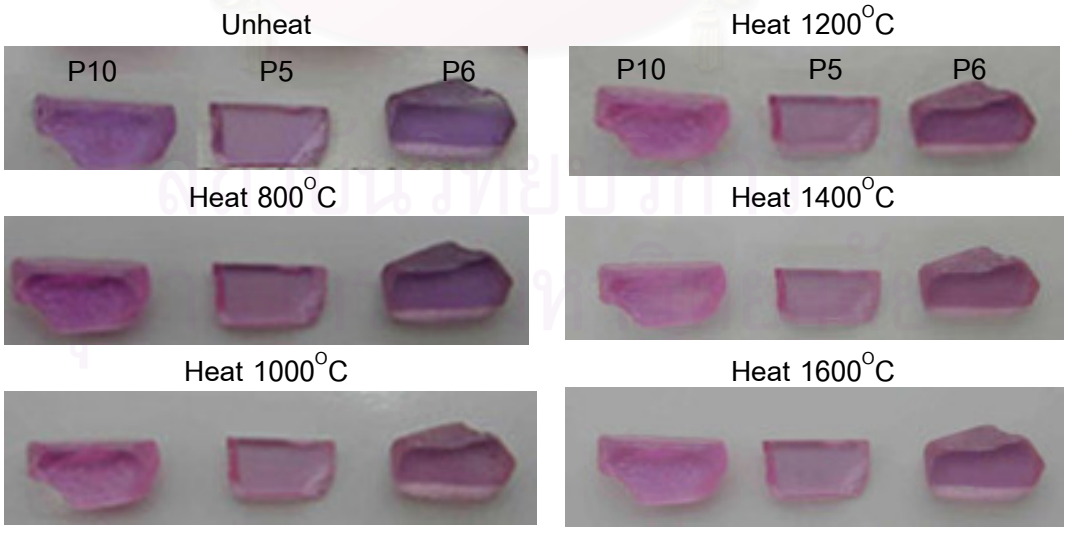

Figure 5.7 Color appearance in pinkish purple sapphire samples.

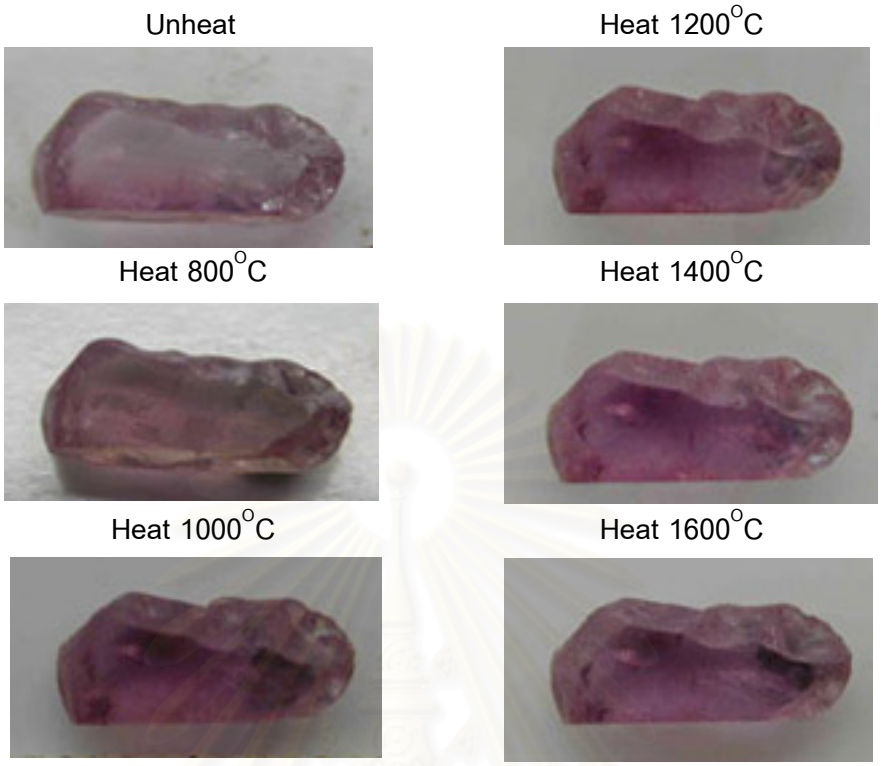

Figure 5.8 Color appearance in brownish purple sapphire (sample no. P11).

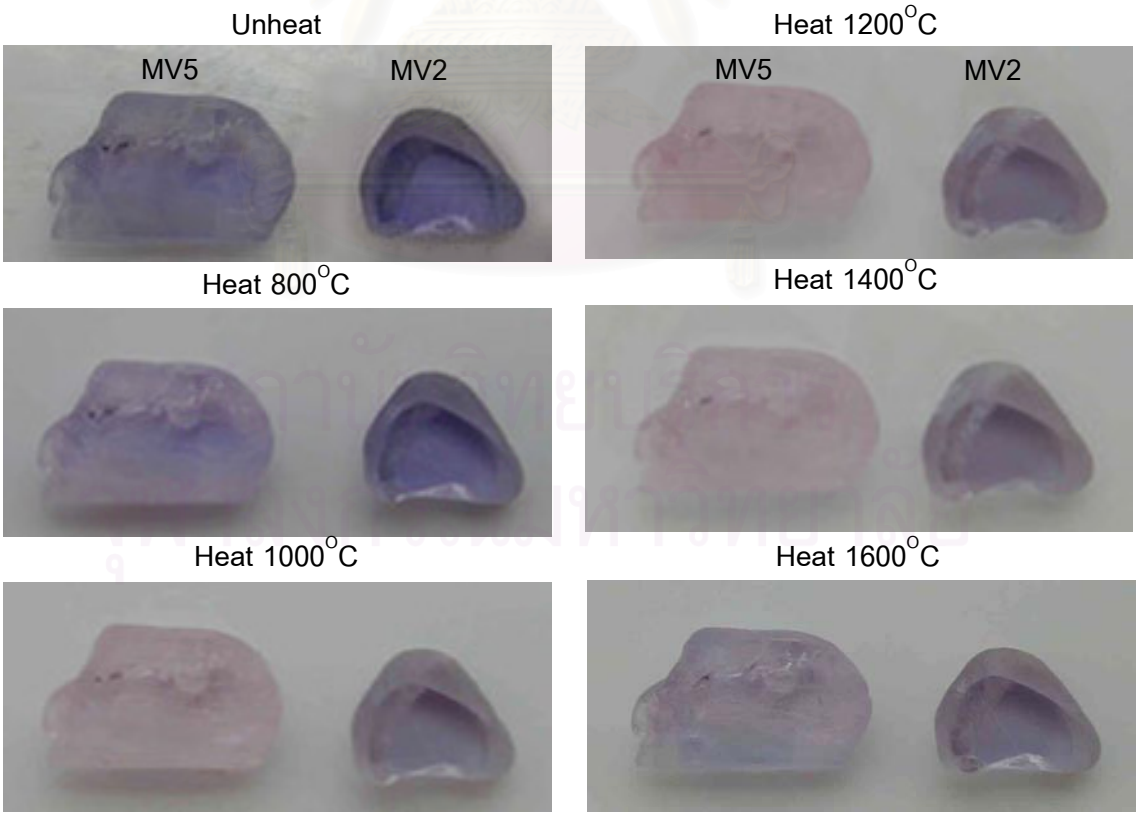

Figure 5.9 Color appearance in medium violet sapphire samples.

The effect of heat treatment on the internal characteristics

The result of this study reveals that when the sapphires were heated at 800°C for 1 hour, most of the internal features were still unchanged. However, a few characteristics can be observed at this temperature. When the same sapphires were re-heated up to 1000°C, 1200°C, 1400°C and 1600°C, each temperature for a period of 1 hour soaking time, many internal characteristics were changed. The change in the internal characteristics can be described in different inclusions as follows:

1. As already mentioned, the zircon occur both as individual crystal and as crystal cluster. Some single crystals and crystal clusters show slight tension crack or discoid even before heating. After step-heating from 800°C to 1600°C, many zircon crystals were still unchanged (Figures 5.10 to 5.15). Generally, the single crystal has a tendency to change at higher temperature than those of the zircon cluster. Some zircon crystals showed slight development of the tension crack surrounding them after heating up to 1000°C and the tension crack was expanded at higher temperatures accompanying by thermal decomposition (appear turbid) (Figures 5.16 to 5.19). These discoid probably result from the different degree of thermal expansion between zircon and host sapphire. Some crystals was partially altered or decomposed into whitish cloudy (turbid) appearance without tension crack when heating up to 1600°C (Figures 5.20 to 5.23). The zircon clusters showed minor tension cracks before heating. These tension cracks were strongly developed after heating at higher temperatures. Some zircon crystals in the cluster began to alter when re–heating to 1200°C (Figures 5.24 to 5.28).

Rankin and Edwards (2003) reported the mottled (turbid) appearance and darkening of zircon inclusion in heat-treated corundum from Chimwadzulu Hill, Malawi. They believed that such feature was due to melting and interaction of zircon with the host corundum at high temperature. They have documented that the original zircons were partially or completely replaced by an intergrowth of monoclinic m-ZrO_2 (baddeleyite) and a glass-like phase which was interpreted as quench melt texture in

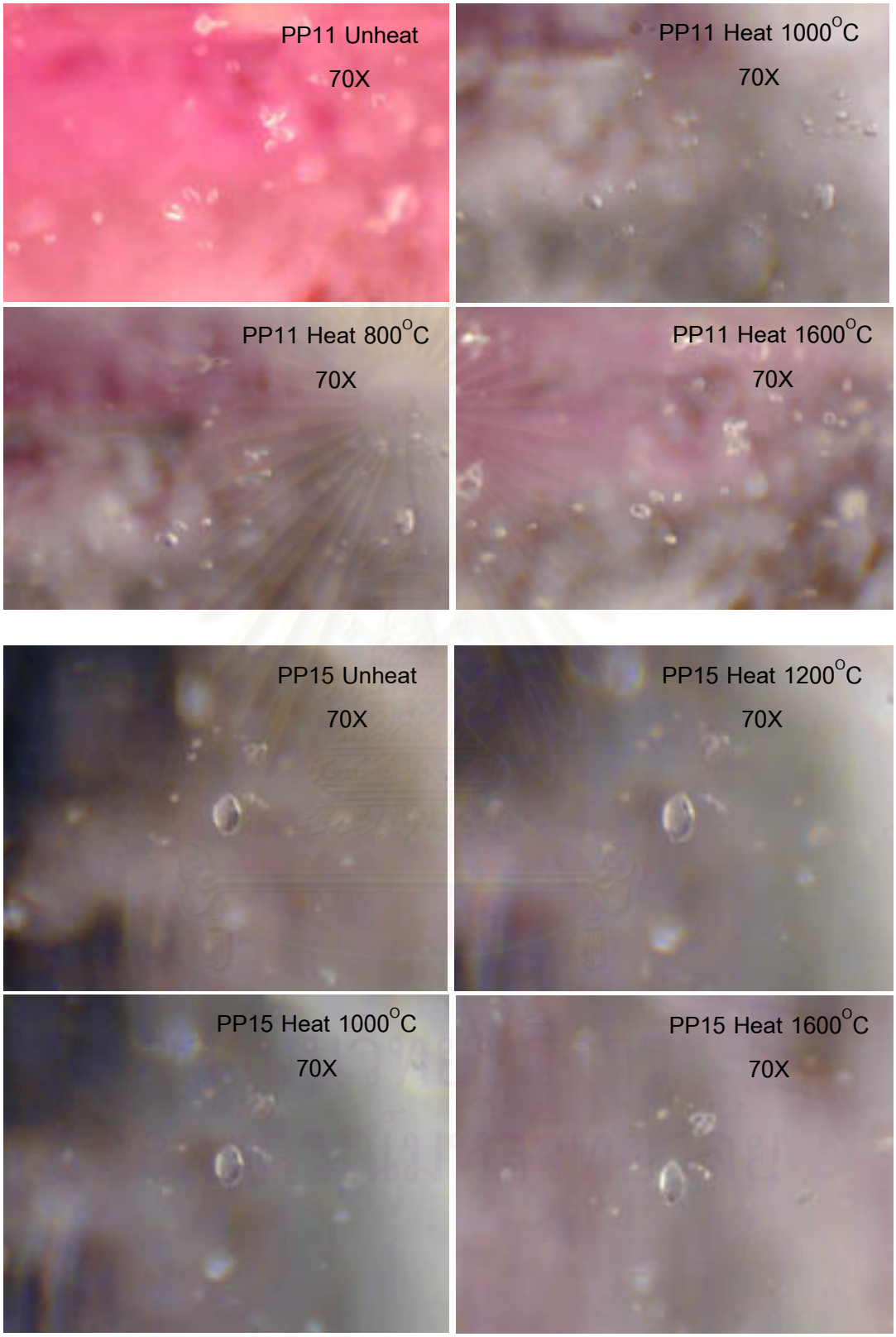

Figure 5.10 Most zircon inclusions in these two sapphire samples were still unchanged after the step-heating from 800°C to 1600°C, each step was hold for 1 hour soaking time.

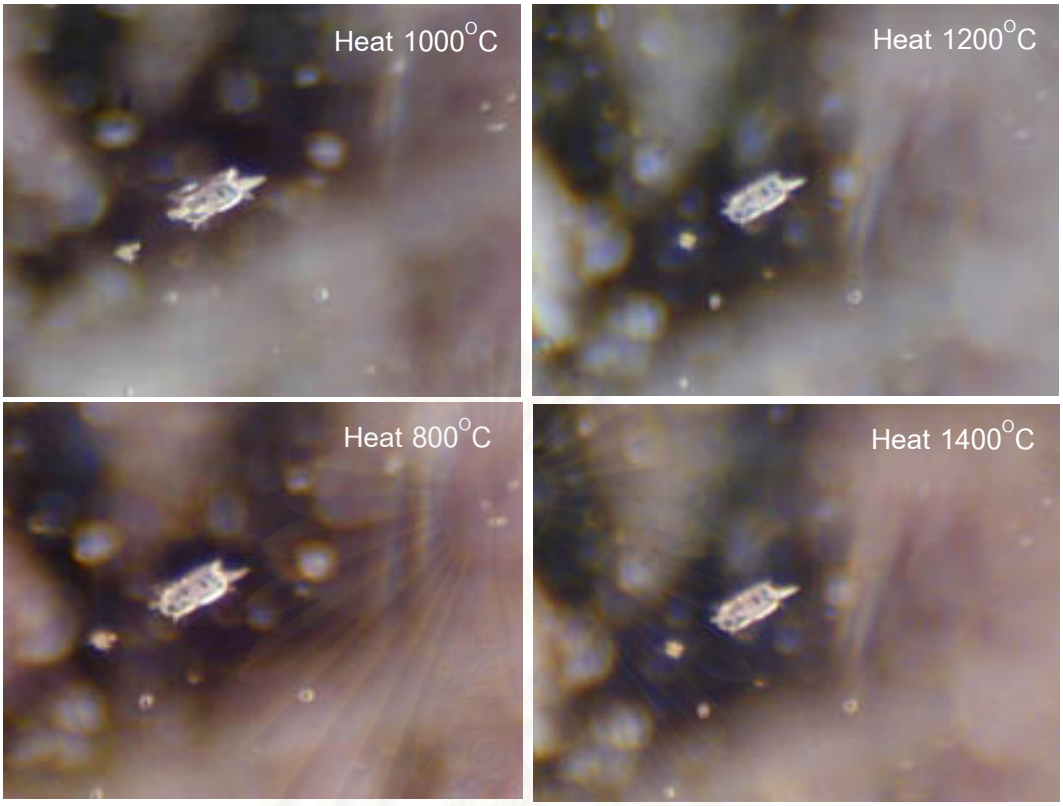

Figure 5.11 A zircon inclusion with slight tension crack was still unchanged after the step-heating from 800°C to 1600°C (sample no. PP15, 70X).

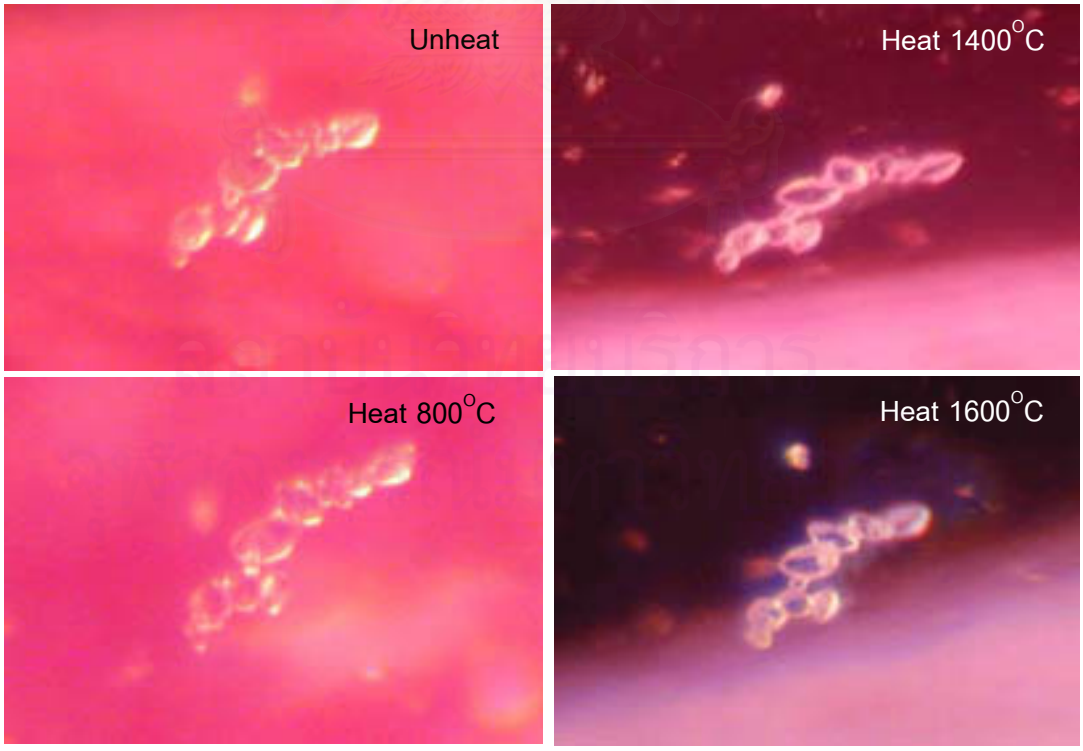

Figure 5.12 A cluster of zircon inclusions was still unchanged after the step-heating from 800°C to 1600°C (sample no. PP6, 140X).

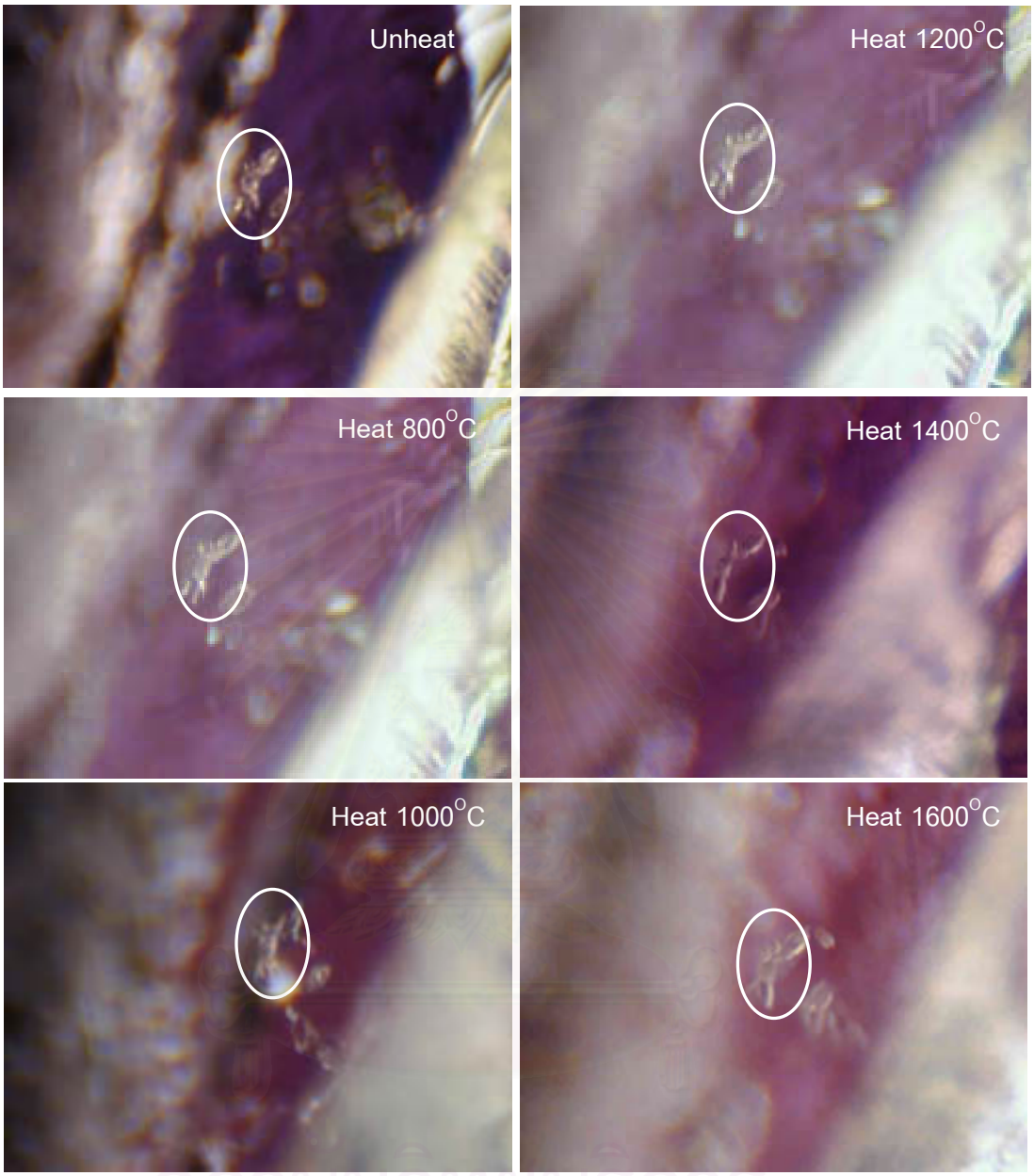

Figure 5.13 Another cluster of zircon inclusions with slight tension disc (in circle) was still unchanged after the step-heating from 800°C to 1600°C (sample no. P16, 70X).

สถาบันวิทยบริการ
จุฬาลงกรณ์มหาวิทยาลัย

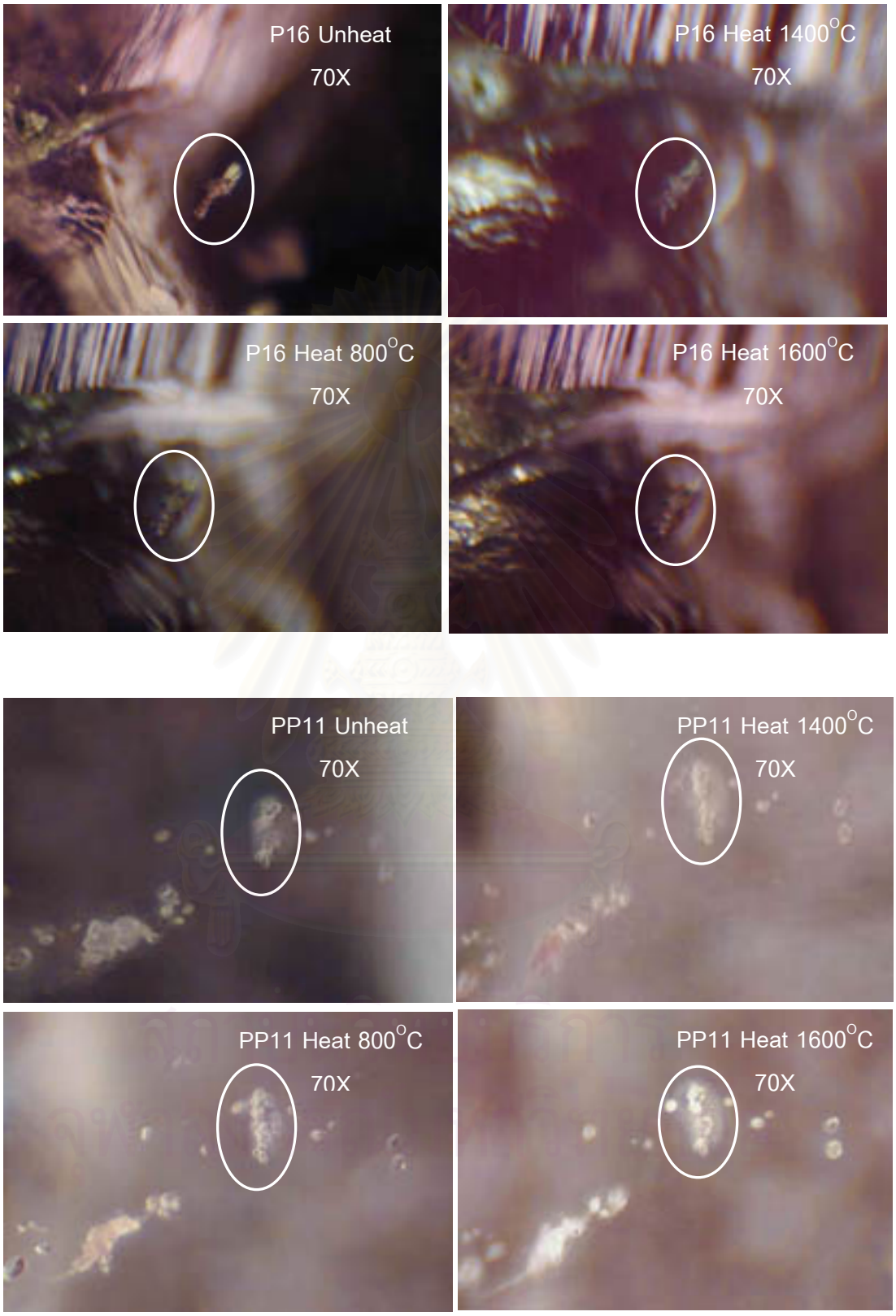

Figure 5.14 Many clusters of zircon inclusions with tension cracks (in circle) were still unchanged after the step-heating from 800°C to 1600°C.

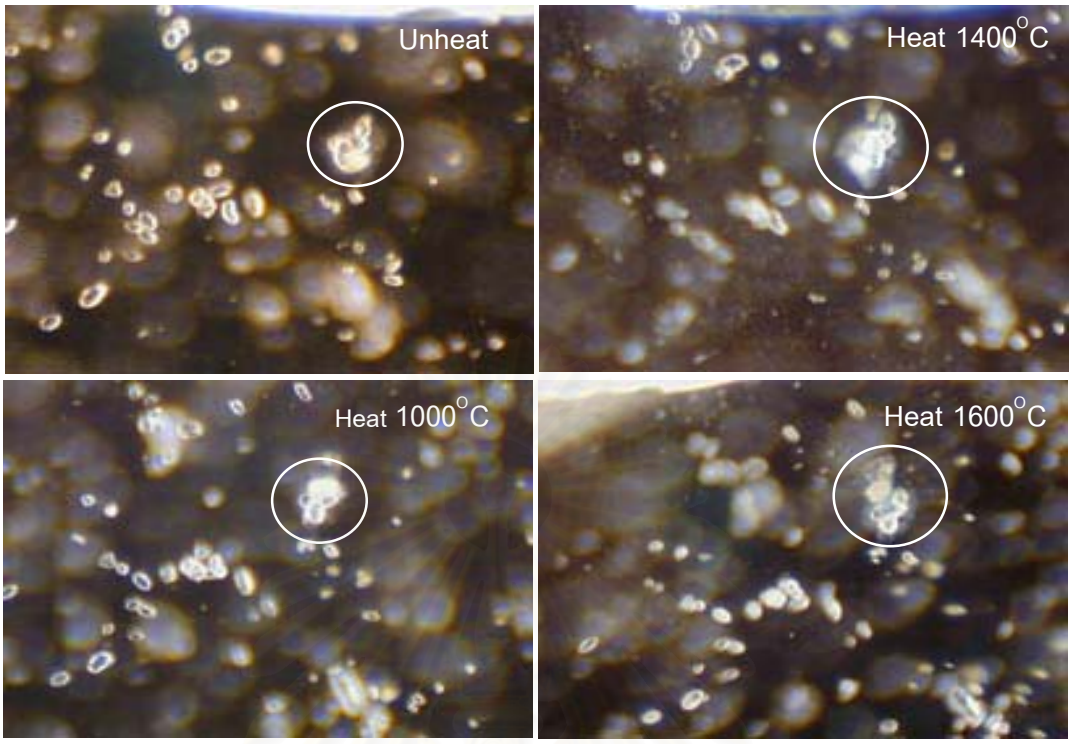

Figure 5.15 Most of individual zircon inclusions were still unchanged after the step-heating from 800°C-1600°C whereas the zircon cluster (in circle) showed slight development of tension crack after heating up to 1000°C. When re-heating up to 1400°C and 1600°C, this tension crack became more obvious (sample no. P6, 70X).

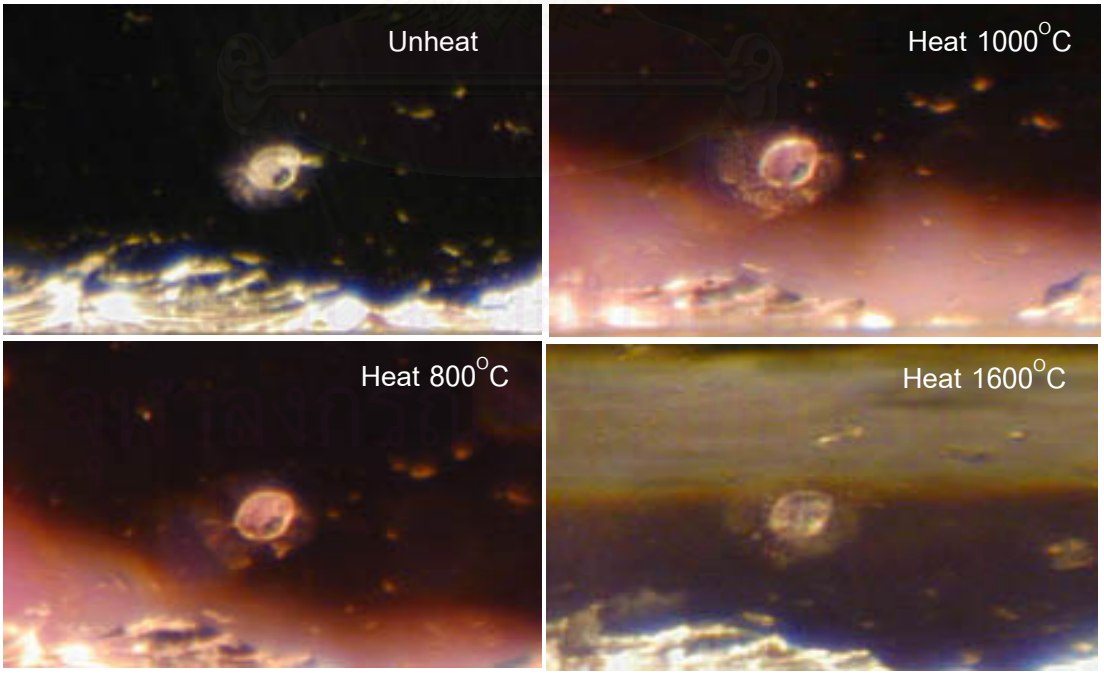

Figure 5.16 A zircon inclusion with slight tension crack was still unchanged after heating to 800°C. When re-heating up to 1000°C-1600°C, this tension crack was obviously expanded (sample no. P5, 140X).

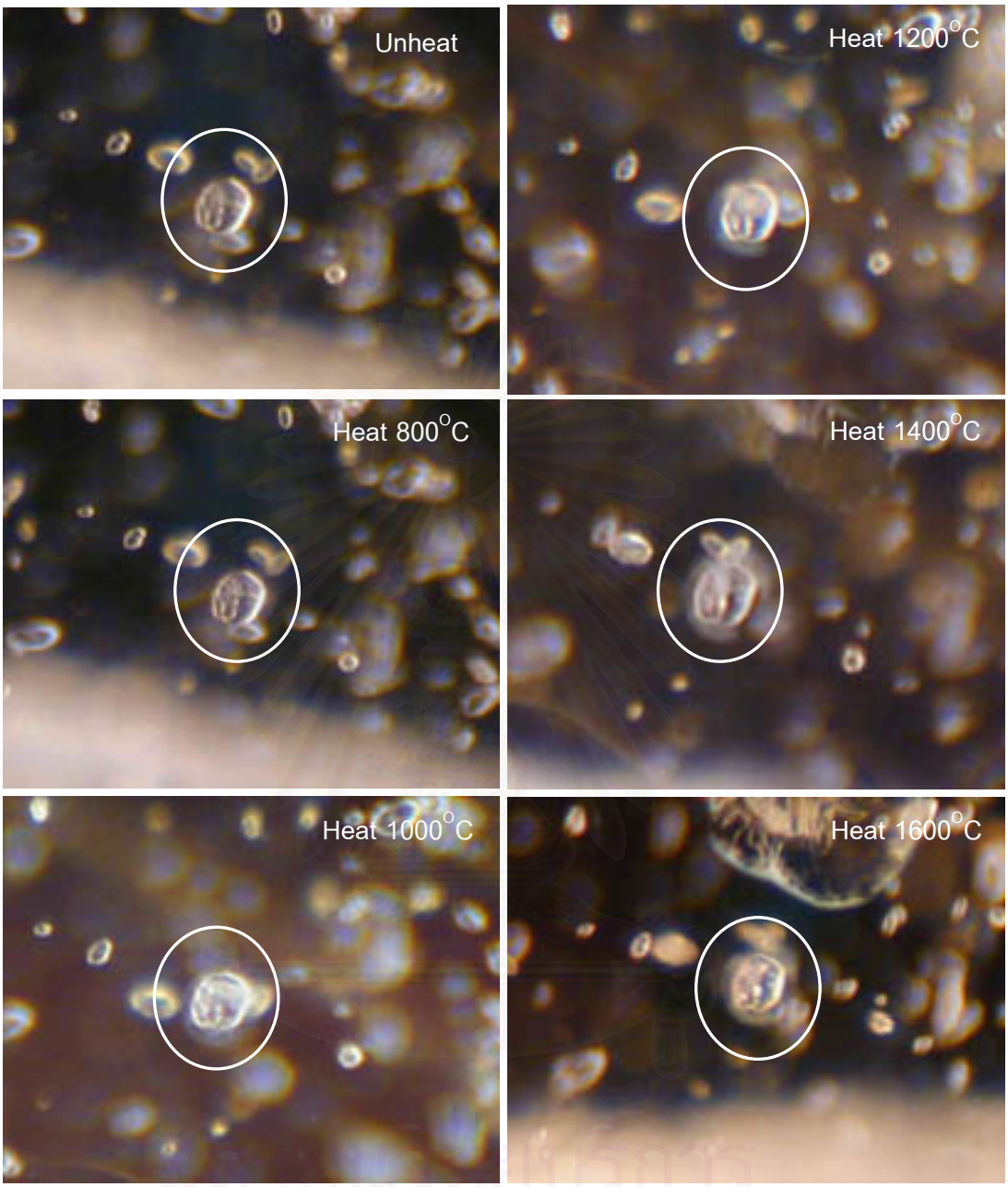

Figure 5.17 A relatively large and clear zircon inclusion (in circle) was still unchanged after heating at 800°C. However, when re-heating up to 1000°C, the crystal began to alter into whitish, cloudy appearance (turbid) with slight development of tension crack. The tension crack became more obvious after re-heating up to 1400°C. The crystal showed stronger decomposition after re-heating up to 1600°C (sample no. P6, 70X).

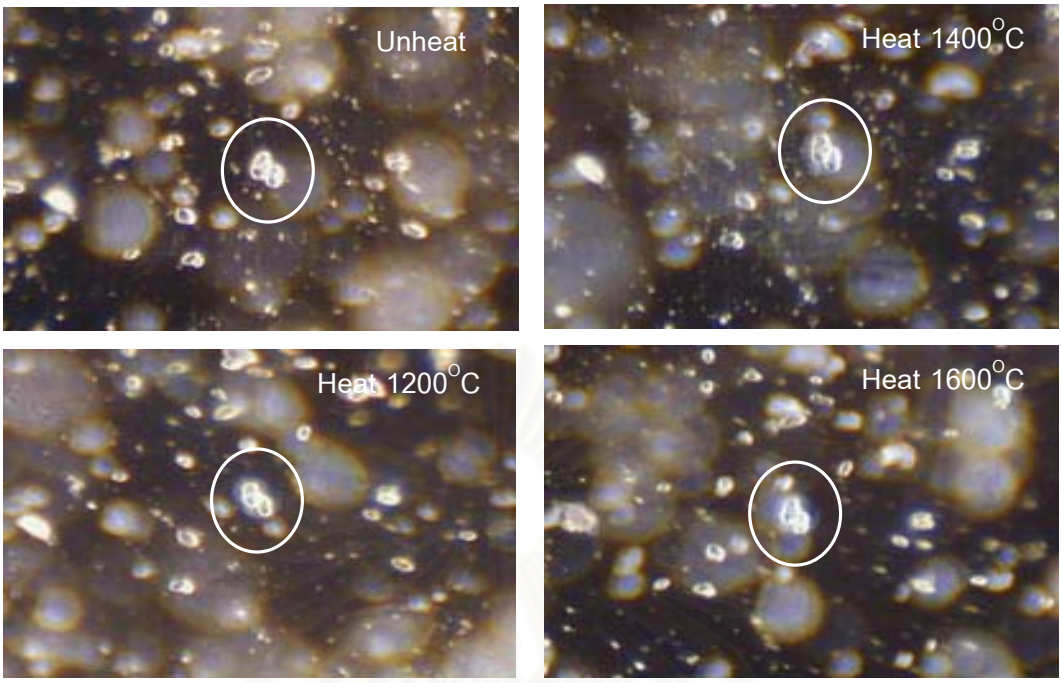

Figure 5.18 Zircon inclusions (in circle) showed the development of tension crack after heating up to 1200°C. When re-heating up to 1600°C, they began to decompose into whitish, cloudy appearance (turbid) with obvious tension crack (sample no. P6, 70X).

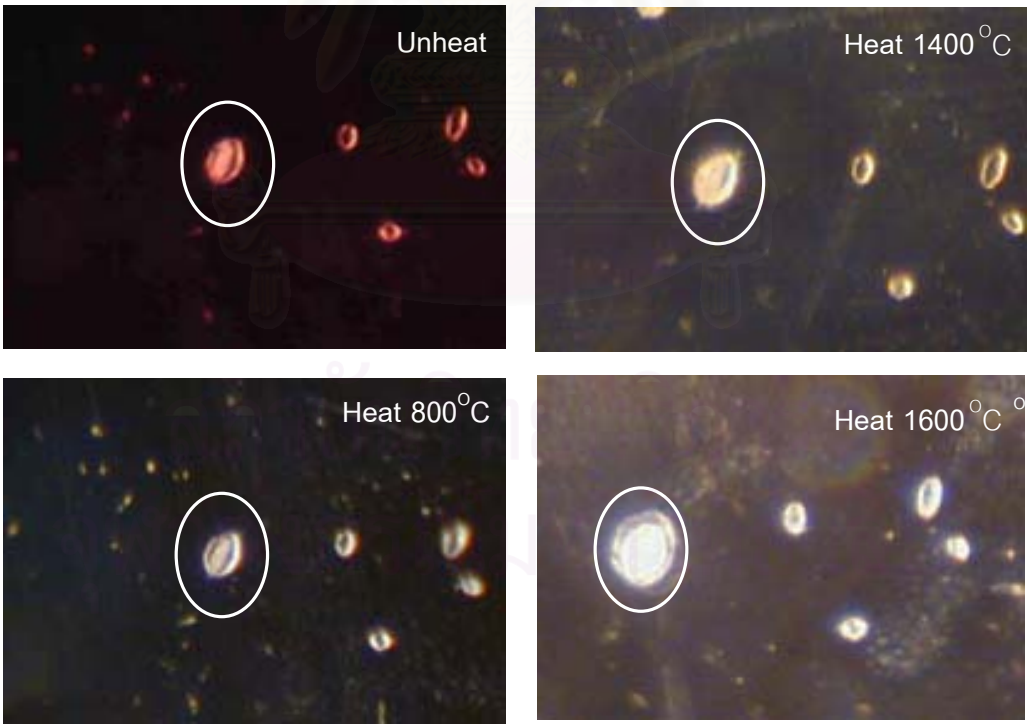

Figure 5.19 Most zircon inclusions were still unchanged after the step-heating from 800°C to 1600°C except the crystal in circle began to alter with slight development of tension crack after heating up to 1400°C. When re-heating up to 1600°C, it was obviously altered into whitish, cloudy appearance (turbid) with well developed tension crack surrounding it (sample no. LP9, 140X).

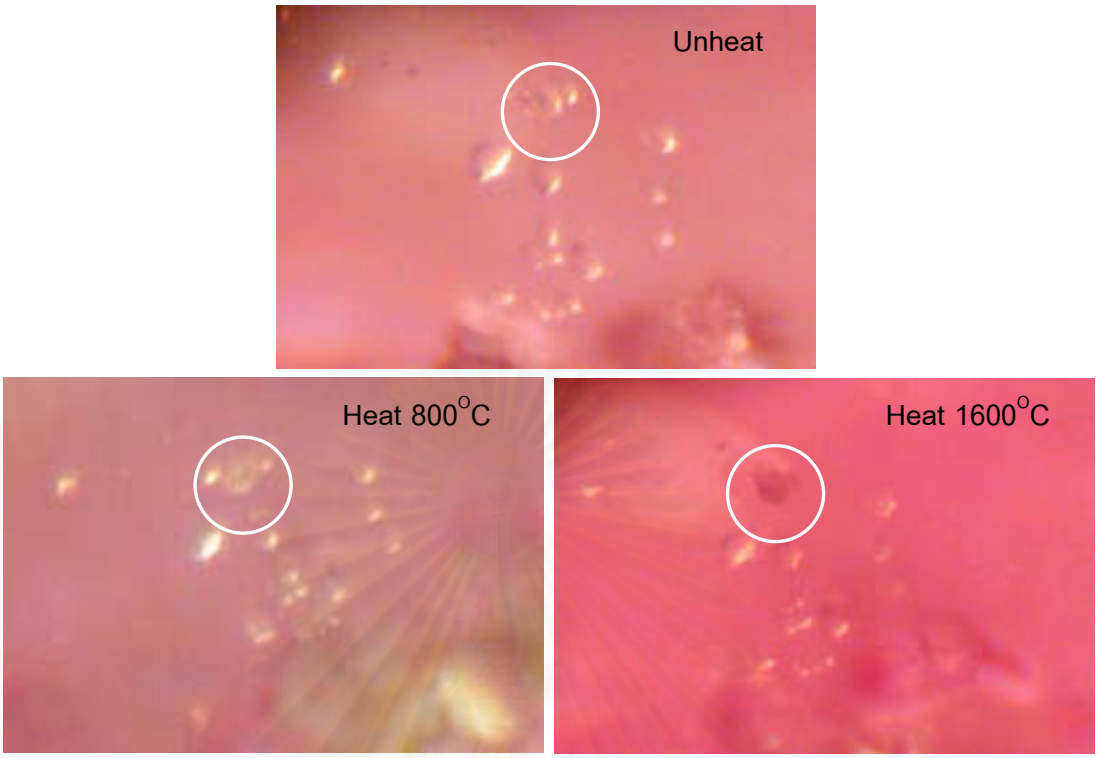

Figure 5.20 Most of the zircon inclusions were still unchanged after the step-heating from 800°C to 1600°C except some crystals in circle appear turbid after heating at 1600°C (sample no. PP6, 140X).

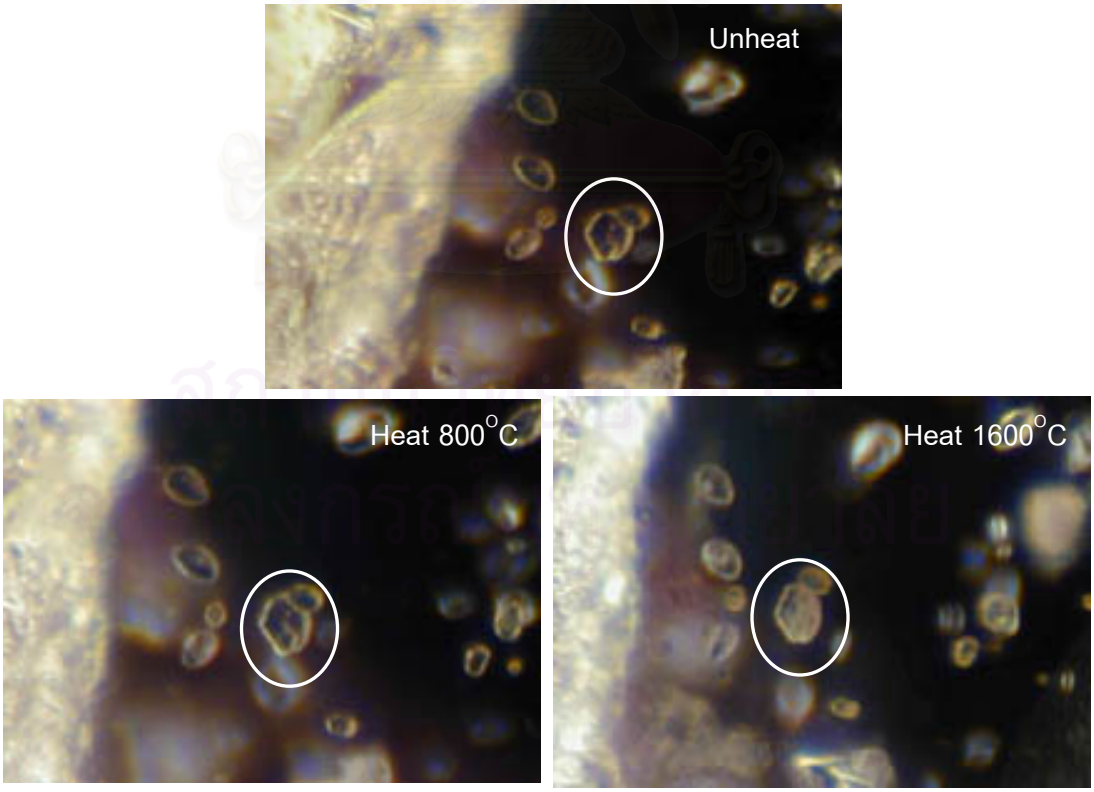

Figure 5.21 Most of the zircon inclusions were still unchanged after the step-heating from 800°C to 1600°C except some crystals in circle appear turbid after heating at 1600°C (sample no. LP3, 140X).

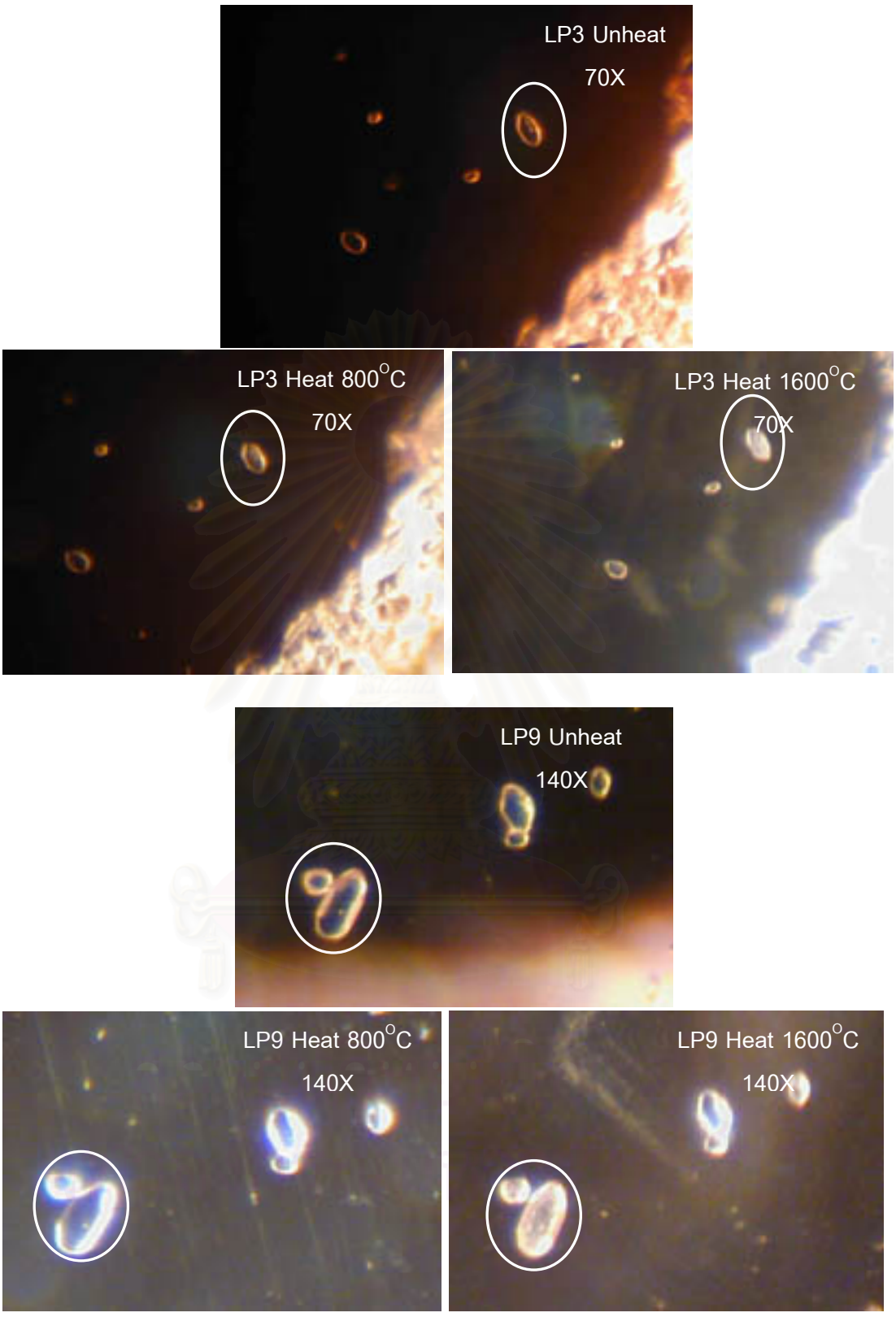

Figure 5.22 Most of the zircon inclusions were still unchanged after the step-heating from 800°C to 1600°C except some crystals in circle appear turbid after heating at 1600°C.

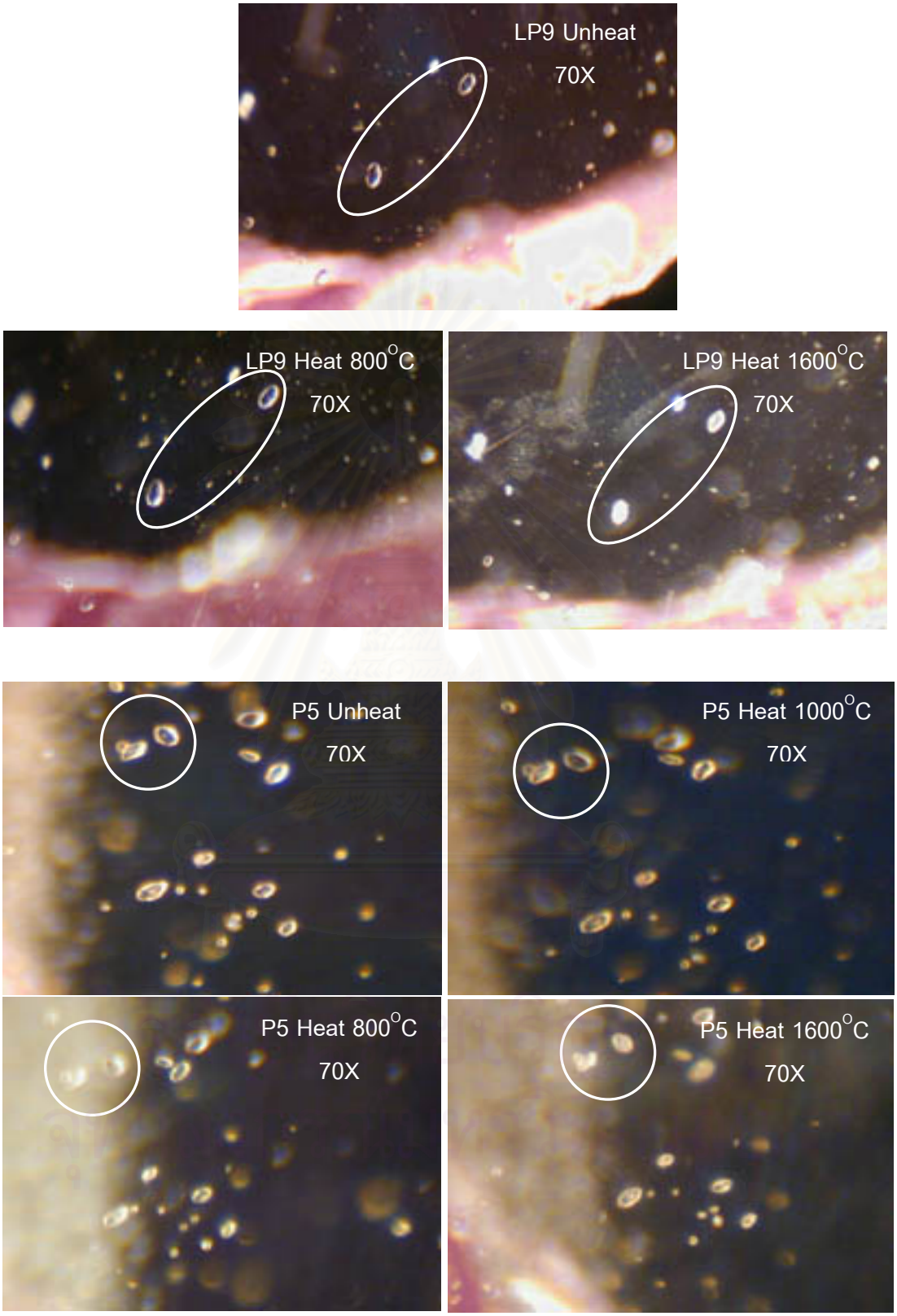

Figure 5.23 Most of the zircon inclusions were still unchanged after the step-heating from 800°C to 1600°C except some crystals in circle appear turbid after heating at 1600°C.

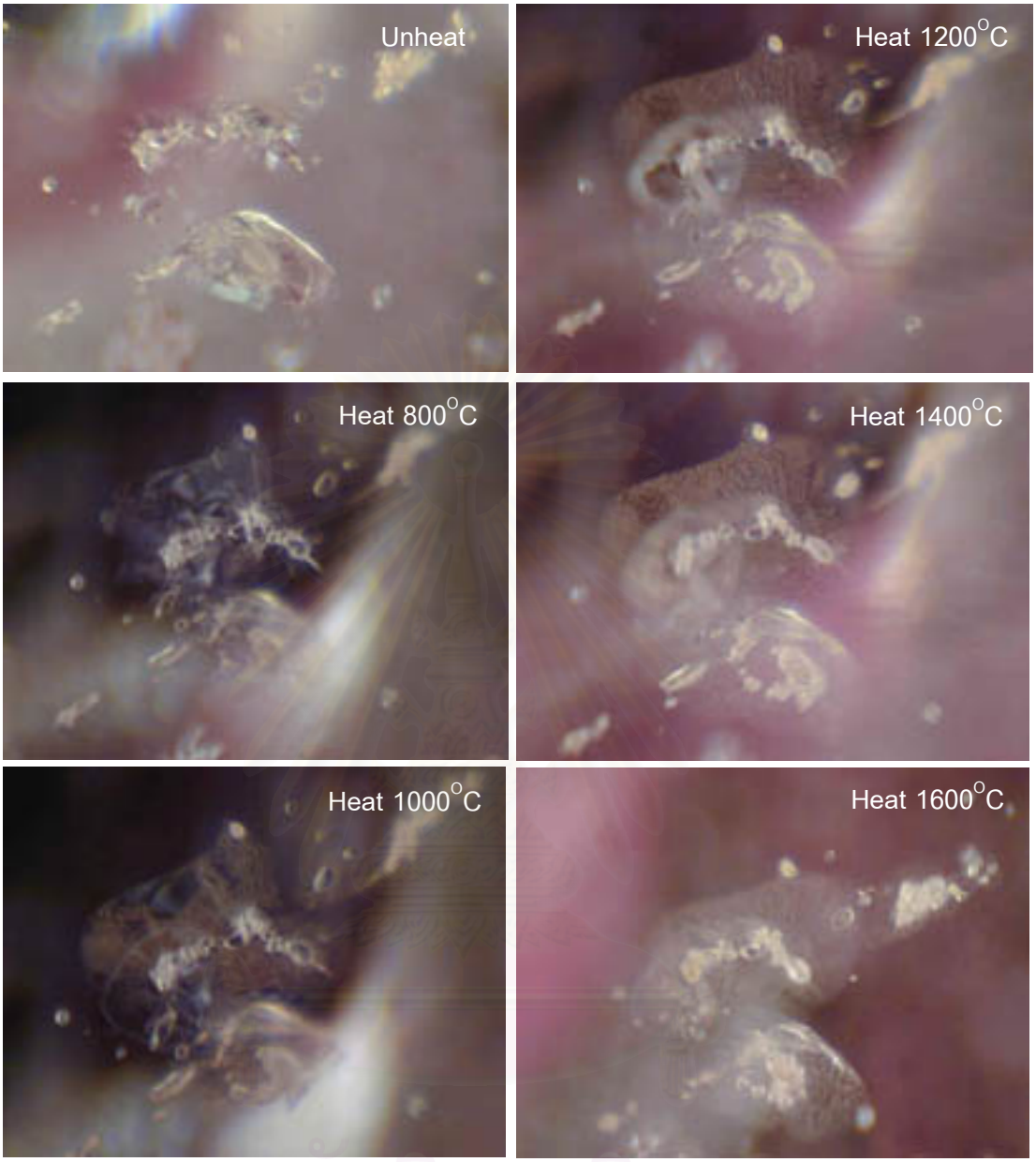

Figure 5.24 Showing zircon clusters with minor tension discs before heating. The tension discs were noticeably expanded after heating at 800°C and became more obvious after re-heating at higher temperatures. It should also be noted that some crystals in zircon clusters appear turbid after heating at 1200°C. The decomposition of those zircon crystals became more pronounced after re-heating to higher temperatures (sample no. PP11, 70X).

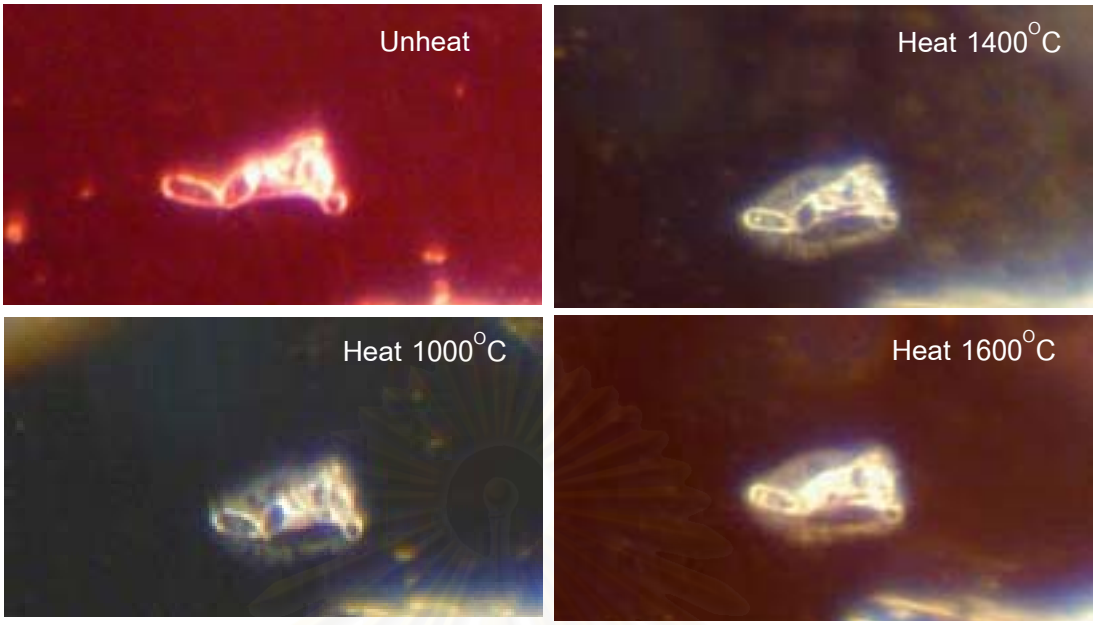

Figure 5.25 A zircon clusters was still unchanged after heating at 800°C. The tension discs began to develop after re-heating to 1000°C. After re-heating from 1400°C to 1600°C, these tension discs became more obvious (sample no. PP4, 140X).

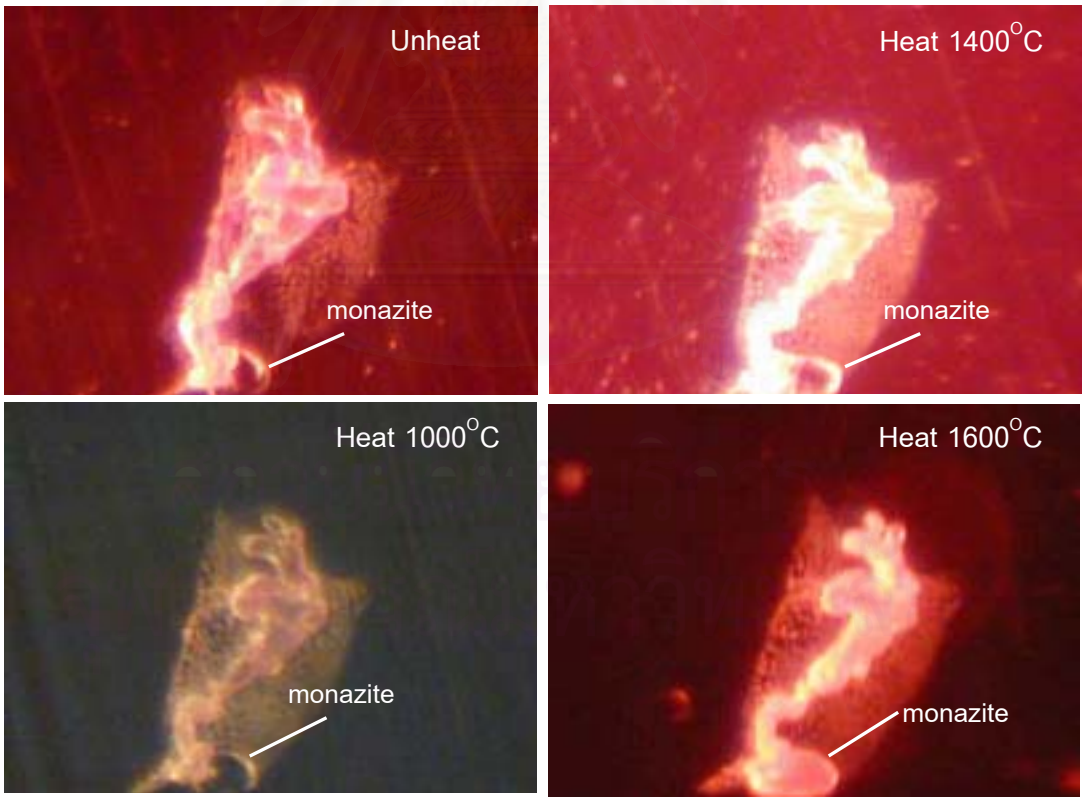

Figure 5.26 A zircon cluster was still unchanged after heating at 800°C but showed a strong development of tension discs after re-heating from 1000°C to 1600°C. Furthermore, most crystals in the cluster appear turbid after heating up to 1400°C while a monazite inclusion began to alter at 1600°C (sample no. PP4, 140X).

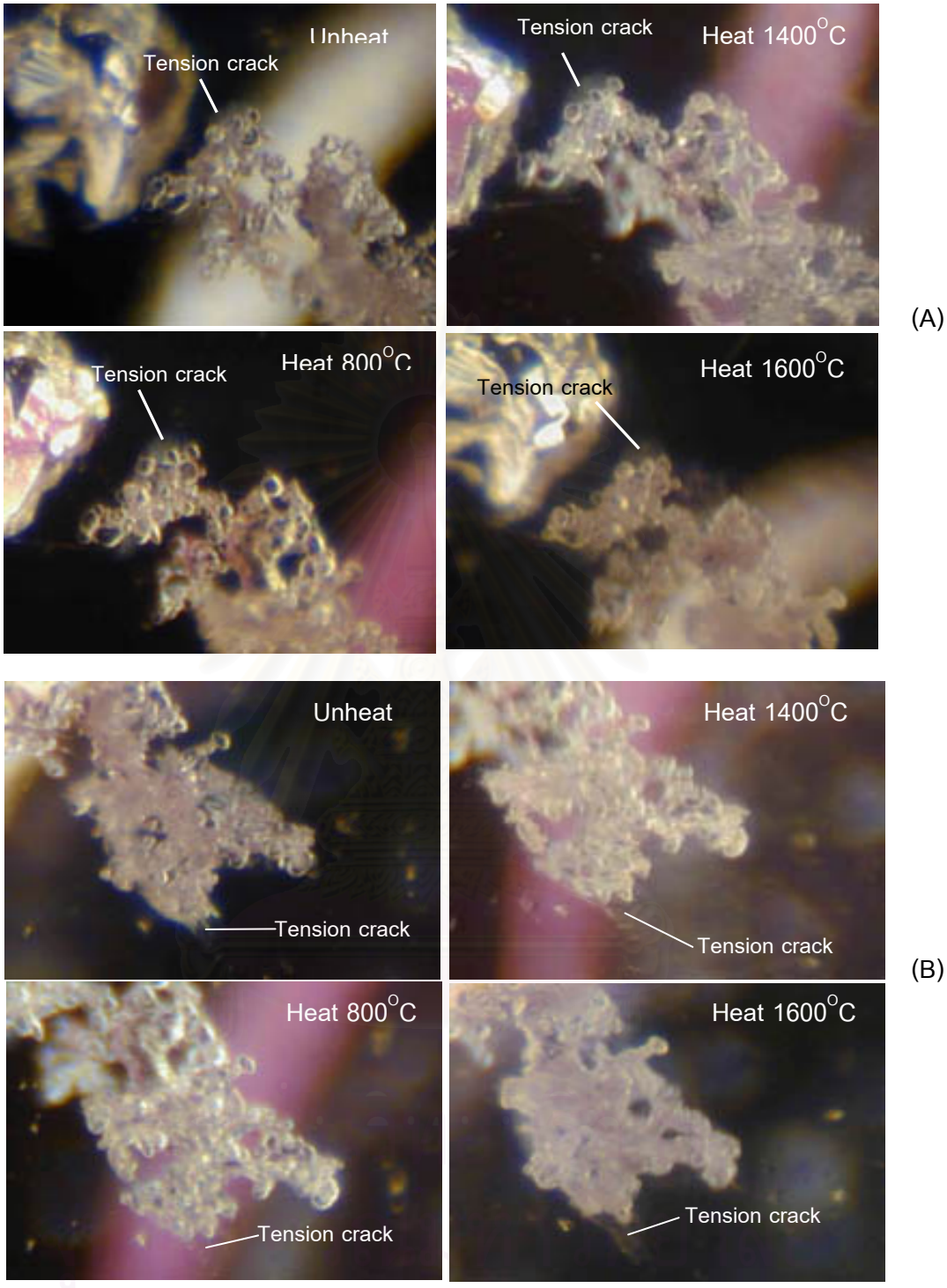

Figure 5.27 Showing zircon clusters with slight tension crack before heating. After heating at 800°C to 1200°C, they were still unchanged (sample no. PP6, 140X).

(A) When re-heating up to 1400°C, some zircon crystals in the clusters began to decompose into whitish cloudy appearance and became obviously decomposed after re-heating up to 1600°C.

(B) After re-heating up to 1400°C, tension crack was extended and some zircon crystals in the clusters began to decompose. These crystals were obviously decomposed when heated up to 1600°C.

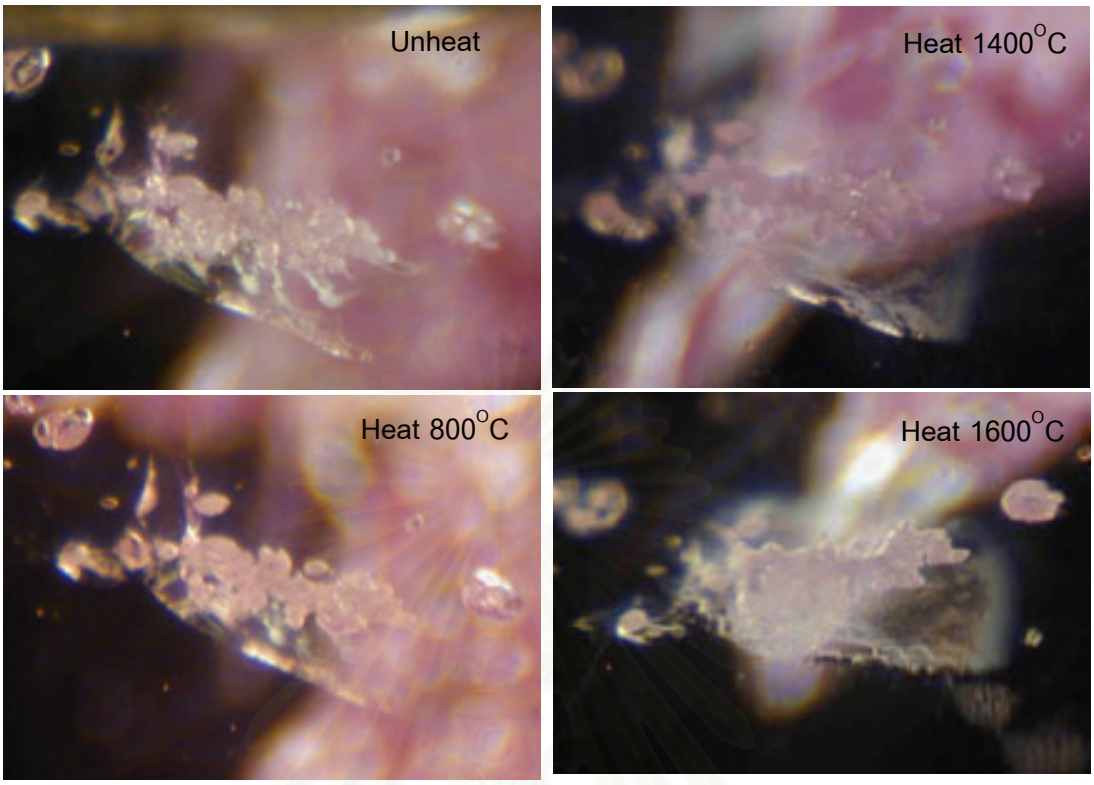

Figure 5.28 Showing zircon clusters with slight tension crack before heating. After heating at 800°C to 1200°C, they were still unchanged. When re-heating up to 1400°C, some zircon crystals in the clusters began to decompose into whitish cloudy appearance and the tension crack was expanded. After re-heating up to 1600°C, the crack appeared more expansive and the crystals clearly turn turbid (sample no. LP3, 70X).

สถาบันวิทยบริการ
จุฬาลงกรณ์มหาวิทยาลัย

the Al_2O_3-ZrO_2-SiO_2 system. Such system was inferred to have occurred above the eutectic temperature of approximately 1750°C. However, we have observed the alteration of some zircon inclusions at much lower temperature in this study. It is possible that such alteration may occur in the intermediate or low (metamict) zircon grains which were more susceptible to the thermal breakdown than the high zircon. This could explain why many zircon inclusions were still unchanged while the others appeared turbid when heated up to 1600°C. It should also be noted that the recognition of the phase change (turbid appearance) in zircon inclusions can provide a useful criterion for detecting the heat-treatment of the host sapphire as it can not be observed in unheated stones. The tension disc around zircon inclusions is however not a good criterion of heat-treatment as it can also be observed in unheated samples.

2. One monazite inclusion was slightly decomposed after the step-heating up to 1600°C (Figure 5.26). Another crystal, however, was still unchanged after the step-heating from 800 °C to 1600°C (Figure 5.29).

3. The mica inclusions were partially altered or appeared slightly turbid with small development of tension crack after heating at 1000°C. The decomposition and tension disc became distinct when re–heating up to 1400°C-1600°C (Figures 5.30 and 5.31).

4. The rutile inclusions occur as the black to dark brown crystals and as thin and long needles, known as rutile silk or rutile needles. The black-dark brown crystals changed to red color with slight development of tension crack after heating at 800°C. When re-heating at higher temperatures they became obviously red color with strong development of tension cracks and also with melted crystal boundary (Figures 5.32 and 5.33).

Rutile silk or needles are long and short tubes which oriented in 3 directions approximately 60°/120° angles. Because rutile silk or needles can fully dissolved in the host corundum, when heated at about its melting point (1825°C) and cooled rapidly. Before the dissolution complete, it passes through several

transformation stage, starting about 1600°C (lowest dissociation point of the rutile) (Themelis, 1992). In this study when heating at 800°C to 1400°C for one hour, rutile silk was still unchanged. After heating at 1600°C for one hour incomplete or partial dissolution of the rutile needles can be observed in host corundum creating certain interrupted dot-like, or hyphen-like pattern, known as dotted needles or resorbed rutile silk (Figures 5.34). However rutile needles in some sapphires can dissolved completely in the host sapphires after heating at 1600 °C (Figure 5.35).

5. Milky or dust zone became clearer when heated at 1600 °C (Figure 5.36).

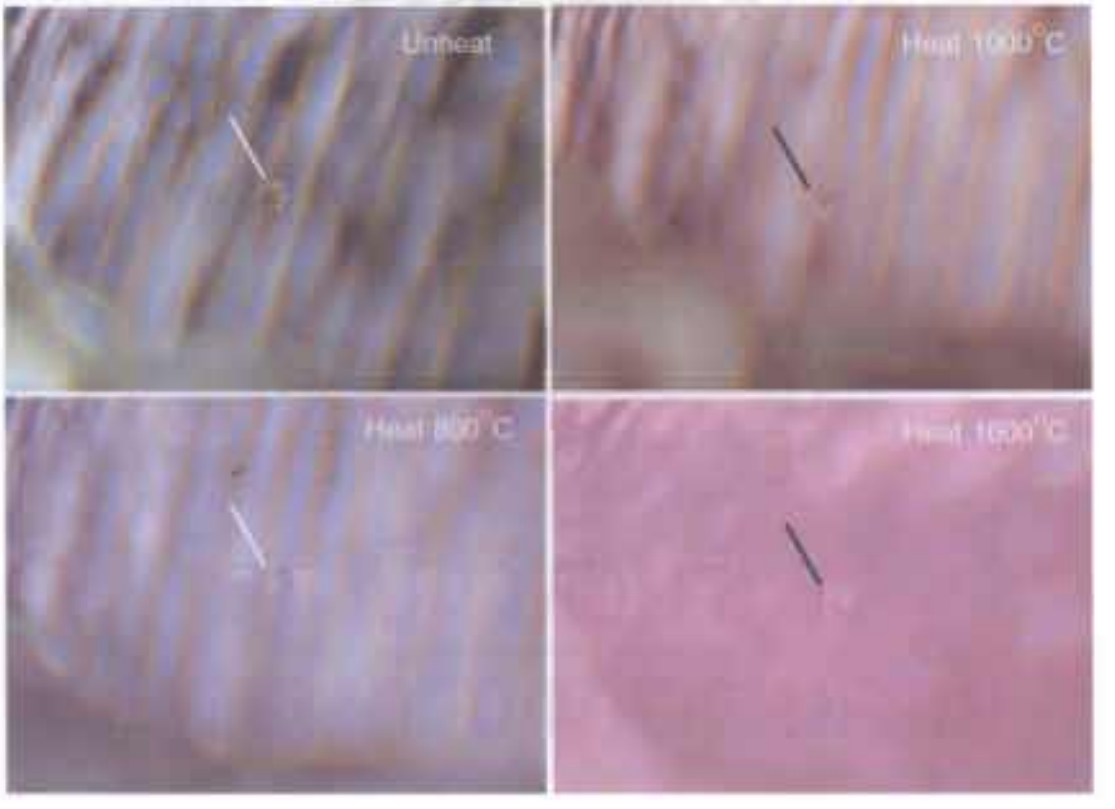

Figure 5.29 A monazite inclusion was still unchanged after the step-heating from 800°C to 1600°C (sample no. P16, 70X).

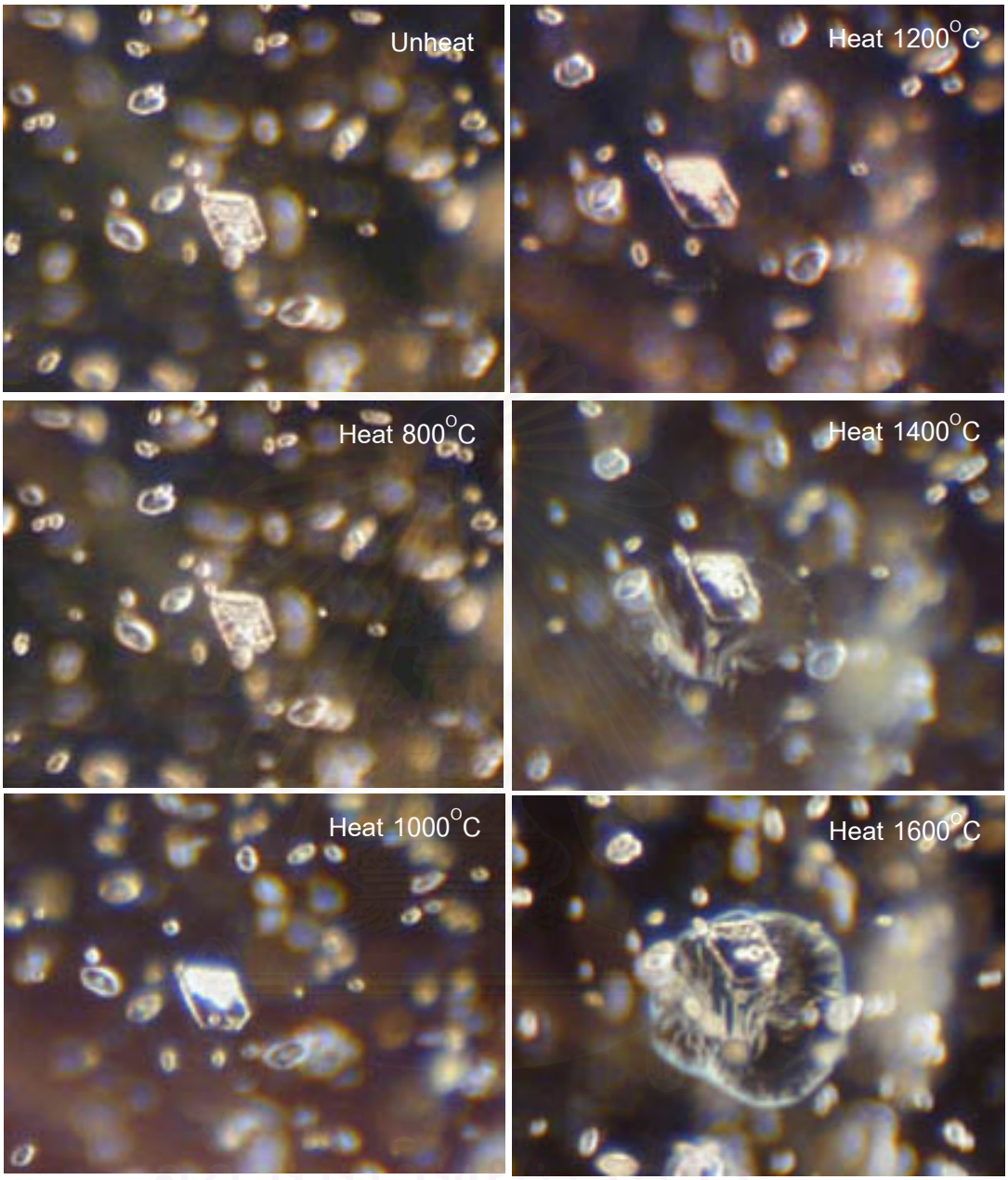

Figure 5.30 A mica inclusion was still remain the same after heating at 800°C. When re-heating up to 1000°C, the crystal began to alter and were obviously altered at higher temperatures. The tension crack start to form around the inclusion at 1200°C, it became more and more obvious when re-heating up to 1400°C and 1600°C (sample no. P6, 70X).

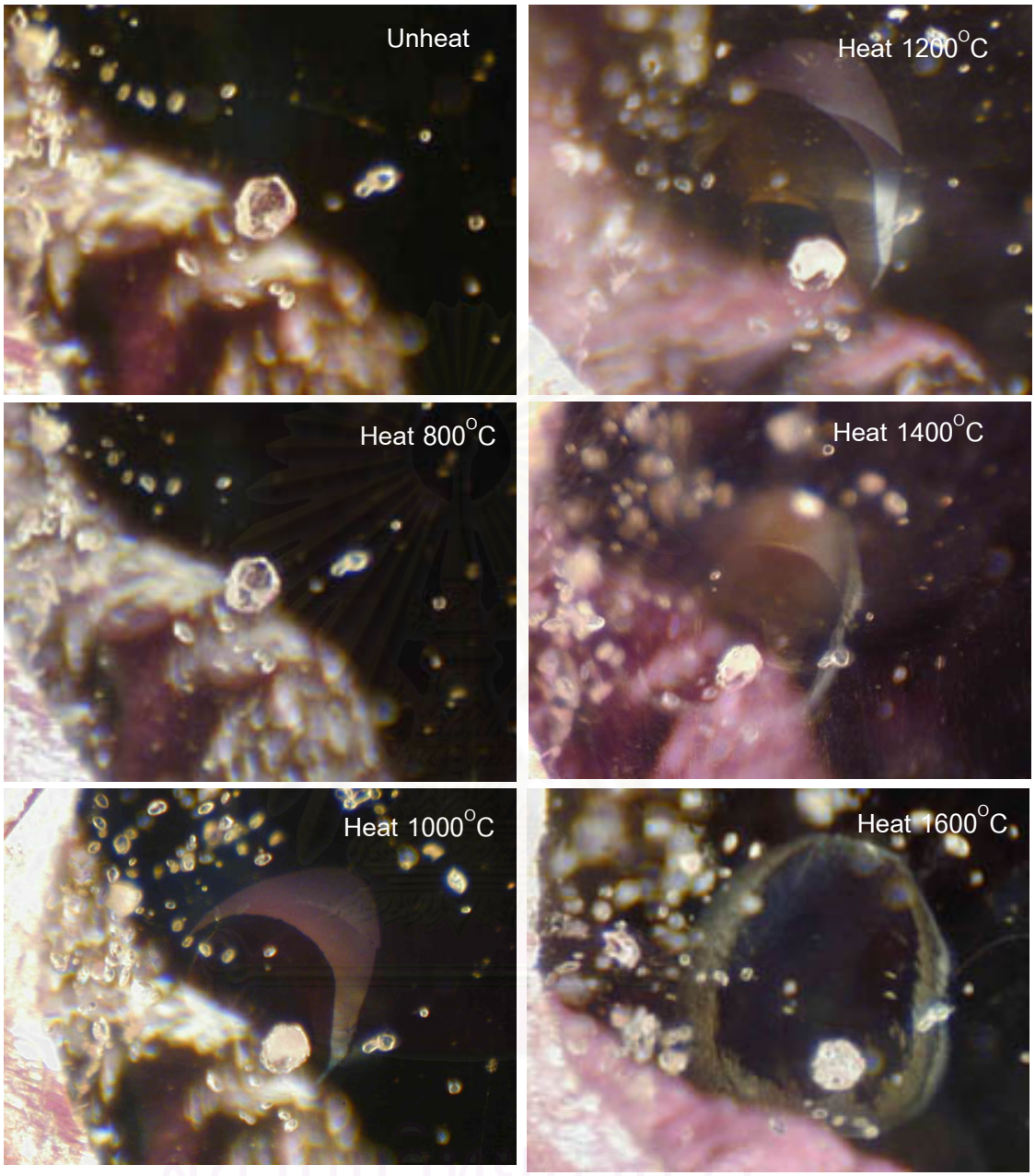

Figure 5.31 Another mica inclusion was still unchanged after heating at 800°C. When re-heating up to 1000°C, it was partially altered or appeared slightly turbid with small development of tension crack. The alteration and tension crack became more and more obvious when re-heating at 1200°C, 1400°C and 1600°C (sample no. LP3, 70X).

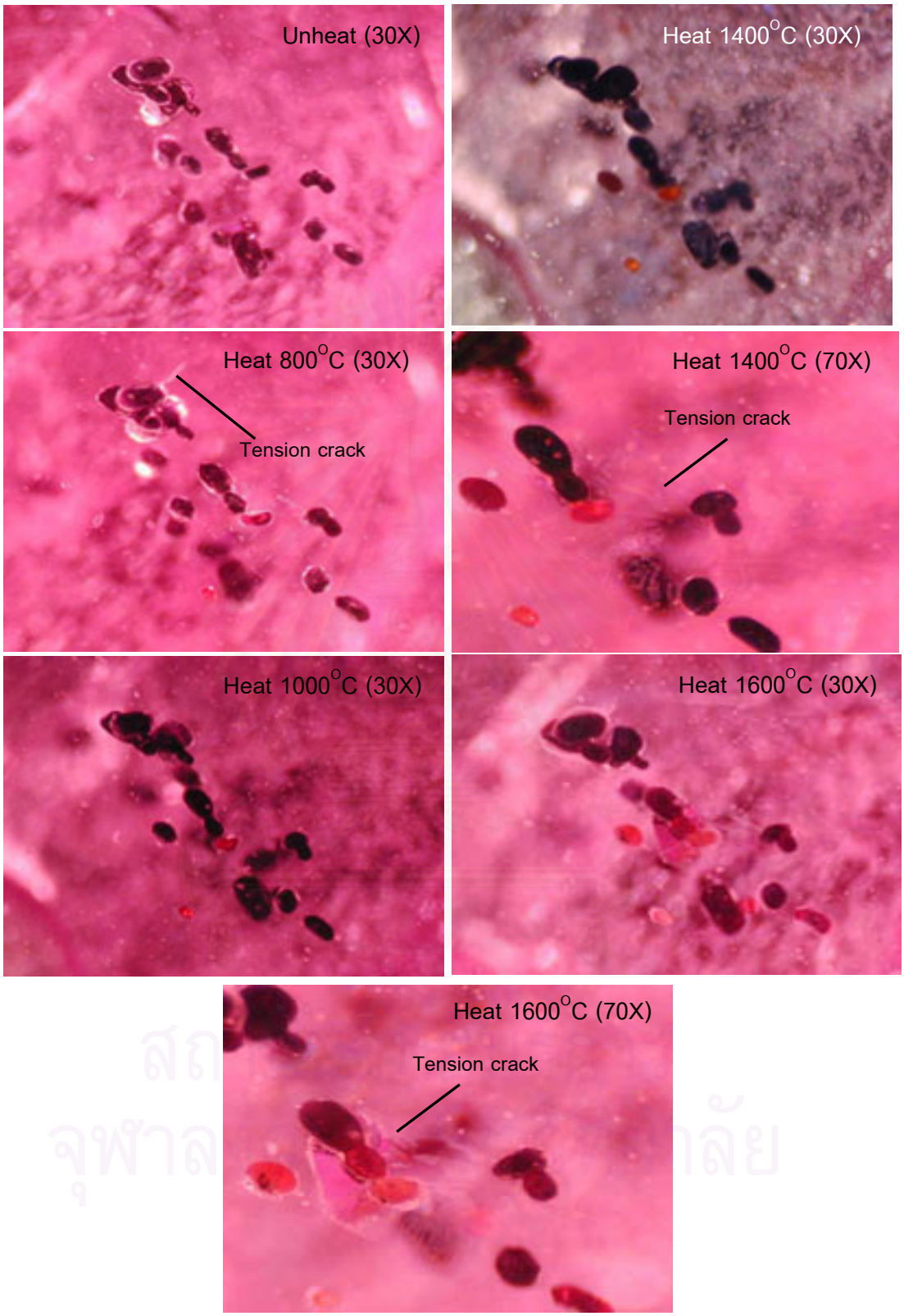

Figure 5.32 Some rutile inclusion changed color from dark brown-black to red with slight development of tension crack after heating at 800°C. When re-heating up to higher temperature (1400°C to 1600°C) the red color were more intense and tension cracks became obvious (sample no. PP3).

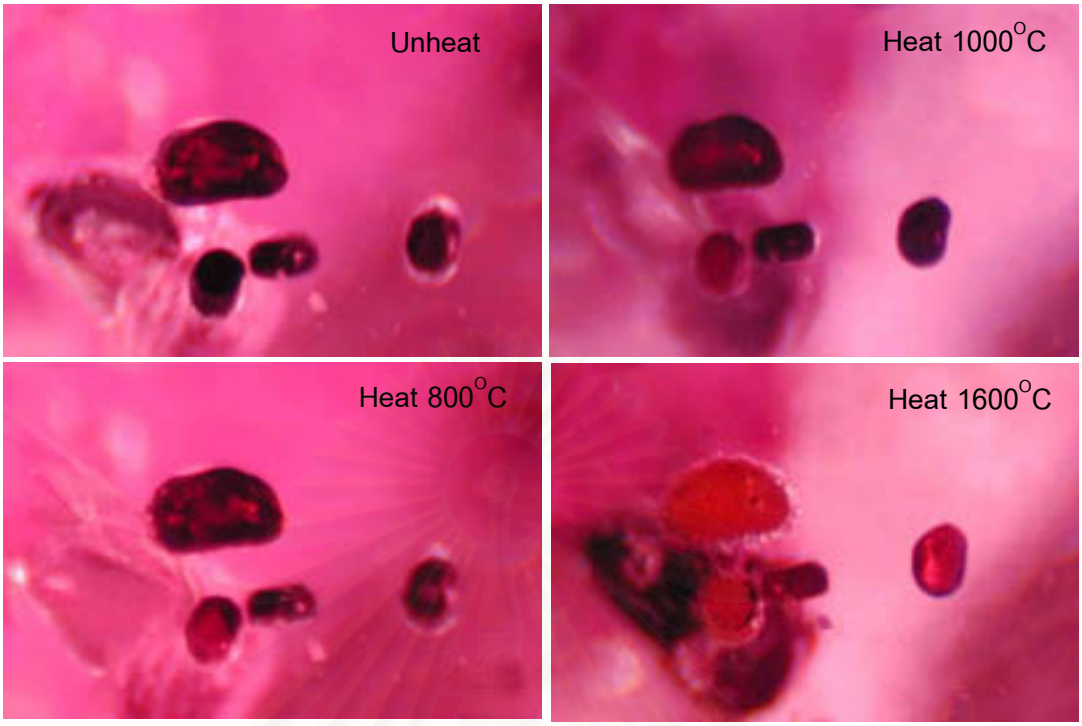

Figure 5.33 Black rutile inclusion slightly changed to red after heating at 800°C. They became obviously red color and formed melted boundary at higher temperatures (sample no. PP3, 70X).

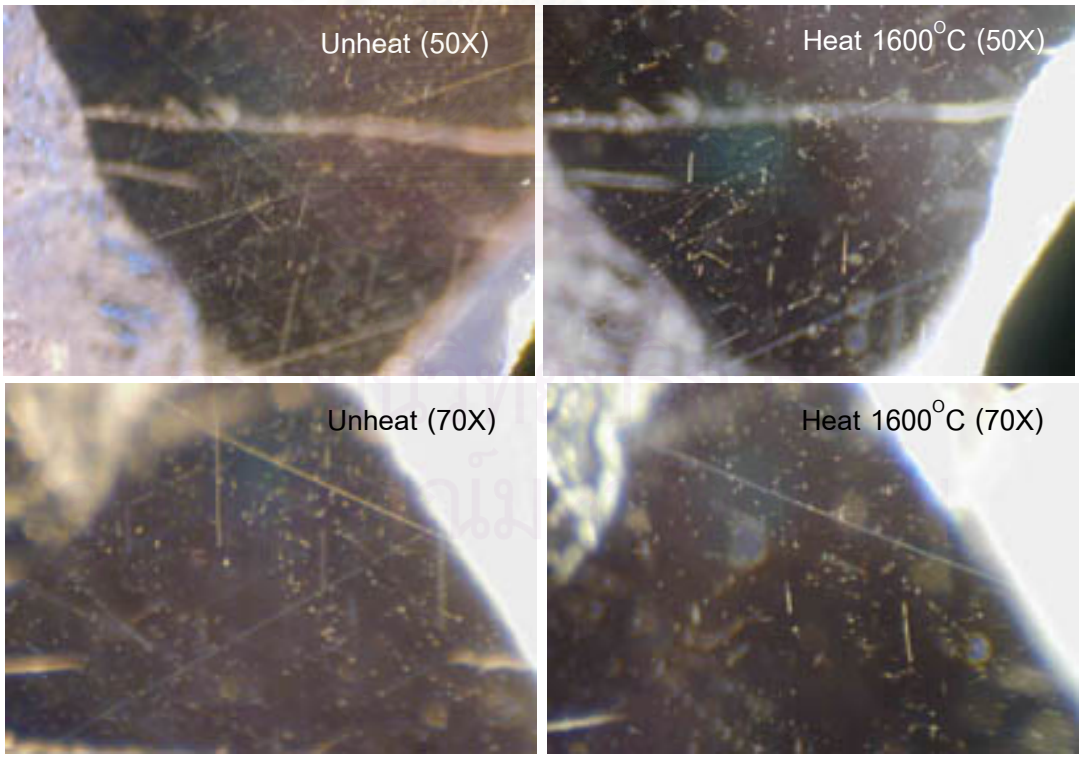

Figure 5.34 Rutile needles intersecting each other at 60°/120° angles was still unchanged after heating at 800°C-1400°C but was partially dissolved in the host sapphire creating dot-like pattern after heating at 1600°C (sample no. MV2).

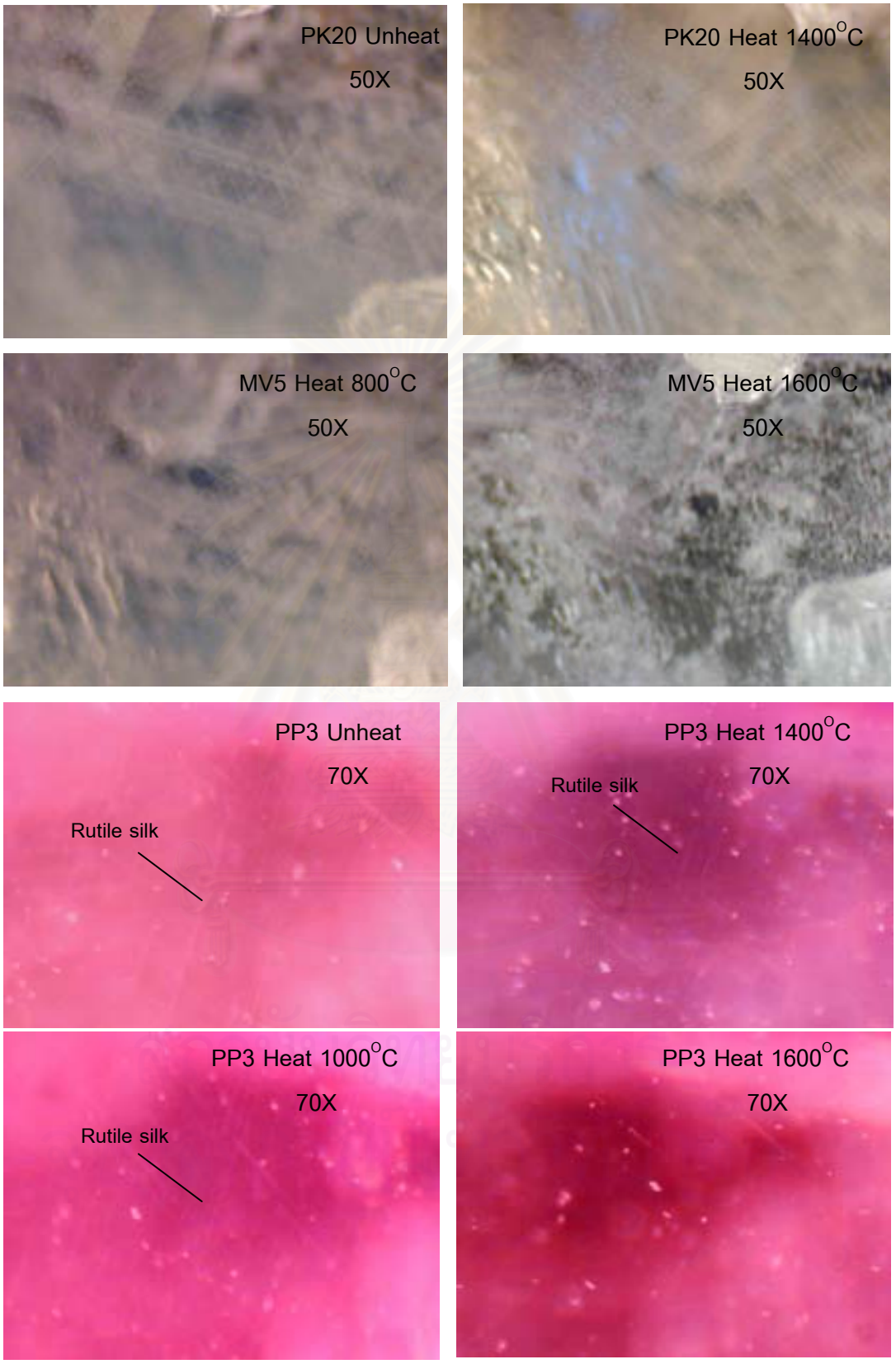

Figure 5.35 Rutile silk or needles completely dissolved in the host sapphire after heating at 1600 °C but was still unchanged after heating at lower temperatures.

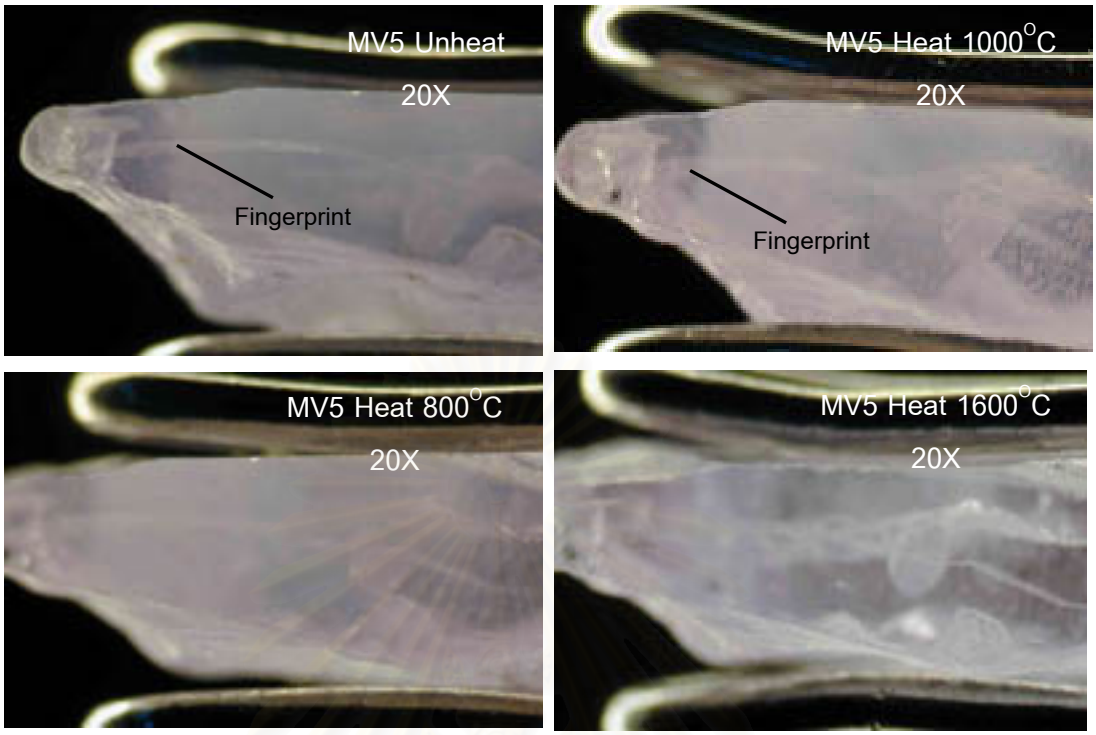

Figure 5.36 Milky or dust zone became clearer when heated at 1600°C.

6. Fingerprints are healed fractures or cracks. When the fluid enters into the host corundum via surface fractures or cracks, which develops in a later stage of the growth process of the corundum. After those fractures are healed it creates inclusions, which are called secondary inclusions. Generally, fingerprints can be observed in unheated and heat-treated sapphires. In some samples, fingerprints were developed after heating at 800°C to 1200°C and more expansive at higher temperatures (Figures 5.37 and 5.38).

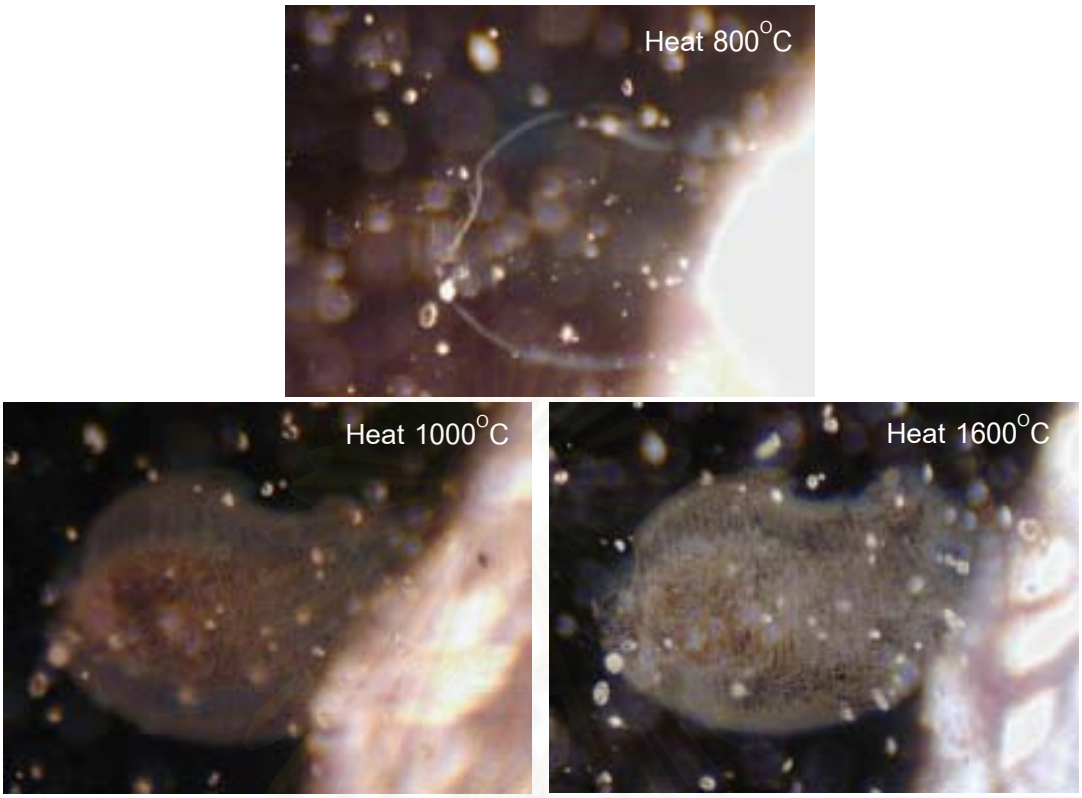

Figure 5.37 Sapphire showed slight development of the fingerprint after heating at 800°C and obviously developed at 1000°C. When re-heating up to 1600°C the fluid inclusion in the fingerprint would be developed into fine pattern (sample no. P6, 70X).

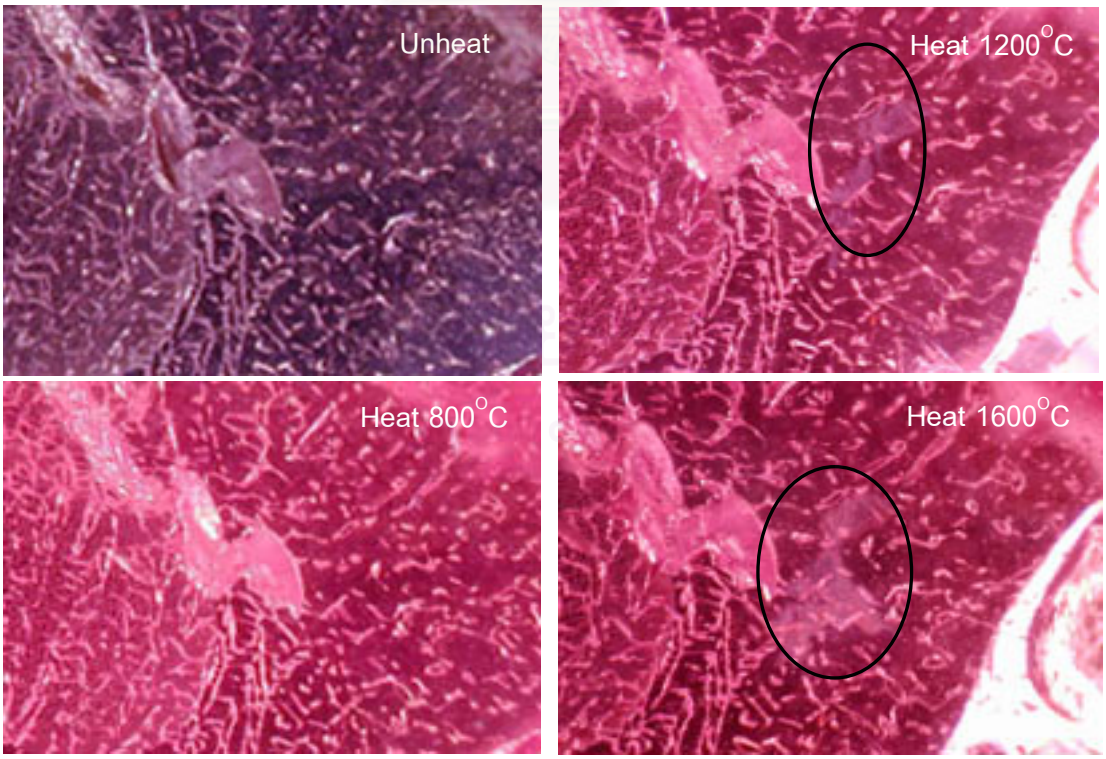

Figure 5.38 Fingerprints in a unheated sapphire were expanded after heating at 1200°C and 1600°C (sample no. PP6, 50X).

FTIR spectra

The FTIR spectra (in % transmittance) of some sapphire samples before and after heating are displayed in Figures 5.39 to 5.46. All FTIR spectra are shown in Appendix V. They show essentially the same pattern. After heating, the H_2O absorption peaks are decreased or disappeared probably due to loosing absorbed water in open fracture or on the surface. All samples (PP6, PP11, PP15, LP3, LP4, LP9, P5 and P16) that do not show OH absorption peak at 3309 cm^{-1} or broad band between 3200 cm^{-1} to 3400 cm^{-1} before heating will also not show this peak or broad band after heating. The very small OH absorption peak or broad band present in some samples (PP3, PP4, PP17, P6, P10, P11, MV2 and MV5) before heating were eliminated after heating. For example, the unheat-treated purplish pink sapphire sample (PP4) shows a weak OH absorption peak at 3309 cm^{-1}. After heating at 1200°C to 1600°C for 1 hour, the purplish overcasted color is reduced and the OH peak disappears (Figure 5.39). The OH peak of pinkish purple sapphire sample (P10) disappears after heating from 1000°C to 1600°C (Figure 5.44). In medium violet sapphire (MV5) the broad band of O-H bonding is disappeared after heating at 800°C to 1400°C (Figure 5.46).

The incorporation of hydrogen in corundum has been a topic studied by many researchers (Eigenmann and Günthard, 1971 and 1972; Eigenmann and others, 1972; Volynets and others, 1972 and 1974; Beran, 1991 cited in Smith, 1995). Most of the previous works reported that the structural bonding of OH groups in corundum have been recorded in verneuil group synthetics of various colors and composition, hydrothermal synthetic rubies and natural corundums, such as Sri Lankan rubies, Montana sapphires, Australian sapphires, Mong Hsu rubies and sapphires from southern Vietnam. The OH absorption peak was much more typically recorded in blue sapphire from basaltic source than ruby or sapphire from metamorphic source. The absorption peak of the OH bonding of hydrothermal synthetic corundum was stronger than other natural and synthetic corundums (Smith, 1995).

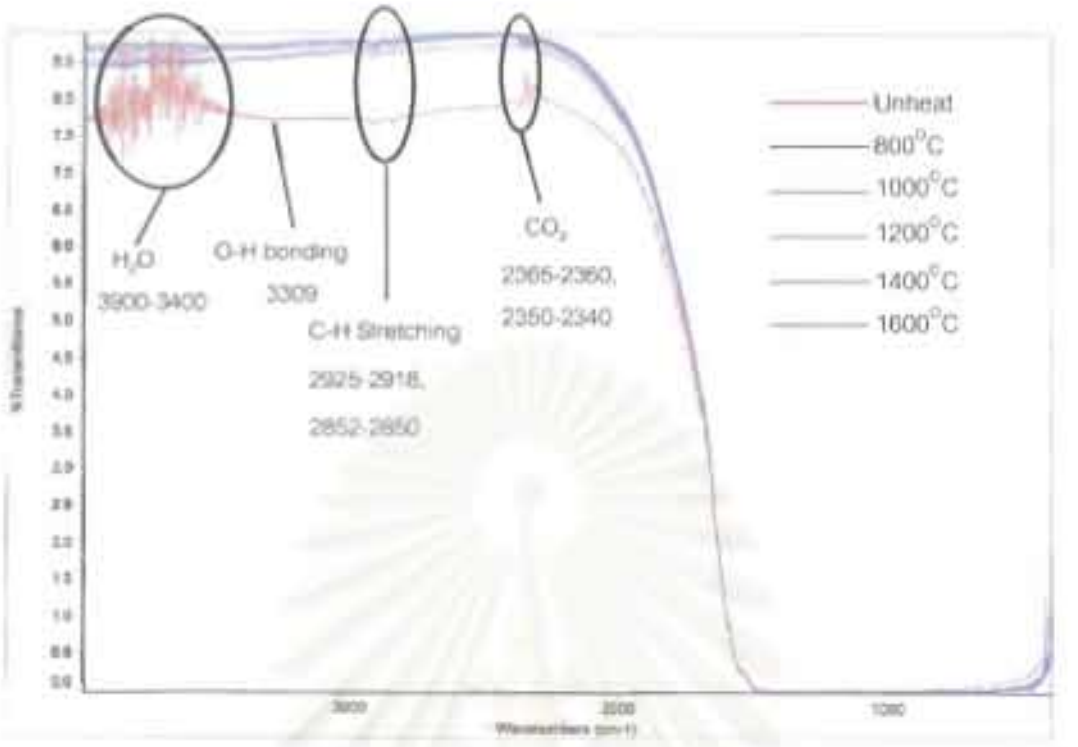

Figure 5.39 FTIR spectra of purplish pink sapphire before and after heating (sample no. PP4)

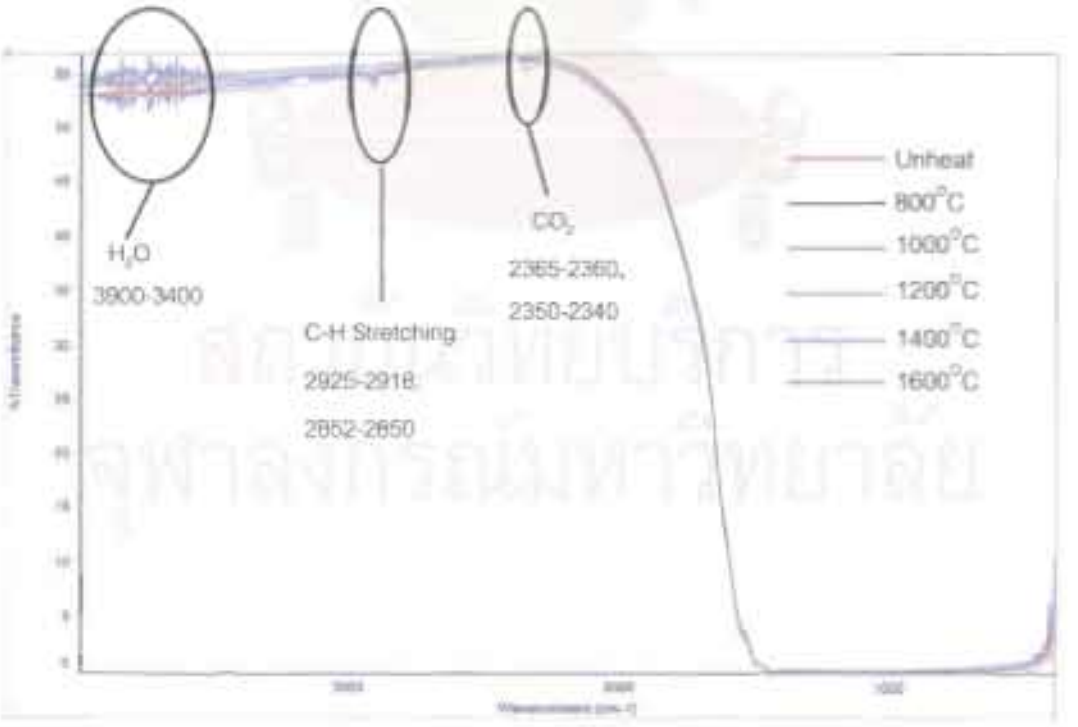

Figure 5.40 FTIR spectra of purplish pink sapphire before and after heating (sample no. LP9)

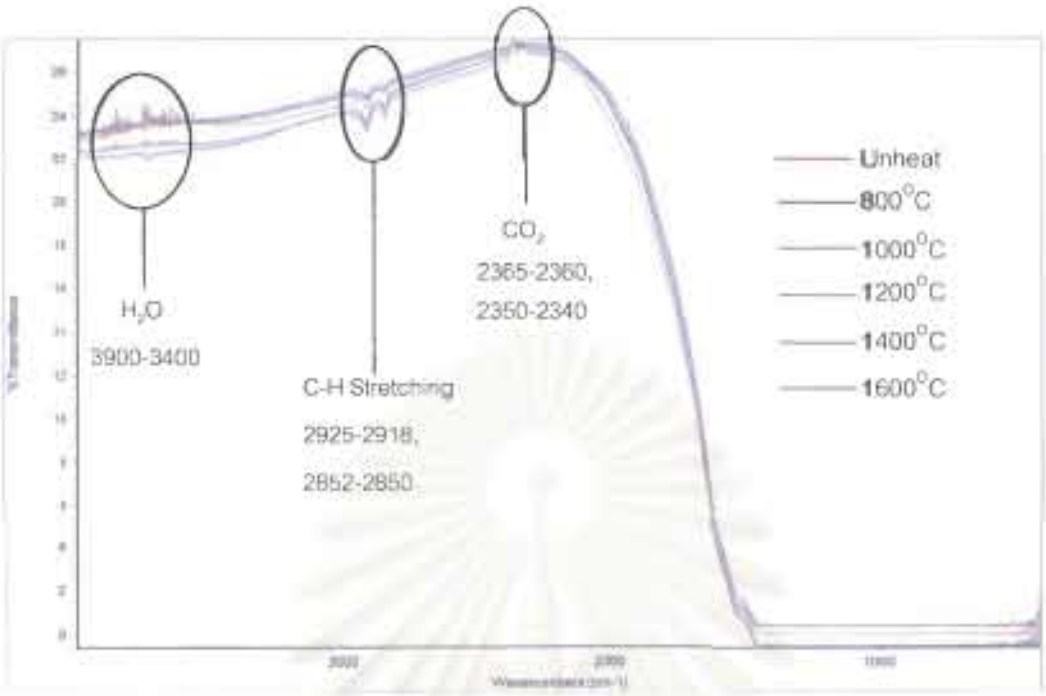

Figure 5.41 FTIR spectra of light orangey pink sapphire before and after heating (sample no. PP15)

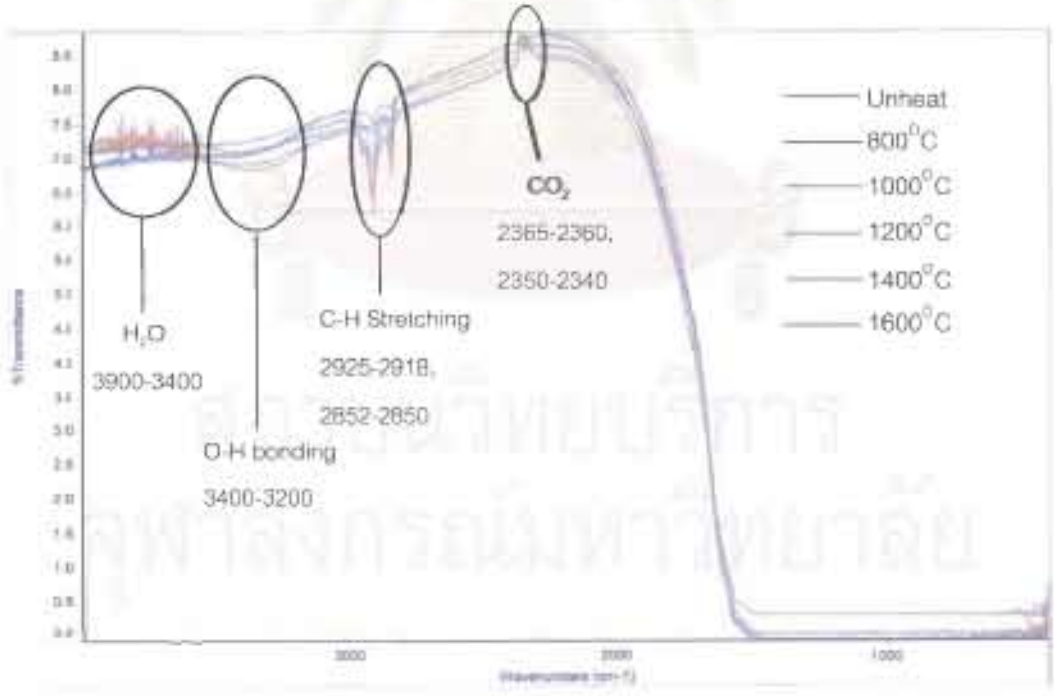

Figure 5.42 FTIR spectra of light orangey pink sapphire before and after heating (sample no. PP17)

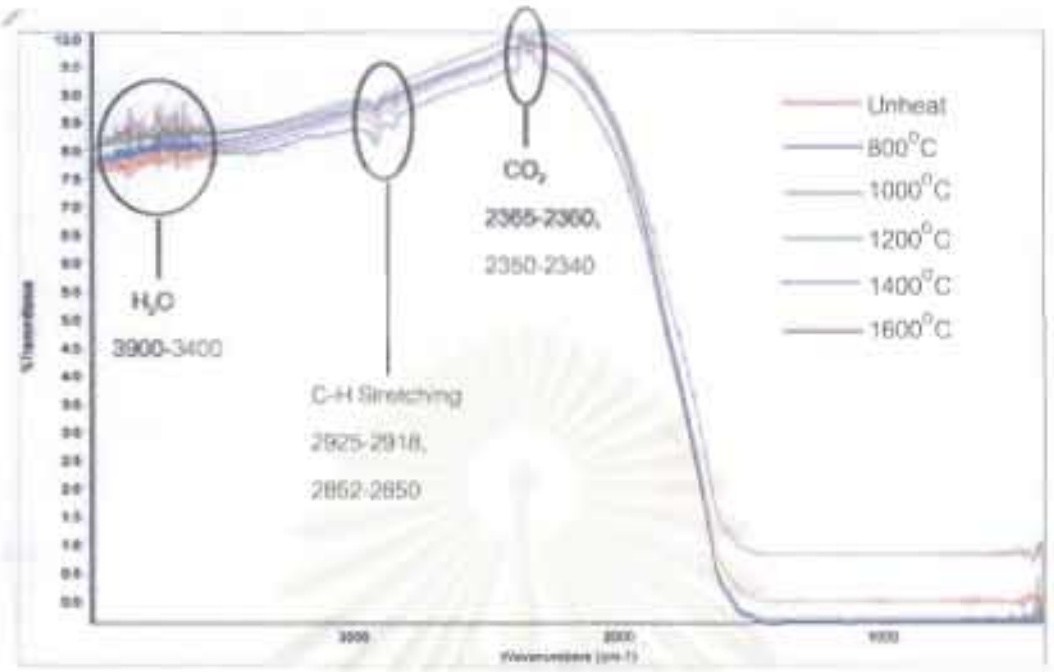

Figure 5.43 FTIR spectra of purple sapphire before and after heating (sample no. P16)

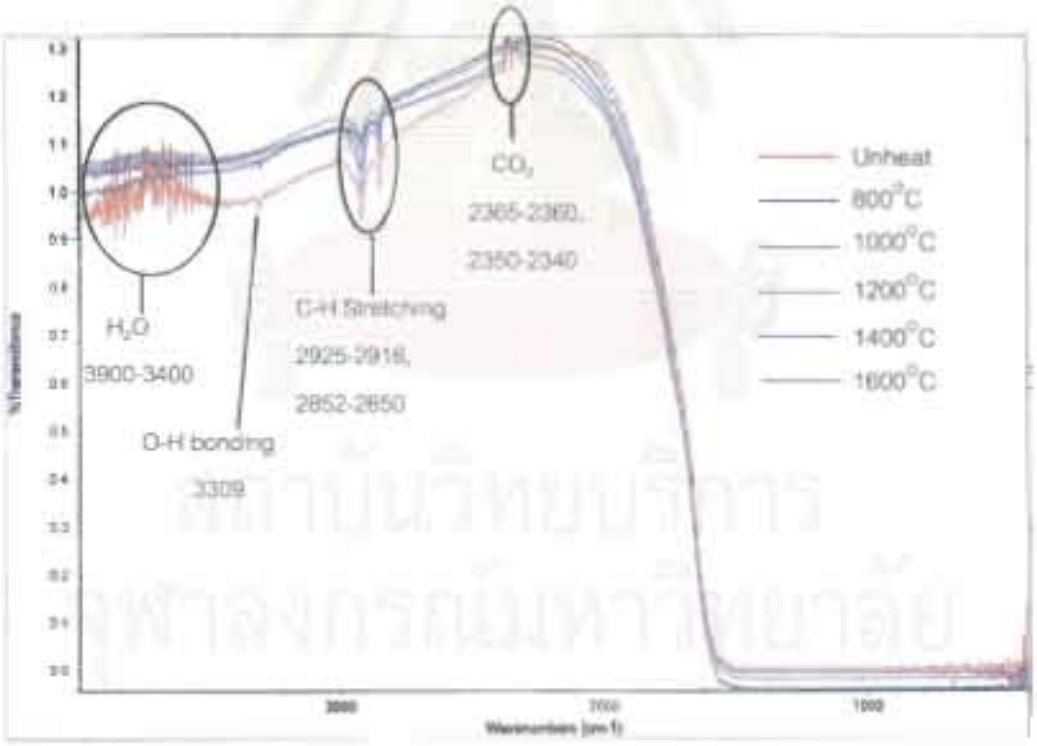

Figure 5.44 FTIR spectra of pinkish purple sapphire before and after heating (sample no. P10)

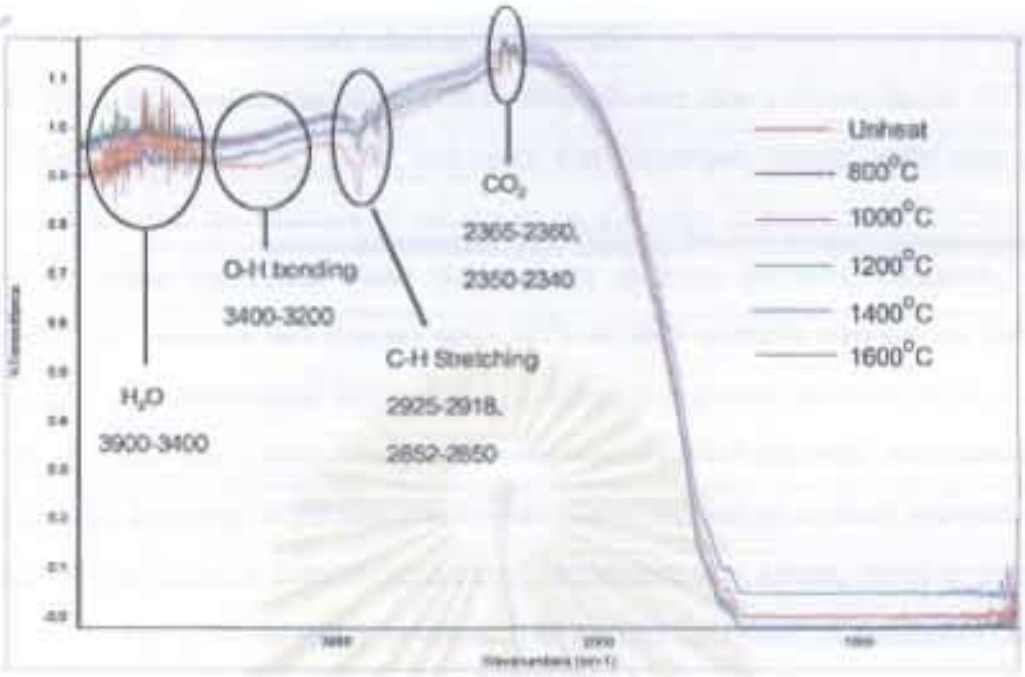

Figure 5.45 FTIR spectra of brownish purple sapphire before and after heating (sample no. P11)

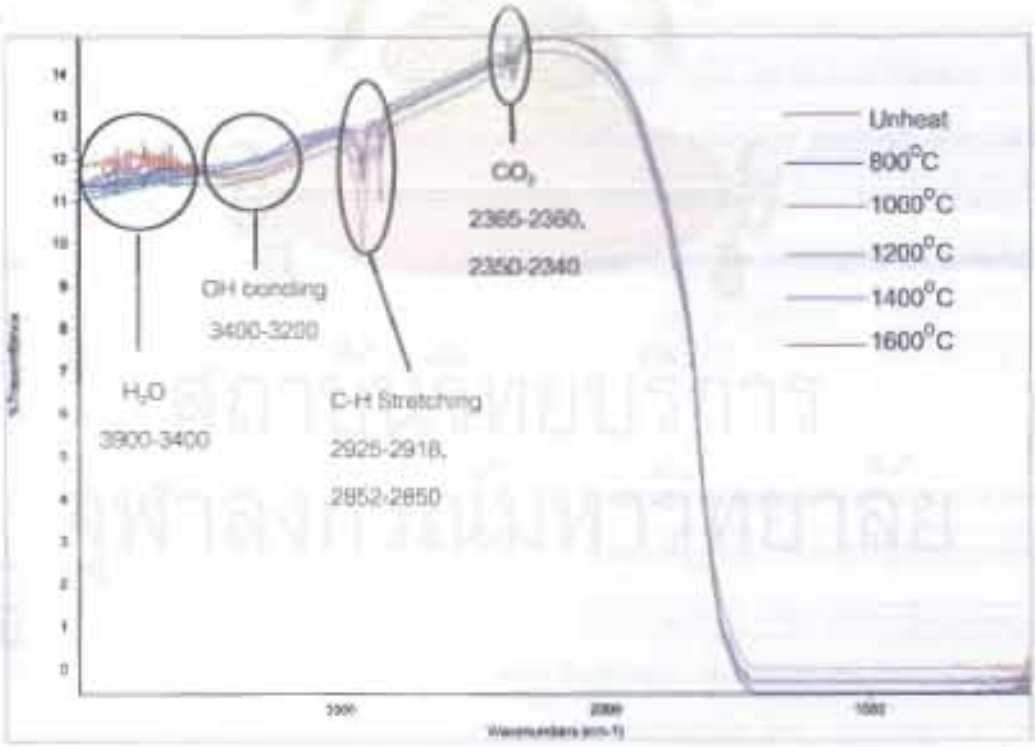

Figure 5.46 FTIR spectra of medium bluish violet sapphire before and after heating (sample no. MV5)

Past researchers cited in Smith (1995), i.e., Eigenmann and Günthard (1971, 1972), Eigenmann and others (1972), Volynets and others (1974), Beran (1991), Moon and Phillips (1994) have indicated that hydrogen atoms were typically incorporated within the structure of corundum as a charge compensation mechanism bound to various transitional metal ions present as trace elements, occupying an interstitial site between two oxygen atom (O^{2-}) or also possibly trapped by cation vacancies. The prominence and number of absorption peaks recorded in the mid-infrared spectrum were dependent on the concentration of O-H bonding. The individual wave number positions of the absorption peaks were dependent on trace element the OH has bonded such as titanium, vanadium, magnesium, iron, silicon, nickel or cobalt. The most typically encountered structural OH groups recorded in corundum were attributed to titanium (Ti), vanadium (V) or iron (Fe) bonds (Smith, 1995). Titanium and iron were the chromophoric trace elements which produced the blue color in corundum via the Fe^{2+}/Ti^{4+} IVCT.

In this study the author suggest that the disappearance of OH absorption peak in heat-treated pink, purple and violet sapphires may be due to heating in an oxidizing atmosphere and may or may not be related to bluish or purplish overcasted color reduction as a result of blue color removal. This has also been demonstrated by Haeger (2001) that the structurally bonded OH group could be destroyed by heating in a gas furnace with slightly oxidizing atmosphere for 5 hours at 1850^{o}C.

UV-VIS-NIR spectra

The absorption of light in the visible range is related directly to the color appearance of ruby and sapphire. Hence by measuring the UV-VIS-NIR absorption spectra of sapphires before and after heating, it should give an important information on the cause of color and color change after heat treatment. In this study the UV-VIS-NIR spectra of pink, purple and violet sapphires were measured and compared on both before and after heat treatment and shown in Appendix III. A few representative spectra that show distinct color change after heating are displayed in Figures 5.47 to 5.49.

It appears that all spectra show the prominent absorption due to Cr^{3+} at 405-410, 555-558 and 693 nm and some samples with additional peaks due to iron at 388 nm (Fe^{3+}) and 450 nm (Fe^{3+}/Fe^{3+} ion pair) both before and after heat treatment.

As shown in Figures 5.47 A, 5.48 A and 5.49 A, there are a clear shift in absorption pattern (mostly up and down direction) of the sample measured before and after heat treatment, in particular on the samples that show distinct color change due to heating. It is, however, not possible to decipher explicitly the cause of color change due to heating from those spectra. This is because those spectra are the sum of subspectra resulting from several causes, e.g., Cr^{3+}, Fe^{2+}/Ti^{4+} IVCT, Fe^{3+}, Fe^{3+}/Fe^{3+} ion pair and also Fe^{2+}/Fe^{3+} IVCT that show a broad absorption band centered at 875 nm (Ferguson and Fielding, 1971 and 1972 cited in Emmett and Douthit, 1993).

The cause of color of ruby and pink sapphire is well understood and is due to Cr^{3+} in trigonal distorted octahedral site in corundum lattice. The absorptions of Cr^{3+} peaked at 405-410, 555-560 and 692-693 nm are well documented (Belyaev, 1980, cited in Haeger, 2001). As pointed out by Haeger (2001), Cr^{3+} is an independent coloring element and do not influence the valence of the other trace elements. It is also not possible to change the content and valence of Cr^{3+} in the corundum lattice by simple heating. Hence absorption intensities due to Cr^{3+} is likely to be the same on both before and after heating (if the spectra were measured from the same sample at exactly the same position on both before and after heating). Therefore by subtracting the spectra of the after from the before heating (Figures 5.47 B, 5.48 B and 5.49 B), the absorption spectra causing by Cr^{3+} should be eliminated completely. The remaining (residue) spectra should reflect the absorption of visible light and should reveal the cause of color change resulting from heating.

As shown in Figure 5.47 A the color of this sample was changed from purple before heating to pink after heating at 1200°C and still remained the same when heated up to 1600°C. The residue spectrum after subtraction (Figure 5.47 B) reveal the presence of asymmetrical absorption band peaked at 610 nm. This band is related to bluish or purplish overcasted color removed after heating.

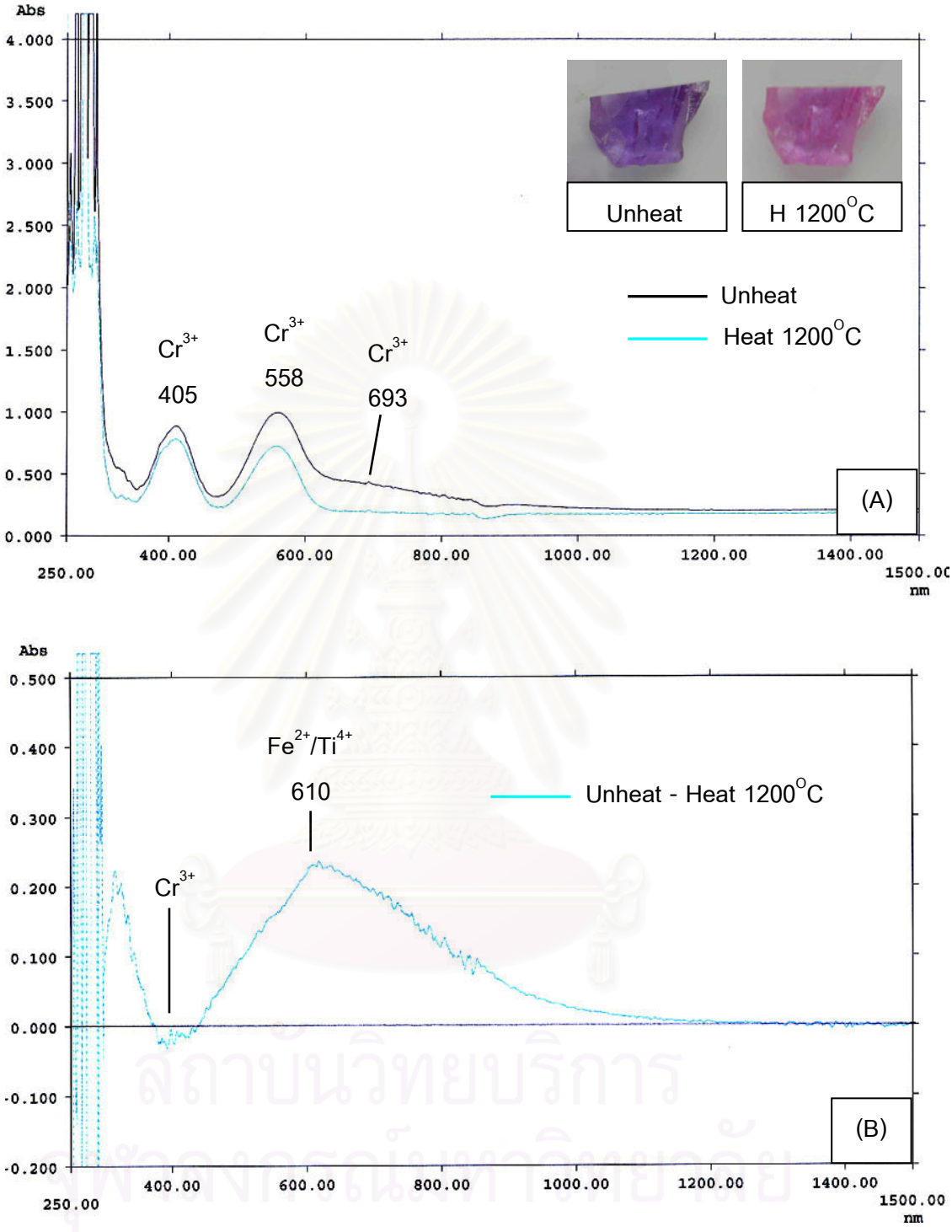

Figure 5.47 The UV-VIS-NIR absorption spectra of the purple sapphire sample (P16) on the vibration plane perpendicular to the c-axis (o-ray)

(A) The spectra of before (purple, unheat) and after (pink) heat treatment at 1200°C

(B) The remaining (residue) spectrum after subtraction of before and after heat-treatment at 1200°C

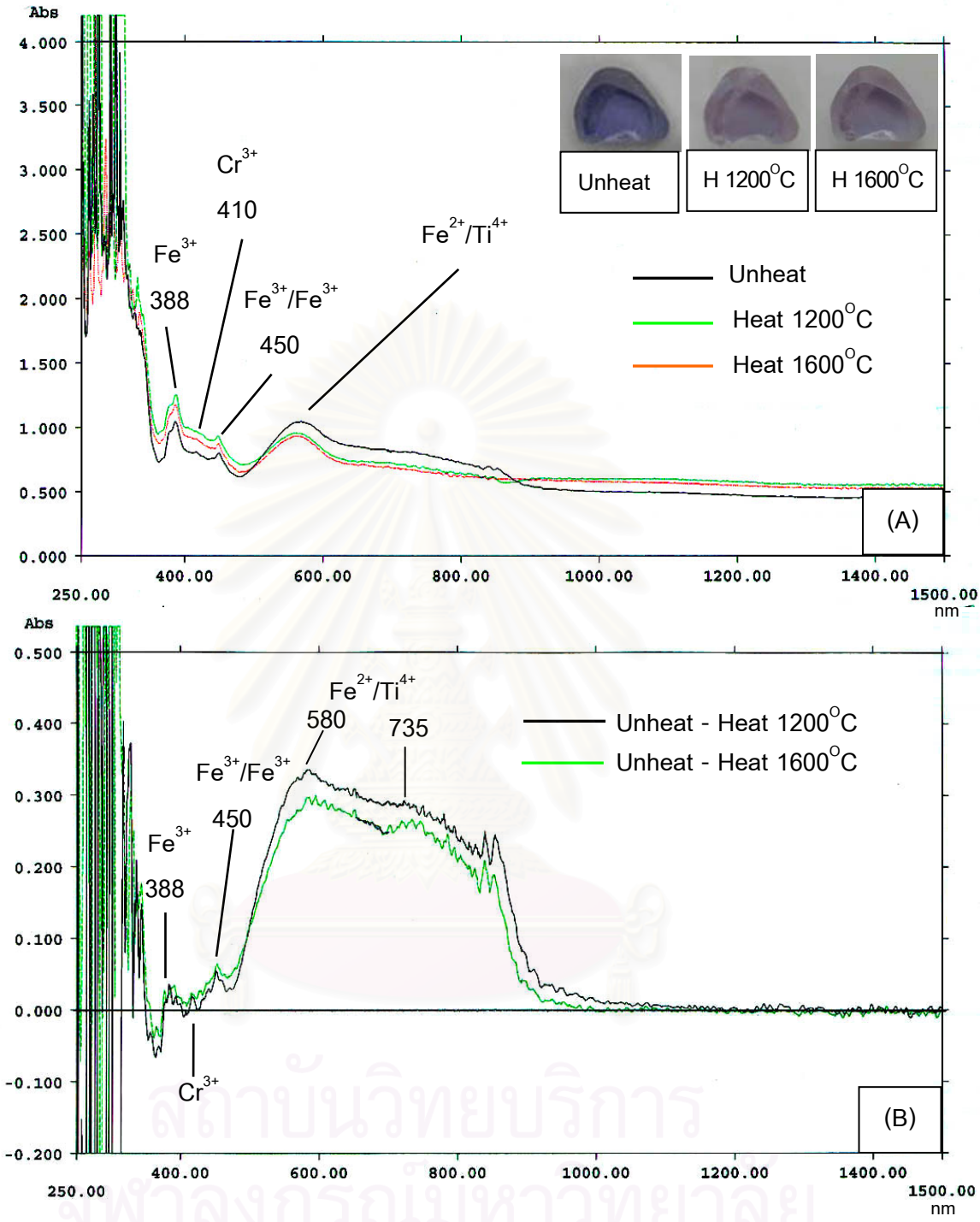

Figure 5.48 The UV-VIS-NIR absorption spectra of the medium violet sapphire sample (MV2) on the vibration plane perpendicular to the c-axis (o-ray)

(A) The spectra of before (medium violet, unheat) and after heat treatment at 1200^{O}C (pale bluish purple) and at 1600^{O}C (bluish purple)

(B) The remaining spectra after subtraction of before and after heat-treatment at 1200^{O}C and 1600^{O}C

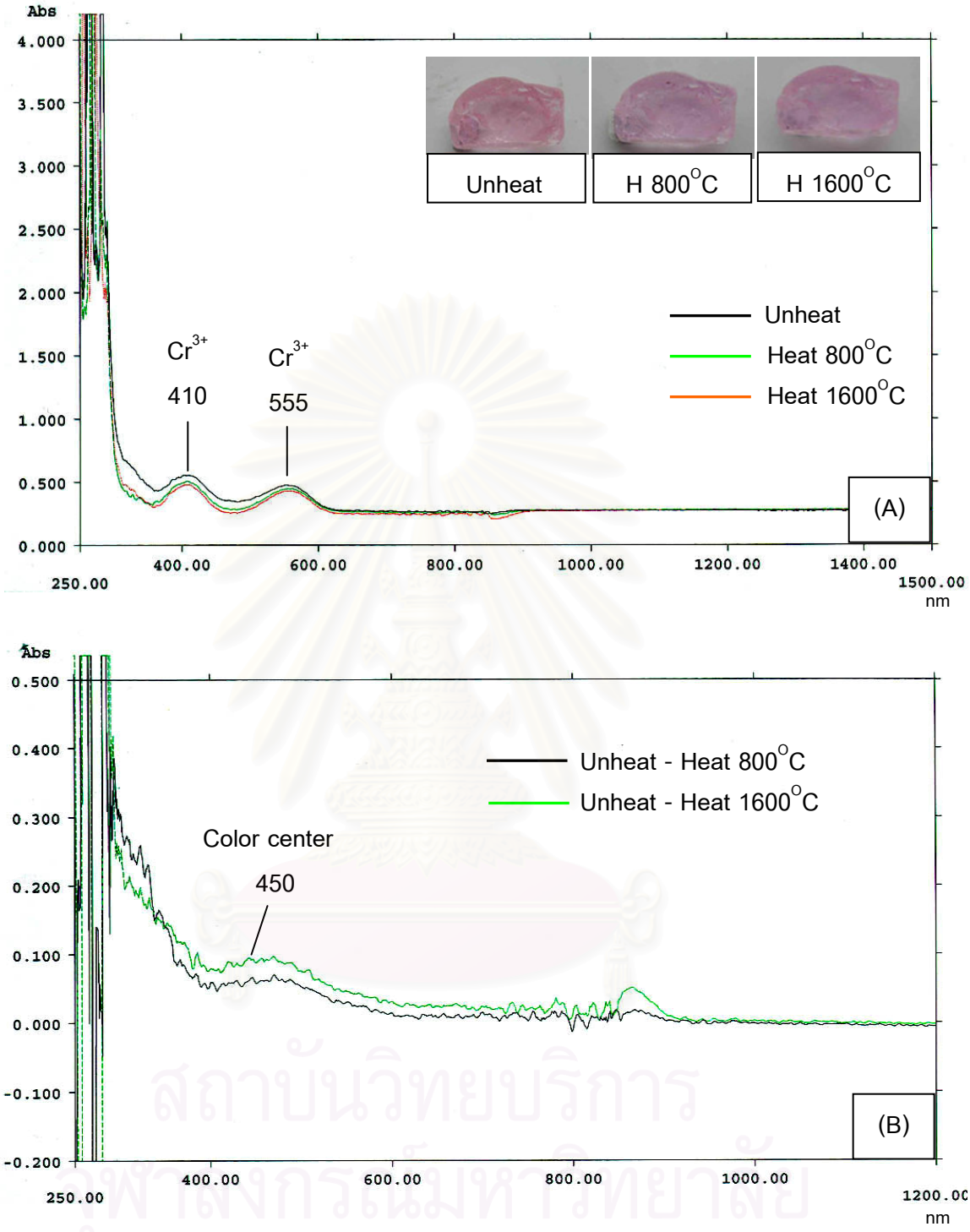

Figure 5.49 The UV-VIS-NIR absorption spectra of the orangey pink sapphire sample (PP17) on the vibration plane perpendicular to the c-axis (o-ray)

(A) The spectra of before (orangey pink, unheat) and after heat treatment at 800°C (pale pink) and at 1600°C (pale pink)

(B) The remaining spectra after subtraction of before and after heat-treatment at 800°C and 1600°C

In Figure 5.48 A the color of this sample was changed from medium violet before heating to pale bluish purple after heating from 1200°C to 1400°C. The bluish color was slightly returned back when heating up to 1600°C. The residue spectra after subtraction (Figure 5.48 B) show a board band peaked at 580 and 735 nm, which corresponds to the Fe^{2+}/Ti^{4+} IVCT (Haeger, 2001) and responsible for the removal of blue component after heating. The small residue spectra peaked at 450 (Fe^{3+}/Fe^{3+} ion pair) and 388 nm (Fe^{3+} ion) can support the idea that the oxidative heating can convert Fe^{2+} to Fe^{3+} in the octahedral site of corundum lattice (Nassau, 1984) in this sample which contain rather high iron content (0.214 weight % Fe_2O_3 analyzed by EDXRF or 0.36-0.37 weight % Fe_2O_3 analyzed by EPMA). It should also be noted that the broad band spectrum of 1200°C is slightly higher than that of 1600 °C which coincides well to the slight return of blue overcasted color when heating at 1600°C. The return of blue hue at 1600°C may be related to the dissolution of rutile needle into the corundum structure (see resorbed rutile silk in Figure 5.34) causing Fe^{2+}/Ti^{4+} IVCT mechanism (by charge compensation even under oxidizing condition, Haeger 2001) to be active one again.

In Figure 5.49 A the color of this sample was changed from orangey pink before heating to pink after heating at 800°C and 1600°C. The spectra are dominated by to Cr^{3+} both before and after heating. The residue spectra after subtraction (Figure 5.51 B) show a continuous increase in absorption toward the UV region and shoulder at 450 nm. This absorption spectra are a typical absorption pattern commonly observed in yellow Sri Lanka sapphire which are known to be caused by color centers (Haeger, 2001; Emmett and Douthit, 1993). The removal of yellow hue by heating can cause the color change from orange to pink. Heating at higher temperature (i.e. at 1600°C) seems to have a stronger influence to destroy this unstable color center than heating at lower temperature (i.e. at 800°C) as the residue spectrum at 1600°C is higher than that at 800°C.

CHAPTER VI
CHEMICAL ANALYSIS

Chemical composition of corundum consists of aluminum oxide (Al_2O_3). All other elements present within it resided as impurities. When it is pure, corundum is colorless, which is rare. If corundums contain chromophoric impurities or color-producing transition metals, they appear in various colors. Important chromophoric impurities are iron (Fe), titanium (Ti), chromium (Cr), and vanadium (V). Chromium produces pink to deep-red color. Iron can give corundum a pale green, yellow and brownish color, but in the presence of titanium also produce blue, blue-green and green color (Nassau, 1984). Vanadium produces violet to purple color.

Energy Dispersive X-ray Fluorescence Spectrometer

Energy Dispersive X-ray Fluorescence Spectrometer (EDXRF) are used to analyze the energy dispersion of electrons which are excited by X-ray. These electrons are excited into a higher energy state in the atom or ejected from the atom. This process thus empties one of the eletronic states of the atom. This state will be filled very rapidly by another higher energy electrons which drops into the empty state and emits the energy. The dispersive energies are different in each elements because each elements have different atomic weight and energy level. Thus, these energies are the characteristic energies and can be used to determine chemical composition.

In this study, the trace element analysis of sapphire samples was carried out by using EDAX Energy Dispersive X-ray Fluorescence Spectrometer (model DX-95) at DMR. The X-ray source is the rhodium (Rh) X-ray tube. The dispersive energy is detected with the Silicon Lithium from 5 eV to 50 eV. Sodium (Na) to uranium (U) elements can be defined for qualitative analysis while chemical concentrations are determined from intensity of energy in terms of semiquantitative analysis. The detection limit of each element is about 0.01 weight %. For a semiquantitative analysis, the energy intensities emitted from sapphire samples are compared with energy intensities of each element in standard natural and synthetic sapphires. The 10 standard sapphires were

analyzed by the Photon (or Particle) Induced X-ray Emission (PIXE) (Sriprasert, per. com.).

Trace Element Analysis by EDXRF

The trace elements of 128 unheated sapphires except light greenish blue, very light yellowish white and colorless sapphires with blue patch, were analyzed as $Fe_2O_{3(total)}$, TiO_2, Cr_2O_3, V_2O_3 and Ga_2O_3 in weight % and listed in Table IV.1 of Appendix IV. Each sample was analyzed only 1 point at the center. These trace element contents are presented as minimum, maximum, average and standard deviation values in Table 6.1. To show the relationship between the trace elements and color of 7 sapphire groups, the average and one standard deviation of chromium, iron, titanium, vanadium and gallium contents were plotted in the variation diagrams of V_2O_3 versus Cr_2O_3, Fe_2O_3 versus TiO_2 and Ga_2O_3 versus Cr_2O_3 (Figures 6.1 to 6.3).

The chromium contents of pink and purple groups as well as violet group with color-change effect are higher than those of the others. In colorless, yellow and green sapphire groups, the chromium contents are lower than detection limit (<0.01 weight %) see Table 6.1, Figures 6.1 and 6.3. Generally, chromium produces red and pink color. If it combines with Fe^{3+} and Fe^{2+}/Ti^{4+} intervalence charge transfer (IVCT) process, it produces violet or purple colors and produces the color-change effect in is sapphire when combines with vanadium (Themelis, 1992).

The average concentrations of vanadium in violet and blue sapphires with color-change groups are distinctly higher than other sapphire without color-change groups (about 0.017-0.021 weight % V_2O_3 in sapphire with color-change and 0.012-0.013 weight % in others; Table 6.1 and Figure 6.1). In pink and purple sapphire groups, the vanadium concentration averages 0.007–0.008 weight % V_2O_3 while the green and colorless groups do not show the vanadium content because the vanadium content is lower than detection limit (<0.01 weight %).

Table 6.1 EDXRF analyzes of some Ilakaka-Sakaraha sapphires (in weight %)

Sample Type	No. of sample	Concentration (wt%)				
		Fe_2O_3	TiO_2	Cr_2O_3	V_2O_3	Ga_2O_3
Pink group	**27**	**0.025-0.609**	**0.008-0.100**	**0.028-0.164**	**<0.010-0.022**	**<0.010-0.009**
		(0.136,0.151)	**(0.028,0.018)**	**(0.064,0.029)**	**(0.008,0.008)**	**(0.009,0.009)**
Purplish pink	12	0.025-0.117	0.012-0.038	0.045-0.164	<0.010-0.022	<0.010-0.047
		(0.061,0.028)	(0.026,0.008)	(0.075,0.033)	(0.010,0.009)	(0.013,0.012)
Light purplish pink	9	0.029-0.506	0.020-0.100	0.034-0.118	<0.010-0.017	<0.010-0.013
		(0.207,0.171)	(0.038,0.024)	(0.067,0.023)	(0.010,0.007)	(0.009,0.005)
Light orangey pink	3	0.105-0.117	0.009-0.055	0.040-0.049	<0.010	<0.010-0.013
		(0.111,0.006)	(0.027,0.025)	(0.044,0.005)	(0.000,0.000)	(0.008,0.007)
Orangey pink	3	0.064-0.609	<0.010-0.027	0.028-0.035	<0.010	<0.010(0.000
		(0.250,0.311)	(0.014,0.014)	(0.032,0.004)	(0.000,0.000)	,0.000)
Purple group	**16**	**0.046-0.791**	**<0.010-0.036**	**0.028-0.087**	**<0.010-0.020**	**<0.010-0.018**
		(0.268,0.248)	**(0.025,0.010)**	**(0.060,0.019)**	**(0.007,0.008)**	**(0.009,0.007)**
Purple	3	0.062-0.114	0.011-0.027	0.051-0.082	<0.010	<0.010-0.018
		(0.096,0.029)	(0.021,0.009)	(0.067,0.015)	(0.000,0.000)	(0.014,0.005)
Pinkish purple	10	0.046-0.572	<0.010-0.036	0.028-0.085	<0.010-0.020	<0.010-0.014
		(0.199,0.156)	(0.026,0.011)	(0.058,0.019)	(0.011,0.008)	(0.008,0.006)
Brownish purple	3	0.442-0.791	0.014-0.036	0.032-0.087	<0.010	<0.010-0.017
		(0.672,0.199)	(0.028,0.012)	(0.062,0.028)	(0.000,0.000)	(0.011,0.009)
Violet group	**6**	**0.062-0.210**	**<0.010-0.053**	**<0.010-0.022**	**<0.010-0.019**	**<0.010-0.017**
		(0.113,0.051)	**(0.030,0.020)**	**(0.010,0.011)**	**(0.012,0.009)**	**(0.009,0.007)**
	***6**	***0.113-0.214**	***0.018-0.044**	***0.033-0.125**	***0.015-0.030**	**<0.010-0.017**
		(0.167,0.045)	**(0.029,0.009)**	**(0.072,0.041)**	**(0.021,0.005)**	**(0.009,0.007)**
Dark violet	*3	*0.129-0.208	*0.018-0.044	*0.065-0.125	*0.019-0.030	<0.010-0.017
		(0.179,0.043)	(0.029,0.014)	(0.103,0.033)	(0.024,0.006)	(0.011,0.010)

Minimum and maximum values are given, along with the average and standard deviation (in parentheses below each range)

*with color-change effect

Table 6.1 EDXRF analyzes of some Ilakaka-Sakaraha sapphires (in weight %) (continued)

Sample Type	No. of	Concentration (wt%)				
	sample	Fe_2O_3	TiO_2	Cr_2O_3	V_2O_3	Ga_2O_3
Medium	3	0.095-0.210	<0.010-0.052	<0.010	<0.010-0.019	<0.010-0.013
violet		(0.135,0.065)	(0.026,0.026)	(0.000,0.000)	(0.006,0.011)	(0.008,0.007)
	*3	*0.113-0.214	*0.026-0.030	*0.033-0.058	*0.015-0.022	<0.010-0.010
		(0.155,0.053)	(0.028,0.002)	(0.041,0.014)	(0.018,0.004)	(0.007,0.006)
Light violet	3	0.062-0.115	0.024-0.053	0.018-0.022	0.016-0.019	<0.010-0.017
		(0.091,0.027)	(0.034,0.016)	(0.020,0.002)	(0.017,0.002)	(0.009,0.009)
Blue group	**51**	**<0.010-0.638**	**<0.010-0.152**	**<0.010-0.022**	**<0.010-0.028**	**<0.010-0.025**
		(0.134,0.119)	**(0.041,0.027)**	**(0.010,0.008)**	**(0.013,0.009)**	**(0.010,0.008)**
	***12**	***0.052-0.440**	**<0.010-0.074**	***0.018-0.100**	**<0.010-0.039**	**<0.010-0.019**
		(0.208,0.115)	**(0.029,0.021)**	**(0.048,0.027)**	**(0.017,0.012)**	**(0.015,0.031)**
Very dark	3	0.032-0.070	0.032-0.152	<0.010	<0.010	<0.010-0.020
blue		(0.046,0.021)	(0.084,0.062)	(0.000,0.000)	(0.000,0.000)	(0.008,0.007)
Dark blue	2	0.088-0.135	0.024-0.052	<0.010	<0.010	0.020-0.025
		(0.112,0.033)	(0.038,0.020)	(0.000,0.000)	(0.000,0.000)	(0.023,0.004)
	*1	*0.384	<0.010	*0.025	<0.010	<0.010
Medium blue	7	<0.010-0.397	<0.010-0.108	<0.010-0.020	<0.010-0.028	<0.010-0.018
		(0.118,0.140)	(0.043,0.035)	(0.010,0.008)	(0.012,0.010)	(0.010,0.007)
	*7	*0.145-0.440	*0.010-0.074	*0.029-0.100	<0.010-0.039	<0.010-0.010
		(0.241,0.096)	(0.039,0.019)	(0.056,0.029)	(0.003,0.012)	(0.169,0.005)
Light blue	14	0.056-0.638	<0.010-0.067	<0.010-0.018	<0.010-0.024	<0.010-0.021
		(0.210,0.171)	(0.034,0.016)	(0.014,0.008)	(0.015,0.007)	(0.011,0.006)
	*4	*0.052-0.179	<0.010-0.038	*0.018-0.032	<0.010-0.019	<0.010-0.019
		(0.105,0.054)	(0.018,0.012)	(0.038,0.025)	(0.014,0.009)	(0.040,0.046)

Minimum and maximum values are given, along with the average and standard deviation (in parentheses below each range)

*with color-change effect

Table 6.1 EDXRF analyzes of some Ilakaka-Sakaraha sapphires (in weight %) (continued)

Sample Type	No. of sample	Concentration (wt%)				
		Fe_2O_3	TiO_2	Cr_2O_3	V_2O_3	Ga_2O_3
Very light blue	15	0.037-0.259 (0.103,0.065)	0.012-0.054 (0.036,0.013)	<0.010-0.017 (0.009,0.007)	<0.010-0.024 (0.013,0.007)	<0.010-0.018 (0.007,0.006)
Extremely light blue	10	0.037-0.212 (0.113,0.049)	<0.010-0.085 (0.046,0.028)	<0.010-0.022 (0.012,0.007)	<0.010-0.024 (0.015,0.007)	<0.010-0.025 (0.011,0.009)
Colorless group	**3**	**0.035-0.062 (0.045,0.015)**	**0.011-0.035 (0.025,0.012)**	**<0.010 (0.000,0.000)**	**<0.010 (0.000,0.000)**	**<0.010-0.013 (0.008,0.007)**
Colorless	1	0.062	0.011	<0.010	<0.010	0.010
Very light bluish	2	0.035-0.038 (0.037,0.002)	0.029-0.035 (0.032,0.004)	<0.010 (0.000,0.000)	<0.010 (0.000,0.000)	<0.010-0.013 (0.007,0.009)
Yellow group	**4**	**0.021-0.232 (0.104,0.099)**	**0.006-0.013 (0.003,0.007)**	**<0.010 (0.000,0.000)**	**<0.010-0.010 (0.003,0.005)**	**<0.010-0.010 (0.003,0.005)**
Orangey yellow	1	0.021	0.013	<0.010	<0.010	<0.010
Light yellow	3	0.030-0.232 (0.132,0.101)	<0.010 (0.000,0.000)	<0.010 (0.000,0.000)	<0.010-0.010 (0.003,0.006)	<0.010-0.010 (0.003,0.006)
Green group	**3**	**0.203-0.766 (0.548,0.302)**	**0.006-0.012 (0.004,0.007)**	**<0.010 (0.000,0.000)**	**<0.010 (0.000,0.000)**	**<0.010 (0.000,0.000)**
Medium green	1	0.203	0.012	<0.010	<0.010	<0.010
Light yellowish green	2	0.675-0.766 (0.721,0.064)	<0.010 (0.000,0.000)	<0.010 (0.000,0.000)	<0.010 (0.000,0.000)	<0.010 (0.000,0.000)

Minimum and maximum values are given, along with the average and standard deviation (in parentheses below each range)

*with color-change effect

สถาบันวิทยบริการ
จุฬาลงกรณ์มหาวิทยาลัย

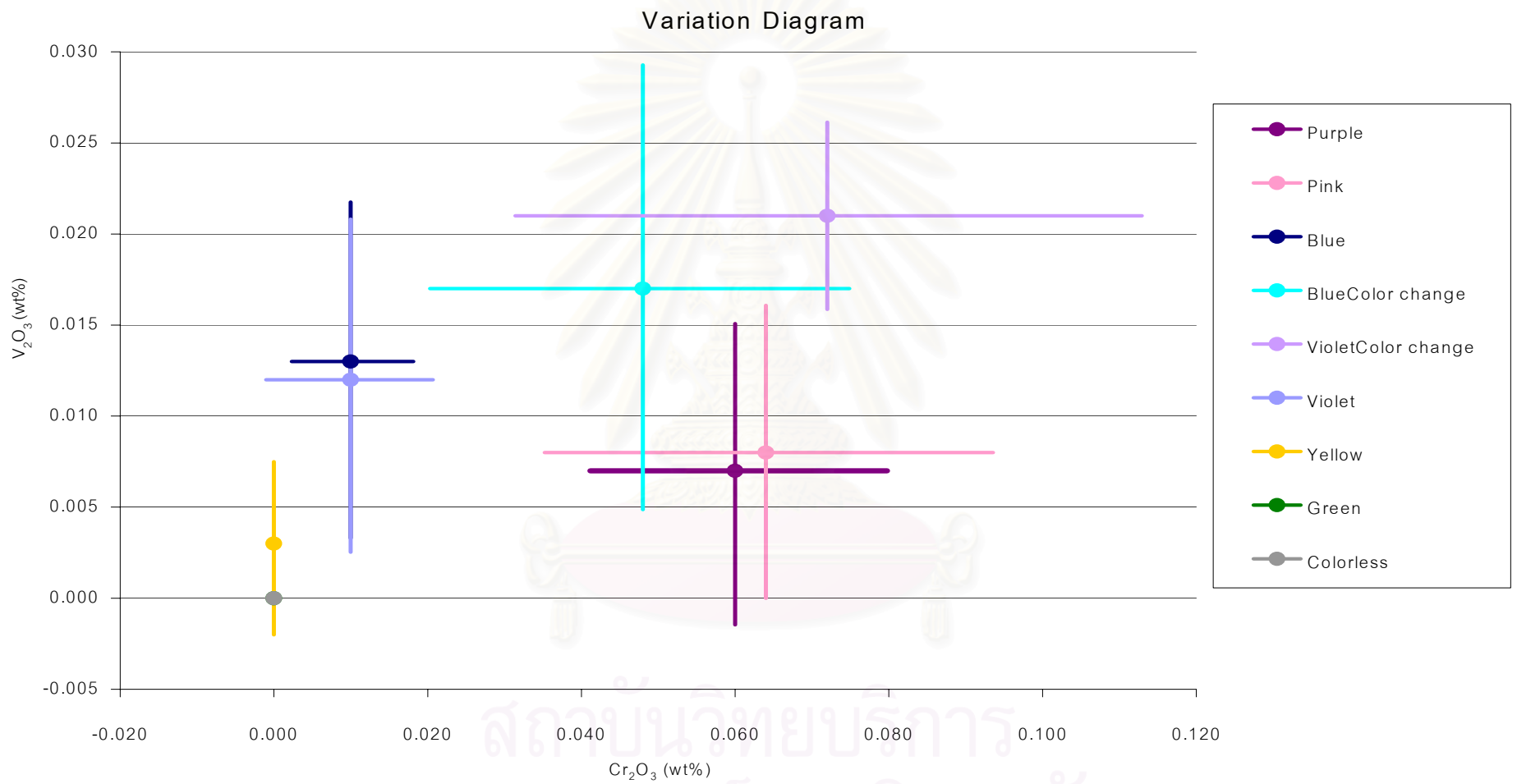

Figure 6.1 Variation diagram of V_2O_3 versus Cr_2O_3 shows the average and one standard deviation of vanadium and chromium contents of 7 sapphire groups by EDXRF.

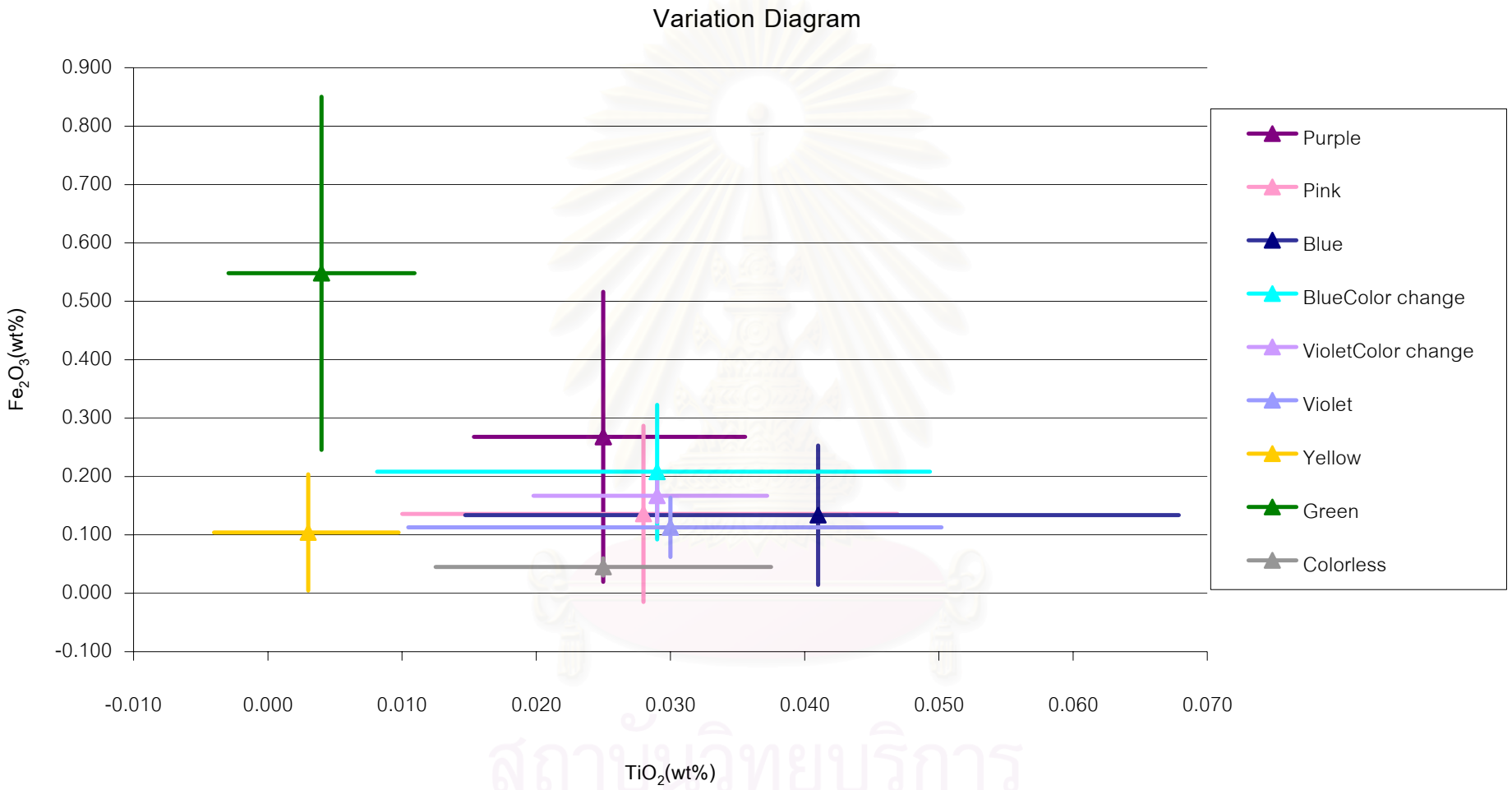

Figure 6.2 Variation diagram of Fe_2O_3 versus TiO_2 shows the average and one standard deviation of iron and titanium contents of 7 sapphire groups by EDXRF.

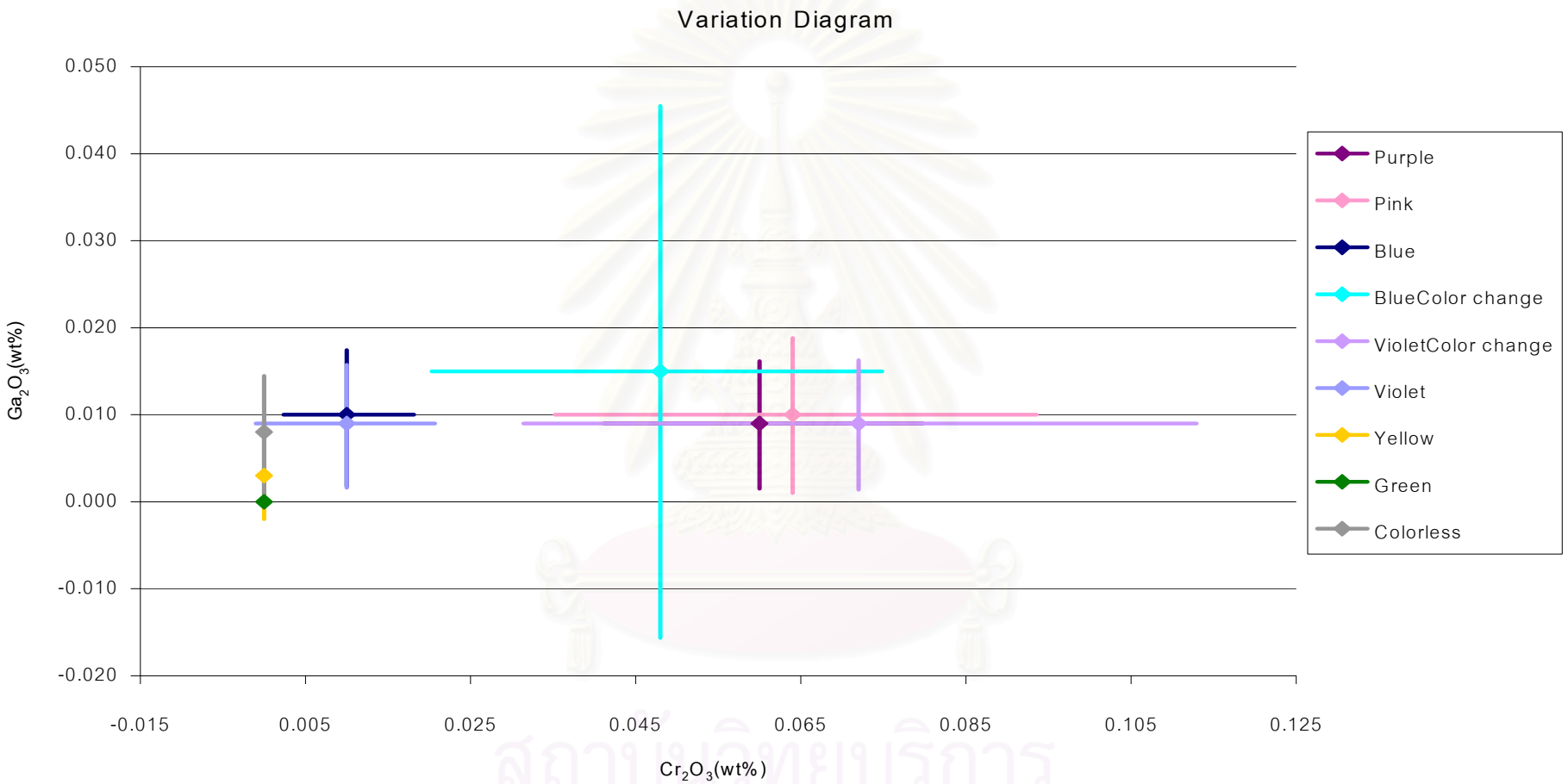

Figure 6.3 Variation diagram of Ga_2O_3 versus Cr_2O_3 shows the average and one standard deviation of gallium and chromium contents of 7 sapphire groups by EDXRF.

The iron content of the green group is the highest (average about 0.548 weight % Fe_2O_3) while the colorless group shows the lowest iron concentrations. The average concentrations of iron in the yellow, blue, violet without color-change and pink sapphire groups are 0.104-0.136 weight % (Table 6.1, Figure 6.2). The iron content of yellow group is only 0.1 weight % on the average but can give yellow color. Hence, the cause of yellow color in Ilakaka-Sakaraha sapphire may by due to color center (Haeger, 2001).

Titanium content in blue sapphire group is the highest (average about 0.041 weight % TiO_2) while the yellow and green groups show the lowest titanium concentrations (average about 0.003-0.004 weight % TiO_2) (Table 6.1, Figure 6.2). The samples with a milky white component (i.e. extremely light blue and very light bluish types) averaged about 0.046 and 0.032 weight % TiO_2 respectively. These sapphires may be heated to develop a blue coloration depending on the sufficient amounts and proper ratio of titanium and iron. Titanium alone can not produce blue coloration in corundum.

The average concentrations of gallium in pink, purple, blue without color-change and violet sapphire groups are about 0.007-0.010 weight % Ga_2O_3. The gallium content of blue with color-change group is the highest (average about 0.015 weight % Ga_2O_3) while the green group does not shows the gallium concentrations (lower than 0.01 weight % Ga_2O_3) see in Table 6.1 and Figure 6.3.

Trace Element Analysis by EPMA

The 16 samples of heat-treated pink, purple and violet sapphires were analyzed using the JEOL Electron Probe Micro-Analyzer (EPMA) model JXA 8900 equiped with EDXRF system at Center of Gemstone Research, Institute of Geosciences, University of Mainz, Germany. Conditions for sample analysis were set at 20 kV and 20 nA with different counting times for each element. The TAP crystal in spectrometer 1 was selected to analyze for Al, Si and Mg with counting times of 40, 40, and 100 seconds, respectively. The PET crystal in spectrometer 2 was used for Ti and Cr with

counting times of 100 seconds. The LiF crystals in spectrometers 3 and 4 were used for V and Ga with counting times of 200 seconds. The LiFH crystal in spectrometers 5 was used for Mn and Fe with counting times of 100 seconds. Standards used were wollastonite for Si, synthetic corundum for Al, pure metal MgO for Mg, pure metal Fe_2O_3 for Fe, pure metal $MnTiO_3$ for Ti and Mn, pure GaAs for Ga, metallic chromium for Cr and pure Vanadium for V. The detection limit of each element is about 0.01 weight % (Sutthirat, per. com.). The major element (Al_2O_3) and trace elements of pink, purple and violet sapphires after step-heating up to 1600^{O}C were analyzed for TiO_2, V_2O_3, Ga_2O_3, $Fe_2O_{3(total)}$, SiO_2, Cr_2O_3, MnO and MgO and listed in Table IV.2 of Appendix IV. Each sample was analyzed about 4-6 points in terms of oxide elements. The values analyzed for each sample are quite similar because most samples are rather homogeneous without color zoning. These oxide element contents were converted into atomic proportion based on 3 oxygen atoms in the formula of corundum (Al_2O_3). Some trace element (Fe_2O_3, TiO_2, Cr_2O_3, V_2O_3 and Ga_2O_3) content of selected pink, purple and violet sapphires are presented as minimum, maximum, average and standard deviation values in Table 6.2. To show the relationship between the trace elements and color of 8 sapphire types, the average and one standard deviation of chromium, iron, titanium, vanadium and gallium contents were plotted in the variation diagrams of V_2O_3 versus Cr_2O_3, Fe_2O_3 versus TiO_2 and Ga_2O_3 versus Cr_2O_3 (Figures 6.4 to 6.6)

The chromium content in purplish pink, purple, brownish purple, pinkish purple and light purplish pink are distinctly higher than those of orangey pink, light orangey pink, medium violet (with and without color-change effects) sappires (Table 6.2, Figure 6.4). The vanadium content in all types of sapphire, on the contrary, are not distinctly different, even in the medium violet with color-change effect, and they are all below 0.01 weight % V_2O_3 on the average (Figure 6.4). Hence color-change effect in this particular sample may not depend only on the amount of V_2O_3.

The iron contents of brownish purple, medium violet (with and without color-change effects), purplish pink, purple, light orangey pink and orangey pink

Table 6.2 Some trace elements content of selected pink, purple and violet sapphires (16 samples) by Electron Probe Micro-Analyzer. The analyzes were performed after the step-heating up to 1600^{O}C.

Sample Type	No. of point	Concentration (weight %)				
		Fe_2O_3	TiO_2	Cr_2O_3	V_2O_3	Ga_2O_3
Pink group	**45**	**0.042-0.310**	**0.000-0.028**	**0.000-0.139**	**0.000-0.025**	**0.000-0.018**
		(0.084,0.079)	**(0.013,0.006)**	**(0.057,0.031)**	**(0.005,0.008)**	**(0.010,0.005)**
Purplish pink	20	0.047-0.068	0.000-0.028	0.042-0.139	0.000-0.025	0.000-0.018
		(0.057,0.007)	(0.014,0.006)	(0.076,0.034)	(0.007,0.010)	(0.011,0.005)
Light purplish pink	14	0.046-0.310	0.000-0.022	0.031-0.079	0.000-0.010	0.000-0.016
		(0.145,0.123)	(0.013,0.006)	(0.056,0.015)	(0.005,0.005)	(0.010,0.005)
Light orangey pink	5	0.062-0.072	0.000-0.012	0.000-0.036	0.000	0.007-0.018
		(0.068,0.004)	(0.008,0.005)	(0.026,0.015)	(0.000,0.000)	(0.011,0.005)
Orangey pink	6	0.042-0.053	0.000-0.016	0.019-0.034	0.000-0.010	0.000-0.015
		(0.047,0.005)	(0.011,0.006)	(0.027,0.006)	(0.005-0.005)	(0.006,0.007)
Purple group	**26**	**0.081-0.660**	**0.010-0.026**	**0.045-0.083**	**0.000-0.017**	**0.000-0.018**
		(0.261,0.214)	**(0.017,0.004)**	**(0.065,0.011)**	**(0.004,0.006)**	**(0.013,0.005)**
Purple	5	0.081-0.088	0.016-0.021	0.068-0.079	0.000-0.017	0.012-0.018
		(0.084,0.003)	(0.018,0.002)	(0.072,0.004)	(0.008,0.008)	(0.015,0.002)
Pinkish purple	16	0.087-0.349	0.010-0.025	0.045-0.071	0.000-0.010	0.000-0.017
		(0.195,0.107)	(0.016,0.004)	(0.058,0.008)	(0.002,0.004)	(0.011,0.005)
Brownish purple	5	0.640-0.660	0.018-0.026	0.074-0.083	0.000-0.010	0.016-0.018
		(0.648,0.008)	(0.022,0.003)	(0.079,0.004)	(0.006,0.005)	(0.015,0.005)
Medium violet	5	0.078-0.096	0.020-0.037	0.014-0.022	0.000-0.017	0.012-0.028
		(0.086-0.007)	(0.028-0.007)	(0.019-0.003)	(0.010-0.006)	(0.019-0.006)
	*5	*0.360-0.371	*0.019-0.025	*0.019-0.030	*0.000-0.010	*0.008-0.020
		(0.366-0.005)	(0.022-0.003)	(0.026-0.004)	(0.006-0.005)	(0.015-0.006)

Minimum and maximum values are given, along with the average and standard deviation (in parentheses below each range)

*with color-change effect

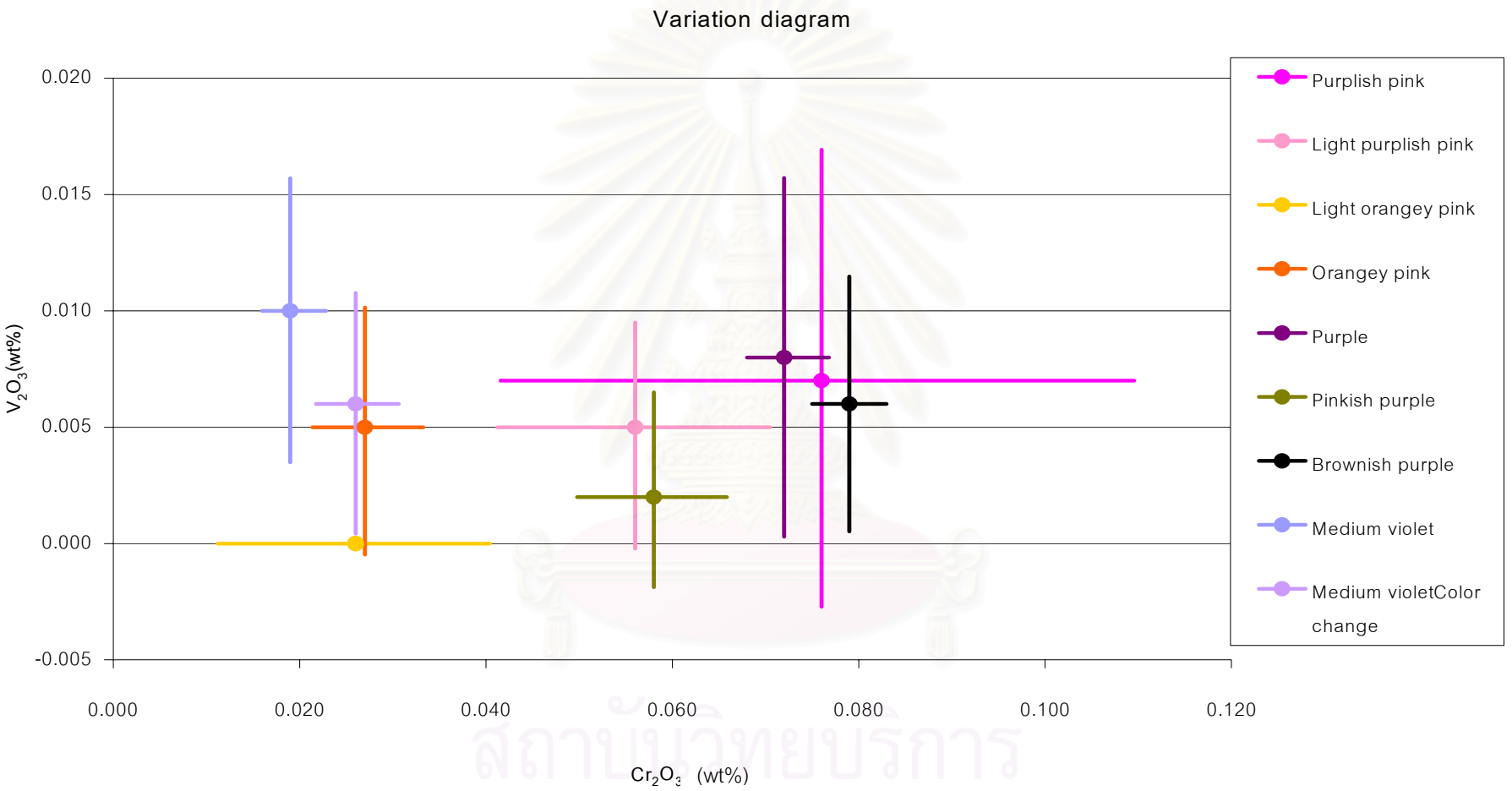

Figure 6.4 Variation diagram of V_2O_3 versus Cr_2O_3 shows the average and one standard deviation of vanadium and chromium contents of 8 sapphire types by EPMA.

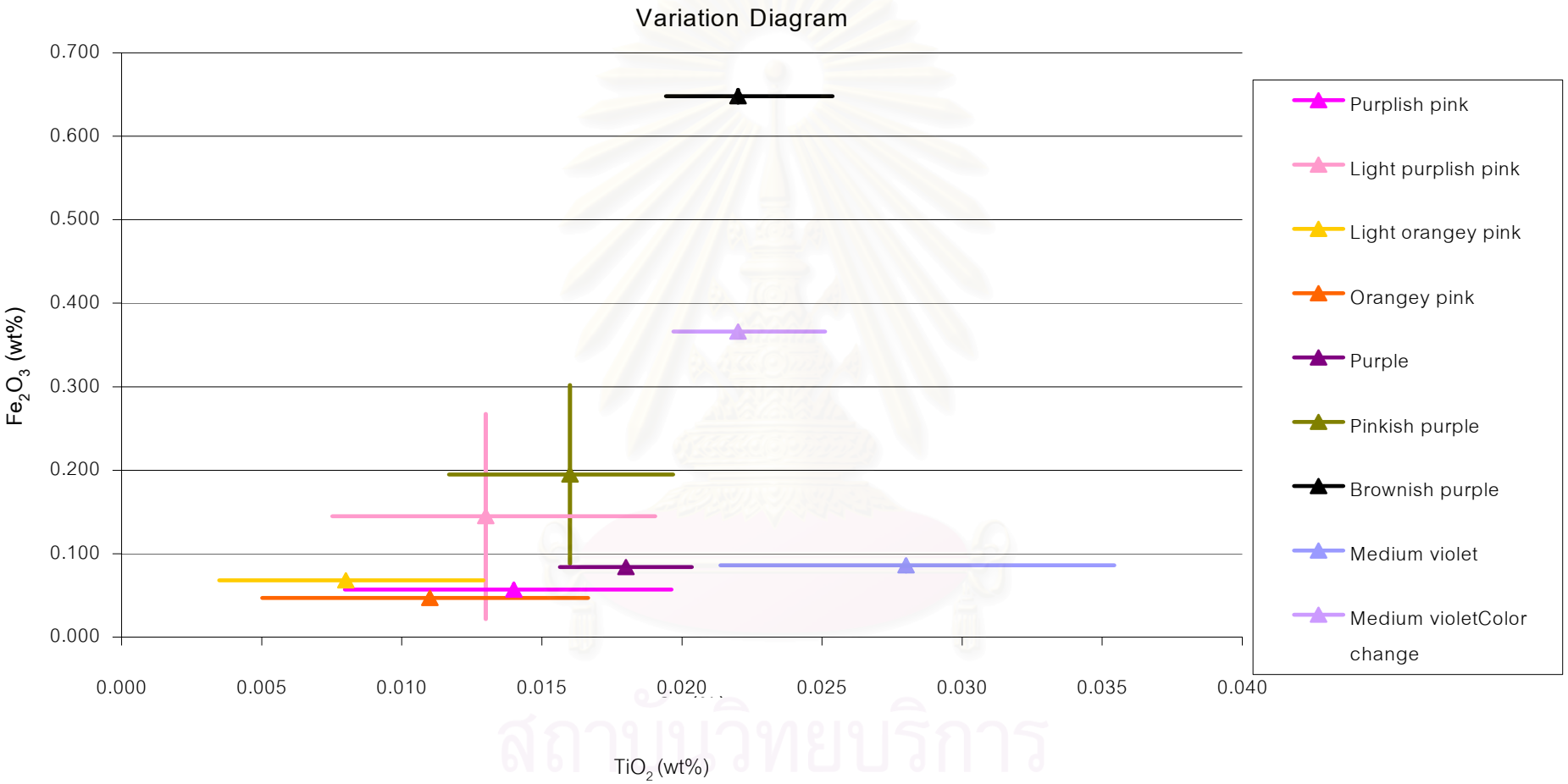

Figure 6.5 Variation diagram of Fe_2O_3 versus TiO_2 shows the average and one standard deviation of iron and chromium contents of 8 sapphire types by EPMA.

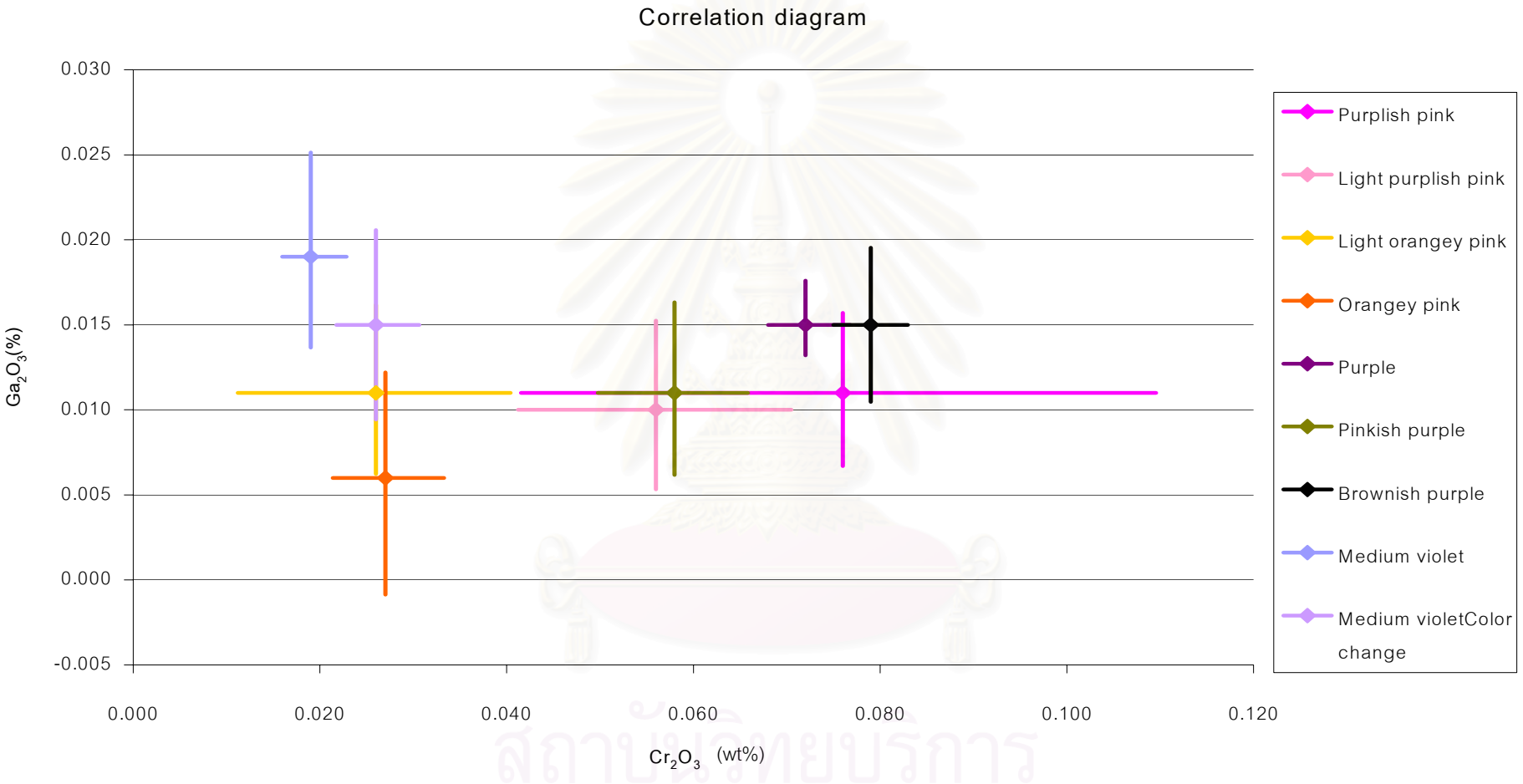

Figure 6.6 Variation diagram of Ga_2O_3 versus Cr_2O_3 shows the average and one standard deviation of gallium and chromium contents of 8 sapphire types by EPMA.

sapphires are fairly uniform (0.047-0.660 weight % Fe_2O_3 on the average). The iron concentration of the brownish purple sample is the highest (Figure 6.5).

Titanium content in medium violet (with and without color-change effects) and brownish purple sapphires are higher than those of the others (average about 0.022-0.028 weight % TiO_2) while the purple and pinkish purple sapphires, which show less blue component than violet sapphire, contain only 0.016-0.018 weight % TiO_2 on the average (Table 6.2, Figure 6.5).

The average gallium concentrations are about 0.006-0.019 weight % Ga_2O_3 and are fairly uniform in all sapphire types (Figure 6.6).

Comparison of trace element content by EDXRF and EPMA

Some selected the trace elements (Cr_2O_3, $Fe_2O_{3(total)}$, TiO_2, V_2O_3 and Ga_2O_3) of sapphire samples analyzed using EPMA are compared with the trace elements content of the same samples analyzed using EDXRF. To present the comparison of trace element analysis between EDXRF and EPMA, the 4 samples which show low, medium and high contents of each oxide element were selected. In each selected sample, the EPMA data is shown as the maximum, minimum and mode values while the EDXRF data is shown as only one value (Figures 6.7 to 6.11).

As shown in Figures 6.7-6.11, TiO_2 content (Figure 6.7) and probably Cr_2O_3 (Figure 6.8), V_2O_3 (Figure 6.9) and Ga_2O_3 (Figure 6.10) content analyzed by EDXRF generally show higher values than those analyzed by EPMA. In contrast, the Fe_2O_3 (Figure 6.11) content analyzed by EDXRF show either higher or lower values than those analyzed by EPMA. Very few data show nearly the same values by both technique. The variation analyzed by EPMA on each sample may be due to compositional inhomogeneity of that sample as well as to the analytical precision of the machine at such low concentration level (noted that Fe_2O_3 values which are an order of magnitude higher than other elements seem to show a good analytical precision). Based on these data it seems to suggest that the present EDXRF technique is rather

poor in both accuracy and precision as compared with the EPMA. Nonetheless the data set obtained from the same EDXRF machine as in this work could still be used to indicate the general trend.

สถาบันวิทยบริการ
จุฬาลงกรณ์มหาวิทยาลัย

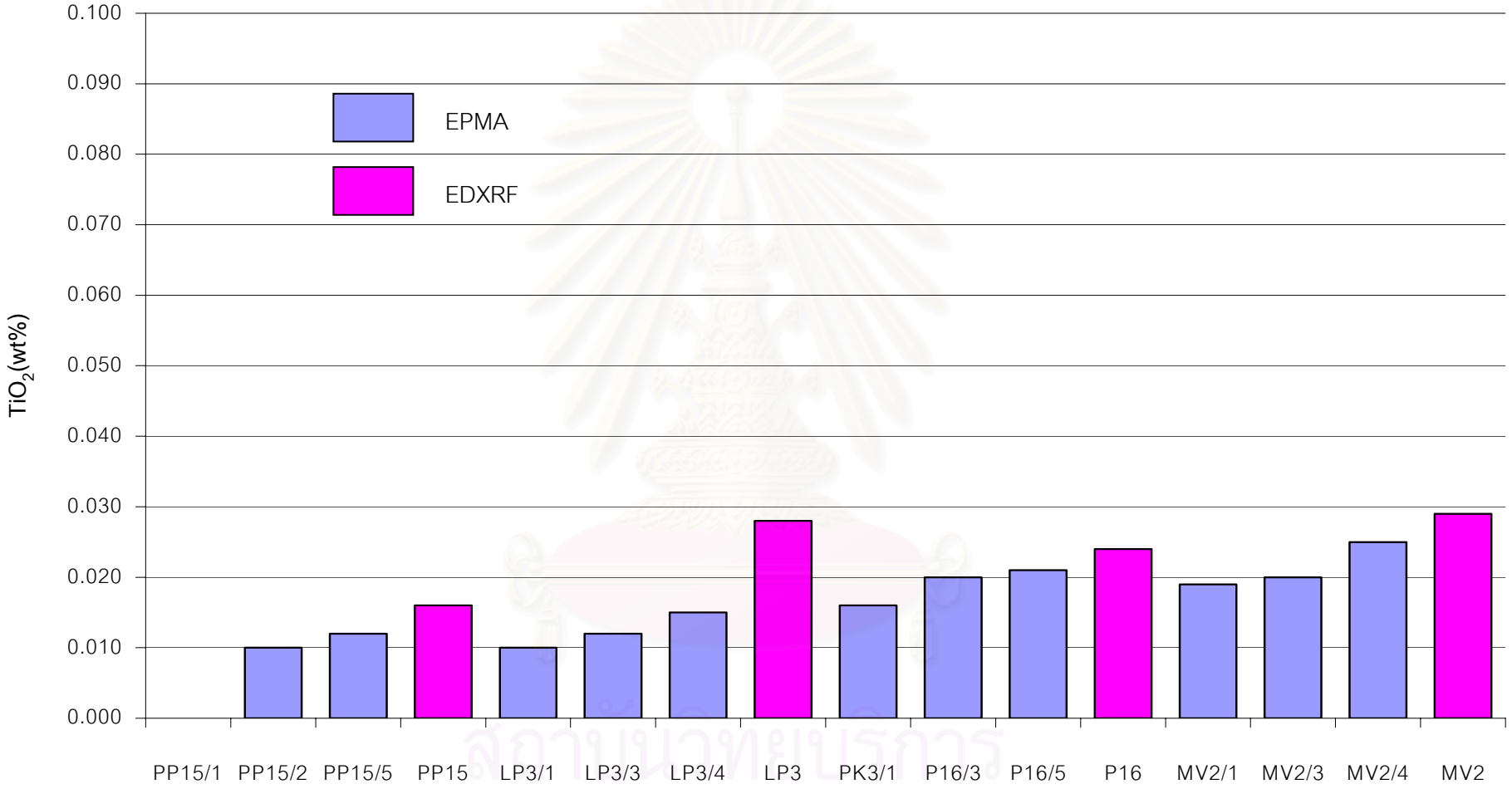

Figure 6.7 Titanium content of some selected pink, purple and violet sapphires (4 samples) by EPMA versus EDXRF; titanium content in PP15/1 is lower than detection limit (<0.01 weight % TiO_2).

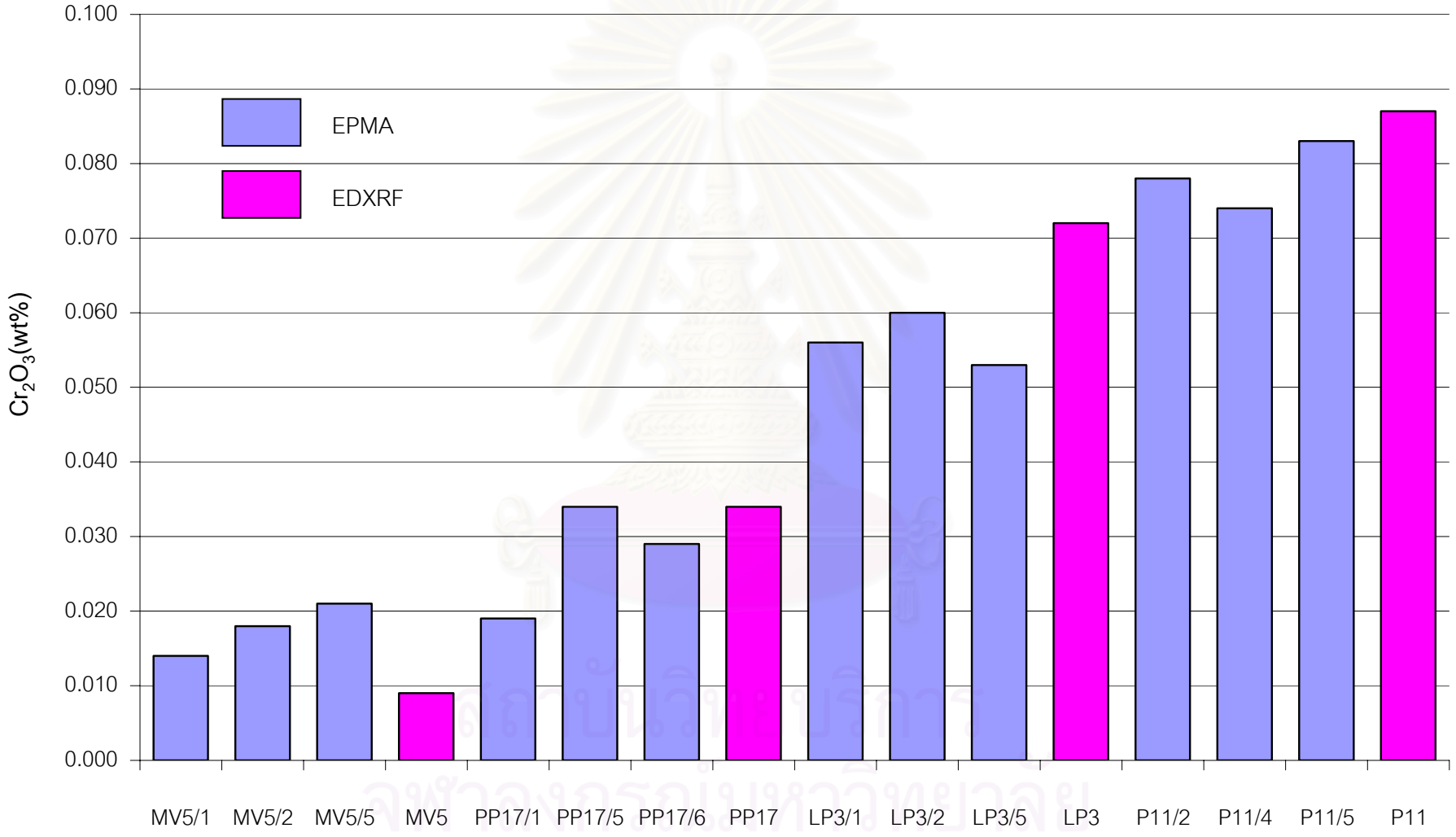

Figure 6.8 Chromium content of some selected pink, purple and violet sapphires (4 samples) by EPMA versus EDXRF.

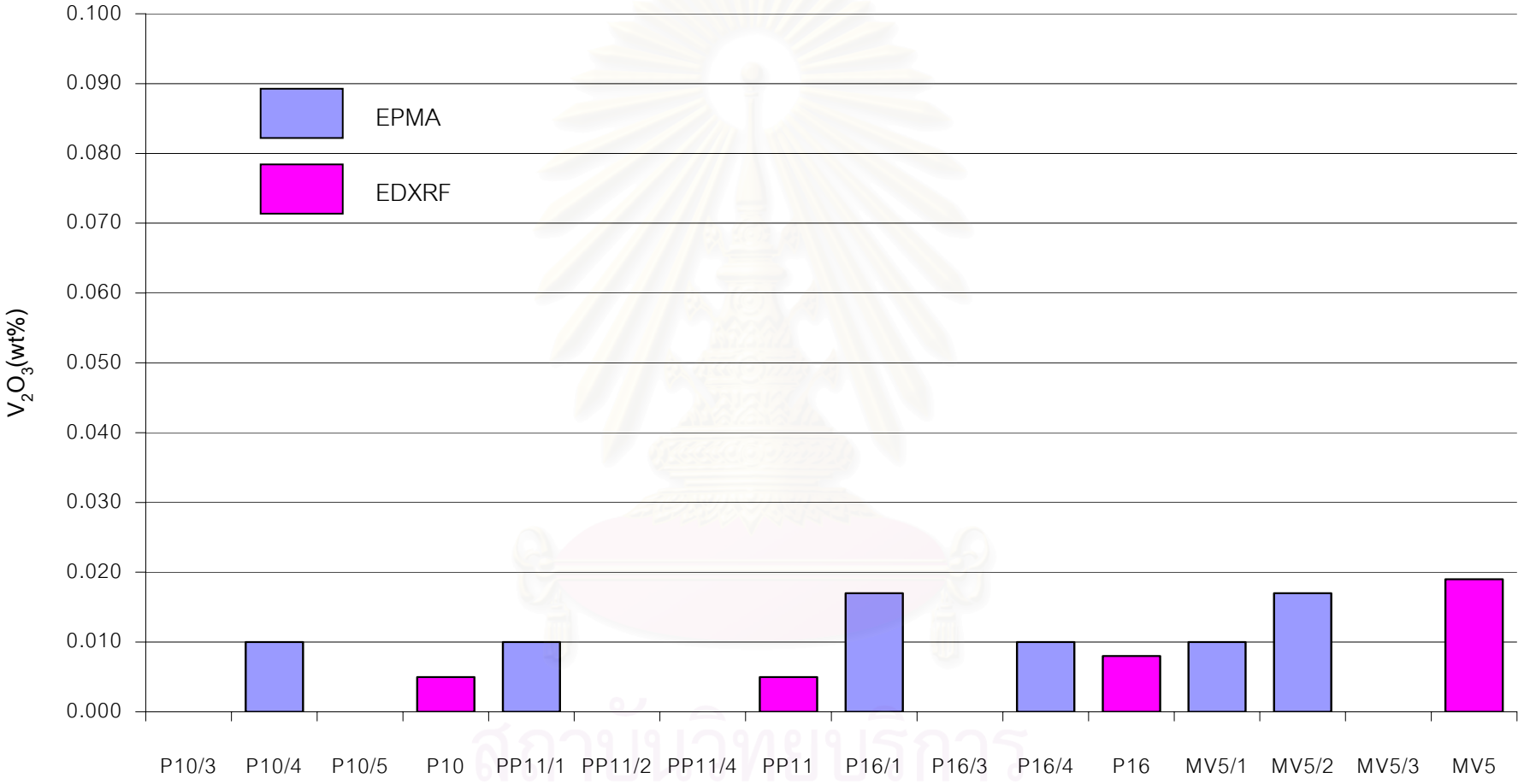

Figure 6.9 Vanadium content of some selected pink, purple and violet sapphires (4 samples) by EPMA versus EDXRF; vanadium contents in P10/3, P10/5, PP11/2, PP11/4, P16/3 and MV5/3 are lower than detection limit (<0.01 weight % V_2O_3).

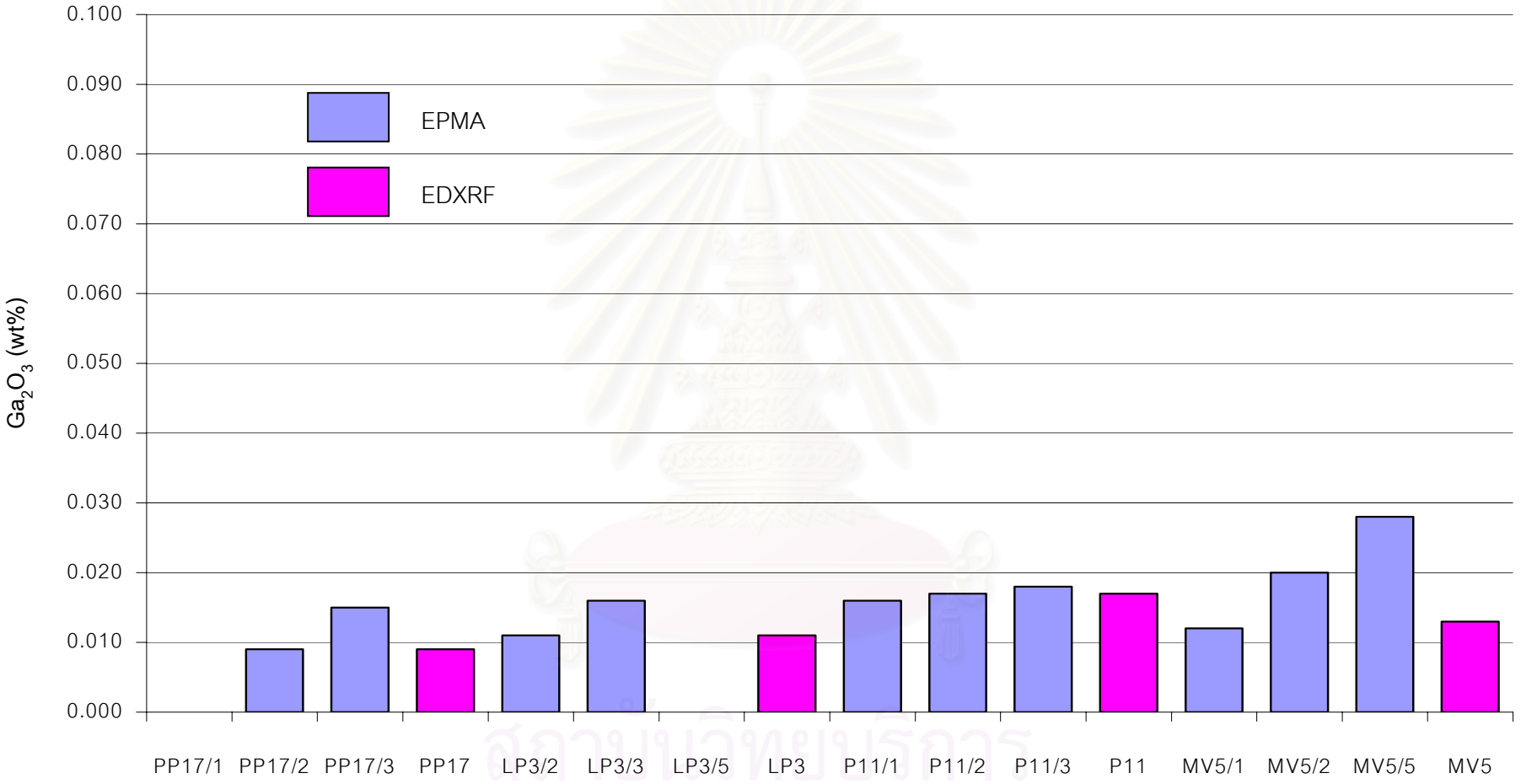

Figure 6.10 Gallium content of some selected pink, purple and violet sapphires (4 samples) by EPMA versus EDXRF; gallium contents in PP17/1 and LP3/5 are lower than detection limit (<0.01 weight % Ga_2O_3).

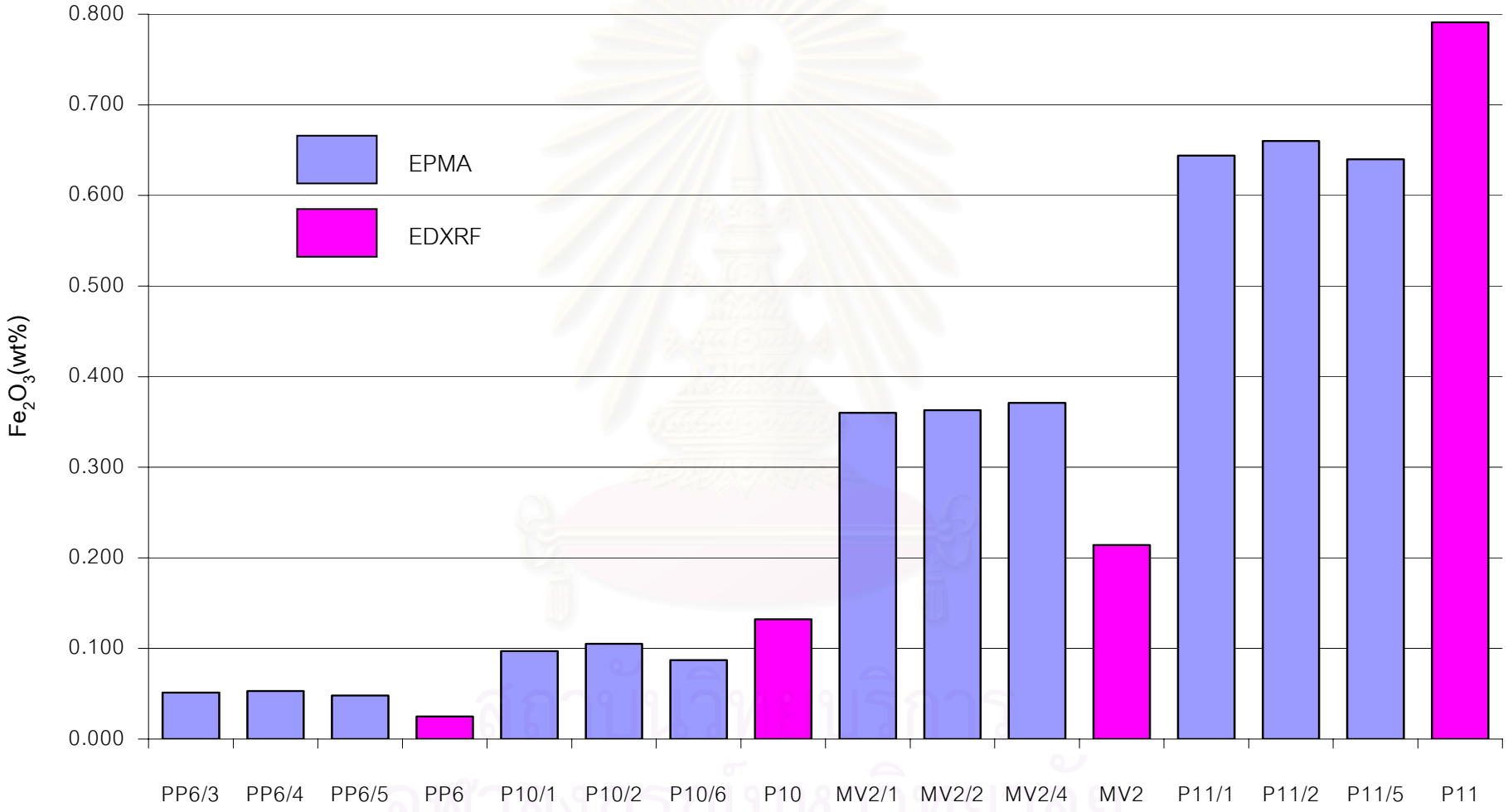

Figure 6.11 Iron content of some selected pink, purple and violet sapphires (4 samples) by EPMA versus EDXRF.

CHAPTER VII
DISCUSSION AND CONCLUSION

Cause of color change in sapphire after heat treatment

The interaction of Mg, Ti and Fe in corundum to create blue or stable yellow color center is well understood (Emmett and Douthit, 1993; Haeger, 2001). Mg and Ti usually form colorless $MgTiO_3$ clusters, known as Geikielite cluster (Haeger, 2001). After the formation of $MgTiO_3$ clusters, the excess of Ti in combination with Fe could form color active $FeTiO_3$ clusters (or so-called color effective $FeTiO_3$ clusters). This clusters can create Fe^{2+}/Ti^{4+} IVCT absorption bands near 580 and 735 nm which are responsible for the coloration of blue sapphire (Emmett and Douthit, 1993; Haeger, 2001). On the contrary, if there is an excess of Mg after the calculation of $MgTiO_3$ clusters, the excess Mg will lead in combination with Fe to produce color active defect center or stable yellow color center. However, in the system where there is no Fe impurity such as in Mg-doped synthetic sapphires, stable brownish violet color center could be produce instead (Wang and others, 1983; Haeger, 2001). The role of Mg was believed to act as stabilizer of the defect center. This model is well illustrated in Figure 7.1 for the corundum heated at $1850^{O}C$ in oxidizing condition and Figure 7.2 with additional Cr^{3+} in the corundum heated at $1750^{O}C$ under oxidizing condition. As shown in Figure 7.2, combination of yellow and pink should produce orange shown in the upper part of the triangle and combination of blue and pink should produce violet or purple shown in the lower part of the triangle. The reason for this was that Cr^{3+} was an additional coloring element for pink or red and it did not influence the valences of the other trace elements (Haeger, 2001).

By plotting the atom moles of Fe, Mg and Ti normalized to 100% of all the sapphires analyzed by EPMA in the triangular diagram in Figure 7.3, the cause of color change after heat treatment can be explained. As shown in Figure 7.3, most data points fall along the line of Mg/Ti ratio of 1:1 or slightly greater than 1. This data therefore suggest that when heat-treated those sapphires in oxidizing atmosphere, most of Mg and Ti would be tied up with the formation of colorless $MgTiO_3$ clusters and at the same

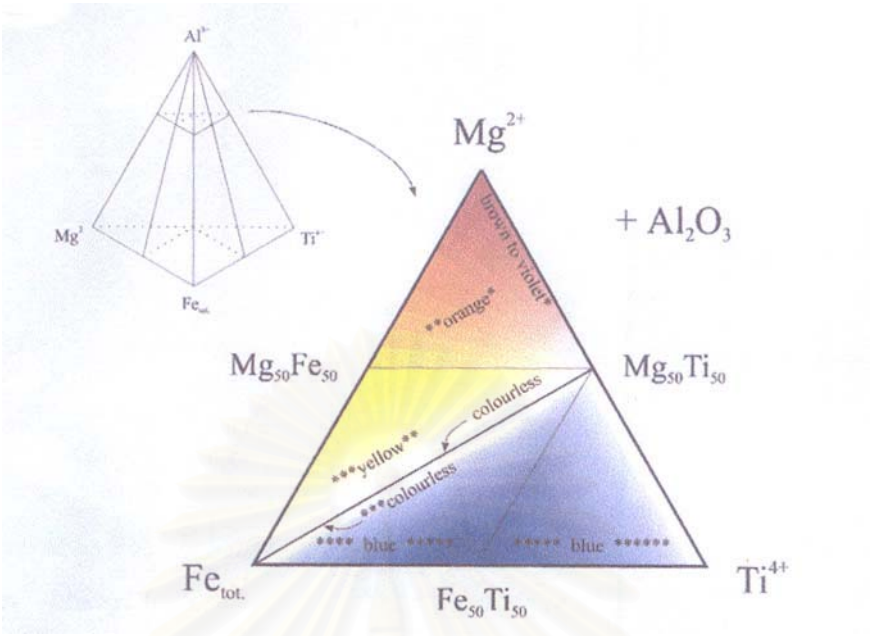

Figure 7.1 Model of sapphires heated at 1850°C in oxidizing atmospheres (Haeger, 2001)

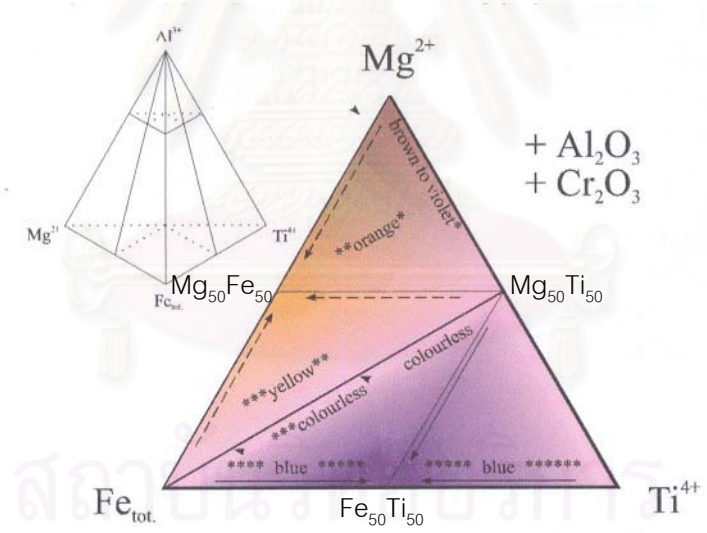

Figure 7.2 Model of corundum heated at 1750°C in oxidizing atmospheres (Haeger, 2001)

*	color center due to Mg	**	color center due to Mg and Fe
***	yellow due to Fe^{3+}	****	Fe^{2+}/Fe^{3+} -charge transfer green due to Fe^{3+}
*****	Fe^{2+}/Ti^{4+} -charge transfer	******	precipitation of TiO_2

time the Fe^{2+} might have been oxidized into Fe^{3+} (Haeger, 2001). Hence the blue overcast originated from Fe^{2+}/Ti^{4+} IVCT process would have been eliminated fairly easily and the stones should turn in pure pink color (Figure 7.2). This is probably the case for most sapphires in this study.

It should be further noted that the presence of blue overcast in the violet and purple samples before heating could imply that at least part of Ti might exist inhomogenously and was not bound originally to $MgTiO_3$ clusters. Hence the unbound Ti could form color active $FeTiO_3$ clusters instead which produce blue hue in the violet and purple sapphires. High temperature annealing would accelerate trace element interaction to their completion and eliminate the blue overcast during the heat treatment.

Further note for the medium violet sapphires (MV2 and MV5), they have the Mg/Ti ratios close to 1 and well within the pink zone of the triangular diagram (Figure 7.3). This is consistent with color change from medium violet before heating to pale bluish purple after heating from $1000^{O}C$ to $1400^{O}C$. However, the stones appear more bluish after heating up to $1600^{O}C$, this phenomenon, nonetheless, can be explained by the dissolution of rutile needle into the corundum structure (see resorbed rutile silk in Figure 5.34) and causing the formation (by charge compensation) of color active $FeTiO_3$ clusters in certain area of the stones. This could make the stones appear bluish once again.

For the light orangey pink (PP15) and orangey pink (PP17) sapphires, these samples turned into pink after heating from $800^{O}C$ to $1600^{O}C$. The Mg/Ti ratios are slightly more than 1 which are still within the pink zone in Figure 7.3. The slight excess of Mg may not be enough to stabilize the yellow color centers in these samples. It commonly requires Mg/Ti ratios of more than 2 to be able to produce yellow color centers under oxidized heating in majority of natural sapphires (Pisutha-Arnond, per. com.).

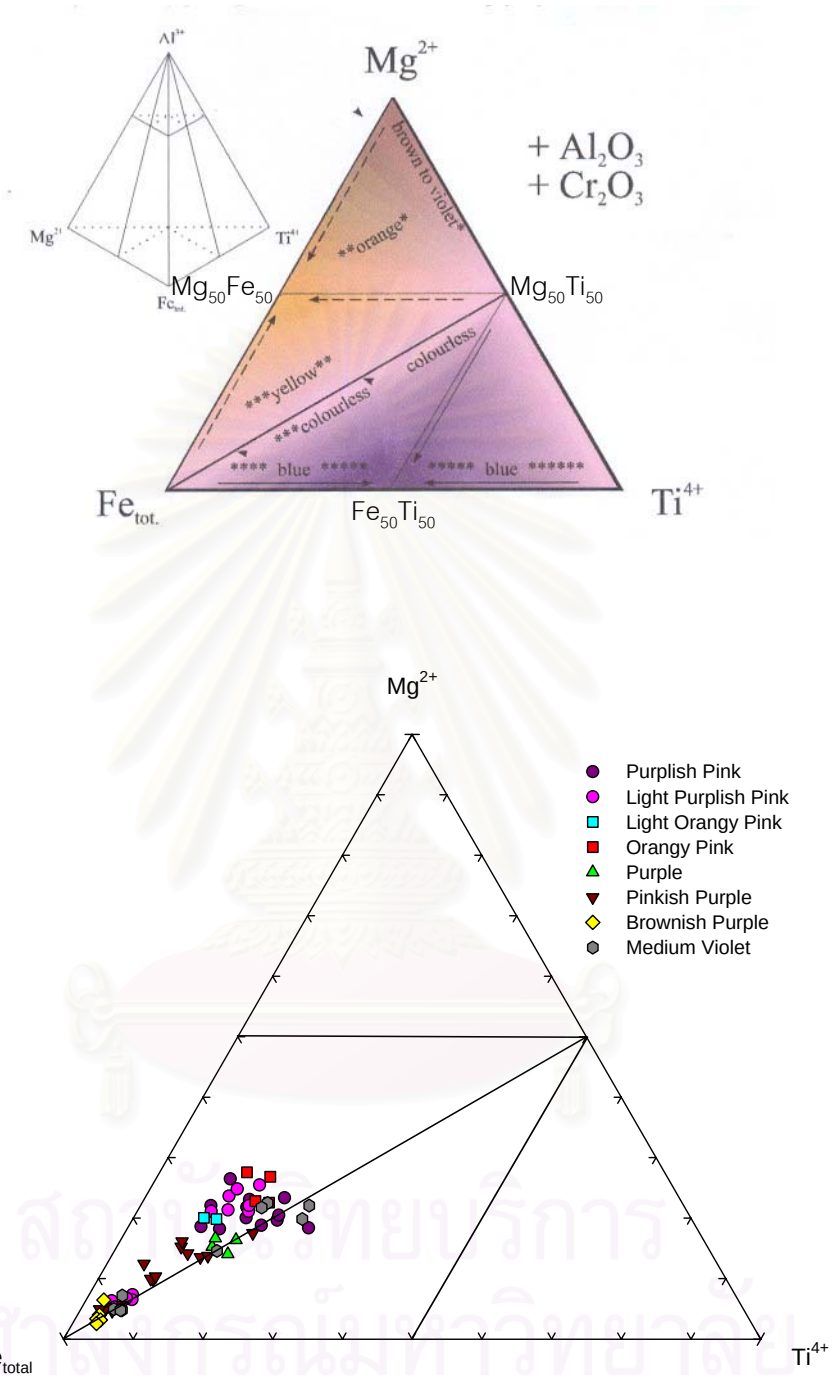

Figure 7.3 Mg, Fe and Ti contents of 16 sapphire samples by EPMA. The analysis was performed after the step-heating up to 1600^{O}C in oxidizing atmosphere. These contents were normalized to 100% and plot in Mg-Fe-Ti triangle in comparison to Al-$Fe_{(total)}$-Ti-Mg model of corundum heated at 1750^{o}C in oxidizing atmospheres.

Conclusions

1. Ilakaka-Sakaraha gem field occur as secondary deposits in alluvial plain and river terrace. The sapphires and accompanying minerals (zircon, spinel, garnet, topaz and chrysoberyl) are being recovered from those deposits which might have been derived from Isalo Group sediments of Middle Triassic to Liassic (Jurassic) in age.

2. The Ilakaka-Sakaraha rough sapphire samples were classified into 7 groups based on the color shade as pink, blue, violet, purple, colorless, yellow and green groups. Most pink, violet and purple sapphires show moderate to strong luminescence in pink to orange color under LWUV which suggest that they may belong to low iron suit of metamorphic-type origin. Only 8 types of pink, purple and violet sapphires namely, purplish pink, light purplish pink, orangey pink, light orangey pink, purple, pinkish purple, brownish purple, medium violet (with and without color-change effects) were selected for heat treatment study.

3. Most pink, purple and violet sapphires are rather clean and homogeneous without color zoning. The most common mineral inclusion is zircon which occurs as single inclusion or as cluster of inclusions with or without tension disc or crack. Other mineral inclusions are monazite, rutile (occurs as crystal or as needles), and mica (colorless and green varieties). The internal features are healed fractures or fingerprints and white dust or minute particles.

4. Heating conditions were selected at 5 maximum temperatures ($800^{O}C$, $1000^{O}C$, $1200^{O}C$, $1400^{O}C$, and $1600^{O}C$) for a period of one hour soaking time at each temperature under oxidizing atmosphere. Generally heat at $1000^{O}C$ for 1 hour is enough to reduce the overcast blue color and it is less likely to damage the stone. For sample with rutile needles or dust that appear milky, the blue color was returned when heating at $1600^{O}C$ such as MV2 and MV5.

5. The whitish, cloudy appearance (turbid) of zircon inclusion can provide a useful criterion for detecting the heat treatment as they can not be observed in unheated stones. However, the tension disc around zircon inclusions is not a good criterion of heat treatment as it can also be observed in unheated samples.

6. The UV-VIS-NIR spectra show the prominent absorption due to Cr^{3+} at 401-412, 553-560 and 692-693 nm in o-ray and some samples (LP9, PP16, P6, P11 and MV2) with additional peaks due to iron at 385-388 nm (Fe^{3+}) and 449-450 nm (Fe^{3+}/Fe^{3+} pairs in o-ray) both before and after heat treatment. For some samples (PP11, PP15, PP17, LP7, P10, P16 and MV5) does not show peaks of Fe^{3+} and Fe^{3+}/Fe^{3+} pairs which has low Fe content (<0.2 weight %), these spectra are similar to those of Mogok ruby that derived from metamorphic source. The remaining (residue) spectra, cause by substracting the spectra of the after from the before heating, should reflect the absorption of visible light and should reveal the cause of color change resulting from heating. For example, the residue spectra of medium violet after subtraction show a board band peaked at 580 and 735 nm, which due to the Fe^{2+}/Ti^{4+} IVCT and responsible for the removal of blue component after heating. The residue spectra of orangey pink sapphire after subtraction show a typical absorption pattern commonly observed in yellow Sri Lanka sapphire which are known to be caused by color centers. After heating at $800^{O}C$ the yellow hue was removed because the heating destroyed this color center.

7. Based on EDXRF analysis, pink, purple and violet with color-change effect groups show higher chromium content than other groups. In blue sapphire group titanium concentration is the highest. The iron content of the green group is the highest while the yellow group show only 0.1 weight % Fe_2O_3 on the average but can give yellow color. Hence, the cause of yellow color in some Ilakaka-Sakaraha sapphires is due to color center. The average concentrations of vanadium in all sapphires with color-change groups are distinctly higher than other sapphire without color-change groups.

8. Based on EPMA analysis, the chromium content in purplish pink, purple, brownish purple, pinkish purple and light purplish pink are distinctly higher than

those of orangey pink, light orangey pink and medium violet (with and without color-change effects) sapphires. The brownish purple sample shows the highest iron concentration. Titanium content in medium violet (with and without color-change effects) and brownish purple sapphires are higher than those of the others. The vanadium concentration in all types of sapphire are not distinctly different (below 0.01 weight % V_2O_3 on the average). All sapphire types show fairly uniform gallium concentrations about 0.006-0.019 weight % Ga_2O_3 on the average.

9. The EPMA analysis reveals that the Mg/Ti ratios of all sapphires are 1:1 or slightly greater than 1. This data therefore suggest that when heat-treated those sapphires in oxidizing atmosphere, most of Mg and Ti would be tied up with the formation of colorless $MgTiO_3$ clusters and at the same time the Fe^{2+} might have been oxidized into Fe^{3+}. Hence the blue overcast originated from Fe^{2+}/Ti^{4+} IVCT process would have been eliminated fairly easily and the stones should turn in pure pink color.

สถาบันวิทยบริการ
จุฬาลงกรณ์มหาวิทยาลัย

REFERENCES

Emmett, J. L., and Douthit, T. R. 1993. Heat Treating the Sapphires of Rock Creek, Montana. Gems&Gemology. 29. 4: 250-272.

Bootsri, K., and Bussai, B. 2001. Some Sapphires from Diego Suarez area, northern Madagascar: the general gemmological properties and their internal characteristics after heat treatment. Senior project report. Department of Geology. Chulalongkorn University: 80 p.

Doomernik. 2001. Sapphire-Seekers in Ilakaka [online]. Available from: http://www.doomernik.com/sapphire/3.html [2001, May 14].

Fritsch, E., and Rossman, G. R. 1988. An update on color in gems. part 3 : colors caused by band gaps and physical phenomena. Gems&Gemology. 24. 2: 81-102.

Gem Mining Resources. 2002. Gemstones in Madagascar [online]. Available from: http://www.gmrcorp.com/page/gem.html [2001, June 15].

Haeger, T. 2001. High Temperature Treatment of Natural Corundum. Proceedings of the International Workshop on Material Characterization by Solid State Spectroscopy. 4-10 April 2001. The Minerals of Vietnam. Hanoi. Vietnam: 1-10

Hansawek, R. 2001. Gem potential and investment opportunity of Madagascar. Proceedings of Seminar on Madagascar's Gems : New Perspectives for Thai Entrepreneurs. 15 February 2001. Department of Mineral Resources. Bangkok, Thailand. Second published: 107-114 (in Thai).

Hughes, R. W. 1997. Ruby&Sapphire. Colorado USA: RWH Publishing.

Inraikhing, K. and Pumpang, S. 2001. Gemmological properties of some Sri Lankan sapphires and their internal characteristics caused by thermal treatment. Senior project report. Department of Geology. Chulalongkorn University: 70 p.

Junprapasir, A. 2000. The gemmological properties and internal characteristics of some sapphires from the Ilakaka area, Madagascar. Senior project report. Department of Geology. Chulalongkorn University: 86 p.

Kiefert, L., Schmetzer, K., Krzemnicki, M. S., Bernhardt, H. J., and Hänni, H. A. 1996. Sapphires from Andranondambo area, Madagascar. Journal of gemmology. 25. 3: 185-209.

Milisenda, C. C., Henn, U., and Hem, J. 2001. New gemstone occurrences in the south-west of Madagascar. Journal of Gemmology. 27. 7: 385-394.

Nassau, K. 1984. Gemstone enhancement. London: Butterworths.

Radelli, L. 1975. Geology and Oil of Sakamena Basin, Malagasy Republic (Madagascar). The American Association of Petroleum Geologists Bulletin. 59. 1: 97-114.

Rankin, A.H., and Edwards, W. 2003. Some effects of extreme heat treatment on zircon inclusions in corundum. Journal of Gemmology. 28. 5: 257-264.

Smith, C. P. 1995. A contribution to understanding the infrared spectra of rubies from Mong Hsu, Myanmar. Journal of Gemmology. 24. 5: 321-334.

Somboon, C. 2000. Internal characteristics of corundum resulting from thermal enhancement. Senior project report. Department of Geology. Chulalongkorn University: 86 p.

Themelis, T. 1992. The Heat Treatment of Ruby and Sapphire: Gemlab Inc.

Wang, H. A., Lee, C. H., and Kröger, F. A. 1983. Point defects in α–Al_2O_3: Mg studied by electrical conductivity, optical absorption, and ESR. Physical Review B. 27. 6: 3821-3841.

Williams, K. P. J., Nelson, J., and Dyer, S. 1997. The Renishaw Raman database of gemmological and mineralogical materials: Renishaw Inc.

จุฬาลงกรณ์มหาวิทยาลัย

APPENDICES

สถาบันวิทยบริการ
จุฬาลงกรณ์มหาวิทยาลัย

APPENDIX I

Table I.1 Showing the gemological properties of some Ilakaka-Sakaraha sapphires.

Table I.2 Color codes of pink, purple and medium violet sapphires before heating based on GIA GemSet color specimens (Retail Set)

สถาบันวิทยบริการ
จุฬาลงกรณ์มหาวิทยาลัย

Table I.1 Showing the gemological properties of some Ilakaka-Sakaraha sapphires.

Sample no.	SG	RI		birefringence	fluorescence	
		n_e	n_o		SWUV	LWUV
Purplish pink						
PP 1	3.95	1.760	1.769	0.009	inert	moderate pink
PP 2	3.94	1.760	1.768	0.008	inert	moderate pink
PP 3	3.96	1.760	1.769	0.009	inert	moderate pink
PP 4	3.97	1.760	1.769	0.009	inert	moderate pink
PP 5	3.98	1.760	1.769	0.009	inert	moderate pink
PP 6	3.94	1.760	1.768	0.008	inert	moderate pink
PP 7	3.96	1.760	1.769	0.009	inert	moderate pink
PP 8	3.97	1.760	1.769	0.009	inert	moderate pink
PP 9	3.95	1.760	1.768	0.008	inert	moderate pink
PP 10	3.96	1.760	1.768	0.008	very weak pink	strong pink
PP 11	3.99	1.760	1.768	0.008	very weak pink	strong pink
PP 12	3.98	1.760	1.768	0.008	very weak pink	strong pink
Light purplish pink						
LP 1	3.97	1.762	1.770	0.008	inert	weak pink
LP 2	3.92	1.760	1.768	0.008	inert	moderate pink
LP 3	3.98	1.760	1.768	0.008	inert	moderate pink
LP 4	3.97	1.760	1.768	0.008	inert	moderate pink
LP 5	3.99	1.762	1.770	0.008	inert	weak pink
LP 6	3.98	1.762	1.770	0.008	inert	weak pink
LP 7	3.99	1.760	1.768	0.008	inert	moderate pink
LP 8	3.92	1.762	1.770	0.008	inert	weak pink
LP 9	3.98	1.762	1.770	0.008	inert	weak pink

Table I.1 Showing the gemological properties of some Ilakaka-Sakaraha sapphires (continued).

Sample no.	SG	RI		birefringence	fluorescence	
		n_e	n_o		SWUV	LWUV
Light orangey pink						
PP 13	4.00	1.760	1.768	0.008	very weak pink	strong orange
PP 14	4.01	1.760	1.768	0.008	weak pink	strong orange
PP 15	3.98	1.760	1.768	0.008	very weak pink	strong pinkish orange
Orangey pink						
PP 16	4.00	1.764	1.772	0.008	inert	very weak pink
PP 17	4.01	1.760	1.768	0.008	weak pink	strong pinkish orange
PP 18	4.01	1.760	1.768	0.008	weak pink	strong orange
Pinkish purple						
P 1	3.97	1.760	1.769	0.009	inert	moderate pink
P 2	3.97	1.761	1.770	0.009	inert	weak pink
P 3	3.98	1.762	1.770	0.008	inert	weak pink
P 4	3.96	1.762	1.770	0.008	inert	weak pink
P 5	4.00	1.760	1.769	0.009	inert	moderate pink
P 6	3.98	1.761	1.770	0.009	inert	weak pink
P 7	3.97	1.760	1.769	0.009	inert	moderate pink
P 8	4.00	1.760	1.768	0.008	very weak pink	strong pink
P 9	4.02	1.760	1.768	0.008	very weak pink	moderate pink
P 10	3.99	1.760	1.768	0.008	very weak pink	strong pink
Brownish purple						
P 11	3.98	1.762	1.770	0.008	inert	very weak pink
P 12	3.96	1.762	1.770	0.008	inert	very weak pink
P 13	3.99	1.762	1.770	0.008	inert	very weak pink

Table I.1 Showing the gemological properties of some Ilakaka-Sakaraha sapphires (continued).

Sample no.	SG	RI		birefringence	fluorescence	
		n_e	n_o		SWUV	LWUV
Purple						
P 14	4.00	1.760	1.768	0.008	very weak pink	strong pink
P 15	4.02	1.760	1.768	0.008	very weak pink	strong pink
P 16	4.01	1.760	1.768	0.008	very weak pink	strong pink
Dark violet						
*DV 1	3.98	1.761	1.769	0.008	inert	moderate orange
*DV 2	3.95	1.761	1.770	0.009	inert	moderate orange
*DV 3	3.99	1.760	1.770	0.010	inert	moderate orange
Medium violet						
*MV 1	3.94	1.760	1.770	0.010	inert	weak orange
*MV 2	4.02	1.762	1.770	0.008	inert	weak orange
*MV 3	3.95	1.760	1.769	0.009	inert	moderate orange
MV 4	3.99	1.760	1.768	0.008	very very weak orange	weak pinkish orange
MV 5	3.97	1.760	1.768	0.008	very very weak orange	moderate pinkish orange
MV 6	3.94	1.760	1.768	0.008	very weak orange	moderate pinkish orange
Light violet						
LV 1	3.95	1.761	1.771	0.010	inert	moderate pinkish orange
LV 2	3.91	1.760	1.769	0.009	inert	moderate orange
LV 3	3.96	1.761	1.770	0.009	inert	weak orange
Very dark blue						
B 1	3.99	1.760	1.768	0.008	inert	inert
B 2	3.97	1.760	1.768	0.008	inert	inert
B 3	3.99	1.760	1.768	0.008	inert	inert

*show color-change effect

สถาบันวิทยบริการ
จุฬาลงกรณ์มหาวิทยาลัย

Table I.1 Showing the gemological properties of some Ilakaka-Sakaraha sapphires (continued).

Sample no.	SG	RI		birefringence	fluorescence	
		n_e	n_o		SWUV	LWUV
Dark blue						
B 4	3.99	1.760	1.768	0.008	inert	inert
B 5	3.93	1.760	1.768	0.008	inert	inert
*B 6	3.97	1.762	1.770	0.008	inert	very weak reddish orange
Medium blue						
B 7	4.00	1.760	1.768	0.008	inert	inert
*B 8	3.97	1.760	1.768	0.008	inert	weak reddish orange
B 9	3.99	1.761	1.769	0.008	inert	inert
B 10	3.94	1.761	1.770	0.009	inert	inert
*B 11	3.92	1.760	1.769	0.009	inert	weak reddish orange
B 12	4.04	1.761	1.770	0.009	inert	inert
*B 13	4.04	1.761	1.770	0.009	inert	moderate reddish orange
*B 14	3.92	1.761	1.769	0.008	inert	weak reddish orange
*B 15	4.00	1.760	1.769	0.009	inert	weak reddish orange
*B 16	3.97	1.761	1.770	0.009	inert	weak reddish orange
*B 17	3.93	1.761	1.770	0.009	inert	weak reddish orange
B 18	3.98	1.761	1.769	0.008	inert	inert
B 19	3.96	1.761	1.769	0.008	inert	inert
B 20	3.96	1.760	1.769	0.009	inert	inert

*show color-change effect

สถาบันวิทยบริการ
จุฬาลงกรณ์มหาวิทยาลัย

Table I.1 Showing the gemological properties of some Ilakaka-Sakaraha sapphires (continued).

Sample no.	SG	RI		birefringence	fluorescence	
		n_e	n_o		SWUV	LWUV
Light blue						
B 21	3.96	1.761	1.770	0.009	inert	inert
B 22	3.92	1.760	1.769	0.009	inert	inert
B 23	3.95	1.760	1.769	0.009	inert	very weak reddish orange
B 24	4.04	1.760	1.769	0.009	inert	very weak reddish orange
B 25	3.95	1.760	1.769	0.009	inert	inert
B 26	3.99	1.761	1.769	0.008	inert	very weak reddish orange
B 27	3.97	1.760	1.769	0.009	inert	inert
*B 28	3.99	1.760	1.770	0.010	inert	moderate reddish orange
*B 29	3.97	1.760	1.768	0.008	inert	moderate reddish orange
*B 30	3.96	1.760	1.770	0.010	inert	moderate orange
B 31	3.97	1.760	1.769	0.009	inert	inert
B 32	3.99	1.760	1.769	0.009	inert	inert
B 33	3.98	1.761	1.770	0.009	inert	inert
B 34	3.99	1.760	1.769	0.009	inert	inert
B 35	3.99	1.761	1.770	0.009	inert	inert
*B 36	4.01	1.760	1.768	0.008	inert	weak reddish orange
B 37	3.99	1.760	1.768	0.008	inert	inert
B 38	3.98	1.760	1.768	0.008	inert	very very weak reddish orange

*show color-change effect

Table I.1 Showing the gemological properties of some Ilakaka-Sakaraha sapphires (continued).

Sample no.	SG	RI		birefringence	fluorescence	
		n_e	n_o		SWUV	LWUV
Very light blue						
B 39	3.96	1.760	1.769	0.009	inert	weak reddish orange
B 40	3.99	1.760	1.769	0.009	inert	weak reddish orange
B 41	3.98	1.760	1.769	0.009	inert	moderate orange
B 42	3.91	1.760	1.769	0.009	inert	weak reddish orange
B 43	3.972	1.760	1.769	0.009	inert	weak reddish orange
B 44	4.00	1.760	1.769	0.009	inert	moderate reddish orange
B 45	3.97	1.760	1.769	0.009	inert	moderate reddish orange
B 46	3.99	1.760	1.768	0.008	inert	weak reddish orange
B 47	3.97	1.760	1.768	0.008	inert	inert
B 48	4.02	1.760	1.768	0.008	inert	inert
B 49	4.00	1.760	1.768	0.008	inert	inert
B 50	3.98	1.760	1.768	0.008	inert	very weak reddish orange
B 51	3.96	1.760	1.768	0.008	inert	very weak reddish orange
B 52	3.98	1.760	1.768	0.008	inert	inert
Extremely light blue						
B 53	3.99	1.760	1.768	0.008	inert	very weak orange

Table I.1 Showing the gemological properties of some Ilakaka-Sakaraha sapphires (continued).

Sample no.	SG	RI		Birefringence	fluorescence	
		n_e	n_o		SWUV	LWUV
Extremely light blue						
B 54	4.00	1.760	1.768	0.008	inert	very weak orange
B 55	3.94	1.760	1.768	0.008	inert	inert
B 56	3.95	1.760	1.769	0.009	inert	inert
B 57	3.95	1.760	1.768	0.008	inert	inert
B 58	3.98	1.760	1.769	0.009	inert	inert
B 59	3.95	1.760	1.768	0.008	inert	inert
B 60	3.96	1.760	1.768	0.008	inert	moderate orange
B 61	3.95	1.760	1.768	0.008	inert	inert
B 62	3.85	1.760	1.768	0.008	inert	inert
Colorless						
W 1	4.00	1.760	1.768	0.008	inert	inert
Very light bluish						
W 2	4.00	1.760	1.768	0.008	inert	inert
W 3	4.00	1.760	1.768	0.008	inert	inert
Orangey yellow						
Y 1	3.99	1.760	1.768	0.008	very weak reddish orange	moderate reddish orange
Medium green						
G 1	4.00	1.763	1.771	0.008	inert	inert
Light yellowish green						
G 2	4.01	1.763	1.771	0.008	inert	very very weak orange
G 3	3.98	1.763	1.771	0.008	inert	inert

สถาบันวิทยบริการ
จุฬาลงกรณ์มหาวิทยาลัย

Table I.2 Color codes of pink, purple and medium violet sapphires before heating based on GIA GemSet color specimens (Retail Set)

Sample no.	Code	Tone, Saturation Hue
Purplish pink		
PP 1	PR/RP 5/3	medium, very slightly brownish Purple - Red
PP 2	PR/RP 5/3	medium, very slightly brownish Purple - Red
PP 3	PR/RP 6/4	medium dark, moderately strong Purple - Red
PP 4	PR/RP 5/3	medium, very slightly brownish Purple - Red
PP 5	PR/RP 5/3	medium, very slightly brownish Purple - Red
PP 6	PR/RP 5/3	medium, very slightly brownish Purple - Red
PP 7	PR/RP 5/3	medium, very slightly brownish Purple - Red
PP 8	PR/RP 4/2	medium light, slightly brownish Purple-Red
PP 9	PR/RP 4/2	medium light, slightly brownish Purple - Red
PP 10	PR/RP 4/2	medium light, slightly brownish Purple-Red
PP 11	PR/RP 5/3	medium, very slightly brownish Purple-Red
PP 12	PR/RP 4/3	medium light, very slightly brownish Purple-Red
Light Purplish pink		
LP 1	R 5/1	medium, brownish Red
LP 2	R 5/1	medium, brownish Red
LP 3	PR/RP 4/3	medium light, very slightly brownish Purple - Red
LP 4	PR/RP 4/3	medium light, very slightly brownish Purple - Red
LP 5	PR/RP 4/3	medium light, very slightly brownish Purple - Red
LP 6	RO/OR 3/2	light, slightly brownish Orange - Red
LP 7	PR/RP 4/3	medium light, very slightly brownish Purple - Red
LP 8	R 5/1	medium, brownish Red
LP 9	PR/RP 4/3	medium light, very slightly brownish Purple - Red
Light orangey pink		
PP 13	Ro/oR 2/3	Very light, very slightly brownish Orange – Red
PP 14	Ro/oR 2/3	Very light, very slightly brownish Orange – Red
PP 15	PR/RP 2/3 + rO 2/3	Very light, very slightly brownish Purple – Red + Very light, very slightly brownish orangey Red

Table I.2 Color codes of pink, purple and medium violet sapphires before heating based on GIA GemSet color specimens (Retail Set) (continued)

Sample no.	Code	Tone, Saturation Hue
Orangey pink		
PP 16	Ro/oR 3/2	light, slightly brownish Orange – Red
PP 17	slpR 2/3 + rO 2/3	very light, very slightly brownish slightly purplish Red + very light, very slightly brownish reddish Orange
PP 18	rO 2/3	very light, very slightly brownish slightly purplish Red + very light, very slightly brownish reddish Orange
Pinkish purple		
P 1	PR/RP 7/4	dark, moderately strong Purple-Red
P 2	oR 4/3 (perpendicular to c-axis)	medium light, very slightly brownish orangey Red
P 3	PR/RP 6/3	medium dark, very slightly brownish Purple-Red
P 4	PR/RP 7/4	dark, moderately strong Purple-Red
P 5	PR/RP 6/3	medium dark, very slightly brownish Purple-Red
P 6	PR/RP 6/3	medium dark, very slightly brownish Purple-Red
P 7	PR/RP 7/4	dark, moderately strong Purple-Red
P 8	P 6/4	medium dark, moderately strong Purple
P 9	PR/RP 4/3	medium light, very slightly brownish Purple-Red
P 10	PR/RP 6/3	medium dark, very slightly brownish Purple-Red
Brownish purple		
P 11	PR/RP 6/3 + oR 4/3	medium dark, very slightly brownish Purple - Red + medium light, very slightly brownish orangey Red
P 12	PR/RP 6/3 + oR 4/3	medium dark, very slightly brownish Purple - Red + medium light, very slightly brownish orangey Red
P 13	rP 5/3 + PR/RP 5/3	medium, very slightly brownish reddish Purple + medium, very slightly brownish Purple - Red

Table I.2 Color codes of pink, purple and medium violet sapphires before heating based on GIA GemSet color specimens (Retail Set) (continued)

Sample no.	Code	Tone, Saturation Hue
Purple		
P 14	P 4/5	medium light, strong Purple
P 15	rP 8/3	very dark, very slightly brownish reddish Purple
P 16	P 6/3	medium dark, very slightly brownish Purple
Medium violet		
MV 1	V 4/3	medium light, very slightly grayish Violet
	*bP 4/4	*medium light, moderately strong bluish Purple
MV 2	V 4/3	medium light, very slightly grayish Violet
	*bP 6/3	*medium dark, very slightly grayish bluish Purple
MV 3	V 4/3	medium light, very slightly grayish Violet
	*bP 6/3	*medium dark, very slightly grayish bluish Purple
MV 4	V 4/4 + rP 5/3	medium light, moderately strong Violet + medium, very slightly brownish reddish Purple
MV 5	V 4/3	medium light, very slightly grayish Violet

* under tungsten lamp

สถาบันวิทยบริการ
จุฬาลงกรณ์มหาวิทยาลัย

List of hue, tone and saturation terms for describing gem colors, with their abbreviations.

HUE			
Purple	P	slightly yellowish Green	slyG
reddish Purple	rP	Green	G
red-purple or purple-red	RP/PR	very slightly bluish Green	VslbG
strongly purplish Red	stpR	bluish Green	BG
strongly purplish Red	stpR	very strongly bluish Green	VstbG
Red	R	Green-Blue or Blue-Green	GB/BG
orange Red	oR	very strongly greenish Blue	VstgB
Red-Orange or Orange-Red	RO/OR	greenish Blue	gB
reddish Orange	rO	very slightly greenish Blue	vslgB
Orange	O	Blue	B
yellowish Orange	yO	violetish Blue	vB
Orange yellowish	Oy	bluish Violet	bV
Yellow	Y	Violet	V
greenish Yellow	gY	bluish Purple	bP
Yellow-Green or Green Yellow	YG/GY	Pink	Pk
strongly yellowish Green	styG	Brown	Br
Yellowish Green	yG		

TONE		SATURATION	
0	colorless or white	1	grayish (brownish)
1	extremely light	2	slightly grayish (brownish)
2	very light	3	very slightly grayish (brownish)
3	light	4	moderately strong
4	medium light	5	strong
5	medium	6	vivid
6	medium dark		
7	dark		
8	very dark		
9	extremely dark		
10	black		

APPENDIX II

FTIR spectra of sapphire before and after heating

Purplish pink: PP3, PP4, PP6, PP11

Light purplish pink: LP3, LP4, LP9

Light orangey pink: PP15

Orangey pink: PP17

Pinkish purple: P5, P6, P10

Brownish purple: P11

Purple: P16

Medium violet: MV2, MV5

สถาบันวิทยบริการ
จุฬาลงกรณ์มหาวิทยาลัย

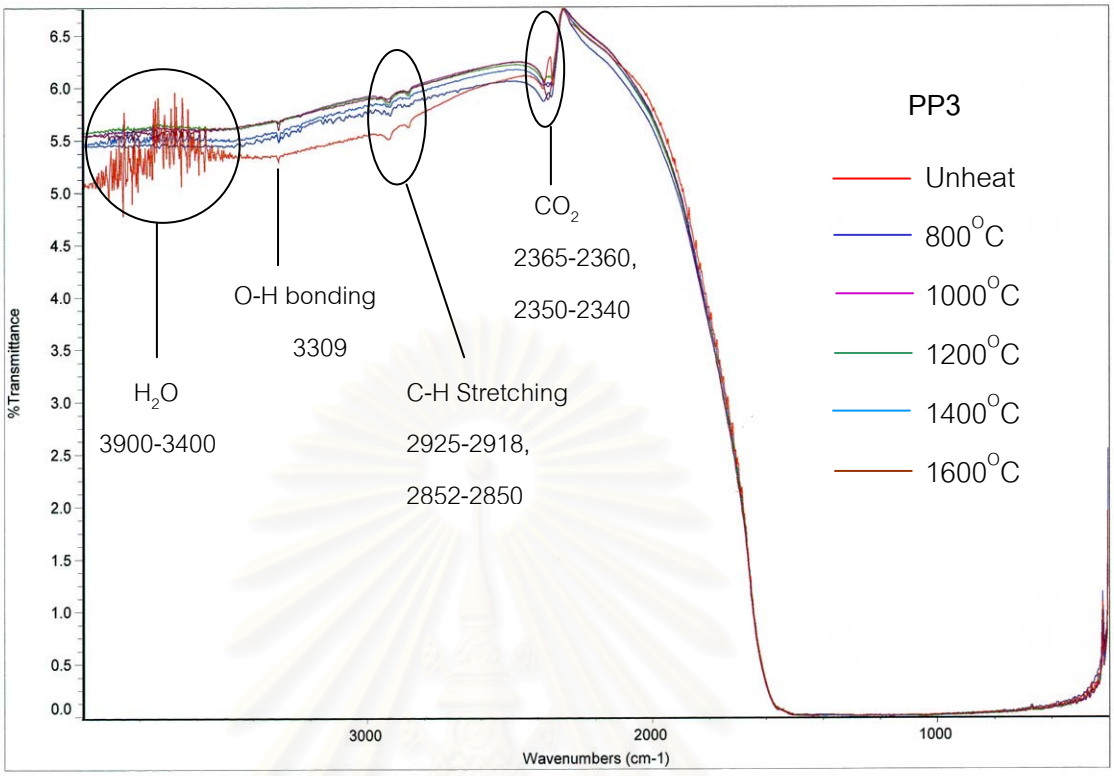
PP3
Unheat
800°C
1000°C
1200°C
1400°C
1600°C
H2O
3900-3400
O-H bonding
3309
C-H Stretching
2925-2918,
2852-2850
CO2
2365-2360,
2350-2340
%Transmittance
Wavenumbers (cm-1)

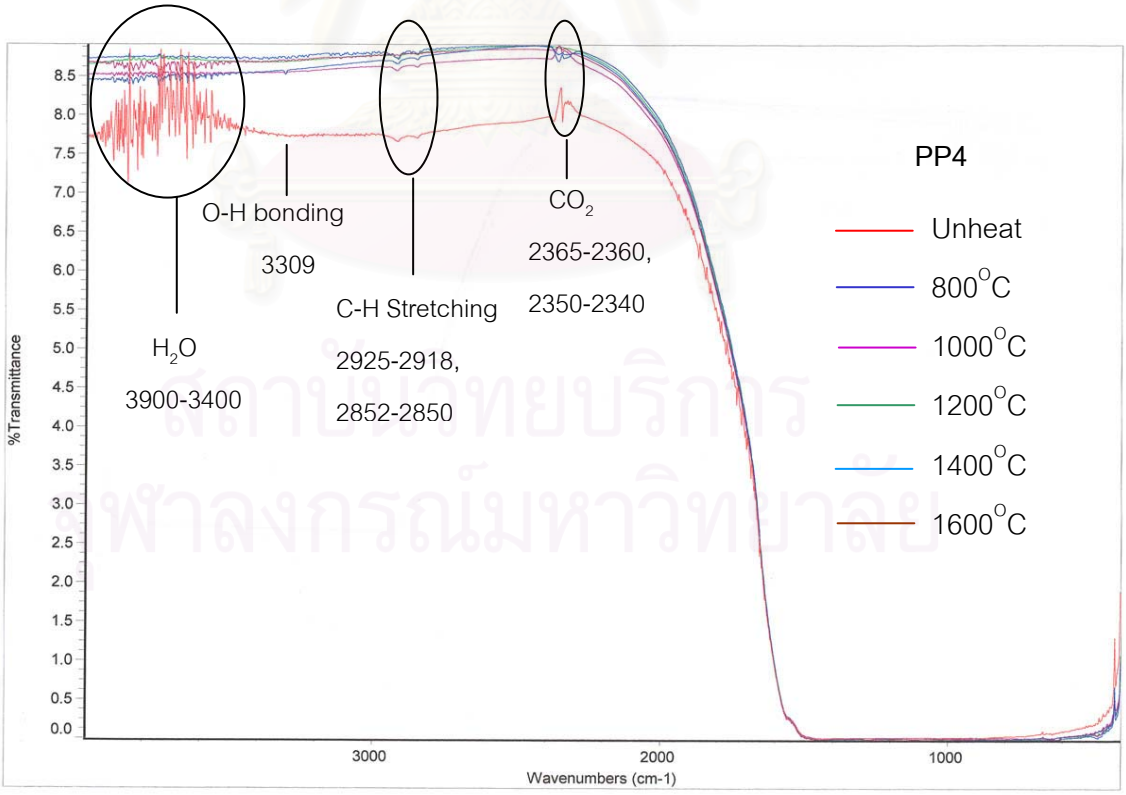
PP4
Unheat
800°C
1000°C
1200°C
1400°C
1600°C
H2O
3900-3400
O-H bonding
3309
C-H Stretching
2925-2918,
2852-2850
CO2
2365-2360,
2350-2340
%Transmittance
Wavenumbers (cm-1)

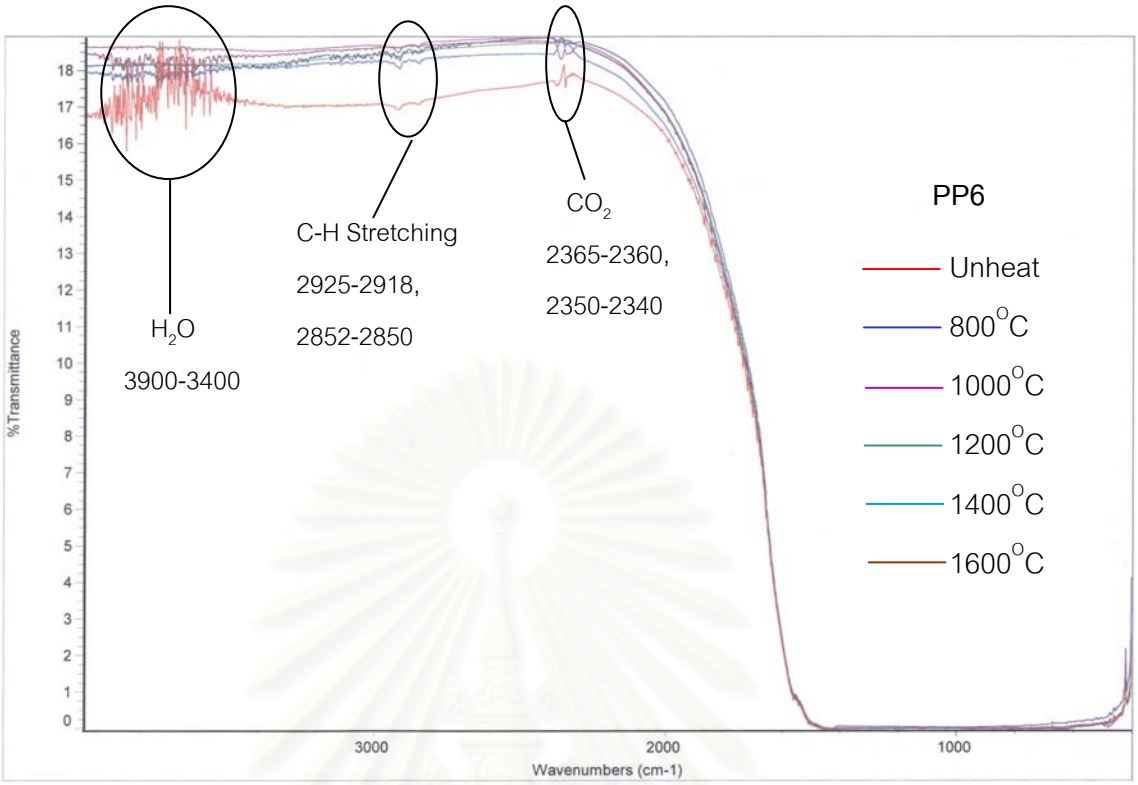

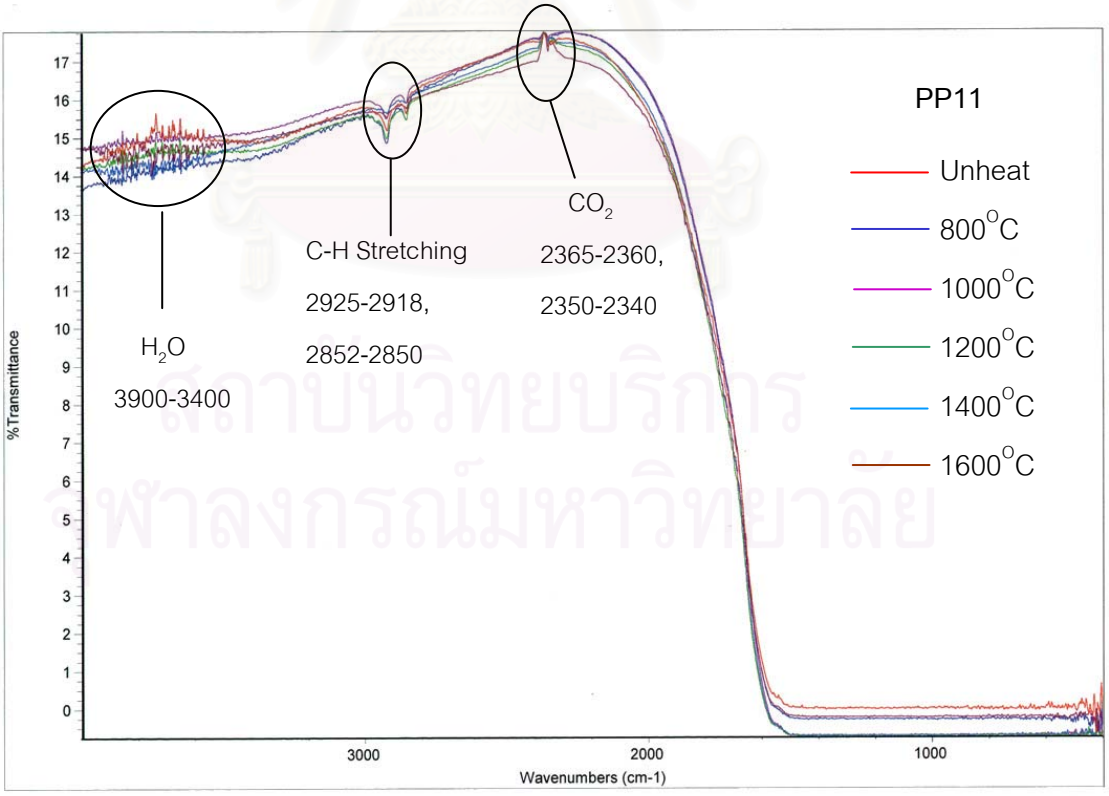

สถาบันวิทยบริการ
จุฬาลงกรณ์มหาวิทยาลัย

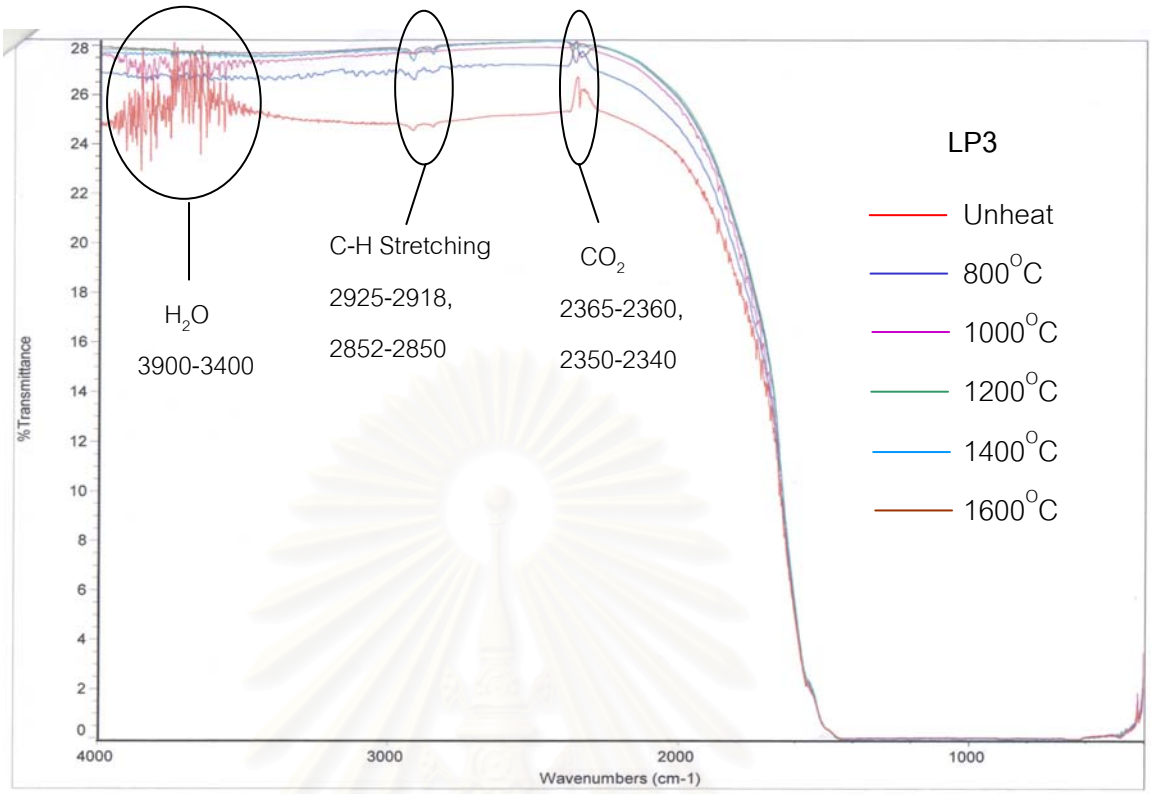
LP3
Unheat
800°C
1000°C
1200°C
1400°C
1600°C
H2O
3900-3400
C-H Stretching
2925-2918,
2852-2850
CO2
2365-2360,
2350-2340
%Transmittance
Wavenumbers (cm-1)
4000
3000
2000
1000

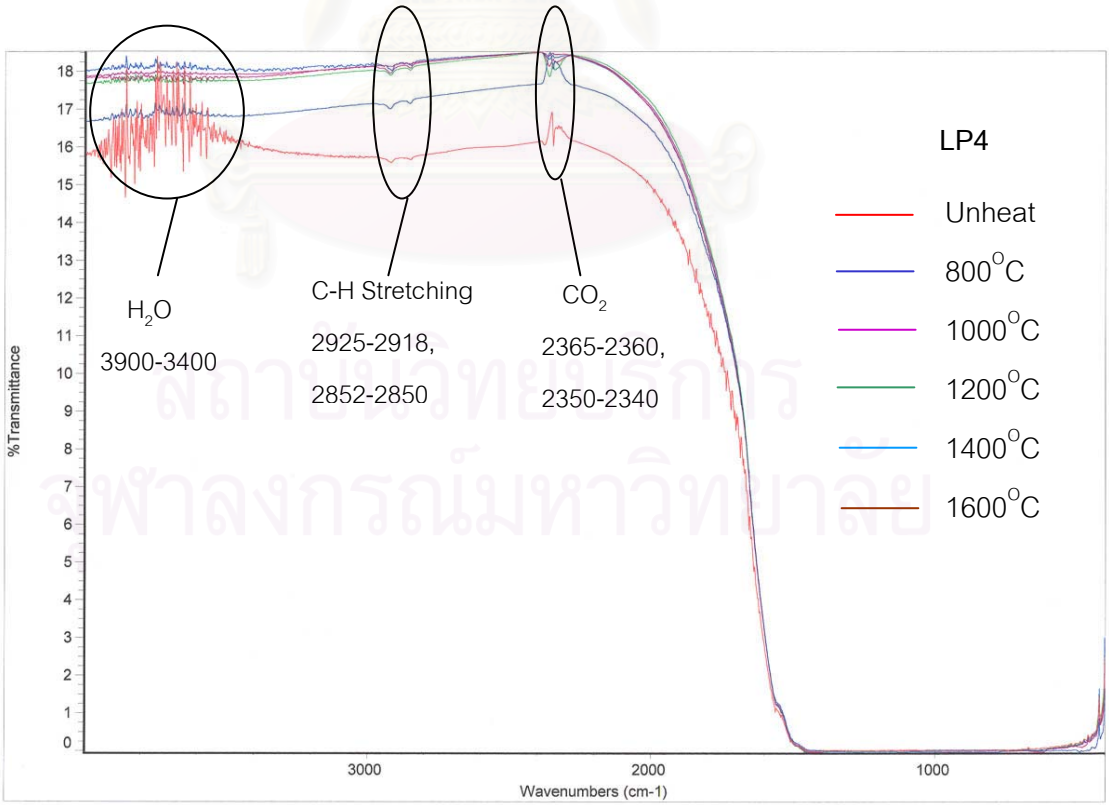
LP4
Unheat
800°C
1000°C
1200°C
1400°C
1600°C
H2O
3900-3400
C-H Stretching
2925-2918,
2852-2850
CO2
2365-2360,
2350-2340
%Transmittance
Wavenumbers (cm-1)
3000
2000
1000

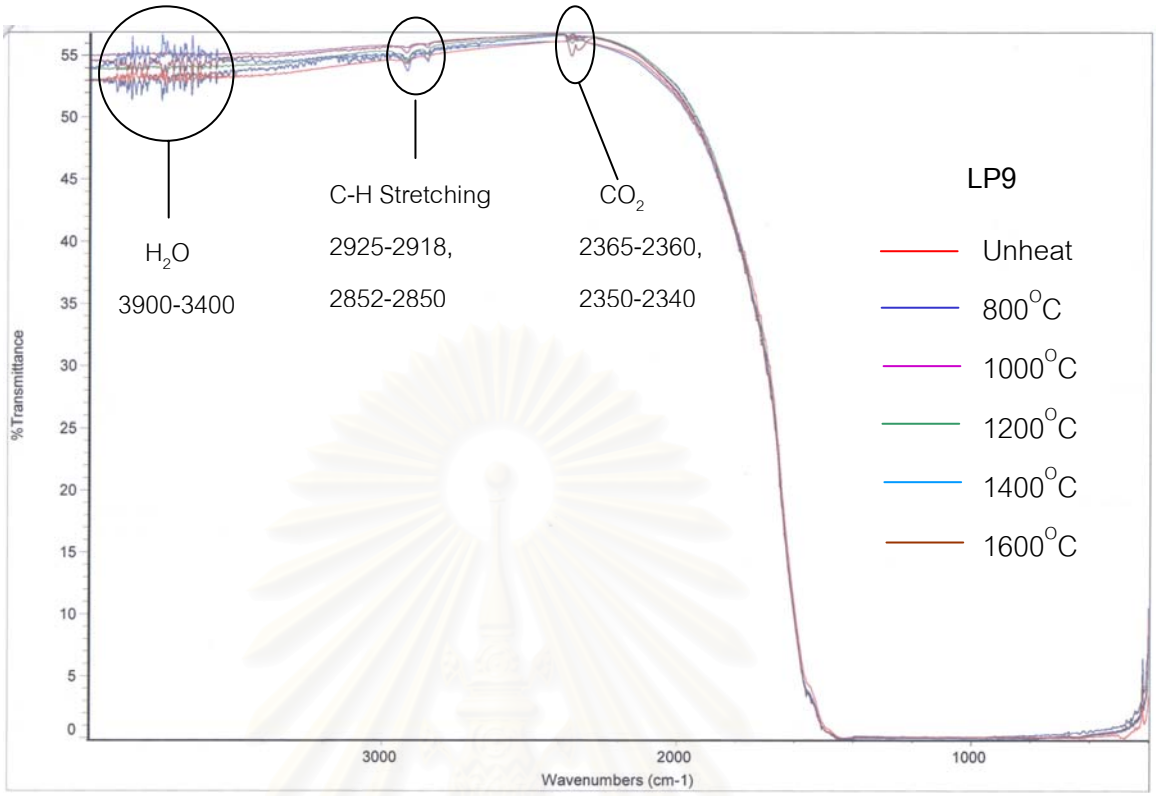
LP9
Unheat
800°C
1000°C
1200°C
1400°C
1600°C
H2O
3900-3400
C-H Stretching
2925-2918,
2852-2850
CO2
2365-2360,
2350-2340
%Transmittance
Wavenumbers (cm-1)

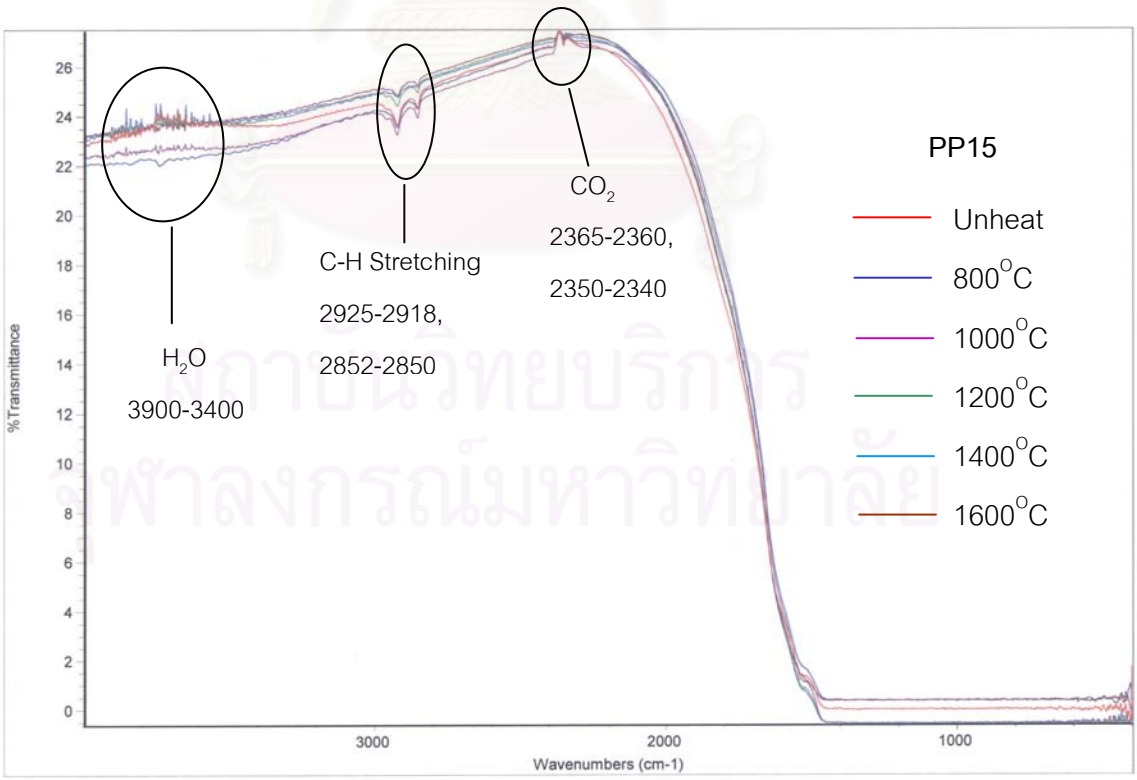
PP15
Unheat
800°C
1000°C
1200°C
1400°C
1600°C
H2O
3900-3400
C-H Stretching
2925-2918,
2852-2850
CO2
2365-2360,
2350-2340
%Transmittance
Wavenumbers (cm-1)

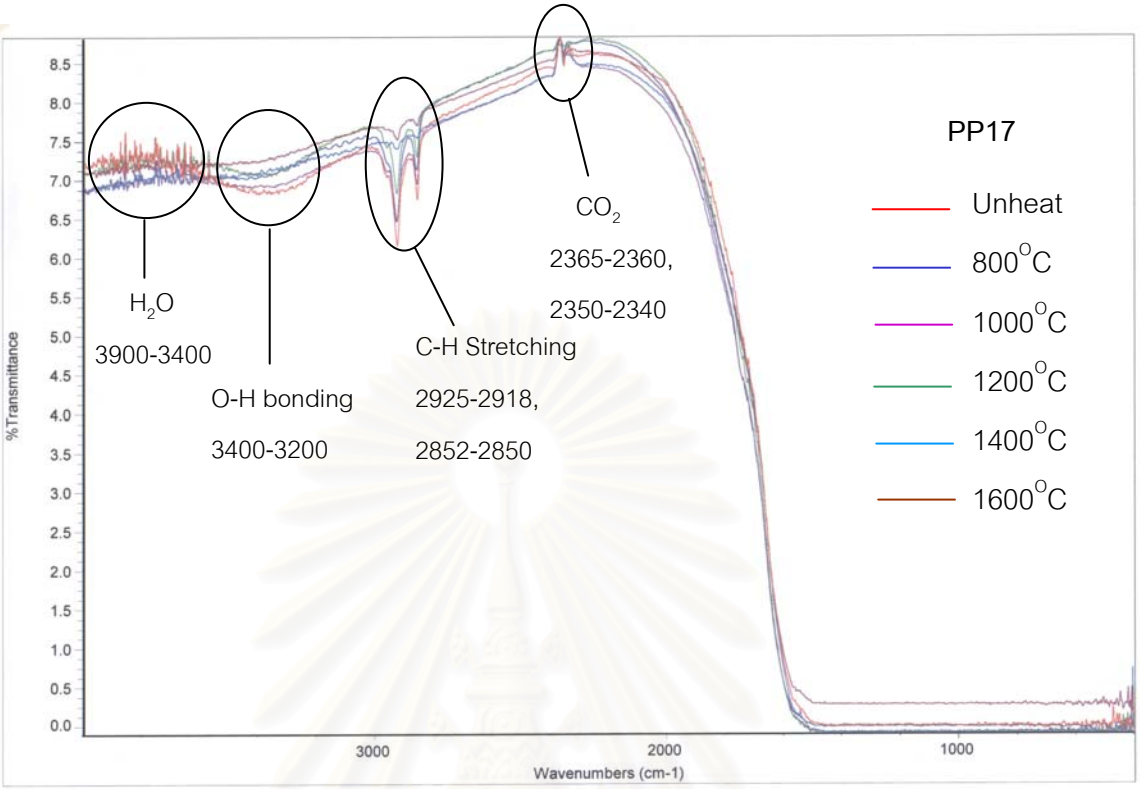
PP17
Unheat
800°C
1000°C
1200°C
1400°C
1600°C
H2O
3900-3400
O-H bonding
3400-3200
C-H Stretching
2925-2918,
2852-2850
CO2
2365-2360,
2350-2340
%Transmittance
Wavenumbers (cm-1)

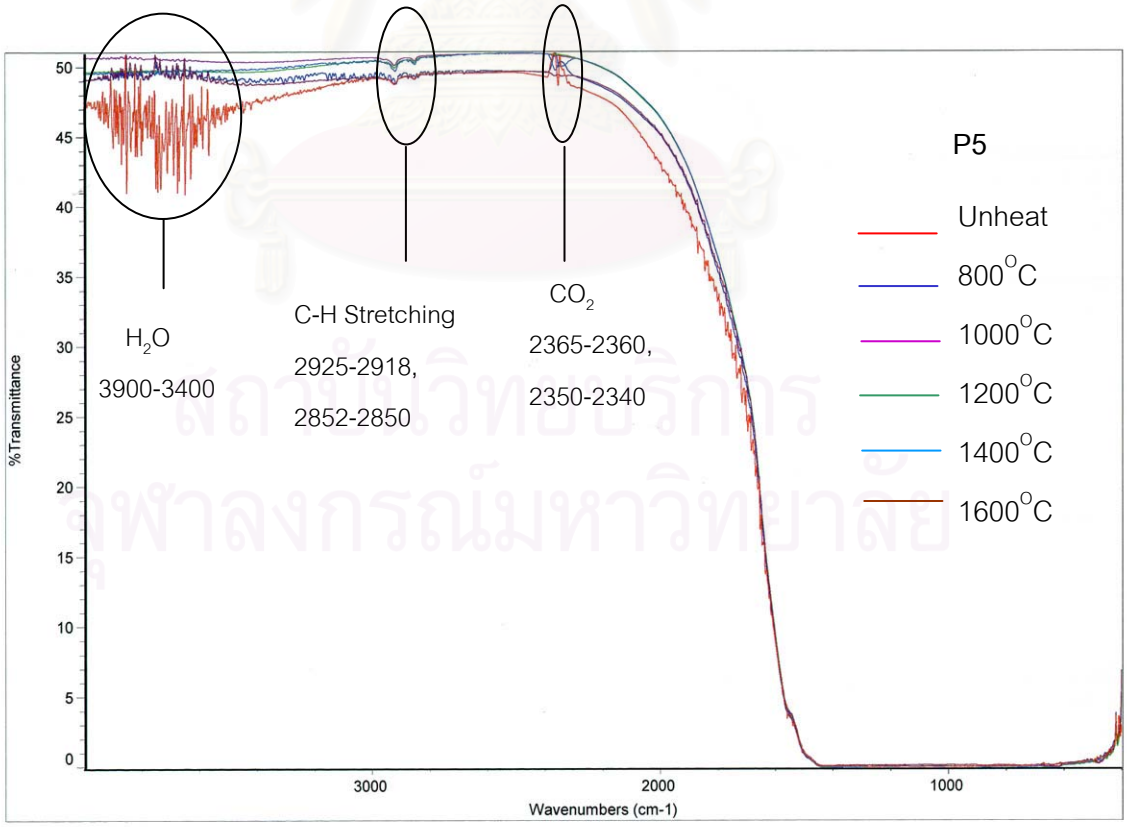
P5
Unheat
800°C
1000°C
1200°C
1400°C
1600°C
H2O
3900-3400
C-H Stretching
2925-2918,
2852-2850
CO2
2365-2360,
2350-2340
%Transmittance
Wavenumbers (cm-1)

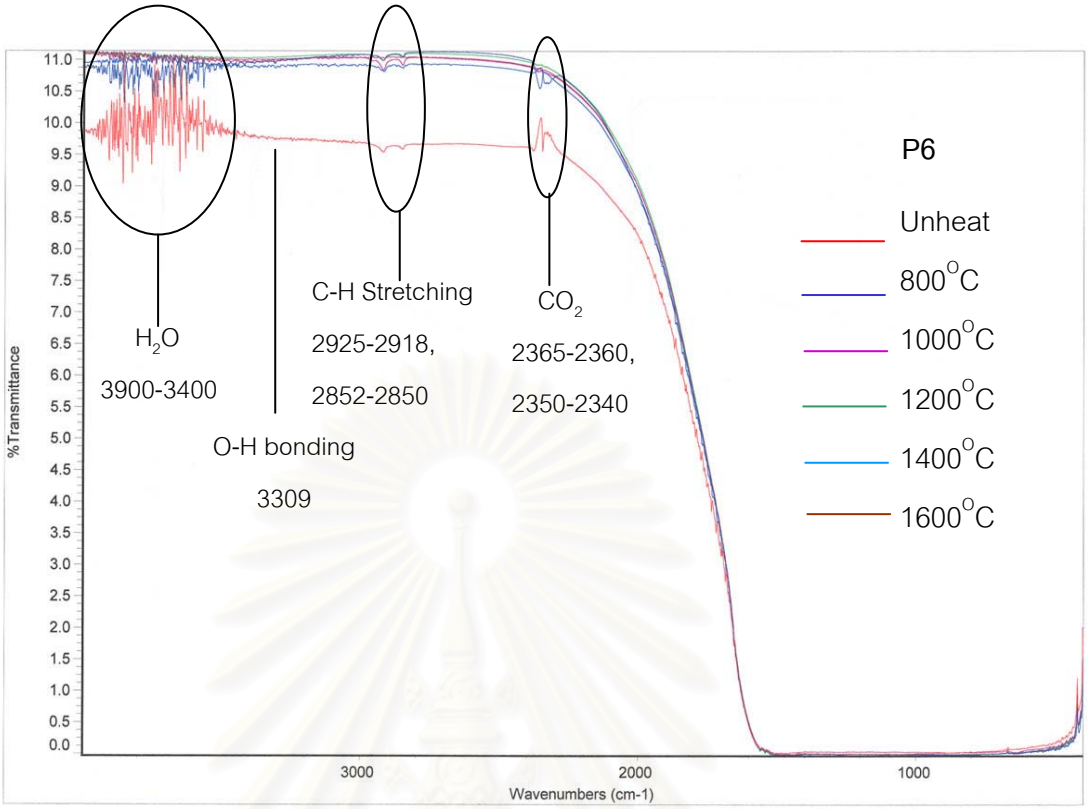
P6
Unheat
800°C
1000°C
1200°C
1400°C
1600°C
H2O
3900-3400
O-H bonding
3309
C-H Stretching
2925-2918,
2852-2850
CO2
2365-2360,
2350-2340
%Transmittance
Wavenumbers (cm-1)

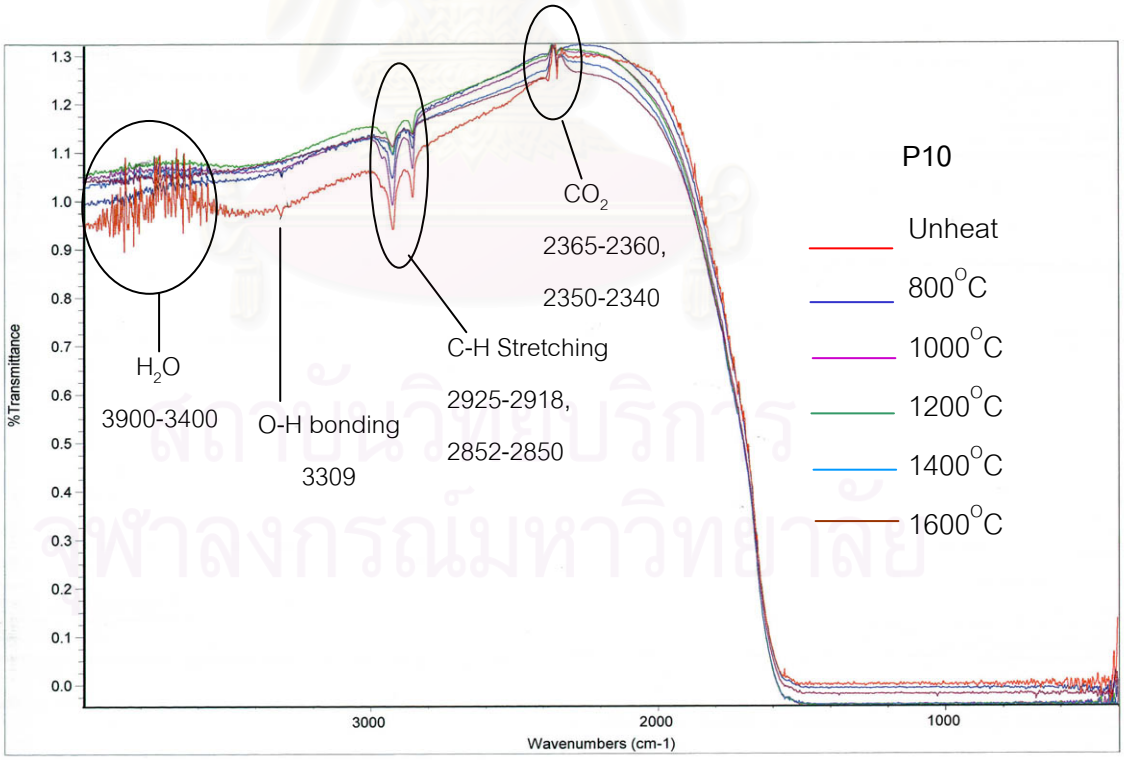
P10
Unheat
800°C
1000°C
1200°C
1400°C
1600°C
H2O
3900-3400
O-H bonding
3309
C-H Stretching
2925-2918,
2852-2850
CO2
2365-2360,
2350-2340
%Transmittance
Wavenumbers (cm-1)

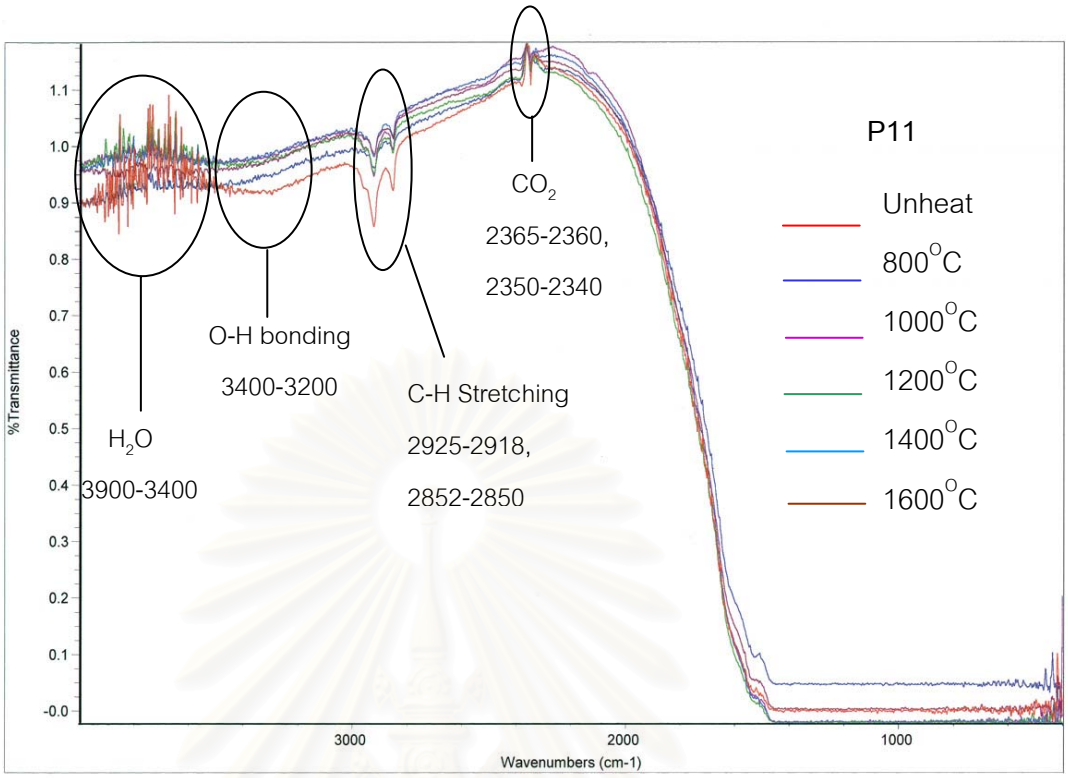
P11
Unheat
800°C
1000°C
1200°C
1400°C
1600°C
H2O
3900-3400
O-H bonding
3400-3200
C-H Stretching
2925-2918,
2852-2850
CO2
2365-2360,
2350-2340
%Transmittance
Wavenumbers (cm-1)

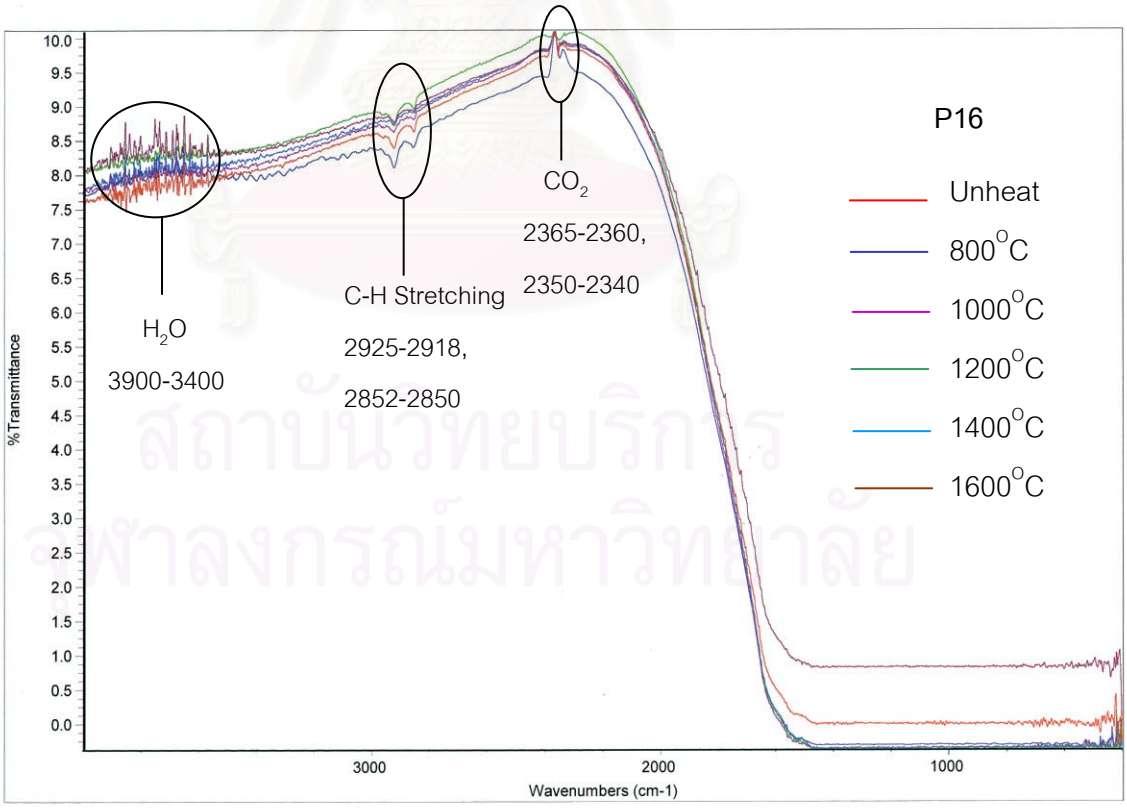
P16
Unheat
800°C
1000°C
1200°C
1400°C
1600°C
H2O
3900-3400
C-H Stretching
2925-2918,
2852-2850
CO2
2365-2360,
2350-2340
%Transmittance
Wavenumbers (cm-1)

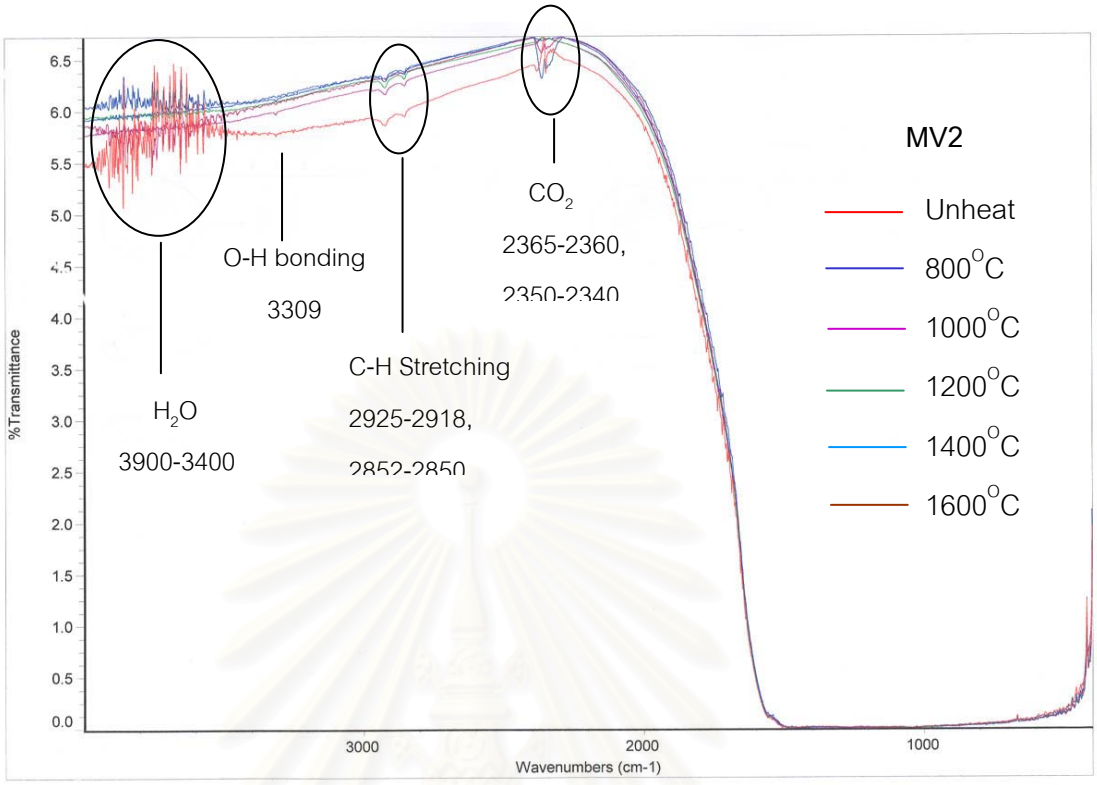
MV2
Unheat
800°C
1000°C
1200°C
1400°C
1600°C
H_2O
3900-3400
O-H bonding
3309
C-H Stretching
2925-2918,
2852-2850
CO_2
2365-2360,
2350-2340
%Transmittance
Wavenumbers (cm-1)

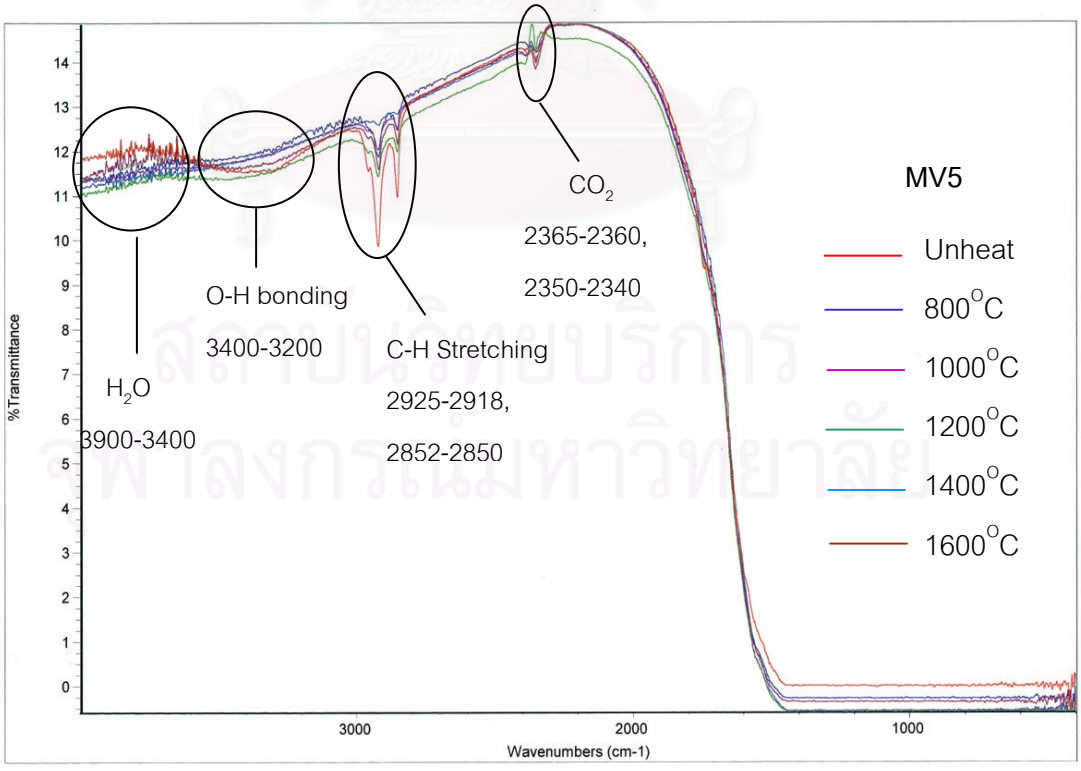
MV5
Unheat
800°C
1000°C
1200°C
1400°C
1600°C
H_2O
3900-3400
O-H bonding
3400-3200
C-H Stretching
2925-2918,
2852-2850
CO_2
2365-2360,
2350-2340
%Transmittance
Wavenumbers (cm-1)

APPENDIX III

UV-VIS-NIR spectra of sapphire before and after heating

Purplish pink: PP3, PP4, PP6, PP11

Light purplish pink: LP3, LP4, LP9

Light orangey pink: PP15

Orangey pink: PP17

Pinkish purple: P5, P6, P10

Brownish purple: P11

Purple: P16

Medium violet: MV2, MV5

สถาบันวิทยบริการ
จุฬาลงกรณ์มหาวิทยาลัย

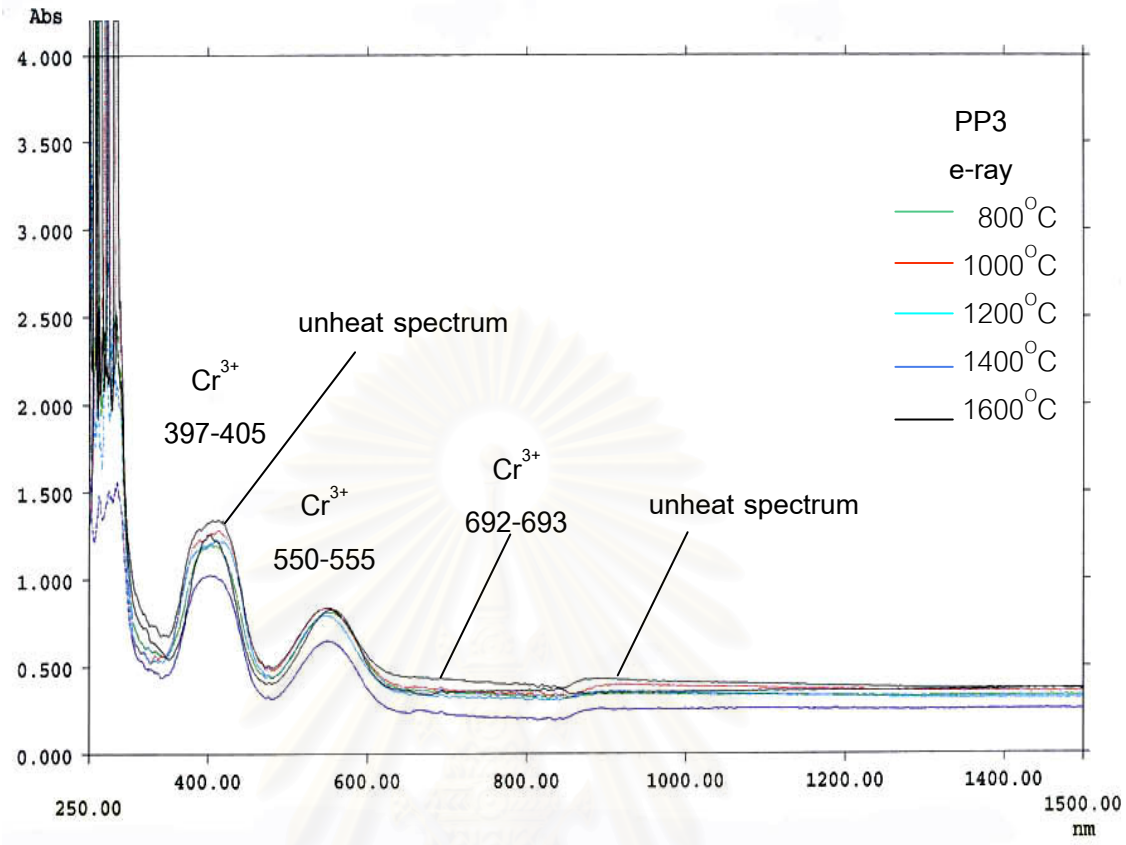

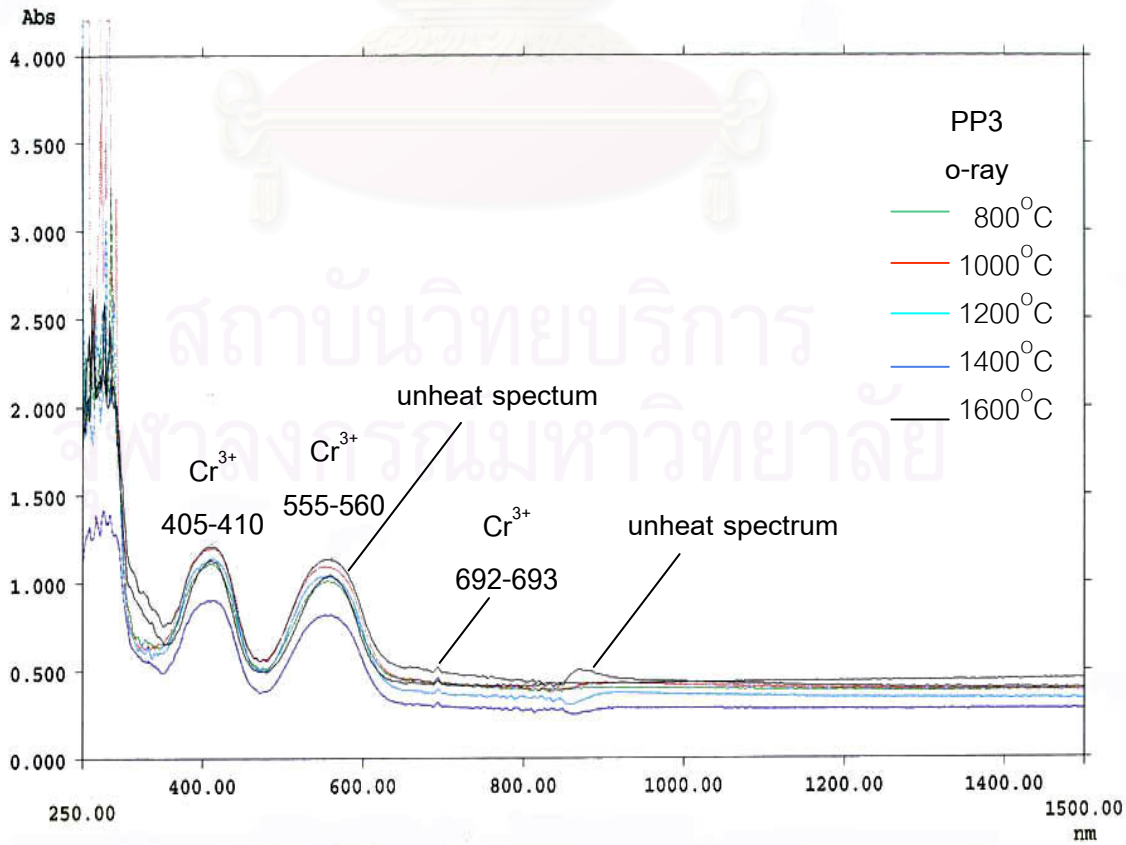

สถาบันวิทยบริการ
จุฬาลงกรณ์มหาวิทยาลัย

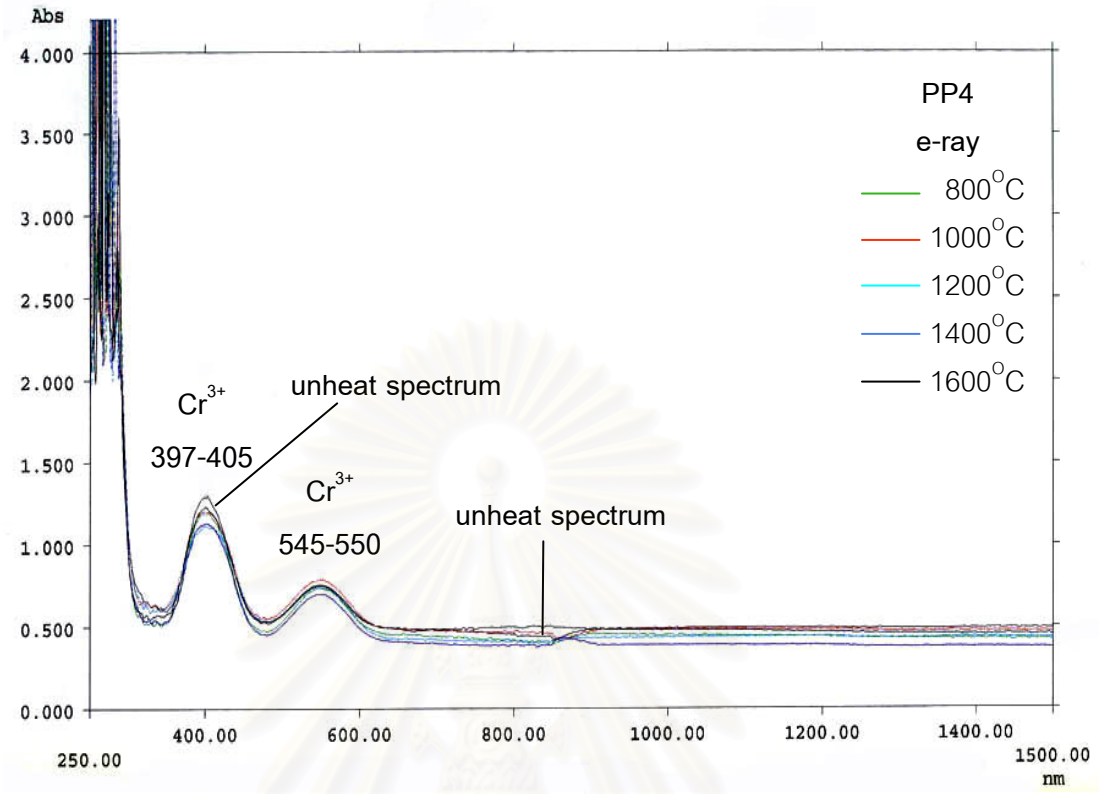
Abs
4.000
3.500
3.000
2.500
2.000
1.500
1.000
0.500
0.000
250.00
400.00
600.00
800.00
1000.00
1200.00
1400.00
1500.00
nm
PP4
e-ray
800°C
1000°C
1200°C
1400°C
1600°C
Cr3+
397-405
unheat spectrum
Cr3+
545-550
unheat spectrum

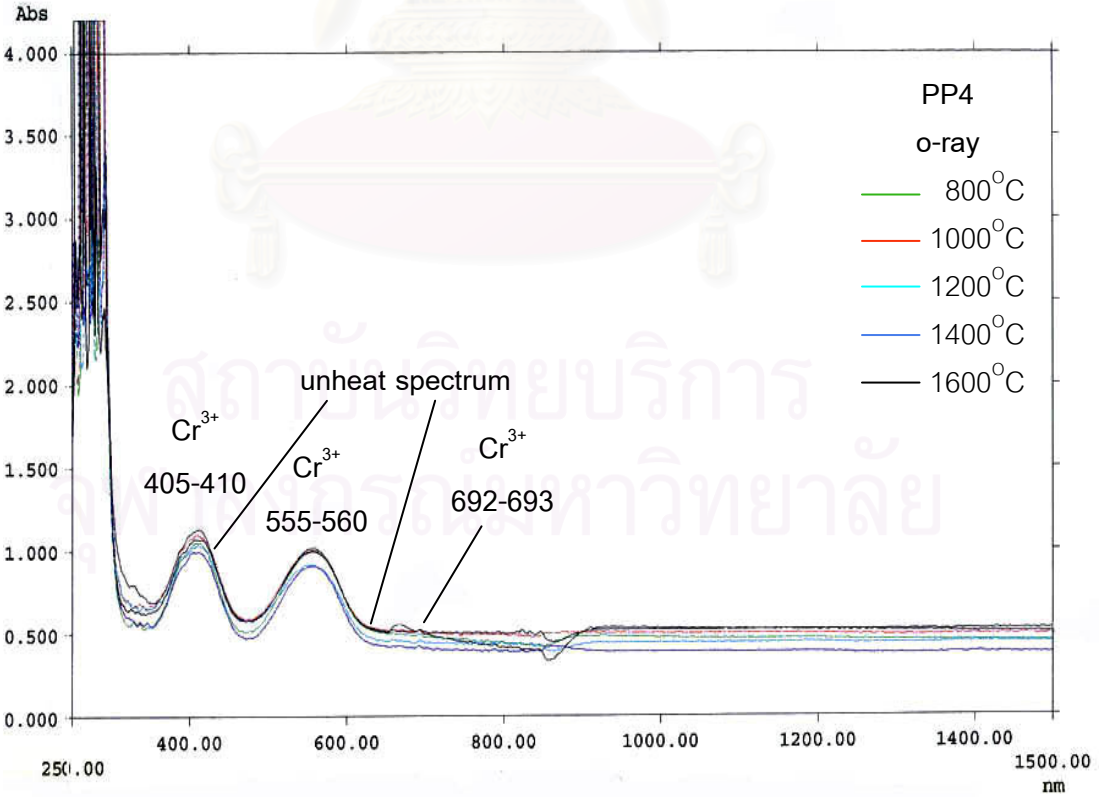
Abs
4.000
3.500
3.000
2.500
2.000
1.500
1.000
0.500
0.000
250.00
400.00
600.00
800.00
1000.00
1200.00
1400.00
1500.00
nm
PP4
o-ray
800°C
1000°C
1200°C
1400°C
1600°C
unheat spectrum
Cr3+
405-410
Cr3+
555-560
Cr3+
692-693

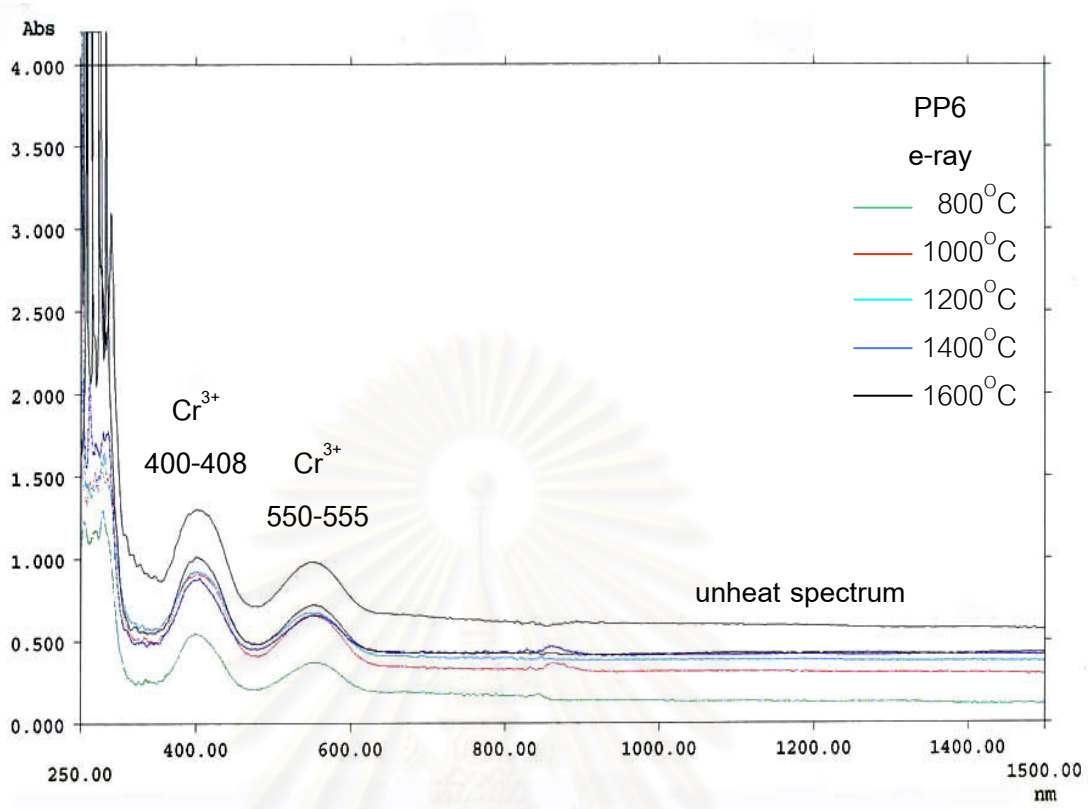
Abs
4.000
3.500
3.000
2.500
2.000
1.500
1.000
0.500
0.000
250.00
400.00
600.00
800.00
1000.00
1200.00
1400.00
1500.00
nm
PP6
e-ray
800°C
1000°C
1200°C
1400°C
1600°C
Cr3+
400-408
Cr3+
550-555
unheat spectrum

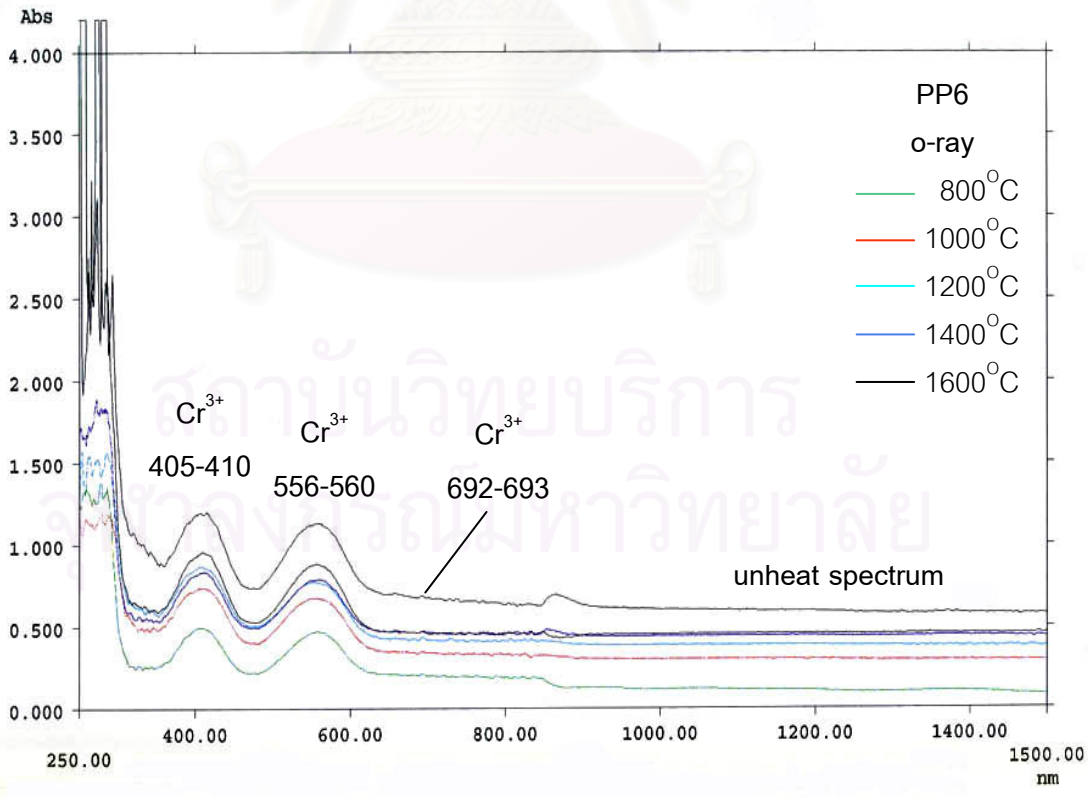
Abs
4.000
3.500
3.000
2.500
2.000
1.500
1.000
0.500
0.000
250.00
400.00
600.00
800.00
1000.00
1200.00
1400.00
1500.00
nm
PP6
o-ray
800°C
1000°C
1200°C
1400°C
1600°C
Cr3+
405-410
Cr3+
556-560
Cr3+
692-693
unheat spectrum

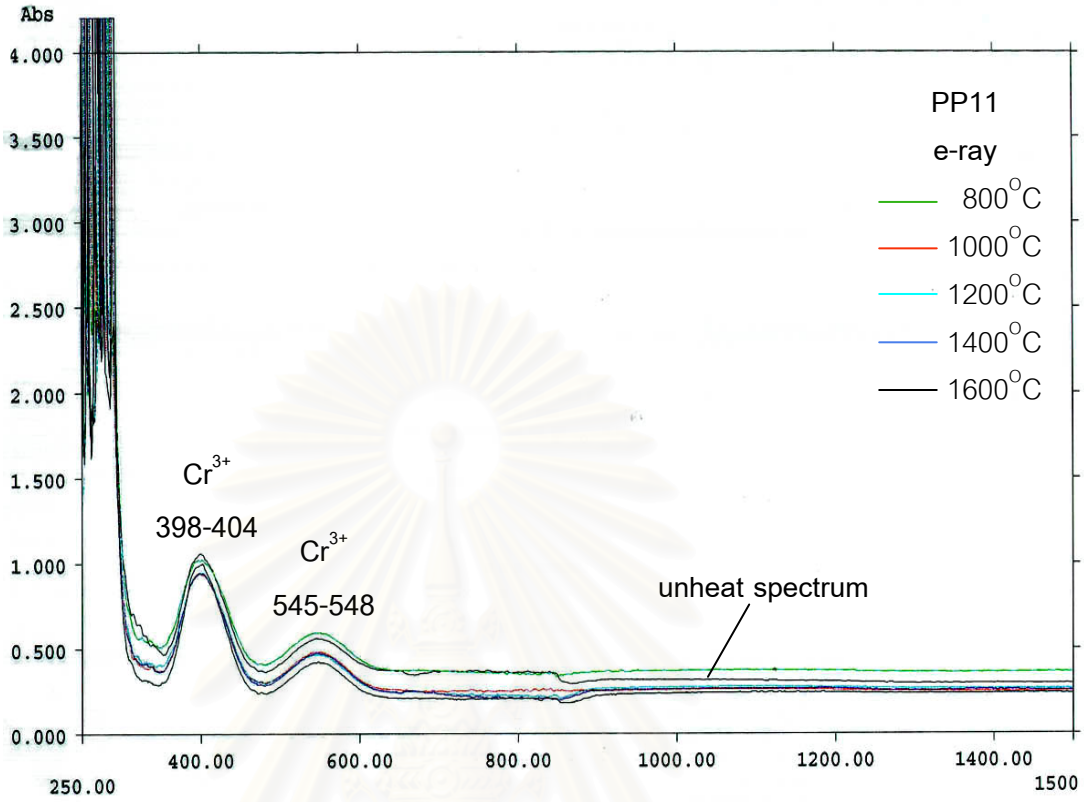

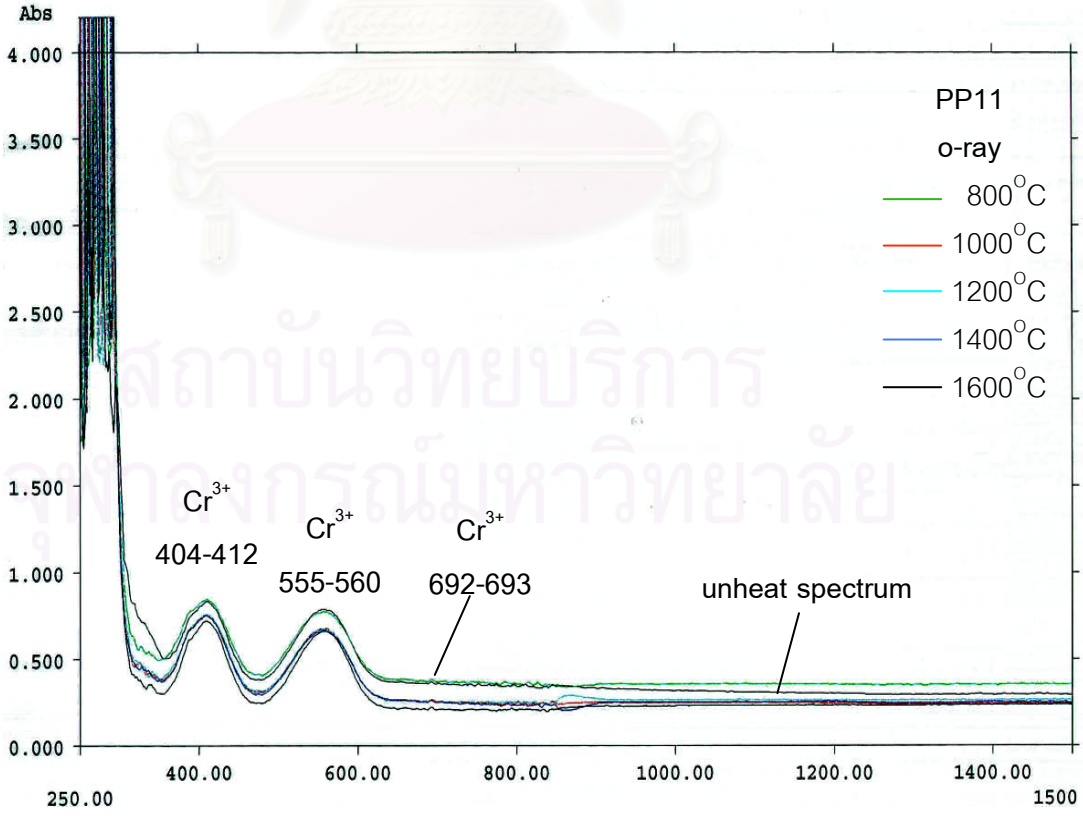

สถาบันวิทยบริการ
จุฬาลงกรณ์มหาวิทยาลัย

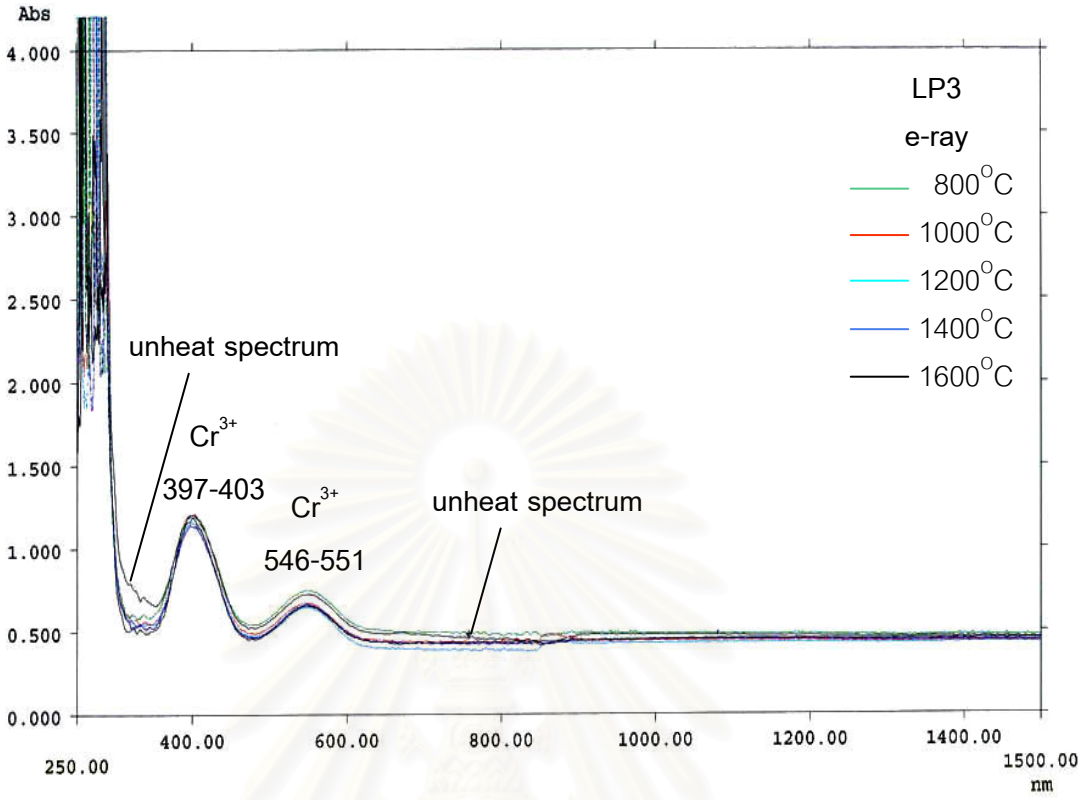
Abs
4.000
3.500
3.000
2.500
2.000
1.500
1.000
0.500
0.000
250.00
400.00
600.00
800.00
1000.00
1200.00
1400.00
1500.00
nm
LP3
e-ray
800°C
1000°C
1200°C
1400°C
1600°C
unheat spectrum
Cr3+
397-403
Cr3+
546-551
unheat spectrum

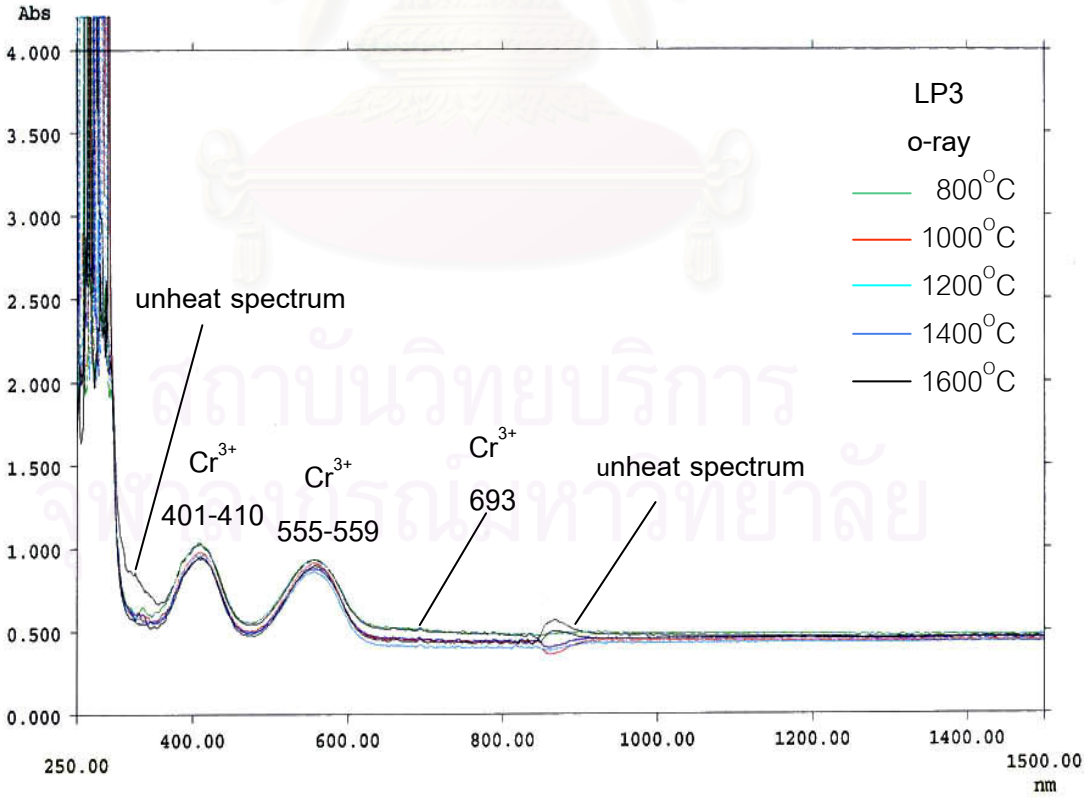
Abs
4.000
3.500
3.000
2.500
2.000
1.500
1.000
0.500
0.000
250.00
400.00
600.00
800.00
1000.00
1200.00
1400.00
1500.00
nm
LP3
o-ray
800°C
1000°C
1200°C
1400°C
1600°C
unheat spectrum
Cr3+
401-410
Cr3+
555-559
Cr3+
693
unheat spectrum

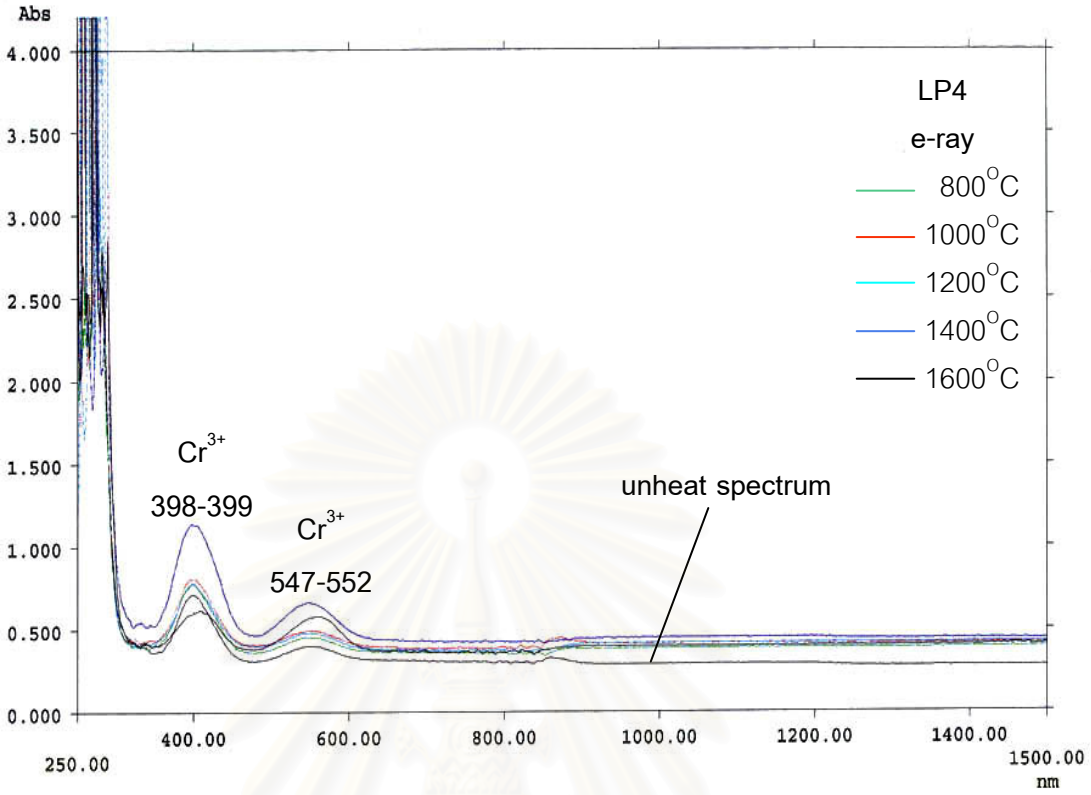

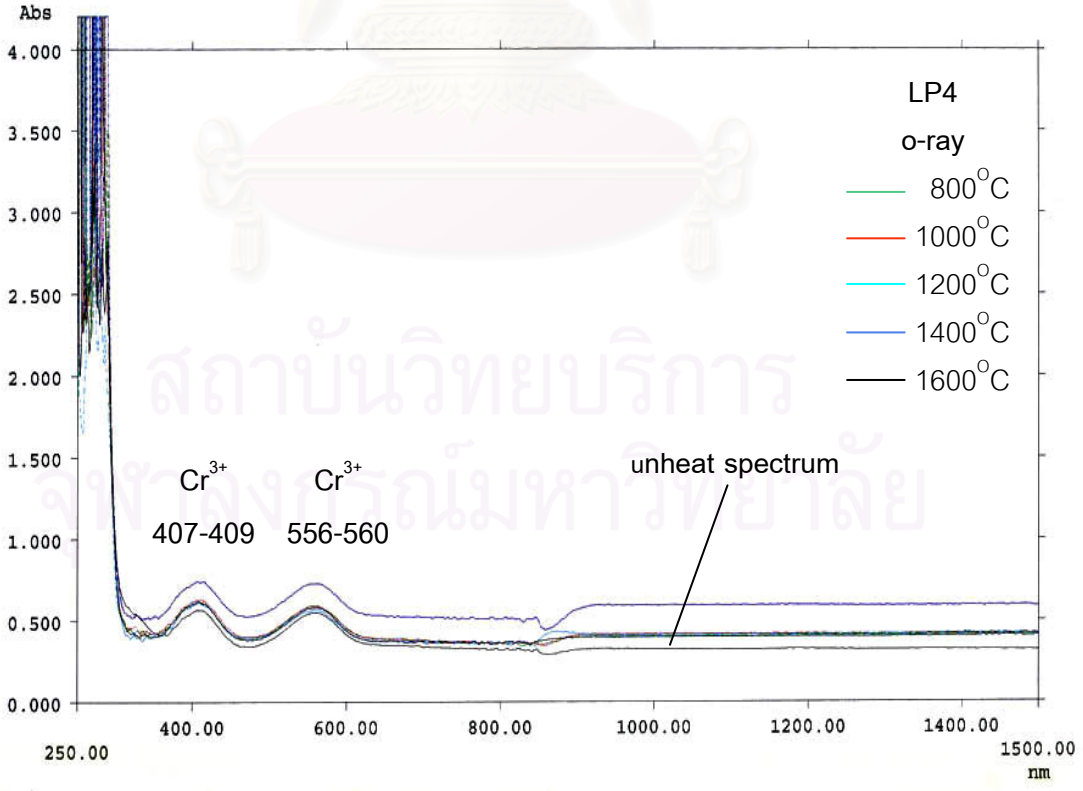

สถาบันวิทยบริการ
จุฬาลงกรณ์มหาวิทยาลัย

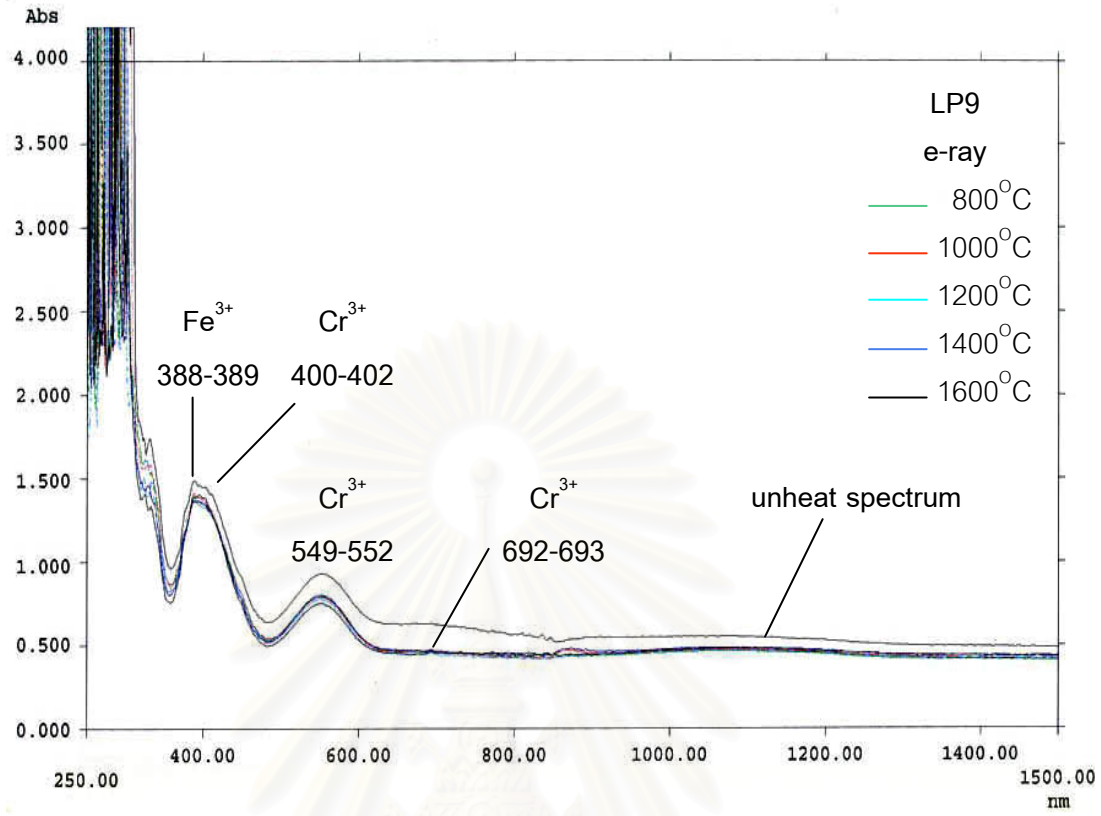
Abs
4.000
3.500
3.000
2.500
2.000
1.500
1.000
0.500
0.000
250.00
400.00
600.00
800.00
1000.00
1200.00
1400.00
1500.00
nm
LP9
e-ray
800°C
1000°C
1200°C
1400°C
1600°C
Fe3+
388-389
Cr3+
400-402
Cr3+
549-552
Cr3+
692-693
unheat spectrum

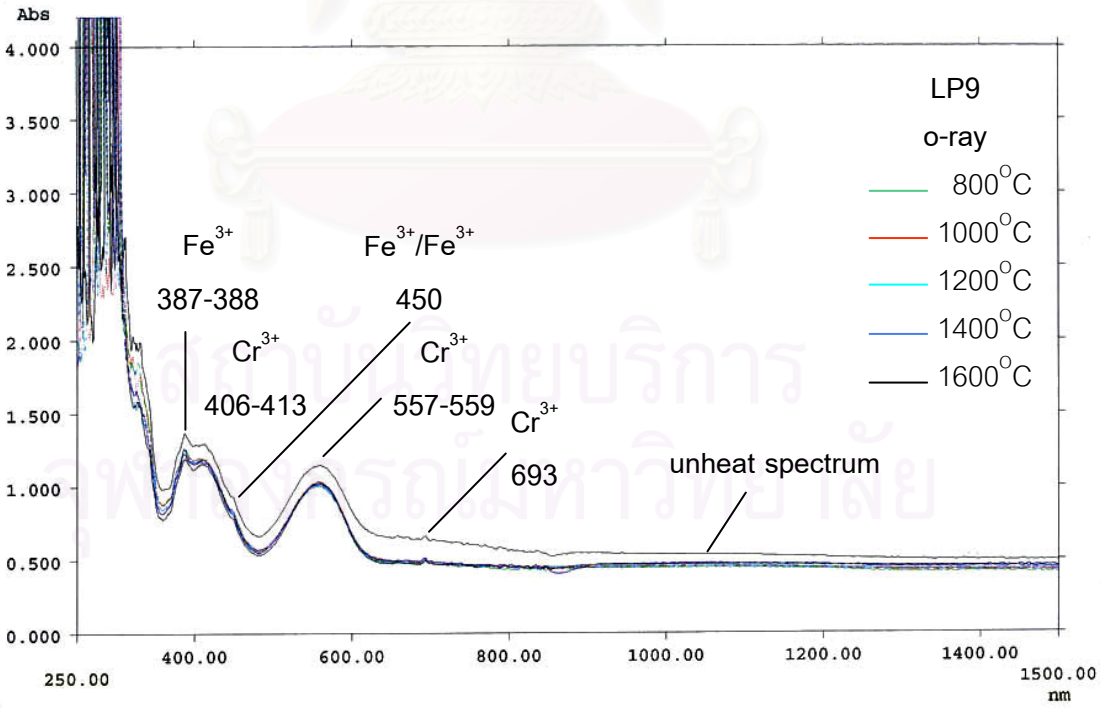
Abs
4.000
3.500
3.000
2.500
2.000
1.500
1.000
0.500
0.000
250.00
400.00
600.00
800.00
1000.00
1200.00
1400.00
1500.00
nm
LP9
o-ray
800°C
1000°C
1200°C
1400°C
1600°C
Fe3+
387-388
Fe3+/Fe3+
450
Cr3+
406-413
Cr3+
557-559
Cr3+
693
unheat spectrum

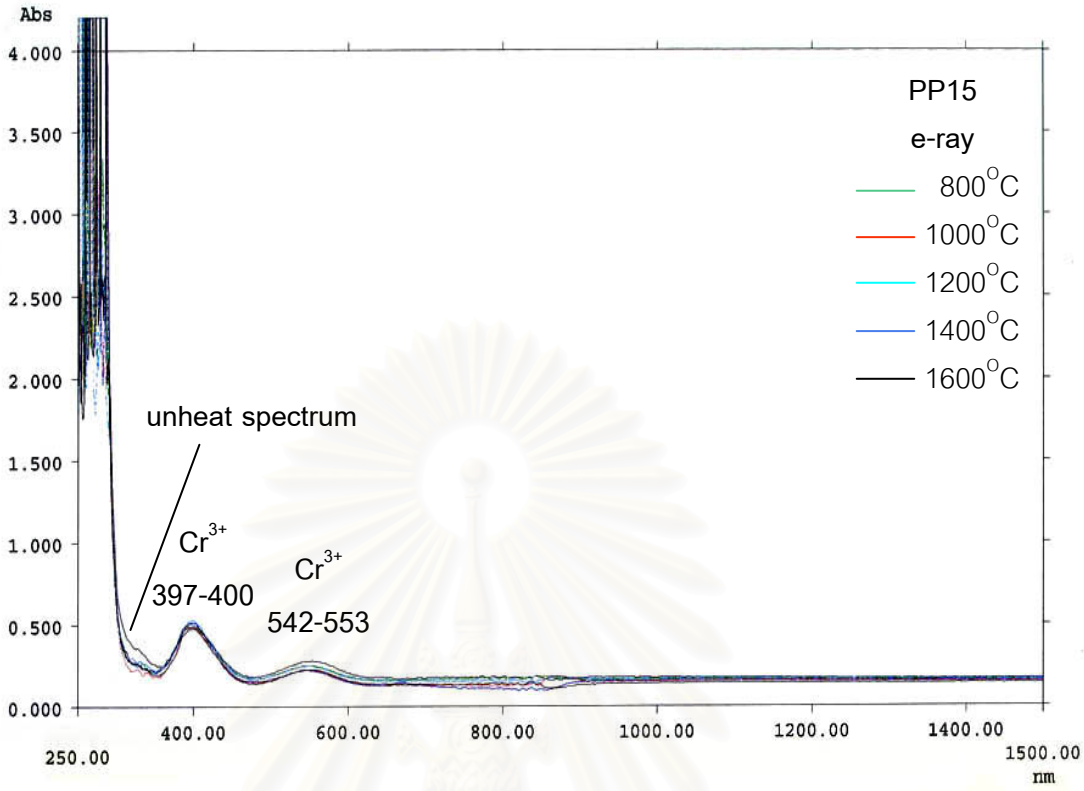
Abs
4.000
3.500
3.000
2.500
2.000
1.500
1.000
0.500
0.000
250.00
400.00
600.00
800.00
1000.00
1200.00
1400.00
1500.00
nm
PP15
e-ray
800°C
1000°C
1200°C
1400°C
1600°C
unheat spectrum
Cr3+
397-400
Cr3+
542-553

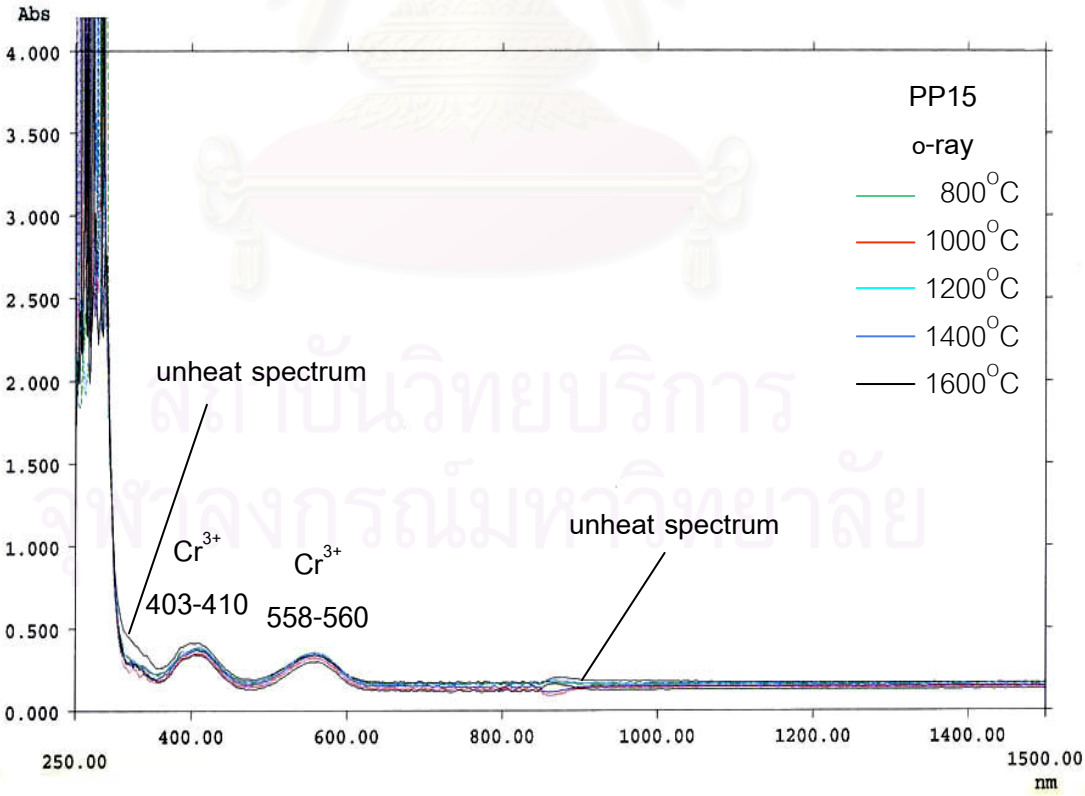
Abs
4.000
3.500
3.000
2.500
2.000
1.500
1.000
0.500
0.000
250.00
400.00
600.00
800.00
1000.00
1200.00
1400.00
1500.00
nm
PP15
o-ray
800°C
1000°C
1200°C
1400°C
1600°C
unheat spectrum
Cr3+
403-410
Cr3+
558-560
unheat spectrum

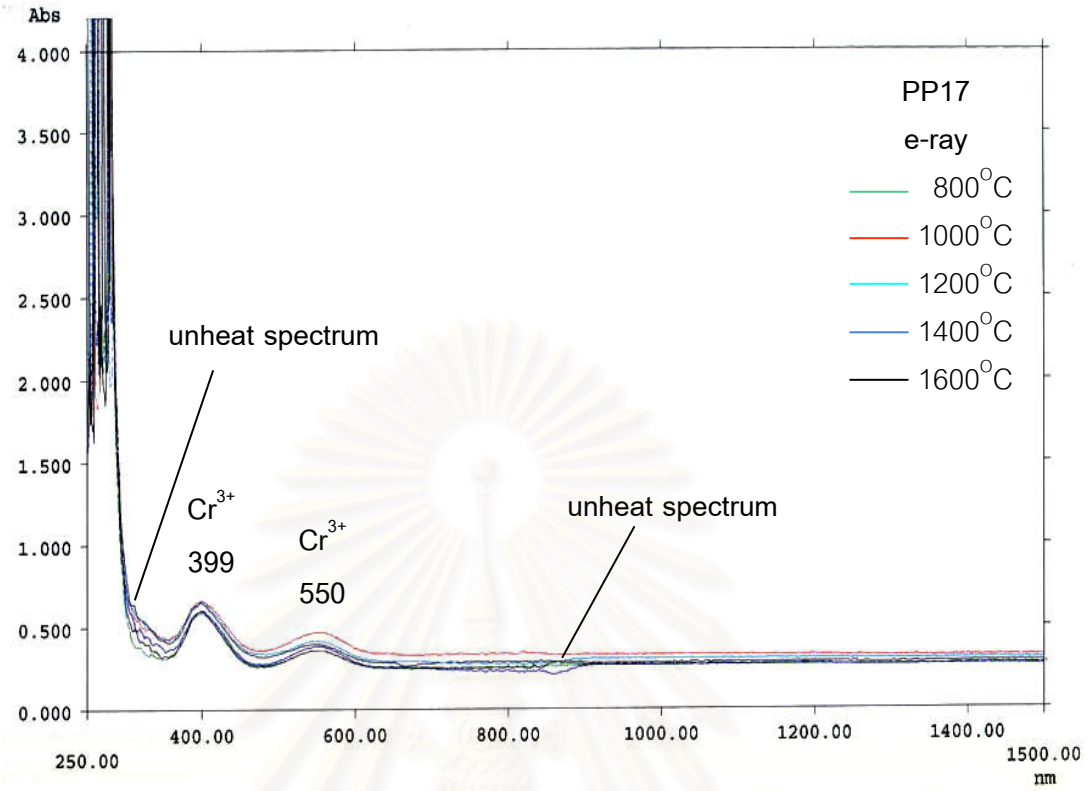

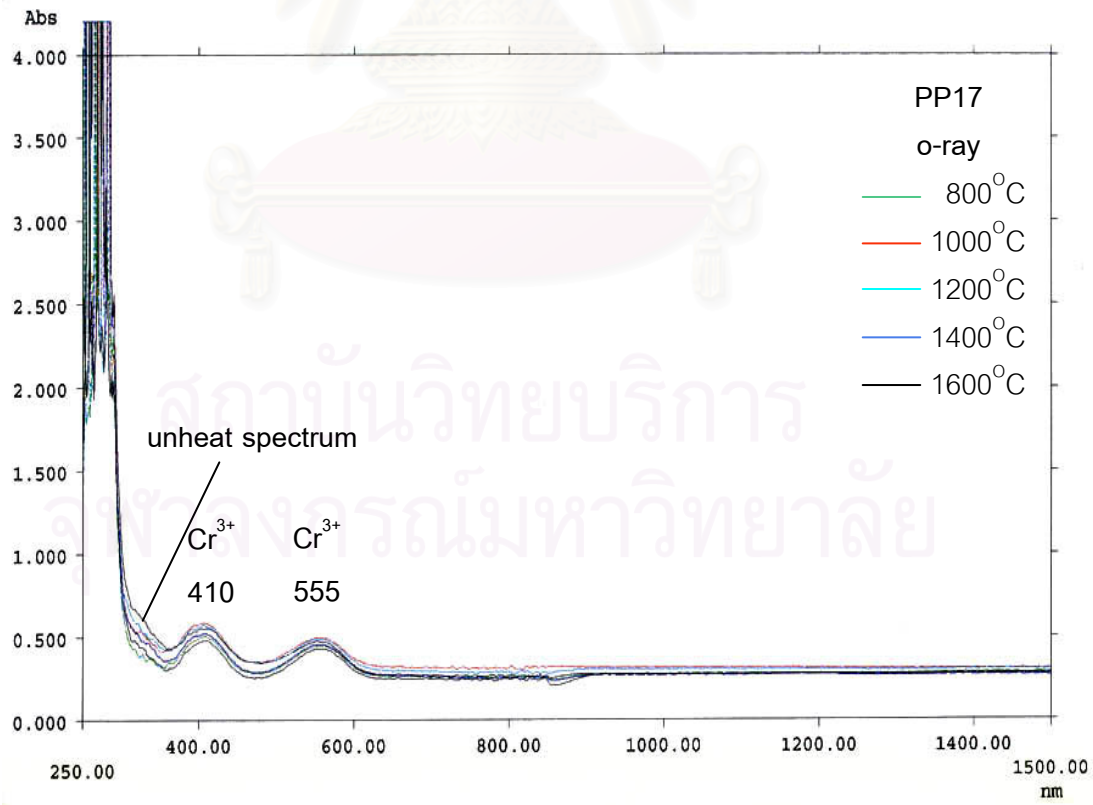

สถาบันวิทยบริการ
จุฬาลงกรณ์มหาวิทยาลัย

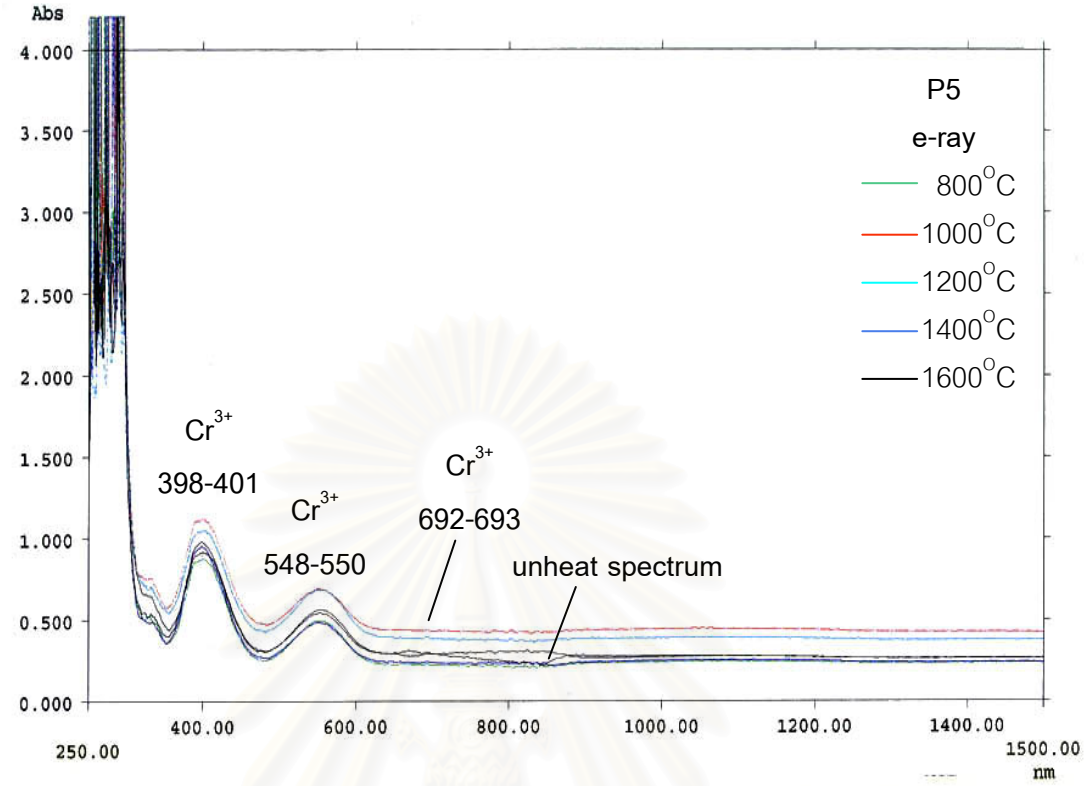
Abs
4.000
3.500
3.000
2.500
2.000
1.500
1.000
0.500
0.000
250.00
400.00
600.00
800.00
1000.00
1200.00
1400.00
1500.00
nm
P5
e-ray
800°C
1000°C
1200°C
1400°C
1600°C
Cr3+
398-401
Cr3+
548-550
Cr3+
692-693
unheat spectrum

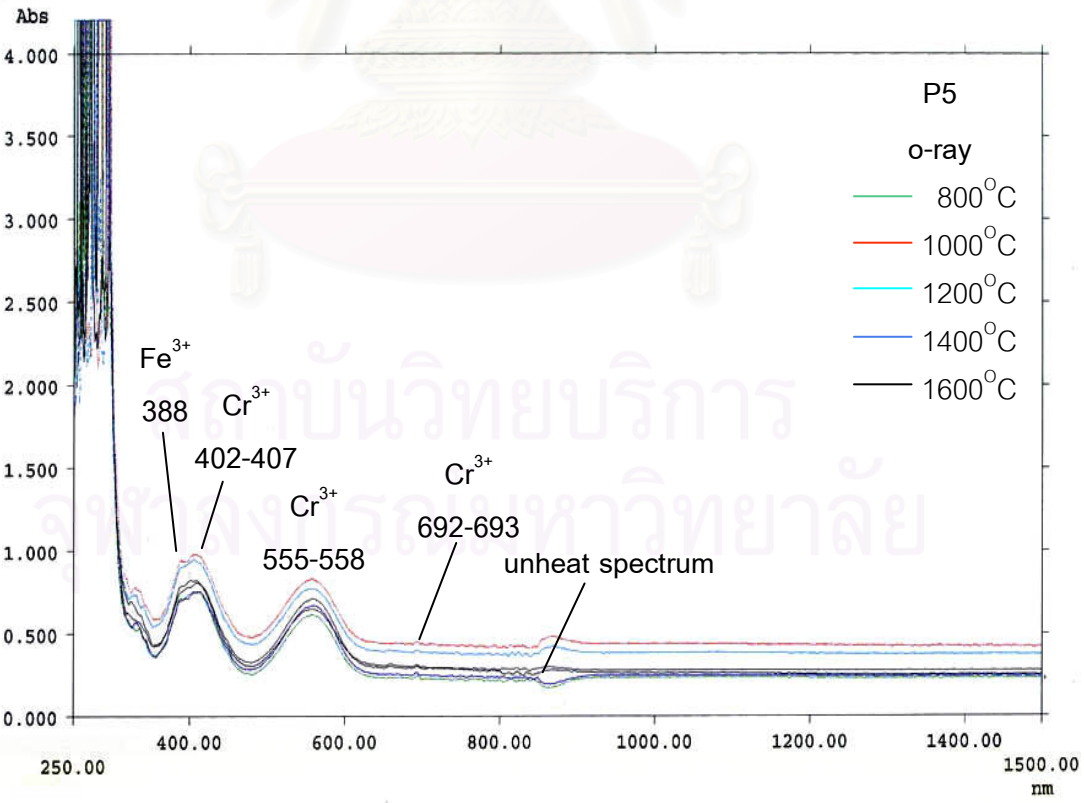
Abs
4.000
3.500
3.000
2.500
2.000
1.500
1.000
0.500
0.000
250.00
400.00
600.00
800.00
1000.00
1200.00
1400.00
1500.00
nm
P5
o-ray
800°C
1000°C
1200°C
1400°C
1600°C
Fe3+
388
Cr3+
402-407
Cr3+
555-558
Cr3+
692-693
unheat spectrum

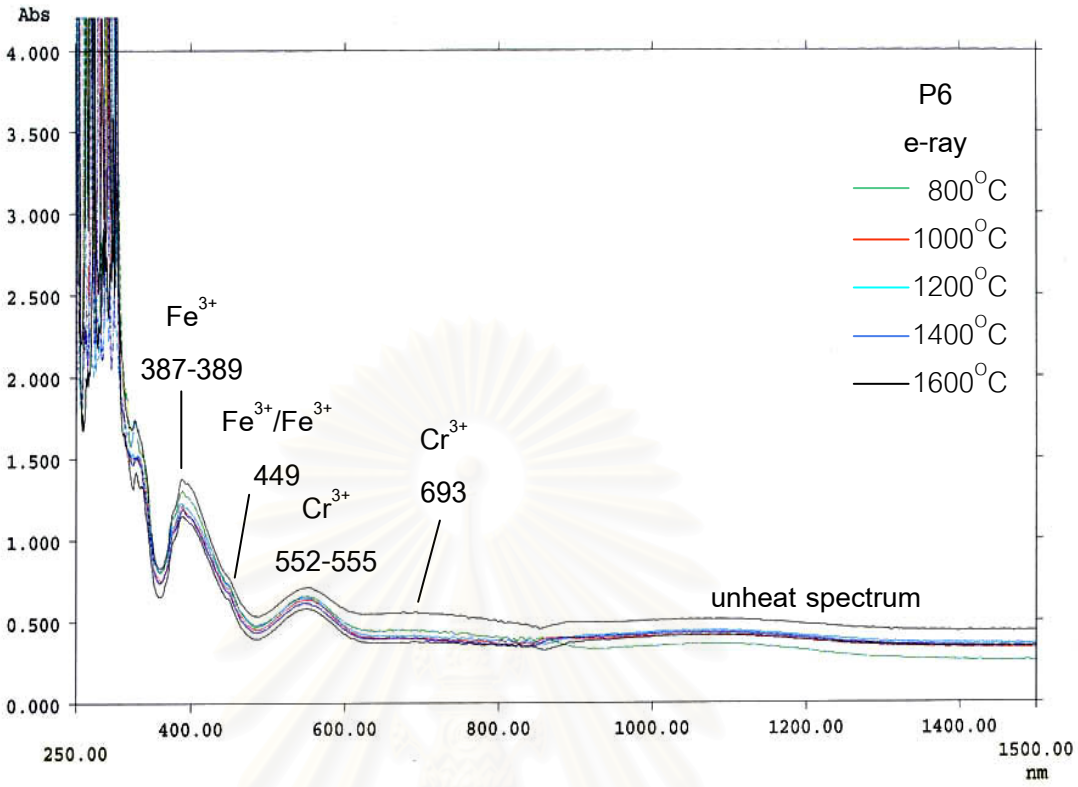
Abs
4.000
3.500
3.000
2.500
2.000
1.500
1.000
0.500
0.000
250.00
400.00
600.00
800.00
1000.00
1200.00
1400.00
1500.00
nm
P6
e-ray
800°C
1000°C
1200°C
1400°C
1600°C
Fe3+
387-389
Fe3+/Fe3+
449
Cr3+
552-555
Cr3+
693
unheat spectrum

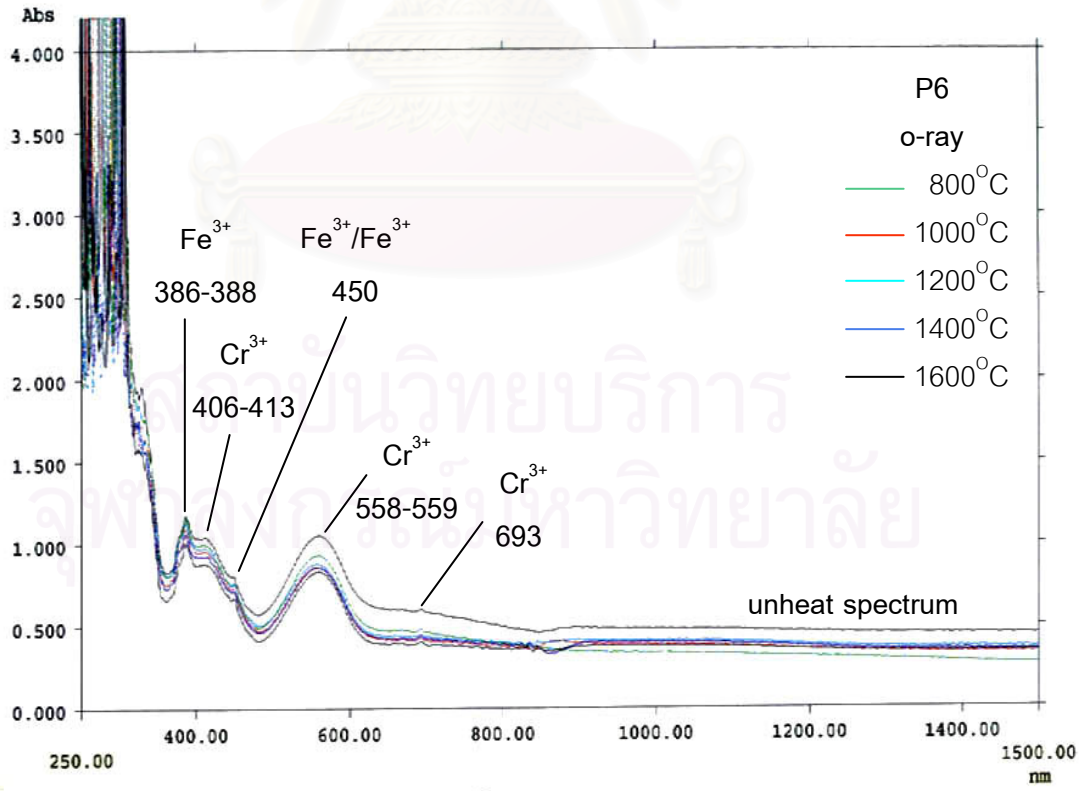
Abs
4.000
3.500
3.000
2.500
2.000
1.500
1.000
0.500
0.000
250.00
400.00
600.00
800.00
1000.00
1200.00
1400.00
1500.00
nm
P6
o-ray
800°C
1000°C
1200°C
1400°C
1600°C
Fe3+
386-388
Fe3+/Fe3+
450
Cr3+
406-413
Cr3+
558-559
Cr3+
693
unheat spectrum

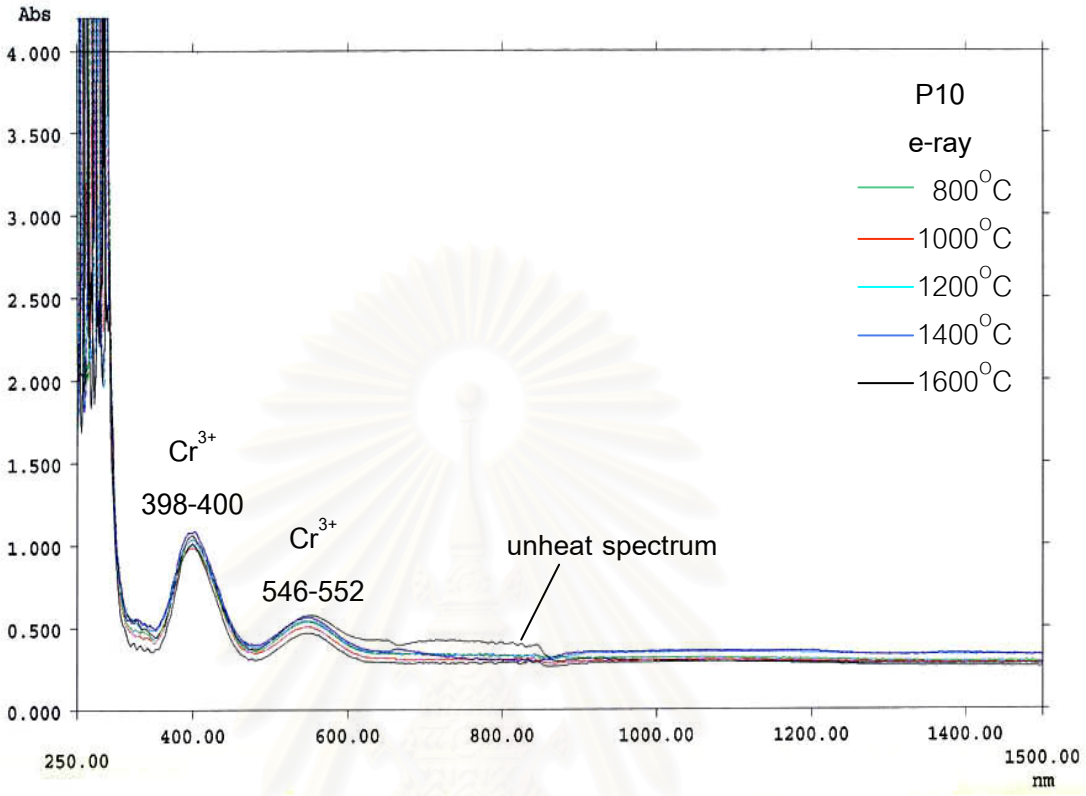

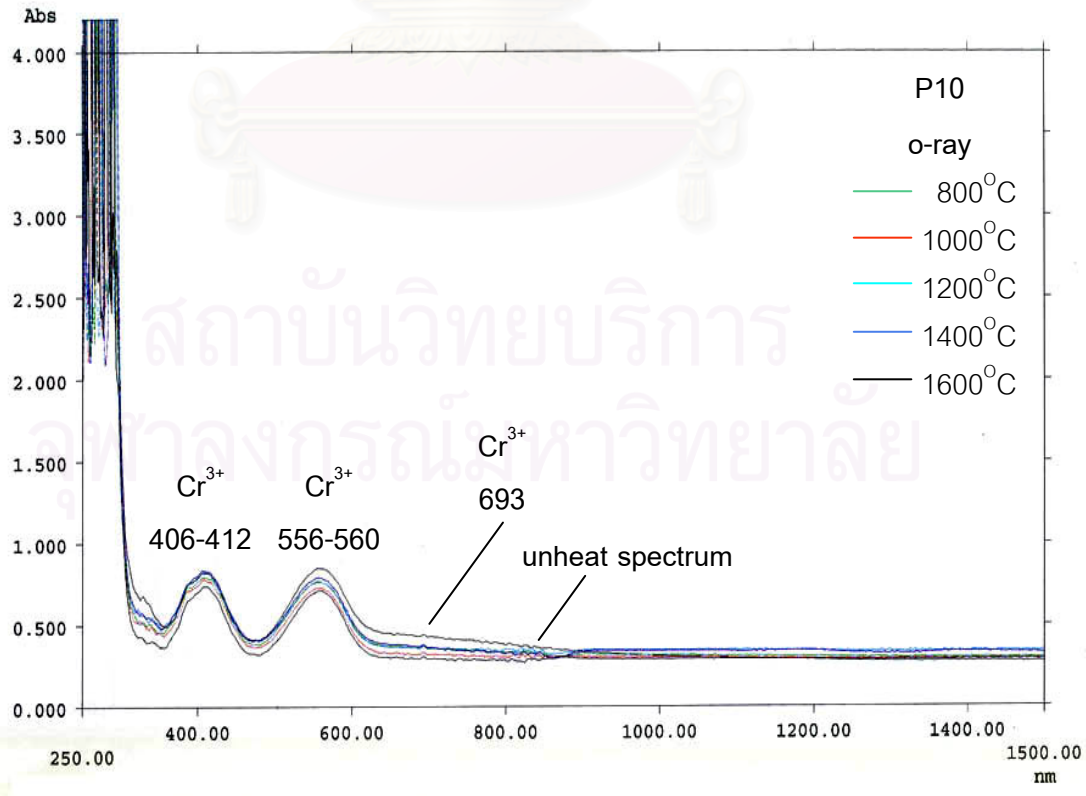

สถาบันวิทยบริการ
จุฬาลงกรณ์มหาวิทยาลัย

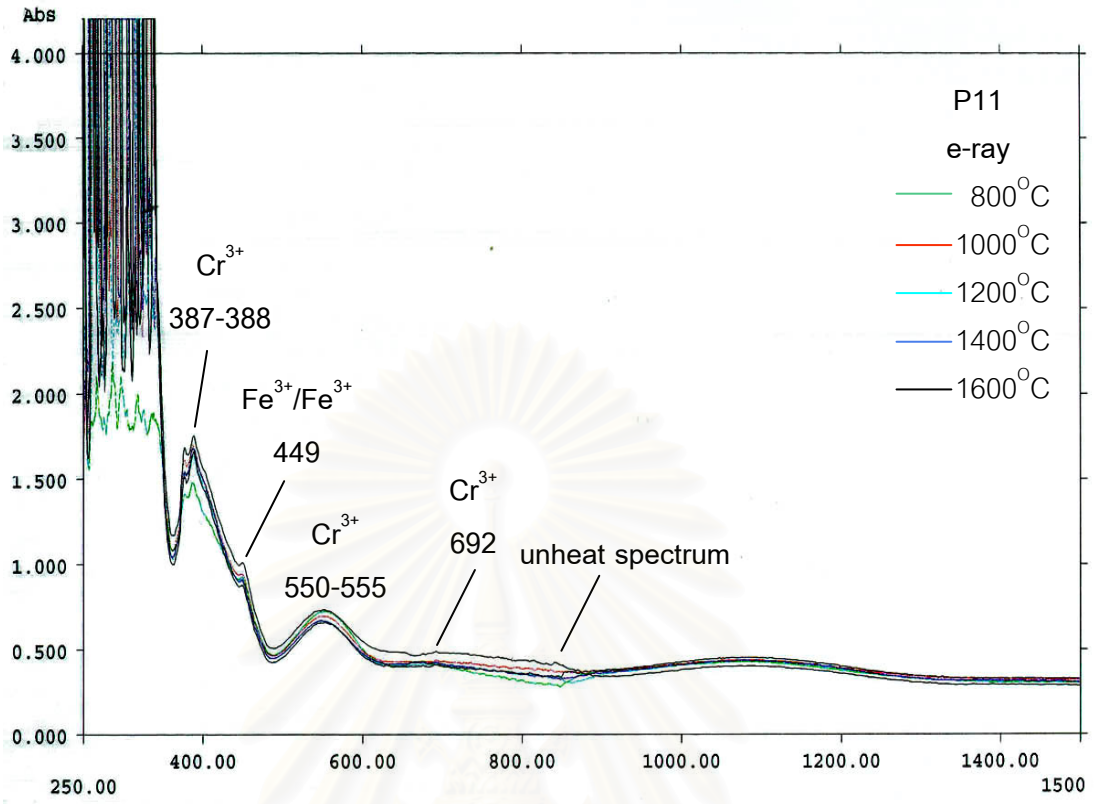
Abs
4.000
3.500
3.000
2.500
2.000
1.500
1.000
0.500
0.000
250.00
400.00
600.00
800.00
1000.00
1200.00
1400.00
1500
P11
e-ray
800°C
1000°C
1200°C
1400°C
1600°C
Cr3+
387-388
Fe3+/Fe3+
449
Cr3+
550-555
Cr3+
692
unheat spectrum

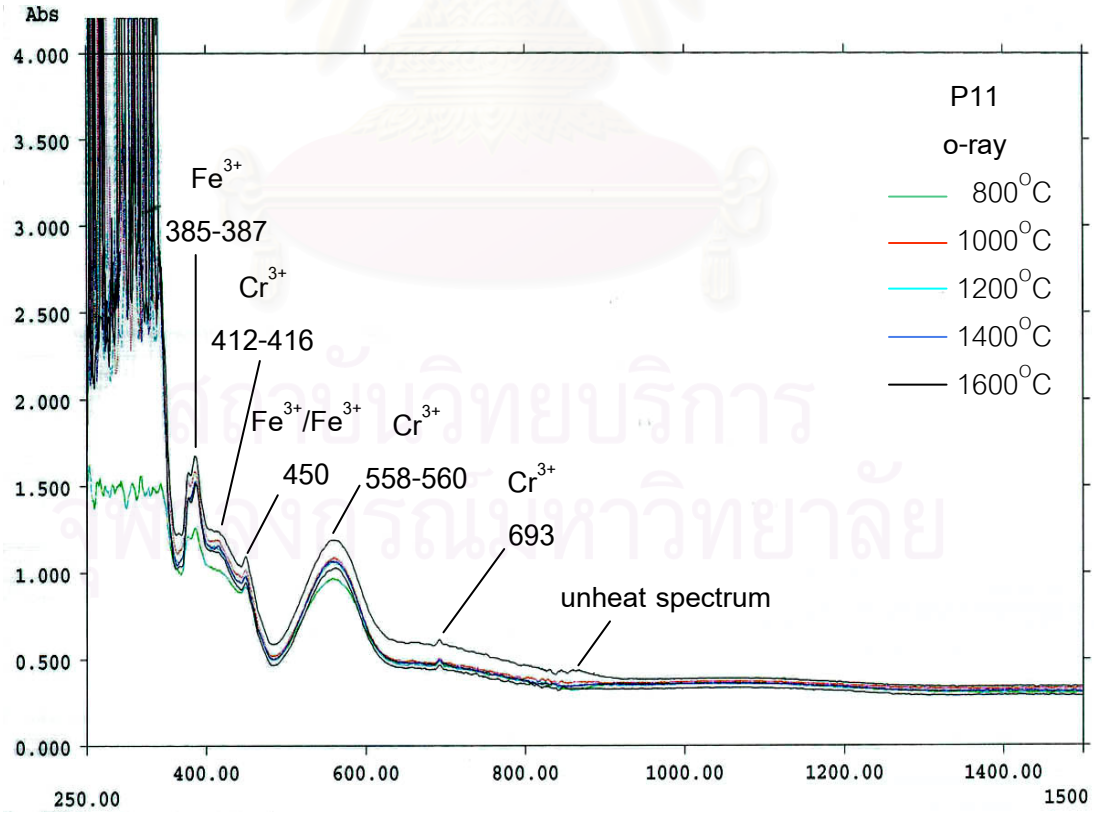
Abs
4.000
3.500
3.000
2.500
2.000
1.500
1.000
0.500
0.000
250.00
400.00
600.00
800.00
1000.00
1200.00
1400.00
1500
P11
o-ray
800°C
1000°C
1200°C
1400°C
1600°C
Fe3+
385-387
Cr3+
412-416
Fe3+/Fe3+
Cr3+
450
558-560
Cr3+
693
unheat spectrum

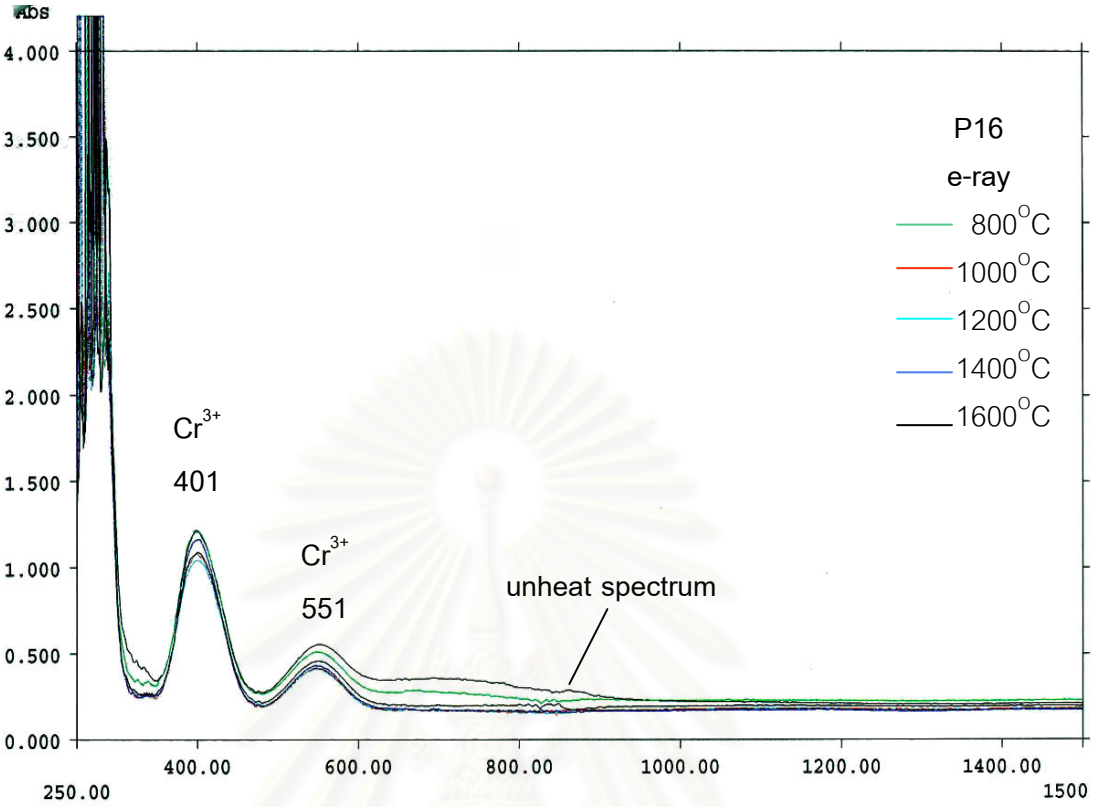

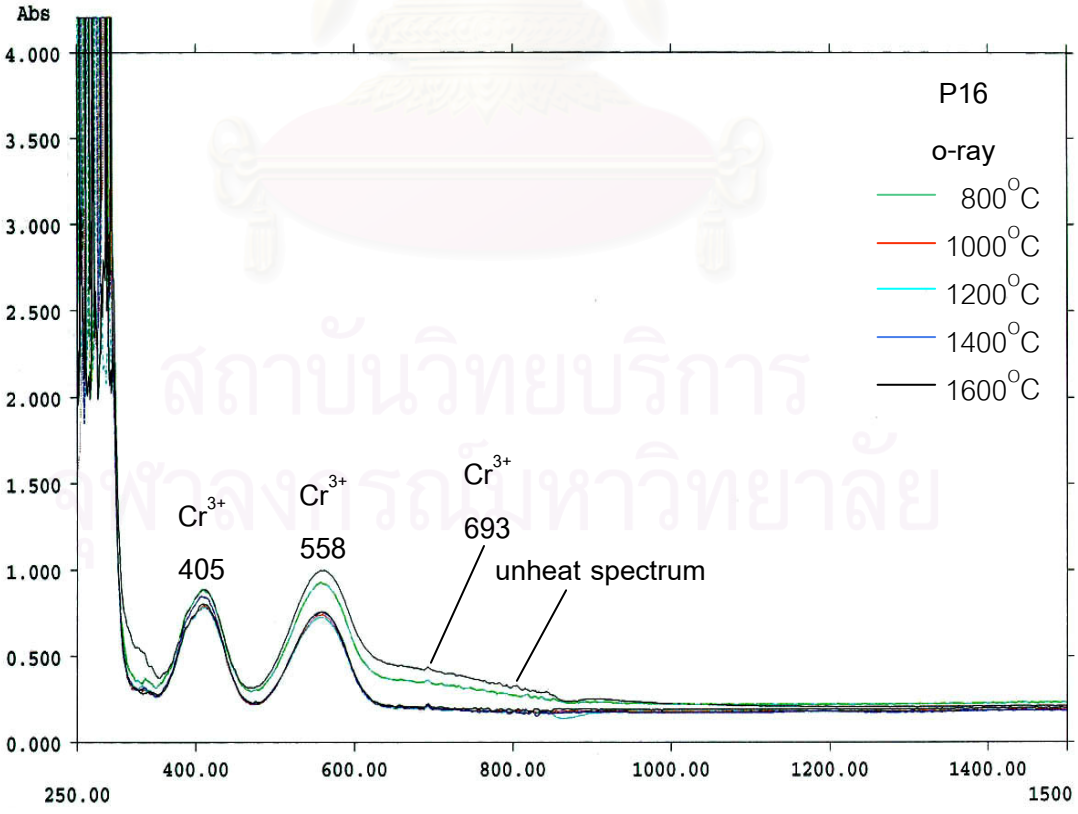

สถาบันวิทยบริการ
จุฬาลงกรณ์มหาวิทยาลัย

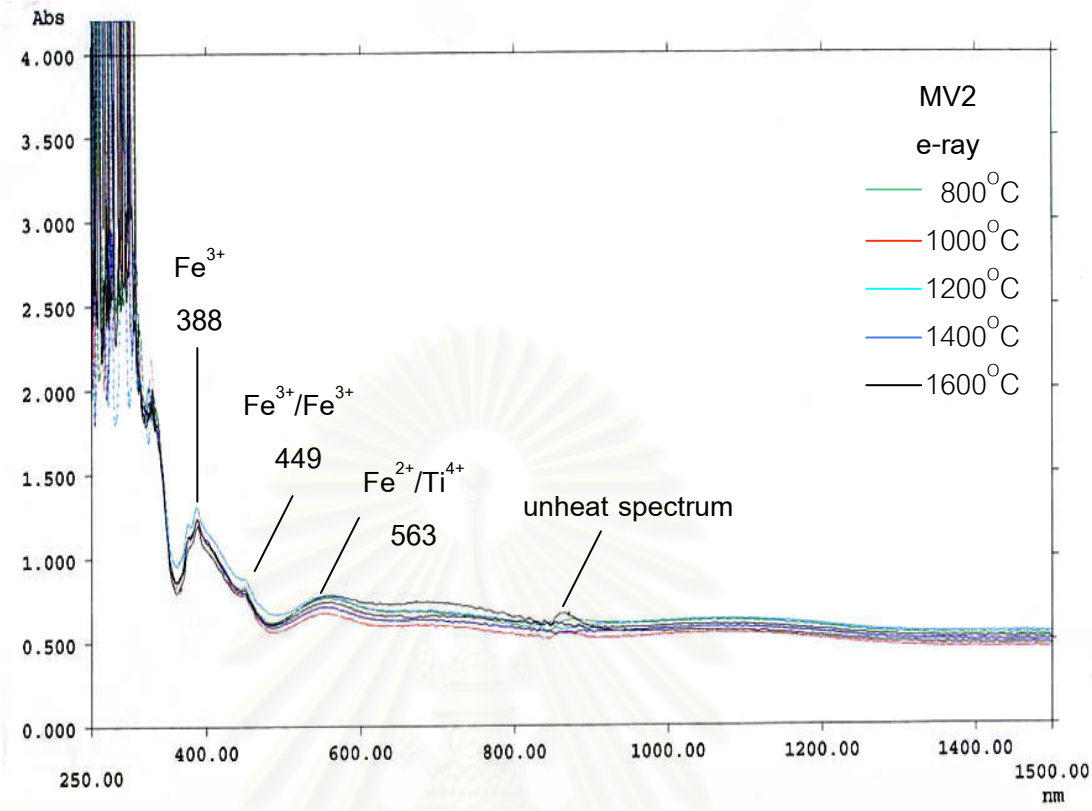
Abs
4.000
3.500
3.000
2.500
2.000
1.500
1.000
0.500
0.000
250.00
400.00
600.00
800.00
1000.00
1200.00
1400.00
1500.00
nm
MV2
e-ray
800°C
1000°C
1200°C
1400°C
1600°C
Fe3+
388
Fe3+/Fe3+
449
Fe2+/Ti4+
563
unheat spectrum

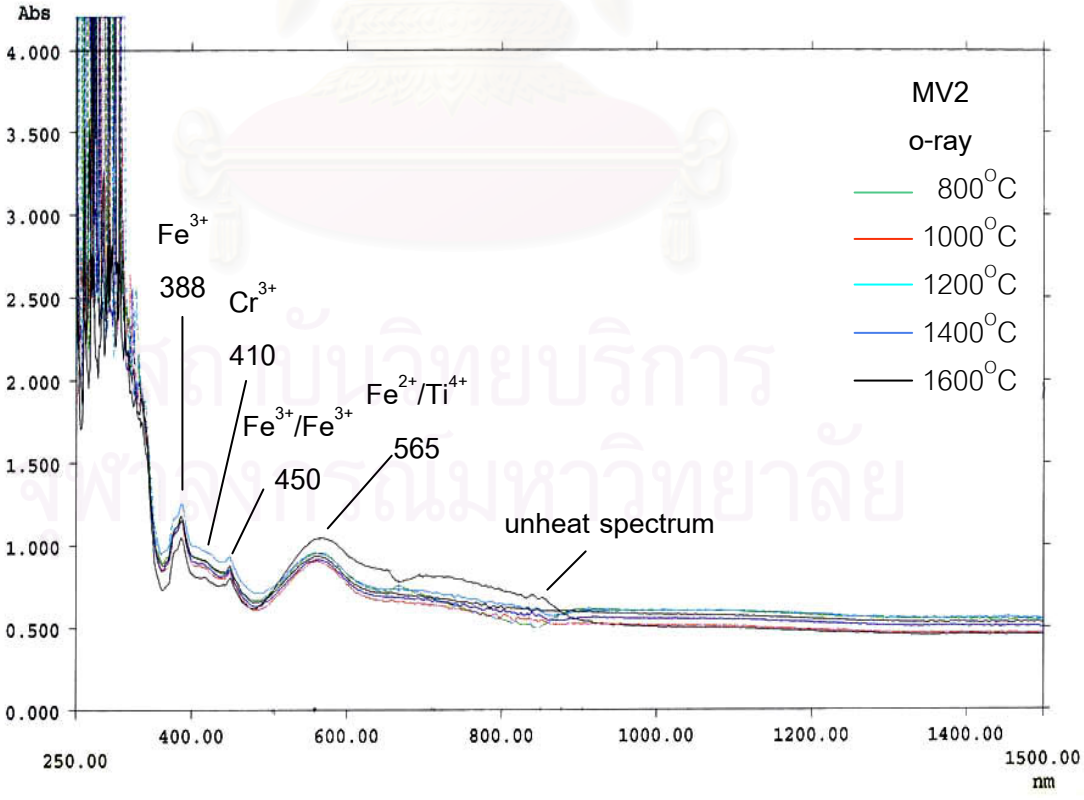
Abs
4.000
3.500
3.000
2.500
2.000
1.500
1.000
0.500
0.000
250.00
400.00
600.00
800.00
1000.00
1200.00
1400.00
1500.00
nm
MV2
o-ray
800°C
1000°C
1200°C
1400°C
1600°C
Fe3+
388
Cr3+
410
Fe3+/Fe3+
450
Fe2+/Ti4+
565
unheat spectrum

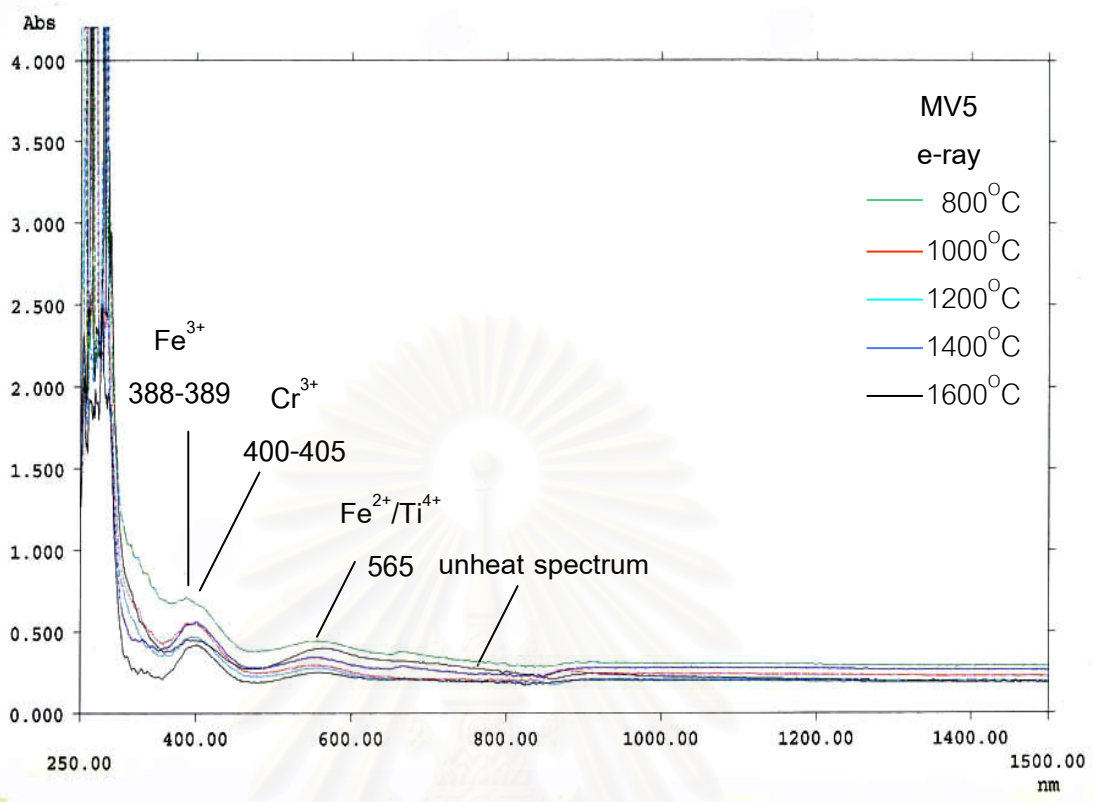
Abs
4.000
3.500
3.000
2.500
2.000
1.500
1.000
0.500
0.000
250.00
400.00
600.00
800.00
1000.00
1200.00
1400.00
1500.00
nm
MV5
e-ray
800°C
1000°C
1200°C
1400°C
1600°C
Fe3+
388-389
Cr3+
400-405
Fe2+/Ti4+
565
unheat spectrum

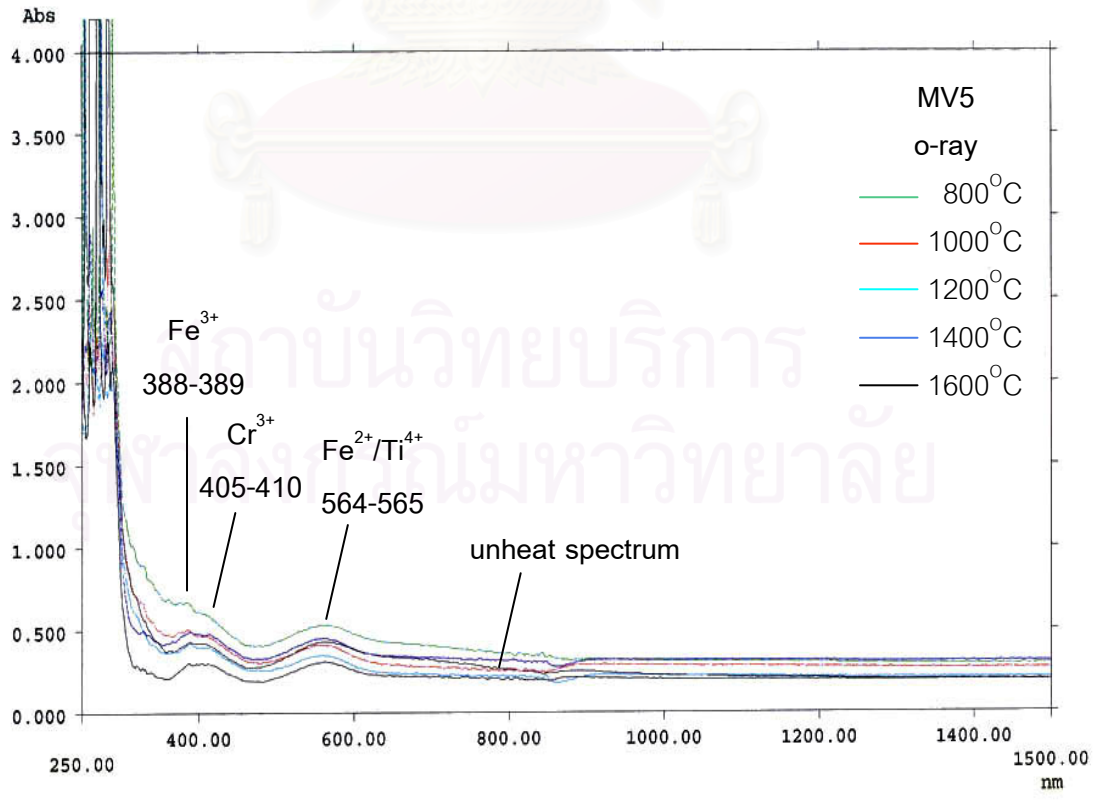
Abs
4.000
3.500
3.000
2.500
2.000
1.500
1.000
0.500
0.000
250.00
400.00
600.00
800.00
1000.00
1200.00
1400.00
1500.00
nm
MV5
o-ray
800°C
1000°C
1200°C
1400°C
1600°C
Fe3+
388-389
Cr3+
405-410
Fe2+/Ti4+
564-565
unheat spectrum

APPENDIX IV

Table IV.1 Showing the trace element content of some Ilakaka-Sakaraha sapphires by Energy Dispersive X-ray Fluorescence (in weight %). The analyzes were performed before heating.

Table IV.2 Showing the major and trace elements content of some selected pink, purple and violet sapphires (16 samples) by Electron Probe Micro-Analyzer. The analyzes were performed after step-heating up to 1600^{O}C.

สถาบันวิทยบริการ
จุฬาลงกรณ์มหาวิทยาลัย

Table IV.1 Showing the trace element content of some Ilakaka-Sakaraha sapphires by Energy Dispersive X-ray Fluorescence (in weight %). The analyzes were performed before heating.

Sample No.	Fe_2O_3	TiO_2	Cr_2O_3	V_2O_3	Ga_2O_3
Purplish pink					
PP1	0.080	0.025	0.089	0.020	0.047
PP2	0.050	0.033	0.066	0.012	<0.010
PP3	0.038	0.037	0.164	<0.010	0.012
PP4	0.040	0.012	0.087	<0.010	0.013
PP5	0.050	0.028	0.050	0.022	<0.010
PP6	0.025	0.028	0.066	0.016	0.011
PP7	0.061	0.024	0.088	0.015	0.011
PP8	0.064	0.038	0.087	0.013	0.010
PP9	0.047	0.028	0.047	0.022	0.010
PP10	0.051	0.013	0.050	<0.010	<0.010
PP11	0.117	0.021	0.066	<0.010	0.015
PP12	0.111	0.025	0.045	<0.010	0.016
Light purplish pink					
LP1	0.381	0.037	0.069	0.017	0.010
LP2	0.065	0.028	0.118	0.016	0.011
LP3	0.045	0.028	0.072	0.013	0.011
LP4	0.029	0.038	0.043	0.010	0.013
LP5	0.214	0.100	0.034	0.009	0.011
LP6	0.506	0.035	0.065	<0.010	<0.010
LP7	0.054	0.026	0.071	0.014	0.012
LP8	0.315	0.020	0.061	0.016	<0.010
LP9	0.250	0.031	0.073	<0.010	0.013
Light orangey pink					
PP13	0.117	<0.010	0.040	<0.010	0.010
PP14	0.110	0.055	0.049	<0.010	0.012
PP15	0.105	0.016	0.042	<0.010	0.013

สถาบันวิทยบริการ
จุฬาลงกรณ์มหาวิทยาลัย

Table IV.1 Showing the trace element content of some Ilakaka-Sakaraha sapphires by Energy Dispersive X-ray Fluorescence (in weight %). The analyzes were performed before heating (continued).

Sample No.	Fe_2O_3	TiO_2	Cr_2O_3	V_2O_3	Ga_2O_3
Orangey pink					
PP16	0.609	0.016	0.028	<0.010	<0.010
PP17	0.076	0.027	0.034	<0.010	0.090
PP18	0.064	0.008	0.035	<0.010	<0.010
Pinkish purple					
P1	0.073	0.028	0.079	0.020	0.011
P2	0.253	0.020	0.062	0.018	<0.010
P3	0.572	0.036	0.070	0.018	0.012
P4	0.282	0.034	0.069	0.010	0.011
P5	0.081	0.026	0.036	0.013	<0.010
P6	0.248	0.035	0.055	0.015	<0.010
P7	0.046	0.029	0.085	0.015	0.013
P8	0.101	0.023	0.035	<0.010	0.013
P9	0.200	<0.010	0.028	<0.010	<0.010
P10	0.132	0.030	0.064	<0.010	0.014
Brownish purple					
P11	0.791	0.034	0.087	<0.010	0.017
P12	0.782	0.036	0.066	<0.010	0.016
P13	0.442	0.014	0.032	<0.010	<0.010
Purple					
P14	0.062	0.011	0.051	<0.010	<0.010
P15	0.114	0.027	0.082	<0.010	0.018
P16	0.112	0.021	0.067	<0.010	0.016
Dark violet					
***DV1**	0.208	0.024	0.119	0.022	0.016
***DV2**	0.199	0.044	0.125	0.030	0.017
***DV3**	0.129	0.018	0.065	0.019	<0.010

*With color-change effect

สถาบันวิทยบริการ
จุฬาลงกรณ์มหาวิทยาลัย

Table IV.1 Showing the trace element content of some Ilakaka-Sakaraha sapphires by Energy Dispersive X-ray Fluorescence (in weight %). The analyzes were performed before heating (continued).

Sample No.	Fe_2O_3	TiO_2	Cr_2O_3	V_2O_3	Ga_2O_3
Medium violet					
*MV1	0.113	0.026	0.033	0.015	0.010
*MV2	0.214	0.029	0.033	0.022	0.010
*MV3	0.138	0.030	0.058	0.018	<0.010
MV4	0.210	0.027	0.010	<0.010	<0.010
MV5	0.099	0.052	0.010	0.019	0.013
MV6	0.095	<0.010	0.010	<0.010	0.011
Light violet					
LV1	0.096	0.053	0.019	0.019	0.017
LV2	0.062	0.024	0.022	0.016	0.011
LV3	0.115	0.026	0.018	0.016	<0.010
Very dark blue					
B1	0.035	0.152	<0.010	<0.010	0.020
B2	0.032	0.067	<0.010	<0.010	<0.010
B3	0.070	0.032	<0.010	<0.010	0.012
Dark blue					
B4	0.088	0.024	<0.010	<0.010	0.020
B5	0.135	0.052	<0.010	<0.010	0.025
*B6	0.384	0.006	0.025	<0.010	<0.010
Medium blue					
B7	0.038	0.012	<0.010	<0.010	<0.010
*B8	0.223	0.010	0.025	<0.010	<0.010
B9	0.397	0.006	<0.010	<0.010	<0.010
B10	0.004	0.039	<0.010	0.011	0.014
*B11	0.235	0.031	0.029	0.013	<0.010

*With color-change effect

สถาบันวิทยบริการ
จุฬาลงกรณ์มหาวิทยาลัย

Table IV.1 Showing the trace element content of some Ilakaka-Sakaraha sapphires by Energy Dispersive X-ray Fluorescence (in weight %). The analyzes were performed before heating (continued).

Sample No.	Fe_2O_3	TiO_2	Cr_2O_3	V_2O_3	Ga_2O_3
Medium blue					
B12	0.007	0.037	0.011	0.011	0.010
*B13	0.145	0.039	0.055	0.024	<0.010
*B14	0.261	0.035	0.100	0.023	<0.010
*B15	0.166	0.074	0.044	0.020	<0.010
*B16	0.216	0.039	0.051	0.030	0.010
*B17	0.440	0.045	0.090	0.039	0.010
B18	0.175	0.058	0.019	0.022	0.012
B19	0.135	0.108	0.013	0.028	0.017
B20	0.084	0.050	0.020	0.014	0.018
Light blue					
B21	0.349	0.029	0.015	0.024	<0.010
B22	0.073	0.038	0.032	0.018	<0.010
B23	0.070	0.022	0.016	0.012	0.014
B24	0.056	0.047	0.019	0.021	0.010
B25	0.144	0.067	0.012	0.012	0.014
B26	0.109	0.025	0.012	0.020	<0.010
B27	0.099	0.036	0.018	0.017	<0.010
*B28	0.083	0.028	0.031	0.019	<0.010
*B29	0.106	0.021	0.074	0.019	0.106
*B30	0.052	0.023	0.018	0.018	0.019
B31	0.389	0.031	0.016	0.017	0.021
B32	0.103	0.039	0.012	0.017	0.011
B33	0.638	0.028	0.017	0.015	0.017
B34	0.142	0.029	0.017	0.017	0.019

*With color change effect

สถาบันวิทยบริการ
จุฬาลงกรณ์มหาวิทยาลัย

Table IV.1 Showing the trace element content of some Ilakaka-Sakaraha sapphires by Energy Dispersive X-ray Fluorescence (in weight %). The analyzes were performed before heating (continued).

Sample No.	Fe_2O_3	TiO_2	Cr_2O_3	V_2O_3	Ga_2O_3
Light blue					
B35	0.111	0.052	0.013	0.024	0.012
*B36	0.179	0.006	0.029	<0.010	0.034
B37	0.282	0.006	<0.010	<0.010	0.015
B38	0.368	0.027	<0.010	<0.010	0.012
Very light blue					
B39	0.054	0.030	0.011	0.024	<0.010
B40	0.086	0.054	0.013	0.024	<0.010
B41	0.047	0.036	0.009	0.015	0.011
B42	0.056	0.042	0.013	0.013	<0.010
B43	0.098	0.044	0.014	0.021	0.018
B44	0.046	0.018	0.014	0.016	<0.010
B45	0.066	0.024	0.017	0.022	0.014
B46	0.037	0.046	0.011	0.018	<0.010
B47	0.259	0.029	0.017	<0.010	0.011
B48	0.203	0.052	0.009	<0.010	0.014
B49	0.095	0.051	0.013	0.022	<0.010
B50	0.153	0.012	<0.010	<0.010	<0.010
B51	0.141	0.030	<0.010	<0.010	<0.010
B52	0.098	0.040	<0.010	<0.010	0.011
Extremly light blue					
B53	0.212	0.011	<0.010	<0.010	0.011
B54	0.037	0.006	<0.010	<0.010	<0.010
B55	0.159	0.064	0.022	0.019	0.025
B56	0.129	0.048	0.015	0.017	0.010
B57	0.054	0.028	0.010	0.017	0.012

สถาบันวิทยบริการ
จุฬาลงกรณ์มหาวิทยาลัย

Table IV.1 Showing the trace element content of some Ilakaka-Sakaraha sapphires by Energy Dispersive X-ray Fluorescence (in weight %). The analyzes were performed before heating (continued).

Sample No.	Fe_2O_3	TiO_2	Cr_2O_3	V_2O_3	Ga_2O_3
Extremly light blue					
B58	0.107	0.085	0.015	0.017	<0.010
B59	0.097	0.047	0.015	0.024	0.014
B60	0.040	0.038	0.013	0.012	0.011
B61	0.105	0.050	0.015	0.018	0.024
B62	0.104	0.085	0.013	0.022	<0.010
Colorless					
W1	0.062	0.011	<0.010	<0.010	0.010
Very light bluish					
W2	0.038	0.035	<0.010	<0.010	<0.010
W3	0.035	0.029	<0.010	<0.010	0.013
Orangey yellow					
Y1	0.021	0.013	<0.010	<0.010	<0.010
Light yellow					
Y2	0.232	<0.010	<0.010	0.010	0.010
Y3	0.030	<0.010	<0.010	<0.010	<0.010
Y4	0.134	<0.010	<0.010	<0.010	<0.010
Medium green					
G1	0.203	0.012	<0.010	<0.010	<0.010
Light yellowish green					
G2	0.766	<0.010	<0.010	<0.010	<0.010
G3	0.675	<0.010	<0.010	<0.010	<0.010

สถาบันวิทยบริการ
จุฬาลงกรณ์มหาวิทยาลัย

Table IV.2 The major and trace elements content of 16 sapphire samples by Electron Probe Micro-Analyzer. The analyses were performed after the step-heating up to 1600^{O}C

	Purplish pink sapphire type																			
	PP3/1	PP3/2	PP3/3	PP3/4	PP3/5	PP11/1	PP11/2	PP11/3	PP11/4	PP11/5	PP4/1	PP4/2	PP4/3	PP4/4	PP4/5	PP6/1	PP6/2	PP6/3	PP6/4	PP6/5
Al_2O_3	99.71	99.79	99.57	99.70	99.86	99.75	99.75	100.00	99.73	99.64	99.37	99.52	99.69	99.92	100.20	99.30	99.62	99.35	99.31	99.62
TiO_2	0.03	0.01	0.02	0.02	0.02	0.01	0.01	0.02	0.02	0.01	0.01	0.01	0.01	0.01	0.01	0.00	0.02	0.02	0.01	0.02
V_2O_3	0.02	0.03	0.02	0.02	0.02	0.01	0.00	0.00	0.00	0.01	0.00	0.00	0.00	0.00	0.00	0.01	0.00	0.00	0.00	0.00
Ga_2O_3	0.02	0.02	0.00	0.01	0.02	0.01	0.01	0.02	0.02	0.01	0.01	0.02	0.01	0.01	0.01	0.01	0.01	0.02	0.01	0.01
Fe_2O_3	0.06	0.06	0.06	0.06	0.06	0.07	0.07	0.07	0.06	0.07	0.06	0.05	0.05	0.06	0.05	0.05	0.05	0.05	0.05	0.05
SiO_2	0.02	0.02	0.02	0.02	0.01	0.02	0.02	0.02	0.02	0.04	0.02	0.01	0.02	0.01	0.00	0.02	0.02	0.02	0.02	0.02
Cr_2O_3	0.13	0.13	0.14	0.13	0.13	0.06	0.05	0.05	0.05	0.04	0.06	0.06	0.06	0.06	0.06	0.06	0.07	0.06	0.06	0.06
MnO	0.00	0.00	0.00	0.00	0.01	0.00	0.01	0.00	0.01	0.01	0.00	0.01	0.01	0.00	0.00	0.01	0.01	0.01	0.01	0.01
MgO	0.01	0.01	0.01	0.01	0.01	0.01	0.01	0.00	0.01	0.01	0.00	0.00	0.00	0.00	0.01	0.01	0.00	0.00	0.01	0.01
Total	99.99	100.06	99.84	99.96	100.14	99.94	99.94	100.17	99.91	99.84	99.52	99.68	99.85	100.07	100.34	99.47	99.78	99.52	99.48	99.78
Formula 3(O)																				
Al	1.9960	1.9963	1.9962	1.9963	1.9962	1.9973	1.9973	1.9976	1.9974	1.9969	1.9978	1.9978	1.9978	1.9979	1.9982	1.9977	1.9977	1.9976	1.9975	1.9976
Ti	0.0004	0.0002	0.0003	0.0003	0.0002	0.0001	0.0002	0.0002	0.0002	0.0001	0.0001	0.0001	0.0002	0.0001	0.0001	0.0000	0.0002	0.0002	0.0002	0.0002
V	0.0002	0.0003	0.0003	0.0003	0.0003	0.0001	0.0000	0.0000	0.0000	0.0001	0.0000	0.0000	0.0000	0.0000	0.0000	0.0001	0.0000	0.0000	0.0000	0.0000
Ga	0.0002	0.0002	0.0000	0.0001	0.0002	0.0001	0.0002	0.0002	0.0002	0.0001	0.0001	0.0002	0.0001	0.0001	0.0001	0.0001	0.0001	0.0002	0.0001	0.0001
Fe	0.0008	0.0007	0.0008	0.0007	0.0008	0.0009	0.0009	0.0008	0.0008	0.0009	0.0007	0.0007	0.0007	0.0007	0.0006	0.0007	0.0006	0.0007	0.0007	0.0006
Si	0.0004	0.0003	0.0003	0.0003	0.0002	0.0004	0.0004	0.0003	0.0003	0.0007	0.0003	0.0002	0.0003	0.0002	0.0000	0.0003	0.0003	0.0003	0.0003	0.0003
Cr	0.0017	0.0017	0.0019	0.0017	0.0018	0.0008	0.0007	0.0007	0.0006	0.0006	0.0008	0.0008	0.0008	0.0008	0.0009	0.0009	0.0009	0.0008	0.0008	0.0008
Mn	0.0000	0.0000	0.0000	0.0000	0.0001	0.0000	0.0001	0.0000	0.0001	0.0001	0.0000	0.0001	0.0001	0.0000	0.0000	0.0001	0.0001	0.0001	0.0001	0.0001
Mg	0.0003	0.0003	0.0003	0.0003	0.0002	0.0002	0.0002	0.0000	0.0003	0.0003	0.0000	0.0000	0.0000	0.0000	0.0003	0.0002	0.0000	0.0000	0.0003	0.0003
Total*	1.9998	1.9999	1.9999	1.9999	2.0000	1.9999	1.9999	1.9998	2.0000	1.9998	1.9999	2.0000	1.9999	1.9999	2.0001	2.0000	1.9999	1.9999	2.0000	2.0000
Mg:Fe:Ti																				
Mg^{2+}	18.379	21.819	19.655	20.467	18.805	18.608	18.228	0.000	20.052	22.061	0.000	0.000	0.000	0.000	26.484	23.360	0.000	0.000	23.090	23.363
Fe_{total}	55.658	62.771	59.522	58.882	62.221	70.961	68.489	80.254	63.762	67.821	84.854	85.489	81.257	85.300	62.827	76.640	75.393	77.280	61.767	56.600
Ti^{4+}	25.963	15.411	20.823	20.651	18.974	10.431	13.283	19.746	16.186	10.118	15.146	14.511	18.743	14.700	10.689	0.000	24.607	22.720	15.144	20.037

0.00 = lower than detection limit

Table IV.2 The major and trace elements content of 16 sapphire samples by Electron Probe Micro-Analyzer. The analyses were performed after the step-heating up to 1600^{O}C (continued).

	Light purplish pink sapphire type													
	LP9/1	LP9/2	LP9/3	LP9/4	LP9/5	LP4/1	LP4/2	LP4/3	LP4/4	LP3/1	LP3/2	LP3/3	LP3/4	LP3/5
Al_2O_3	99.53	98.80	99.16	99.43	99.25	99.34	99.41	99.65	99.85	100.29	99.95	100.22	100.17	99.77
TiO_2	0.02	0.02	0.01	0.02	0.02	0.01	0.01	0.00	0.01	0.01	0.01	0.01	0.02	0.01
V_2O_3	0.00	0.00	0.00	0.00	0.01	0.01	0.01	0.01	0.01	0.01	0.00	0.00	0.00	0.01
Ga_2O_3	0.01	0.01	0.01	0.01	0.01	0.01	0.02	0.02	0.00	0.01	0.01	0.02	0.01	0.00
Fe_2O_3	0.30	0.29	0.31	0.30	0.31	0.05	0.05	0.06	0.05	0.06	0.06	0.06	0.06	0.06
SiO_2	0.03	0.01	0.02	0.02	0.02	0.02	0.02	0.02	0.02	0.02	0.02	0.02	0.02	0.02
Cr_2O_3	0.06	0.06	0.07	0.08	0.08	0.04	0.04	0.03	0.04	0.06	0.06	0.06	0.06	0.05
MnO	0.01	0.00	0.00	0.00	0.00	0.00	0.00	0.01	0.01	0.00	0.00	0.01	0.01	0.00
MgO	0.01	0.01	0.01	0.01	0.01	0.01	0.01	0.01	0.01	0.01	0.00	0.01	0.01	0.01
Total	99.98	99.22	99.59	99.86	99.71	99.49	99.57	99.81	100.00	100.47	100.11	100.40	100.35	99.93
Formula 3(O)														
Al	1.9939	1.9943	1.9942	1.9942	1.9937	1.9978	1.9976	1.9978	1.9978	1.9975	1.9977	1.9974	1.9974	1.9976
Ti	0.0003	0.0003	0.0002	0.0002	0.0003	0.0002	0.0001	0.0000	0.0001	0.0001	0.0001	0.0002	0.0002	0.0002
V	0.0000	0.0000	0.0000	0.0000	0.0001	0.0001	0.0001	0.0001	0.0001	0.0001	0.0000	0.0000	0.0000	0.0001
Ga	0.0001	0.0002	0.0001	0.0001	0.0001	0.0001	0.0002	0.0002	0.0000	0.0001	0.0001	0.0002	0.0001	0.0000
Fe	0.0039	0.0038	0.0040	0.0039	0.0040	0.0006	0.0007	0.0007	0.0006	0.0008	0.0008	0.0008	0.0008	0.0007
Si	0.0004	0.0002	0.0003	0.0003	0.0004	0.0003	0.0004	0.0004	0.0004	0.0003	0.0003	0.0003	0.0003	0.0003
Cr	0.0009	0.0009	0.0009	0.0011	0.0010	0.0005	0.0006	0.0004	0.0005	0.0007	0.0008	0.0007	0.0008	0.0007
Mn	0.0001	0.0000	0.0000	0.0000	0.0000	0.0000	0.0000	0.0002	0.0002	0.0000	0.0000	0.0001	0.0001	0.0000
Mg	0.0003	0.0003	0.0003	0.0002	0.0003	0.0003	0.0003	0.0003	0.0003	0.0003	0.0000	0.0003	0.0003	0.0003
Total*	1.9999	1.9999	1.9999	1.9999	1.9999	1.9999	1.9999	2.0000	2.0000	1.9999	1.9999	2.0000	2.0000	1.9999
Mg:Fe:Ti														
Mg^{2+}	7.322	6.510	6.321	5.294	6.759	25.464	23.640	26.134	24.825	21.120	0.000	21.348	21.121	22.061
Fe_{total}	86.426	86.922	89.910	89.958	87.558	59.120	64.433	73.866	62.650	68.224	85.921	65.728	62.896	62.356
Ti^{4+}	6.252	6.569	3.769	4.748	5.683	15.416	11.927	0.000	12.525	10.655	14.079	12.924	15.983	15.582

0.00 = lower than detection limit

Table IV.2 The major and trace elements content of 16 sapphire samples by Electron Probe Micro-Analyzer. The analyses were performed after the step-heating up to 1600^{O}C (continued).

	Light orangey pink sapphire type					Orangey pink sapphire type						Purple sapphire type				
	PP15/1	PP15/2	PP15/3	PP15/4	PP15/5	PP17/1	PP17/2	PP17/3	PP17/4	PP17/5	PP17/6	P16/1	P16/2	P16/3	P16/4	P16/5
Al_2O_3	99.64	99.83	99.73	99.72	99.77	99.26	99.40	99.06	99.15	99.44	99.41	98.66	98.82	98.39	98.82	99.05
TiO_2	0.00	0.01	0.01	0.01	0.01	0.00	0.01	0.01	0.02	0.01	0.01	0.02	0.02	0.02	0.02	0.02
V_2O_3	0.00	0.00	0.00	0.00	0.00	0.01	0.01	0.01	0.00	0.00	0.00	0.02	0.01	0.00	0.01	0.00
Ga_2O_3	0.02	0.01	0.01	0.02	0.01	0.00	0.01	0.02	0.01	0.00	0.00	0.02	0.02	0.02	0.02	0.01
Fe_2O_3	0.06	0.07	0.07	0.07	0.07	0.04	0.04	0.04	0.05	0.05	0.05	0.08	0.09	0.08	0.08	0.09
SiO_2	0.02	0.02	0.02	0.02	0.02	0.01	0.02	0.02	0.02	0.02	0.02	0.02	0.02	0.02	0.02	0.03
Cr_2O_3	0.00	0.03	0.03	0.03	0.04	0.02	0.03	0.02	0.03	0.03	0.03	0.07	0.07	0.08	0.07	0.07
MnO	0.01	0.01	0.01	0.01	0.00	0.01	0.01	0.01	0.00	0.00	0.00	0.00	0.00	0.01	0.00	0.00
MgO	0.00	0.01	0.00	0.00	0.01	0.00	0.01	0.01	0.01	0.00	0.01	0.01	0.00	0.01	0.01	0.01
Total	99.74	99.99	99.88	99.87	99.92	99.36	99.54	99.20	99.29	99.56	99.54	98.90	99.04	98.63	99.05	99.27
Formula 3(O)																
Al	1.9985	1.9978	1.9978	1.9979	1.9977	1.9987	1.9979	1.9979	1.9980	1.9983	1.9980	1.9966	1.9970	1.9965	1.9967	1.9967
Ti	0.0000	0.0001	0.0001	0.0001	0.0002	0.0000	0.0002	0.0001	0.0002	0.0002	0.0002	0.0002	0.0002	0.0003	0.0002	0.0003
V	0.0000	0.0000	0.0000	0.0000	0.0000	0.0001	0.0001	0.0001	0.0000	0.0000	0.0000	0.0002	0.0002	0.0000	0.0001	0.0000
Ga	0.0002	0.0001	0.0001	0.0002	0.0001	0.0000	0.0001	0.0002	0.0001	0.0000	0.0000	0.0002	0.0002	0.0002	0.0002	0.0001
Fe	0.0008	0.0009	0.0009	0.0009	0.0009	0.0006	0.0005	0.0006	0.0007	0.0006	0.0007	0.0011	0.0011	0.0010	0.0011	0.0011
Si	0.0003	0.0003	0.0004	0.0003	0.0003	0.0002	0.0003	0.0004	0.0003	0.0003	0.0004	0.0004	0.0003	0.0004	0.0004	0.0004
Cr	0.0000	0.0004	0.0004	0.0004	0.0005	0.0003	0.0004	0.0003	0.0004	0.0005	0.0004	0.0010	0.0009	0.0011	0.0010	0.0009
Mn	0.0001	0.0001	0.0001	0.0001	0.0000	0.0001	0.0002	0.0001	0.0000	0.0000	0.0000	0.0000	0.0000	0.0001	0.0000	0.0000
Mg	0.0000	0.0003	0.0000	0.0000	0.0003	0.0000	0.0003	0.0003	0.0003	0.0000	0.0003	0.0002	0.0000	0.0003	0.0003	0.0002
Total*	1.9999	2.0000	1.9999	1.9999	1.9999	2.0000	2.0000	1.9999	1.9999	1.9998	1.9999	1.9999	1.9998	1.9999	1.9999	1.9998
Mg:Fe:Ti																
Mg^{2+}	0.000	20.052	0.000	0.000	19.851	0.000	26.844	27.591	22.564	0.000	22.824	15.263	0.000	16.401	16.677	14.060
Fe_{total}	100.000	69.832	88.893	87.184	68.131	100.000	56.905	59.881	59.222	78.132	61.055	71.047	83.339	67.051	69.862	69.388
Ti^{4+}	0.000	10.116	11.107	12.816	12.018	0.000	16.251	12.528	18.214	21.868	16.121	13.690	16.661	16.549	13.461	16.551

0.00 = lower than detection limit

Table IV.2 The major and trace elements content of 16 sapphire samples by Electron Probe Micro-Analyzer. The analyses were performed after the step-heating up to 1600^{O}C (continued).

	Pinkish purple sapphire type															
	P10/1	P10/2	P10/3	P10/4	P10/5	P10/6	P5/1	P5/2	P5/3	P5/4	P5/5	P6/1	P6/2	P6/3	P6/4	P6/5
Al_2O_3	99.56	99.43	99.16	98.83	99.32	99.07	98.69	98.53	99.14	99.11	99.70	99.81	99.41	99.65	99.30	99.25
TiO_2	0.02	0.02	0.01	0.02	0.01	0.03	0.02	0.01	0.02	0.02	0.02	0.02	0.02	0.01	0.02	0.01
V_2O_3	0.00	0.01	0.00	0.01	0.00	0.00	0.00	0.00	0.00	0.00	0.00	0.01	0.00	0.00	0.00	0.01
Ga_2O_3	0.01	0.01	0.02	0.01	0.01	0.01	0.02	0.02	0.01	0.00	0.01	0.01	0.01	0.02	0.01	0.00
Fe_2O_3	0.10	0.11	0.10	0.09	0.09	0.09	0.17	0.17	0.16	0.17	0.17	0.34	0.35	0.34	0.34	0.34
SiO_2	0.03	0.02	0.02	0.02	0.02	0.02	0.02	0.02	0.02	0.02	0.02	0.02	0.02	0.02	0.02	0.02
Cr_2O_3	0.06	0.06	0.05	0.05	0.06	0.05	0.07	0.07	0.07	0.07	0.07	0.05	0.05	0.05	0.05	0.05
MnO	0.01	0.01	0.01	0.01	0.01	0.00	0.01	0.00	0.01	0.01	0.00	0.01	0.01	0.00	0.01	0.01
MgO	0.01	0.01	0.01	0.01	0.01	0.01	0.01	0.01	0.01	0.00	0.01	0.01	0.01	0.01	0.01	0.01
Total	99.79	99.66	99.37	99.06	99.53	99.27	99.00	98.83	99.44	99.39	99.99	100.28	99.88	100.11	99.77	99.69
Formula 3(O)																
Al	1.9967	1.9968	1.9970	1.9968	1.9971	1.9970	1.9957	1.9958	1.9958	1.9962	1.9959	1.9937	1.9937	1.9938	1.9937	1.9941
Ti	0.0002	0.0002	0.0002	0.0002	0.0001	0.0003	0.0002	0.0001	0.0002	0.0002	0.0002	0.0002	0.0002	0.0002	0.0003	0.0001
V	0.0000	0.0001	0.0000	0.0001	0.0000	0.0000	0.0000	0.0000	0.0000	0.0000	0.0000	0.0001	0.0000	0.0000	0.0000	0.0001
Ga	0.0002	0.0001	0.0002	0.0002	0.0001	0.0001	0.0002	0.0002	0.0001	0.0000	0.0001	0.0001	0.0001	0.0002	0.0001	0.0000
Fe	0.0012	0.0013	0.0013	0.0012	0.0012	0.0011	0.0021	0.0022	0.0021	0.0021	0.0022	0.0043	0.0045	0.0044	0.0044	0.0043
Si	0.0004	0.0003	0.0003	0.0003	0.0003	0.0004	0.0004	0.0004	0.0004	0.0003	0.0003	0.0004	0.0004	0.0004	0.0003	0.0003
Cr	0.0008	0.0008	0.0007	0.0007	0.0007	0.0006	0.0009	0.0009	0.0010	0.0009	0.0009	0.0007	0.0007	0.0007	0.0007	0.0007
Mn	0.0001	0.0001	0.0001	0.0001	0.0001	0.0000	0.0001	0.0000	0.0001	0.0001	0.0000	0.0001	0.0001	0.0000	0.0001	0.0001
Mg	0.0002	0.0003	0.0003	0.0002	0.0003	0.0003	0.0003	0.0003	0.0003	0.0000	0.0003	0.0003	0.0002	0.0002	0.0003	0.0002
Total*	1.9999	2.0000	2.0000	2.0000	2.0000	1.9999	1.9999	1.9999	1.9999	1.9999	1.9999	1.9999	1.9999	1.9999	1.9999	2.0000
Mg:Fe:Ti																
Mg^{2+}	13.527	14.172	15.263	13.735	16.133	17.512	9.867	12.458	9.966	0.000	10.339	5.272	4.634	4.770	5.635	4.915
Fe_{total}	73.583	75.104	75.496	72.406	74.914	64.082	82.169	82.224	82.492	91.670	81.599	90.472	90.691	91.754	88.680	92.331
Ti^{4+}	12.890	10.724	9.240	13.859	8.953	18.406	7.964	5.318	7.542	8.330	8.061	4.256	4.675	3.476	5.685	2.755

0.00 = lower than detection limit

Table IV.2 The major and trace elements content of 16 sapphire samples by Electron Probe Micro-Analyzer. The analyses were performed after the step-heating up to 1600^{O}C (continued).

	Brownish purple sapphire type					Medium violet sapphire type									
	P11/1	P11/2	P11/3	P11/4	P11/5	MV2/1	MV2/2	MV2/3	MV2/4	MV2/5	MV5/1	MV5/2	MV5/3	MV5/4	MV5/5
Al_2O_3	99.15	99.41	99.39	99.46	99.48	99.05	99.27	99.33	99.36	99.50	100.12	100.19	100.24	99.96	100.02
TiO_2	0.02	0.02	0.03	0.02	0.02	0.02	0.02	0.02	0.03	0.02	0.04	0.03	0.03	0.02	0.02
V_2O_3	0.00	0.01	0.01	0.01	0.00	0.00	0.01	0.01	0.00	0.01	0.01	0.02	0.00	0.01	0.01
Ga_2O_3	0.02	0.02	0.02	0.02	0.01	0.02	0.01	0.02	0.01	0.02	0.01	0.02	0.02	0.02	0.03
Fe_2O_3	0.64	0.66	0.65	0.65	0.64	0.36	0.36	0.36	0.37	0.37	0.08	0.08	0.09	0.08	0.10
SiO_2	0.02	0.02	0.02	0.02	0.05	0.02	0.01	0.02	0.02	0.02	0.02	0.02	0.02	0.02	0.01
Cr_2O_3	0.08	0.08	0.08	0.07	0.08	0.03	0.03	0.03	0.02	0.03	0.01	0.02	0.02	0.02	0.02
MnO	0.00	0.00	0.01	0.01	0.00	0.00	0.01	0.01	0.01	0.00	0.01	0.01	0.01	0.01	0.00
MgO	0.01	0.01	0.01	0.01	0.02	0.01	0.01	0.02	0.01	0.01	0.02	0.01	0.02	0.02	0.01
Total	99.94	100.23	100.21	100.28	100.30	99.51	99.73	99.81	99.82	99.98	100.32	100.40	100.44	100.16	100.22
Formula 3(O)															
Al	1.9895	1.9891	1.9892	1.9892	1.9888	1.9938	1.9939	1.9935	1.9938	1.9936	1.9970	1.9970	1.9971	1.9972	1.9972
Ti	0.0003	0.0003	0.0003	0.0003	0.0002	0.0002	0.0003	0.0003	0.0003	0.0003	0.0005	0.0004	0.0003	0.0003	0.0003
V	0.0000	0.0001	0.0001	0.0001	0.0000	0.0000	0.0001	0.0001	0.0000	0.0001	0.0001	0.0002	0.0000	0.0001	0.0001
Ga	0.0002	0.0002	0.0002	0.0002	0.0001	0.0002	0.0001	0.0002	0.0001	0.0002	0.0001	0.0002	0.0002	0.0002	0.0003
Fe	0.0083	0.0084	0.0082	0.0083	0.0082	0.0046	0.0047	0.0047	0.0048	0.0047	0.0010	0.0010	0.0011	0.0011	0.0012
Si	0.0003	0.0004	0.0003	0.0004	0.0009	0.0004	0.0002	0.0003	0.0003	0.0003	0.0004	0.0003	0.0003	0.0003	0.0002
Cr	0.0011	0.0010	0.0011	0.0010	0.0011	0.0004	0.0003	0.0004	0.0003	0.0004	0.0002	0.0002	0.0003	0.0003	0.0003
Mn	0.0000	0.0000	0.0001	0.0001	0.0000	0.0000	0.0001	0.0001	0.0002	0.0000	0.0001	0.0001	0.0001	0.0001	0.0000
Mg	0.0004	0.0003	0.0003	0.0002	0.0006	0.0003	0.0003	0.0004	0.0003	0.0003	0.0004	0.0004	0.0004	0.0004	0.0003
Total*	1.9999	1.9999	1.9999	1.9999	1.9998	1.9999	2.0000	2.0000	1.9999	1.9999	1.9999	1.9999	2.0000	2.0000	1.9999
Mg:Fe:Ti															
Mg^{2+}	3.998	3.369	3.146	2.574	6.477	4.968	4.870	7.201	4.765	4.776	22.062	19.852	22.504	21.739	14.589
Fe_{total}	92.832	93.515	93.103	93.964	90.966	90.270	89.233	87.955	89.225	89.440	53.712	55.825	59.464	60.713	70.690
Ti^{4+}	3.170	3.116	3.751	3.463	2.557	4.762	5.897	4.844	6.010	5.783	24.225	24.323	18.032	17.548	14.721

0.00 = lower than detection limit

BIOGRAPHY

Miss Krittaya Pattamalai was born in August 24, 1970, at Bangkok. She graduated with a bachelor degree in geology from the Department of Geology, Faculty of science, Chiang Mai University in 1993. At present, she works at the Research and Development Encouragement Division, Bureau of Mineral Resources, Department of Mineral Resources and also studies in a Master program in geology at Chulalongkorn University.

สถาบันวิทยบริการ
จุฬาลงกรณ์มหาวิทยาลัย